

Kähler metrics and gauge kinetic functions for intersecting D6-branes on toroidal orbifolds

- The complete perturbative story -

Gabriele Honecker

*Institut für Physik (WA THEP), Johannes-Gutenberg-Universität, D - 55099 Mainz,
Germany* Gabriele.Honecker@uni-mainz.de

Abstract

We systematically derive the perturbatively exact holomorphic gauge kinetic function, the open string Kähler metrics and closed string Kähler potential on intersecting D6-branes by matching open string one-loop computations of gauge thresholds with field theoretical gauge couplings in $\mathcal{N} = 1$ supergravity. We consider all cases of bulk, fractional and rigid D6-branes on $T^6/\Omega\mathcal{R}$ and the orbifolds $T^6/(\mathbb{Z}_N \times \Omega\mathcal{R})$ and $T^6/(\mathbb{Z}_2 \times \mathbb{Z}_{2M} \times \Omega\mathcal{R})$ without and with discrete torsion, which differ in the number of bulk complex structures and in the bulk Kähler potential. Our analysis includes all supersymmetric configurations of vanishing and non-vanishing angles among D6-branes and O6-planes, and all possible Wilson line and displacement moduli are taken into account. The shape of the Kähler moduli turns out to be orbifold independent but angle dependent, whereas the holomorphic gauge kinetic functions obtain three different kinds of one-loop corrections: a Kähler moduli dependent one for some vanishing angle independently of the orbifold background, another one depending on complex structure moduli only for fractional and rigid D6-branes, and finally a constant term from intersections with O6-planes. These results are of essential importance for the construction of the related effective field theory of phenomenologically appealing D-brane models.

As first examples, we compute the complete perturbative gauge kinetic functions and Kähler metrics for some $T^6/\mathbb{Z}_2 \times \mathbb{Z}_2$ examples with rigid D-branes of [1]. As a second class of examples, the Kähler metrics and gauge kinetic functions for the fractional QCD and leptonic D6-brane stacks of the Standard Model on T^6/\mathbb{Z}'_6 from [2] are given.

Contents

1	Introduction	3
2	The gauge thresholds revisited	4
2.1	Geometry, three-cycles and RR tadpole cancellation	5
2.2	$SU(N)$, $SO(2N)$ and $Sp(2N)$ gauge thresholds on fractional and rigid D6-branes	18
2.3	Comments on anomaly-free $U(1)$ gauge groups	37
3	Kähler metrics, Kähler potential and holomorphic gauge kinetic function at one loop	38
3.1	Tree level gauge kinetic function	38
3.2	One-loop results for T^6 and T^6/\mathbb{Z}_2 and $T^6/\mathbb{Z}_2 \times \mathbb{Z}_2$ with $\eta = \pm 1$	41
3.3	Kähler metrics and holomorphic gauge kinetic functions for $SO(2M)$ and $Sp(2M)$	58
3.4	Gauge kinetic functions for anomaly-free $U(1)$ s	60
4	Example on $T^6/\mathbb{Z}_2 \times \mathbb{Z}_2$: Magnetised D9-branes vs. D6-branes at angles	63
4.1	Examples 1 and 2 by Angelantonj <i>et al.</i> revisited	65
4.2	Example 3 by Angelantonj <i>et al.</i> revisited	68
5	Example on T^6/\mathbb{Z}'_6: the Standard Model on fractional D6-branes	72
6	Conclusions and Outlook	76
A	Reformulations of the Möbius strip contributions to the gauge thresholds	93
B	Tree level gauge couplings for various orbifolds	96
B.1	The T^6/\mathbb{Z}_4 and $T^6/\mathbb{Z}_2 \times \mathbb{Z}_4$ orientifolds	96
B.2	The T^6/\mathbb{Z}'_6 and $T^6/\mathbb{Z}_2 \times \mathbb{Z}_6$ orientifolds	98
B.3	The T^6/\mathbb{Z}_6 and $T^6/\mathbb{Z}_2 \times \mathbb{Z}'_6$ orientifolds	100
C	Details of the $T^6/\mathbb{Z}_2 \times \mathbb{Z}_2$ models with magnetised T-duals	101
C.1	Example 1	102
C.2	Example 3	104
	References	108

1 Introduction

Over recent years, considerable progress has been made in constructing supersymmetric globally consistent string theory vacua with Standard Model gauge group and matter content, see e.g. [3–8, 2] and the review articles [9–14] for intersecting D6-branes, [15–18] for heterotic orbifolds, [19, 20] for heterotic Calabi-Yau compactifications with $SU(N)$ bundles and [21–24] for $U(N)$ bundles, the review [25] and references therein for globally defined F-theory models and [26, 27] for Gepner models.

Establishing the existence of Standard Model vacua, however, also requires the matching of the low-energy effective action, in particular recovering the perturbative gauge and Yukawa couplings of the Standard Model group and particles. Partial results at tree level can generically be obtained by dimensional reduction of the supergravity and D-brane Chern-Simons and Born-Infeld actions in combination with charge selection rules, see e.g. [28] and [29–31] for very early and very recent works on D6-branes, respectively. The exact dependence on moduli fields and numerical values at one loop, however, requires more powerful techniques of conformal field theory. The well-known methods from heterotic orbifolds, e.g. [32, 33], have been translated to the case of *bulk* D6-branes in IIA string theory on the six-torus and its T-dual variants of D-branes in the IIB theory, by identifying orbifold twists on the heterotic side with intersection angles in IIA and magnetic background fields in IIB, see e.g. the reviews [34, 11].¹ But realistic string spectra require the use of *rigid* or at least *fractional* D-branes in order to project out adjoint moduli which would be responsible for arbitrary continuous breakings of the gauge group along flat directions. These types of D6-branes on orbifolds of the type IIA string with at least one \mathbb{Z}_2 subsymmetry, which leads to new non-trivial contributions to the one-string-loop gauge threshold computation as worked out in [40], possess new chiral configurations at some vanishing intersection angle, and the particle generations can emerge from various intersection sectors of orbifold-image D6-branes for orbifolds other than $\mathbb{Z}_2 \times \mathbb{Z}_2$.

The aim of the present article is to consistently and compactly formulate the perturbatively exact holomorphic gauge kinetic function, the bulk Kähler potential and open string Kähler metrics for (factorisable) toroidal orbifold backgrounds of type IIA orientifolds in the most general possible set-up, i.e. by including all (untilted and tilted) background lattices and all (discrete or continuous) displacements and Wilson lines in such a way that it can be readily applied to the existing Standard Model-like spectra on fractional D6-branes on T^6/\mathbb{Z}'_6 [41, 2, 40] and T^6/\mathbb{Z}_6 [6, 42] as well as expected new models on orbifolds with discrete

¹Field theory results on Kähler metrics and gauge thresholds at the orbifold point in the type IIB string, which are *not* T-dual to the intersecting D6-brane scenario include e.g. the globally consistent models of [35–37] and the local models of [38, 39].

torsion. To this end, the previously computed gauge threshold corrections [43–45, 40] are carefully regrouped for all backgrounds into lattice sums with beta function coefficients as prefactors plus constant terms from intersections with O6-planes and complex structure moduli dependent contributions on fractional and rigid D6-branes only. While the first kind of correction has been used before to derive Kähler metrics, e.g. on the six-torus in [44], the two other kinds are to our knowledge fully appreciated here for the first time.

The paper is organised as follows. In section 2 we review the geometric set-up and computation of gauge thresholds at open string one-loop. The focus is on the comparison of bulk, fractional and rigid D6-branes, and all gauge thresholds are reformulated such that the beta function coefficients appear as prefactors, wherever possible. This is essential for the correct identification of the Kähler metrics in section 3. In section 2, we furthermore focus, besides the unitary groups, on symplectic and orthogonal gauge factors as well as (anomalous) single $U(1)$ s and anomaly-free massless linear combinations of Abelian gauge factors, all of which have to our knowledge not been discussed in detail before.

In section 3, the matching of the stringy gauge thresholds from the previous section with the supergravity expressions is performed for each case, and the Kähler metrics and perturbatively exact holomorphic gauge kinetic functions are extracted. The discussion includes all factorisable toroidal orbifolds with different numbers $h_{21}^{\text{bulk}} = 3, 1, 0$ of bulk complex structures, possible one-loop field redefinitions, and all gauge groups $SU(N)$, $SO(2M)$, $Sp(2M)$ and $U(1)$.

The use of the generic results is demonstrated in two classes of examples, first in section 4 on rigid D6-branes in the $T^6/\mathbb{Z}_2 \times \mathbb{Z}_2$ background with discrete torsion dual to the magnetised D9/D5-brane set-up of [1], and finally in section 5, the generic expressions are applied to the Standard Model on fractional D6-branes in the T^6/\mathbb{Z}'_6 orbifold background of [41, 2, 40], which was the original motivation for studying the field theory on various kinds of D6-branes, in particular including chiral matter at some vanishing angle, in detail. Section 6 contains our conclusions, and technical details on the rewriting of the gauge threshold amplitudes with Möbius strip topology, the tree-level gauge couplings for orbifolds with different numbers $h_{21}^{\text{bulk}} = 3, 1, 0$ of bulk complex structures and details on the three-cycles and intersection numbers of the $T^6/\mathbb{Z}_2 \times \mathbb{Z}_2$ examples dual to those in [1] are collected in appendices A to C.

2 The gauge thresholds revisited

In this section, we review the computation of the gauge thresholds for rigid D6-branes by means of the magnetic background field method on the least discussed orbifold background

$T^6/\mathbb{Z}_2 \times \mathbb{Z}_{2M}$ with discrete torsion. Our discussion includes all possible supersymmetric D6-brane configurations at three or one vanishing angle or with all three angles non-vanishing. We comment on changes in the normalisation for all other known bulk and fractional D6-branes on the factorisable six-torus T^6 , orbifolds with one generator T^6/\mathbb{Z}_N and with two generators $T^6/\mathbb{Z}_2 \times \mathbb{Z}_{2M}$ without discrete torsion.

To this means, we discuss the background geometry and cycles in section 2.1 and then briefly review the gauge threshold amplitudes in section 2.2. Tables 6, 8, 10 and 11 contain the complete result for beta function coefficients and gauge thresholds from bifundamental and adjoint matter of $SU(N_a)$ on all toroidal orbifold backgrounds ($T^6/\mathbb{Z}_2 \times \mathbb{Z}_{2M}$ with discrete torsion, T^6 and T^6/\mathbb{Z}_3 , $T^6/\mathbb{Z}_2 \times \mathbb{Z}_{2M}$ without discrete torsion, T^6/\mathbb{Z}_{2N} , respectively) under considerations, and tables 7, 9, 10 and 12 give the analogous result for symmetric and antisymmetric matter. In section 2.3, we discuss the situation for Abelian gauge factors. This complete presentation of all possible cases serves as preparation for determining the holomorphic gauge kinetic function and Kähler metrics for each case in section 3.

2.1 Geometry, three-cycles and RR tadpole cancellation

2.1.1 Orbifolds, compactification lattices and one-cycles

Throughout this paper we consider intersecting D6-branes on the factorisable six-torus, $T^6 = T^2_{(1)} \times T^2_{(2)} \times T^2_{(3)}$, and its orbifolds with all possibilities of one generator,

$$T^6/\mathbb{Z}_N : \quad \theta : z_i \rightarrow e^{2\pi i v_i} z_i,$$

or all choices of two generators containing a $\mathbb{Z}_2 \times \mathbb{Z}_2$ subgroup,

$$T^6/\mathbb{Z}_2 \times \mathbb{Z}_{2M} : \quad \theta : z_i \rightarrow e^{2\pi i v_i} z_i \quad \text{and} \quad \omega : z_i \rightarrow e^{2\pi i w_i} z_i,$$

acting on the complex coordinates z_i of the two-tori $T^2_{(i)}$. The corresponding shift vectors for these orbifolds, which are singular limits of Calabi-Yau threefolds, are listed in table 1.

The \mathbb{Z}_2 rotations are consistent with any choice of two-torus lattice, whereas a \mathbb{Z}_4 rotation requires a square torus and a \mathbb{Z}_3 (or \mathbb{Z}_6) rotation requires a rhombus with acute angle $\pi/3$. The situation is depicted in figure 1 for \mathbb{Z}_2 and figure 2 for \mathbb{Z}_4 and \mathbb{Z}_3 symmetries, respectively. The orientifold projection $\Omega\mathcal{R}$ in Type IIA string theory contains an anti-holomorphic involution \mathcal{R} on the compact space. On the factorisable torus, the involution is simply given by complex conjugation,

$$\mathcal{R} : z_i \rightarrow \bar{z}_i.$$

$T^6 /$	\vec{v}	$T^6 /$	\vec{v}	\vec{w}
\mathbb{Z}_3	$\frac{1}{3}(1, -2, 1)$	$\mathbb{Z}_2 \times \mathbb{Z}_2$	$\frac{1}{2}(1, -1, 0)$	$\frac{1}{2}(0, 1, -1)$
\mathbb{Z}_4	$\frac{1}{4}(1, -2, 1)$	$\mathbb{Z}_2 \times \mathbb{Z}_4$	$\frac{1}{2}(1, -1, 0)$	$\frac{1}{4}(0, 1, -1)$
\mathbb{Z}_6	$\frac{1}{6}(1, -2, 1)$	$\mathbb{Z}_2 \times \mathbb{Z}_6$	$\frac{1}{2}(1, -1, 0)$	$\frac{1}{6}(0, 1, -1)$
\mathbb{Z}'_6	$\frac{1}{6}(1, 2, -3)$	$\mathbb{Z}_2 \times \mathbb{Z}'_6$	$\frac{1}{2}(1, -1, 0)$	$\frac{1}{6}(-2, 1, 1)$

Table 1: Left: shift vectors for all toroidal orbifolds on factorisable tori with one generator. The two-tori are ordered such that the $\mathbb{Z}_2 \equiv \mathbb{Z}_2^{(2)}$ sub-symmetry leaves the second two-torus invariant. Right: shift vectors for all toroidal orbifolds with two generators and $\mathbb{Z}_2 \times \mathbb{Z}_2$ sub-group. For each of these orbifolds, there exist two inequivalent choices of the phase, $\eta = \pm 1$, with which one \mathbb{Z}_2 sub-group acts on the twisted states of the other \mathbb{Z}_2 and preserves either the two- or three-cycles. These are the orbifolds ‘without discrete torsion’ ($\eta = 1$) and ‘with discrete torsion’ ($\eta = -1$).

This constrains the shape of the \mathbb{Z}_2 invariant tori to be ‘untilted’ (rectangular) or ‘tilted’ parameterised by the discrete choices $b = 0, 1/2$ of the real part of the complex structure, cf. figure 1, which in the T-dual IIB language correspond to two discrete choices of the B -field. For the \mathbb{Z}_4 and \mathbb{Z}_3 invariant lattices, there exist two inequivalent orientations w.r.t. the $\Re(z)$ axis: for the **A**-lattice the basic one-cycle π_{2i-1} spans the real axis, and for the **B**-type lattice the real axis extends along $\pi_{2i-1} + \pi_{2i}$. The untilted and titled torus differ in the number of parallel $\Omega\mathcal{R}$ invariant O6-planes, $N_{\Omega\mathcal{R}}^{(i)} = 2(1 - b_i)$. The Hodge numbers (h_{11}, h_{21}) for all toroidal orbifolds listed in table 1 can be found in the appendix of [46] together with the decomposition (h_{11}^+, h_{11}^-) into massless vectors and Kähler moduli in dependence of the lattice orientations. For those orbifolds with $\mathbb{Z}_2 \times \mathbb{Z}_2$ sub-symmetry, also all inequivalent choices of discrete torsion and some exotic O6-plane are taken into account in [46].

Any one-cycle on the two-torus $T_{(i)}^2$ can be expressed in terms of the coprime wrapping numbers (n_a^i, m_a^i) along the basic lattice vectors π_{2i-1} and π_{2i} . The angle of such an one-cycle w.r.t. the \mathcal{R} invariant axis is given by

$$\tan(\pi\phi_a^{(i)}) = \begin{cases} \frac{m_a^i + b_i n_a^i}{n_a^i} \frac{R_2^{(i)}}{R_1^{(i)}} & \mathbb{Z}_2(\mathbf{a}, \mathbf{b}) \\ \frac{m_a^i}{n_a^i} & \mathbb{Z}_4(\mathbf{A}) \\ \frac{m_a^i - n_a^i}{m_a^i + n_a^i} & \mathbb{Z}_4(\mathbf{B}) \\ \sqrt{3} \frac{m_a^i}{2n_a^i + m_a^i} & \mathbb{Z}_3(\mathbf{A}) \\ \frac{1}{\sqrt{3}} \frac{m_a^i - n_a^i}{m_a^i + n_a^i} & \mathbb{Z}_3(\mathbf{B}) \end{cases}, \quad (1)$$

and relative angles between $D6_a$ and $D6_b$ -branes as well as with the $\Omega\mathcal{R}\theta^n\omega^m$ invariant

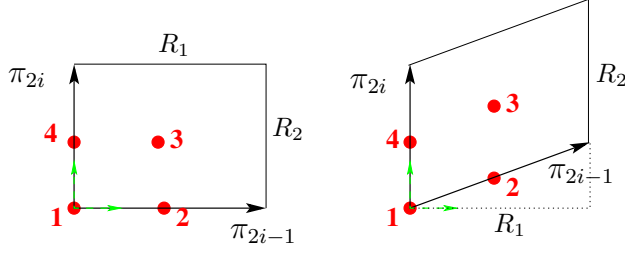


Figure 1: The \mathbb{Z}_2 invariant ‘untilted’ **a**-type (left) and ‘tilted’ **b**-type (right) tori, which are parameterised by $b = 0, \frac{1}{2}$, respectively. The \mathbb{Z}_2 fixed points are depicted in blue. The points 1, 4 are invariant under \mathcal{R} , whereas the other two points are on the tilted torus exchanged under \mathcal{R} , $2 \xrightarrow{\mathcal{R}} 2 + 2b$ and $3 \xrightarrow{\mathcal{R}} 3 - 2b$. The untilted torus with $R_1 = R_2 = r$ corresponds to the **A**-type \mathbb{Z}_4 invariant lattice in figure 2. The tilted torus for $R_2/R_1 = 2, 2\sqrt{3}, 2/\sqrt{3}$ corresponds to the **B**-type \mathbb{Z}_4 lattice and the **A**- and **B**-type \mathbb{Z}_3 (and \mathbb{Z}_6) invariant lattices in figure 2 with radii $r = \sqrt{2}R_2, R_2/\sqrt{3}, R_2$, respectively.

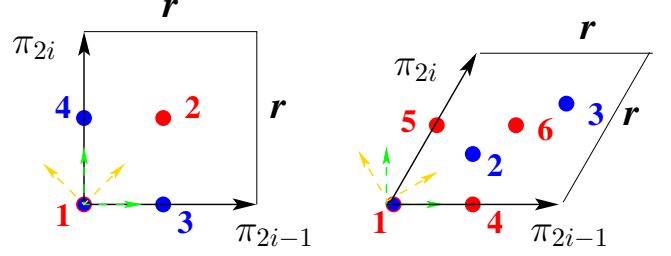


Figure 2: The \mathbb{Z}_4 (left) and \mathbb{Z}_3 (right) invariant lattices. For the **A** orientation (with green coordinate axes), π_{2i-1} spans the $\Re(z)$ axis, and on the **B** lattice (axes in yellow), the $\Re(z)$ axis extends along $\pi_{2i-1} + \pi_{2i}$. The \mathbb{Z}_4 invariant points 1, 2 (left, in red) are \mathcal{R} invariant, the additional \mathbb{Z}_2 fixed points $3 \xleftrightarrow{\mathbb{Z}_4} 4$ (left, in blue) are \mathcal{R} invariant on the **A**-lattice, but are permuted under \mathcal{R} on the **B**-lattice. The \mathbb{Z}_3 invariant points $2 \xleftrightarrow{\mathbb{Z}_3} 3$ (right, in blue) are exchanged under \mathcal{R} on the **A** orientation and are invariant on the **B**-lattice. The \mathbb{Z}_2 fixed points $6 \xrightarrow{\mathbb{Z}_3} 5 \xrightarrow{\mathbb{Z}_3} 4$ (right, in red) contain one point fixed under \mathcal{R} , the other two are exchanged under \mathcal{R} . The origin 1 is fixed under the full \mathcal{R} and \mathbb{Z}_6 symmetry.

O6-plane are given by

$$\phi_{ab}^{(i)} \equiv \phi_b^{(i)} - \phi_a^{(i)} \quad \text{and} \quad \phi_{a, \Omega \mathcal{R} \theta^n \omega^m}^{(i)} \equiv \phi_{\Omega \mathcal{R} \theta^n \omega^m}^{(i)} - \phi_a^{(i)},$$

where our notation is chosen to fit with the $T^6/\mathbb{Z}_2 \times \mathbb{Z}_{2M}$ orbifold backgrounds in [46]. For the O6-plane, we used the notation that the action of the orbifold generator produces a new one-cycle with the following torus wrapping numbers,

$$(n_a^i, m_a^i) \xrightarrow{\text{rotation by } 2\pi v_i} (n_{(\omega a)}^i, m_{(\omega a)}^i) = \begin{cases} (-n_a^i, -m_a^i) & w_i = \frac{1}{2} \\ (-m_a^i, n_a^i) & w_i = \frac{1}{4} \\ (-m_a^i, n_a^i + m_a^i) & w_i = \frac{1}{6} \end{cases}, \quad (2)$$

where the \mathbb{Z}_2 rotation applies to all allowed lattice orientations and the \mathbb{Z}_4 and \mathbb{Z}_6 rotation to those depicted in figure 2. All the orbifold rotations listed in table 1 can be obtained from these basic relations.

A \mathbb{Z}_3 symmetry with generator ω produces one orbifold invariant orbit consisting of three toroidal cycles at relative angles $\pm \frac{2\pi i}{3}$, and there exists one orbit of $\Omega \mathcal{R} \omega^n$ ($n = 0, 1, 2$)

invariant O6-planes. A \mathbb{Z}_4 symmetry provides orbifold invariant orbits of two toroidal cycles, and there exist two distinct orbits of O6-planes, $\Omega\mathcal{R}\omega^{2k}$ and $\Omega\mathcal{R}\omega^{2k+1}$ at angles $-(2k)\pi w_i$ and $-(2k+1)\pi w_i$ w.r.t. the $\Omega\mathcal{R}$ invariant plane, which we denote by $\Omega\mathcal{R}$ and $\Omega\mathcal{R}\mathbb{Z}_4$ invariant O6-plane orbits. A \mathbb{Z}_6 symmetry again contains the orbits of \mathbb{Z}_3 invariant cycles, but has two distinct orbits $\Omega\mathcal{R}\omega^{2k}$ and $\Omega\mathcal{R}\omega^{2k+1}$ of O6-planes at angles $-(2k)\pi w_i$ and $-(2k+1)\pi w_i$ w.r.t. the $\Omega\mathcal{R}$ invariant plane, which we denote by one of their representatives as the $\Omega\mathcal{R}$ and $\Omega\mathcal{R}\mathbb{Z}_2$ invariant orbits. For orbifolds with $\mathbb{Z}_2 \times \mathbb{Z}_2$ sub-symmetry, four different orbits of O6-planes $\Omega\mathcal{R}$ and $\Omega\mathcal{R}\mathbb{Z}_2^{(i)}$ with $i = 1, 2, 3$ arise as will be detailed further in section 2.1.2.

The one-cycle intersection number on the two-torus is antisymmetric in its subscripts and given by

$$I_{ab}^{(i)} \equiv n_a^i m_b^i - m_a^i n_b^i. \quad (3)$$

In section 2.2, we use the fact that (at least in the defining region $0 \leq |\phi_{ab}^{(i)}| < 1$) the signs of intersection numbers and relative angles are identical,

$$\text{sgn}(\phi_{ab}^{(i)}) = \text{sgn}(I_{ab}^{(i)}),$$

and that for supersymmetric D6-brane configurations, the maximal angle comes with the opposite sign of the other two leading to

$$\sum_{i=1}^3 \text{sgn}(\phi_{ab}^{(i)}) = - \prod_{i=1}^3 \text{sgn}(\phi_{ab}^{(i)}).$$

These relations permit to replace intersection numbers by their absolute values in the computation of gauge thresholds and beta function coefficients by means of the magnetic background field method as briefly reviewed below in section 2.2.

The complex structure moduli dependent quantity

$$V_{ab}^{(i)} \equiv \left\{ \begin{array}{cc} \frac{R_1^{(i)}}{R_2^{(i)}} n_a^i n_b^i + \frac{R_2^{(i)}}{R_1^{(i)}} (m_a^i + b_i n_a^i)(m_b^i + b_i n_b^i) & \mathbb{Z}_2(\mathbf{a}, \mathbf{b}) \\ n_a^i n_b^i + m_a^i m_b^i & \mathbb{Z}_4(\mathbf{A}, \mathbf{B}) \\ \frac{1}{\sqrt{3}}(2 n_a^i n_b^i + n_a^i m_b^i + m_a^i n_b^i + 2 m_a^i m_b^i) & \mathbb{Z}_3(\mathbf{A}, \mathbf{B}) \end{array} \right\} = \left\{ \begin{array}{cc} \frac{(L_a^{(i)})^2}{\text{Vol}(T_{(i)}^2)} & \phi_{ab}^{(i)} = 0 \\ I_{ab}^{(i)} \cot(\pi \phi_{ab}^{(i)}) & \phi_{ab}^{(i)} \neq 0 \end{array} \right. \quad (4)$$

is symmetric in its subscripts and for $a = b$ computes the square of the length $L_a^{(i)}$ (in units of the two-torus volume $\text{Vol}(T_{(i)}^2)$) of the one-cycle wrapped by the D6_a-brane along $T_{(i)}^2$. Note in particular the following correspondences between specific angles, intersection numbers and $(\text{length})^2$,

$$I_{ab}^{(i)} = 0 \quad \Leftrightarrow \quad \pi \phi_{ab}^{(i)} = 0, \quad V_{ab}^{(i)} = 0 \quad \Leftrightarrow \quad \pi \phi_{ab}^{(i)} = \pm \frac{\pi}{2},$$

which simplify the expressions for beta function coefficients and gauge thresholds. For later use, we define the dimensionless real Kähler modulus

$$v_i \equiv \frac{\text{Vol}(T_{(i)}^2)}{\alpha'} = \begin{cases} \frac{R_1^{(i)} R_2^{(i)}}{\alpha'} & \mathbb{Z}_2(\mathbf{a}, \mathbf{b}) \\ \frac{r_{(i)}^2}{\alpha'} & \mathbb{Z}_4(\mathbf{A}, \mathbf{B}) \\ \frac{\sqrt{3}}{2} \frac{r_{(i)}^2}{\alpha'} & \mathbb{Z}_3(\mathbf{A}, \mathbf{B}) \end{cases}$$

in slight abuse of the symbol v_i , which was used above also for entries of the shift vector generating the orbifold rotation θ . Since the meaning should be clear from the context throughout this article, we refrain from introducing a new symbol.

Last but not least, the intersection numbers and generalised volume forms involving some O6-plane are in all computations weighted with the number $N_{\Omega\mathcal{R}\theta^n\omega^m}^{(i)} = 2(1-b_i)$ of parallel O6-planes on the two-torus $T_{(i)}^2$,

$$\tilde{I}_a^{\Omega\mathcal{R}\theta^n\omega^m, (i)} \equiv 2(1-b_i) I_{a, \Omega\mathcal{R}\theta^n\omega^m}^{(i)}, \quad \tilde{V}_a^{\Omega\mathcal{R}\theta^n\omega^m, (i)} \equiv 2(1-b_i) V_{a, \Omega\mathcal{R}\theta^n\omega^m}^{(i)}. \quad (5)$$

For use in later sections, it is useful to explicitly compute the intersection numbers for D6-branes perpendicular to some O6-plane. In [40], we already made use of the fact that

$$\begin{aligned} a \perp \Omega\mathcal{R}\mathbb{Z}_2^{(l)} \text{ on } T_{(i)}^2 : \quad |\tilde{I}_a^{\Omega\mathcal{R}\mathbb{Z}_2^{(l)}, (i)}| &= 2, \\ a \perp \Omega\mathcal{R}\mathbb{Z}_2^{(l)} \text{ on } T_{(i)}^2 \times T_{(j)}^2 : \quad \tilde{I}_a^{\Omega\mathcal{R}\mathbb{Z}_2^{(l)}, (i,j)} &= -4, \end{aligned} \quad (6)$$

where the minus sign in the second line arises due to supersymmetry. In the same spirit, the (length)² for one-cycles parallel to some O6-plane are given by

$$a \uparrow\uparrow \Omega\mathcal{R}\mathbb{Z}_2^{(l)} \text{ on } T_{(i)}^2 : \quad \tilde{V}_a^{\Omega\mathcal{R}\mathbb{Z}_2^{(l)}, (i)} = \begin{cases} \frac{2}{1-b_i} \frac{R_1^{(i)}}{R_2^{(i)}} & \mathbb{Z}_2(\mathbf{a}, \mathbf{b}) & l = i \\ 2(1-b_i) \frac{R_2^{(i)}}{R_1^{(i)}} & \mathbb{Z}_2(\mathbf{a}, \mathbf{b}) & l \neq i \\ 2 & \mathbb{Z}_4(\mathbf{A}, \mathbf{B}) \\ \frac{2}{\sqrt{3}} & \mathbb{Z}_6(\mathbf{A}) & l = i; \quad \mathbb{Z}_6(\mathbf{B}) \quad l \neq i \\ 2\sqrt{3} & \mathbb{Z}_6(\mathbf{A}) & l \neq i; \quad \mathbb{Z}_6(\mathbf{B}) \quad l = i \end{cases},$$

since $N_{\Omega\mathcal{R}\mathbb{Z}_2^{(l)}}^{(i)} = 2(1-b_i)$ on the \mathbb{Z}_2 invariant two-torus, $N_{\Omega\mathcal{R}\mathbb{Z}_2^{(l)}}^{(i)} = 1$ on the $\mathbb{Z}_3(\mathbb{Z}_6)$ invariant two-torus, and $N_{\Omega\mathcal{R}\mathbb{Z}_2^{(l)}}^{(i)} = 2$ if the O6-plane lies in the orbit formed by $(n_{\Omega\mathcal{R}\mathbb{Z}_2^{(l)}}^i, m_{\Omega\mathcal{R}\mathbb{Z}_2^{(l)}}^i) = (1, 0), (0, 1)$ on the \mathbf{A} -type \mathbb{Z}_4 invariant lattice, but $N_{\Omega\mathcal{R}\mathbb{Z}_2^{(l)}}^{(i)} = 1$ if the orbit contains $(n_{\Omega\mathcal{R}\mathbb{Z}_2^{(l)}}^i, m_{\Omega\mathcal{R}\mathbb{Z}_2^{(l)}}^i) = (1, 1), (1, -1)$, and vice versa on the \mathbb{Z}_4 invariant \mathbf{B} -type lattice.

For the sake of brevity of the expressions pertaining to the lattice sums in the Möbius strip contributions to the gauge thresholds in section 2.2, we also introduce a weighted two-torus volume depending on the two-torus shape,

$$\tilde{v}_i \equiv \frac{v_i}{1 - b_i}. \quad (7)$$

The notation in this section fully agrees with the one in [40] and will be extended to bulk and exceptional three-cycles in the following section.

2.1.2 Three-cycles and RR tadpole cancellation

In this section, we briefly review the construction of fractional and rigid three-cycles, discuss their intersection numbers and implications for the normalisation of the beta function coefficients in terms of toroidal and exceptional intersection numbers in the computation of the gauge thresholds in section 2.2. We also comment on a rewritten version of the RR tadpole cancellation conditions, which serves as a cross-check and completion for the relative normalisation of the different contributions to the gauge thresholds. In the text, we focus on the technically most complicated case of $T^6/(\mathbb{Z}_2 \times \mathbb{Z}_{2M} \times \Omega\mathcal{R})$ with discrete torsion² and refer to tables 2, 3 and 4 for a comparison with compactifications on $T^6/\Omega\mathcal{R}$, $T^6/(\mathbb{Z}_2 \times \mathbb{Z}_{2M} \times \Omega\mathcal{R})$ without discrete torsion and $T^6/(\mathbb{Z}_N \times \Omega\mathcal{R})$, which have been studied to a greater extent in the literature before, see e.g. [52, 6, 41].

There exist two different basic building blocks to three-cycles on toroidal orbifolds: The first one consists of the omnipresent bulk three-cycles, which are the superposition of all orbifold images of a given factorisable torus three-cycle

$$\Pi_a^{\text{bulk}} = 4 \sum_{m=0}^{M-1} \Pi_{(\omega^m a)}^{\text{torus}} \quad \text{with} \quad \Pi_a^{\text{torus}} \equiv \bigotimes_{i=1}^3 (n_a^i \pi_{2i-1} + m_a^i \pi_{2i}), \quad (8)$$

where ω is the generator of \mathbb{Z}_{2M} and the factor 4 arises from the $\mathbb{Z}_2 \times \mathbb{Z}_2$ subgroup of $\mathbb{Z}_2 \times \mathbb{Z}_{2M}$.

²For presentations of intersecting D6-branes on $T^6/(\mathbb{Z}_N \times \mathbb{Z}_M \times \Omega\mathcal{R})$ orbifolds without discrete torsion see [47], for the first chiral models on $T^6/\mathbb{Z}_2 \times \mathbb{Z}_2$ and $T^6/\mathbb{Z}_2 \times \mathbb{Z}_4$ without torsion see [3, 4] and [5, 48], respectively, and for early discussions of $T^6/\mathbb{Z}_2 \times \mathbb{Z}_2$ with discrete torsion on factorisable tori see [49] and on non-factorisable tori [50, 51], which is completed and extended to all $T^6/\mathbb{Z}_2 \times \mathbb{Z}_{2M}$ orbifolds on factorisable tori with and without discrete torsion in [46].

In the presence of a $\mathbb{Z}_2^{(i)}$ sub-symmetry which leaves the two-torus $T_{(i)}^2$ invariant and for discrete torsion (and $2M \neq 4$) parameterised by $\eta = -1$, there exist exceptional three-cycles,

$$\Pi_a^{\mathbb{Z}_2^{(i)}} = 2 (-1)^{\tau_a^{\mathbb{Z}_2^{(i)}}} \sum_{m=0}^{M-1} \sum_{(\alpha\beta) \in T_{(j)}^2 \times T_{(k)}^2} c_{\alpha\beta}^{(i)} \left(e_{\omega^m(\alpha\beta)}^{(i)} \otimes \pi_{(\omega^m a)}^{(i)} \right), \quad (9)$$

where $\tau_a^{\mathbb{Z}_2^{(i)}} \in \{0, 1\}$ parameterises the $\mathbb{Z}_2^{(i)}$ eigenvalue, $c_{\alpha\beta}^{(i)} = \pm 1$ depends on the combination of displacements and Wilson lines $(\vec{\sigma}_a, \vec{\tau}_a)$ along $T_{(j)}^2 \times T_{(k)}^2$ with (i, j, k) cyclic permutations of $(1, 2, 3)$, and $(\alpha\beta)$ runs over four $\mathbb{Z}_2^{(i)}$ fixed points on $T_{(j)}^2 \times T_{(k)}^2$. For more details on the fixed points, exceptional two-cycles $e_{\omega^m(\alpha\beta)}^{(i)}$ and their sign prefactors $c_{\alpha\beta}^{(i)}$ the reader is referred to appendix A of [40]. The global factor of 2 stems from the sum over images under the second independent $\mathbb{Z}_2^{(j)}$ symmetry inside $\mathbb{Z}_2 \times \mathbb{Z}_{2M}$ in the presence of discrete torsion (i.e. $\eta = -1$).

Fractional three-cycles on $T^6/\mathbb{Z}_2 \times \mathbb{Z}_{2M}$ with discrete torsion ($\eta = -1$) are of the form

$$\Pi_a = \frac{1}{4} \left(\Pi_a^{\text{bulk}} + \sum_{i=1}^3 \Pi_a^{\mathbb{Z}_2^{(i)}} \right). \quad (10)$$

For $2M = 2$, these three-cycles are completely rigid, i.e. have no adjoint matter and are stuck at the $\mathbb{Z}_2 \times \mathbb{Z}_2$ fixed points on each two-torus. For $2M = 6, 6'$, the three-cycles are also stuck at the $\mathbb{Z}_2 \times \mathbb{Z}_2$ fixed points, but adjoint matter can arise at intersections of a given torus cycle a with its orbifold images $(\omega^m a)_{m=1,2}$. For a small number of combinations of wrapping numbers (n_a^i, m_a^i) and discrete displacements and Wilson lines $(\vec{\sigma}_a, \vec{\tau}_a)$, no such adjoint matter arises, see appendix B.2.1 of [46] for a complete classification. Since this detail is not relevant for the present discussion, we refer to D6-branes on three cycles of the form (10) as ‘rigid’.

The O6-planes on the same orbifold background are non-dynamical objects, which are also stuck at the $\mathbb{Z}_2 \times \mathbb{Z}_2$ fixed points, but only wrap a fraction of a bulk three-cycle,

$$\Pi_{O6} = \frac{1}{4} \Pi_{O6}^{\text{bulk}} = \sum_{n=0}^1 \sum_{m=0}^{2M-1} \eta_{\Omega\mathcal{R}\theta^n \omega^m} N_{\Omega\mathcal{R}\theta^n \omega^m} \Pi_{\Omega\mathcal{R}\theta^n \omega^m}^{\text{torus}},$$

where $\eta_{\Omega\mathcal{R}\theta^n \omega^m} = \pm 1$ denotes an ordinary or exotic O6-plane, and the assignment is subject to the consistency condition relating the choice of discrete torsion $\eta = \pm 1$ and the

assignment of exotic O6-planes (for a more detailed discussion see [49, 46]),

$$\eta = \eta_{\Omega\mathcal{R}} \prod_{i=1}^3 \eta_{\Omega\mathcal{R}\mathbb{Z}_2^{(i)}} \quad \text{and} \quad \eta_{\Omega\mathcal{R}\theta^n\omega^m} = \begin{cases} \eta_{\Omega\mathcal{R}} & (n, m) = (\text{even}, \text{even}) \\ \eta_{\Omega\mathcal{R}\mathbb{Z}_2^{(1)}} & (\text{even}, \text{odd}) \\ \eta_{\Omega\mathcal{R}\mathbb{Z}_2^{(2)}} & (\text{odd}, \text{odd}) \\ \eta_{\Omega\mathcal{R}\mathbb{Z}_2^{(3)}} & (\text{odd}, \text{even}) \end{cases}. \quad (11)$$

Note that (n, m) here denote the exponents of the orbifold generators θ and ω . This is distinguished from the one-cycle wrapping numbers (n_a^i, m_a^i) throughout the article by keeping track of the sub- and superscripts, and it will also be clear from the context.

For later convenience we also define the sign acting on the $\mathbb{Z}_2^{(i)}$ twisted cycles upon orientifolding,

$$\eta_{\mathbb{Z}_2^{(i)}} \equiv \eta_{\Omega\mathcal{R}} \cdot \eta_{\Omega\mathcal{R}\mathbb{Z}_2^{(i)}}. \quad (12)$$

The three-cycles wrapped by D6-branes and O6-planes are tabulated and compared to the six-torus for all factorisable T^6/\mathbb{Z}_N and $T^6/\mathbb{Z}_2 \times \mathbb{Z}_{2M}$ orbifolds without and with discrete torsion in table 2.

Comparison of the bulk, exceptional and fractional 3-cycles on $T^6, T^6/\mathbb{Z}_N$ and $T^6/\mathbb{Z}_2 \times \mathbb{Z}_{2M}$					
$T^6/$	Π_{D6_a}	Π_{O6}	$\Pi_{D6_a}^{\text{bulk}} =$	$\Pi_{D6_a}^{\mathbb{Z}_2^{(i)}} =$	$\Pi_{O6}^{\text{bulk}} =$
just T^6	Π_a^{torus}	Π_{O6}^{torus}	—	—	—
\mathbb{Z}_3	Π_a^{bulk}	Π_{O6}^{bulk}	$\sum_{n=0}^2 \Pi_{(\theta^n a)}^{\text{torus}}$	—	$\sum_{n=0}^2 N_{\Omega\mathcal{R}\theta^n} \Pi_{\Omega\mathcal{R}\theta^n}^{\text{torus}}$
\mathbb{Z}_{2N}	$\frac{1}{2} (\Pi_a^{\text{bulk}} + \Pi_a^{\mathbb{Z}_2})$	$\frac{1}{2} \Pi_{O6}^{\text{bulk}}$	$2 \sum_{n=0}^{N-1} \Pi_{(\theta^n a)}^{\text{torus}}$	$(-1)^{\tau_a^{(i)}} \sum_{n=0}^{N-1} \sum_{(\alpha\beta) \in T_{(j)}^2 \times T_{(k)}^2} c_{\alpha\beta}^{(2)} \left(e_{\theta^n(\alpha\beta)}^{(2)} \otimes \pi_{(\theta^n a)}^{(2)} \right)$	$2 \sum_{n=0}^{2N-1} N_{\Omega\mathcal{R}\theta^n} \Pi_{\Omega\mathcal{R}\theta^n}^{\text{torus}}$
$\mathbb{Z}_2 \times \mathbb{Z}_{2M}$ $\eta = 1$	$\frac{1}{2} \Pi_a^{\text{bulk}}$	$\frac{1}{4} \Pi_{O6}^{\text{bulk}}$	$4 \sum_{m=0}^{M-1} \Pi_{(\omega^m a)}^{\text{torus}}$	—	$4 \sum_{n=0}^1 \sum_{m=0}^{2M-1} N_{\Omega\mathcal{R}\theta^n\omega^m} \Pi_{\Omega\mathcal{R}\theta^n\omega^m}^{\text{torus}}$
$\mathbb{Z}_2 \times \mathbb{Z}_{2M}$ $\eta = -1$ for $2M \neq 4$	$\frac{1}{4} \left(\Pi_a^{\text{bulk}} + \sum_{i=1}^3 \Pi_a^{\mathbb{Z}_2^{(i)}} \right)$	$\frac{1}{4} \Pi_{O6}^{\text{bulk}}$	$4 \sum_{m=0}^{M-1} \Pi_{(\omega^m a)}^{\text{torus}}$	$2 (-1)^{\tau_a^{(i)}} \sum_{m=0}^{M-1} \sum_{(\alpha\beta) \in T_{(j)}^2 \times T_{(k)}^2} c_{\alpha\beta}^{(i)} \left(e_{\omega^m(\alpha\beta)}^{(i)} \otimes \pi_{(\omega^m a)}^{(i)} \right)$	$4 \sum_{n=0}^1 \sum_{m=0}^{2M-1} \eta_{\Omega\mathcal{R}\theta^n\omega^m} N_{\Omega\mathcal{R}\theta^n\omega^m} \Pi_{\Omega\mathcal{R}\theta^n\omega^m}^{\text{torus}}$

Table 2: The fractional multiplicities for three-cycles wrapped by D6-branes, Π_{D6_a} , and O6-planes, Π_{O6} , for all relevant toroidal orbifold backgrounds are compared in the first columns. The explicit expressions of the bulk and exceptional contributions to each fractional three-cycle are given in the last three columns. $\eta = 1$ denotes orbifolds without discrete torsion, and $\eta = -1$ corresponds to orbifolds with discrete torsion.

In this article, we exclude the case $T^6/\mathbb{Z}_2 \times \mathbb{Z}_4$ with discrete torsion in order to avoid a more cumbersome notation. This is due to the fact that for $\mathbb{Z}_2 \times \mathbb{Z}_4$, the discrete torsion

factor does not affect the \mathbb{Z}_2 twisted sectors, and therefore there are no exceptional three-cycles at \mathbb{Z}_2 fixed points independently of the choice of discrete torsion. The shape of the fractional three-cycles in table 2 on which D6-branes on $\mathbb{Z}_2 \times \mathbb{Z}_4$ wrap *independently of the choice of discrete torsion* is the one listed for $\eta = 1$, but the existence of an exotic O6-plane in the presence of discrete torsion leads to the shape of the orientifold invariant three-cycle wrapped by the O6-planes given for $\eta = -1$. More details on this particular orbifold background can be found in [46].

The relative prefactors of fractional three-cycles of D6-branes and O6-planes carry over to the normalisation of the tree-level gauge couplings, the beta function coefficients and threshold corrections in terms of intersection numbers and (length)². In this section, we focus on the intersection numbers and beta function coefficients. More details on the gauge threshold corrections are given in section 2.2, and the complete expressions for the Kähler metrics and gauge couplings at one loop are presented in section 3 for each of the bulk, fractional and rigid D6-branes introduced here.

The one-cycle intersection numbers in (3) are generalised to intersection numbers for the bulk and exceptional three-cycles in (8), (9), which read

$$\Pi_a^{\text{torus}} \circ \Pi_b^{\text{torus}} \equiv -I_{ab} = -\prod_{i=1}^3 I_{ab}^{(i)}, \quad e_{\alpha\beta}^{(i)} \circ e_{\gamma\delta}^{(j)} = -2 \delta^{ij} \delta_{\alpha\gamma} \delta_{\beta\delta}.$$

For $T^6/\mathbb{Z}_2 \times \mathbb{Z}_{2M}$ with discrete torsion, the combinatorial factor of $1/4M$ for intersection numbers of bulk three-cycles and $1/2M$ for the exceptional three-cycles together with a simplification of the double sum over orbifold images using relations, e.g. $I_{(\omega^k a)(\omega^l b)}^{(i)} = I_{(\omega^{k-l} a)_b}^{(i)}$, leads to the bulk and exceptional three-cycle intersection numbers in terms of a single sum over orbifold images,

$$\begin{aligned} \Pi_a^{\text{bulk}} \circ \Pi_b^{\text{bulk}} &= \frac{1}{4M} \left(4 \sum_{m=0}^{M-1} \Pi_{(\omega^m a)}^{\text{torus}} \right) \circ \left(4 \sum_{m'=0}^{M-1} \Pi_{(\omega^{m'} b)}^{\text{torus}} \right) = -4 \sum_{m=0}^{M-1} I_{(\omega^m a)_b}, \\ \Pi_a^{\mathbb{Z}_2^{(i)}} \circ \Pi_b^{\mathbb{Z}_2^{(i)}} &\equiv -4 \sum_{m=0}^{M-1} I_{(\omega^m a)_b}^{\mathbb{Z}_2^{(i)}} = -4 \sum_{m=0}^{M-1} I_{(\omega^m a)_b}^{(i)} I_{(\omega^m a)_b}^{\mathbb{Z}_2^{(i)},(j \cdot k)} \\ \text{with } I_{(\omega^m a)_b}^{\mathbb{Z}_2^{(i)},(j \cdot k)} &= (-1)^{\tau_a^{\mathbb{Z}_2^{(i)}} + \tau_b^{\mathbb{Z}_2^{(i)}}} \sum_{(\alpha_a \beta_a), (\gamma_b \delta_b) \in T_{(j)}^2 \times T_{(k)}^2} \left(c_{\alpha_a \beta_a}^{(i)} c_{\gamma_b \delta_b}^{(i)} \right) \delta_{(\omega^m \alpha_a) \gamma_b} \delta_{(\omega^m \beta_a) \delta_b}. \end{aligned}$$

In contrast to earlier works [41, 2, 40, 46], we perform the sum here on the first subscript. This is due to the fact that the contributions from intersections with O6-planes are most clearly arranged for the $T^6/\mathbb{Z}_2 \times \mathbb{Z}_2$ orbifold, and we can reduce our computations and notation to this particular background by treating $a \dots (\omega^{M-1} a)$ as separate D6-branes. In

other words, the $4M$ intersections of D6-brane a with all $\Omega\mathcal{R}\theta^n\omega^m$ invariant O6-planes are replaced by M sets of intersections of the branes $(\omega^m a)$ with the four orbits of O6-planes $\Omega\mathcal{R}$ and $\Omega\mathcal{R}\mathbb{Z}_2^{(i)}$ ($i = 1, 2, 3$).

For the weighted intersection numbers (5) with O6-planes, the assignments (11) of some exotic O6-plane need to be taken into account. For some given D6 _{a} -brane, all intersection numbers with different D6 _{b} -branes and the O6-planes are given on the r.h.s. of table 3 for each of the toroidal orbifolds considered in this article.

Chiral spectrum		3-cycle intersection numbers on various orbifolds		
		$T^6/$	$-\Pi_a \circ \Pi_b$	$-\Pi_a \circ \Pi_{O6}$
rep.	net chirality χ	just T^6	I_{ab}	$\tilde{I}_a^{\Omega\mathcal{R}}$
$(\mathbf{N}_a, \overline{\mathbf{N}}_b)$	$\Pi_a \circ \Pi_b$	\mathbb{Z}_3	$\sum_{n=0}^2 I_{(\theta^n a)b}$	$\sum_{n=0}^2 \tilde{I}_{(\theta^n a)}^{\Omega\mathcal{R}}$
$(\mathbf{N}_a, \mathbf{N}_b)$	$\Pi_a \circ \Pi_{b'}$	\mathbb{Z}_{2N}	$\sum_{n=0}^{N-1} \frac{I_{(\theta^n a)b} + I_{(\theta^n a)b}^{\mathbb{Z}_2}}{2}$	$\sum_{n=0}^{N-1} \frac{\tilde{I}_{(\theta^n a)}^{\Omega\mathcal{R}} + \tilde{I}_{(\theta^n a)}^{\Omega\mathcal{R}\mathbb{Z}_2}}{2}$
(\mathbf{Anti}_a)	$\frac{\Pi_a \circ \Pi_{a'} + \Pi_a \circ \Pi_{O6}}{2}$	$\mathbb{Z}_2 \times \mathbb{Z}_{2M}$ with $\eta = 1$	$\sum_{m=0}^{M-1} I_{(\omega^m a)b}$	$\sum_{m=0}^{M-1} \frac{\tilde{I}_{(\omega^m a)}^{\Omega\mathcal{R}} + \sum_{i=1}^3 \tilde{I}_{(\omega^m a)}^{\Omega\mathcal{R}\mathbb{Z}_2^{(i)}}}{2}$
(\mathbf{Sym}_a)	$\frac{\Pi_a \circ \Pi_{a'} - \Pi_a \circ \Pi_{O6}}{2}$	$\mathbb{Z}_2 \times \mathbb{Z}_{2M}$ with $\eta = -1$ for $2M \neq 4$	$\sum_{m=0}^{M-1} \frac{I_{(\omega^m a)b} + \sum_{i=1}^3 I_{(\omega^m a)b}^{\mathbb{Z}_2^{(i)}}}{4}$	$\sum_{m=0}^{M-1} \frac{\eta_{\Omega\mathcal{R}} \tilde{I}_{(\omega^m a)}^{\Omega\mathcal{R}} + \sum_{i=1}^3 \eta_{\Omega\mathcal{R}\mathbb{Z}_2^{(i)}} \tilde{I}_{(\omega^m a)}^{\Omega\mathcal{R}\mathbb{Z}_2^{(i)}}}{4}$

Table 3: Left: the multiplicities χ of chiral matter states at D6-brane intersections are given in terms of three-cycle intersection numbers. Right: explicit expression for (minus) the three-cycle intersection numbers of the bulk and fractional and rigid D6-branes in table 2. The beta function coefficients are computed from the total amount of (chiral plus non-chiral) matter at intersections of D6-branes. The total amount $\varphi^{ab} \supset |\chi^{ab}|$ of matter is given in terms of absolute values of individual contributions to the net-chiralities χ^{ab} .

The total amount of (chiral plus non-chiral) matter at the intersections of two different stacks of D6-branes is given by the sum over the absolute values of the contributions to the net-chirality from the various sectors $(\omega^m a)b$,

$$\varphi^{ab} \equiv \sum_{m=0}^{M-1} \tilde{\varphi}^{(\omega^m a)b} = \sum_{m=0}^{M-1} \left| \frac{I_{(\omega^m a)b} + \sum_{i=1}^3 I_{(\omega^m a)b}^{\mathbb{Z}_2^{(i)}}}{4} \right| \quad \text{for } T^6/\mathbb{Z}_2 \times \mathbb{Z}_{2M} \text{ with discrete torsion,} \quad (13)$$

and analogously for D6-branes at non-vanishing angles on all other orbifold backgrounds. At this point it is important to notice that $\tilde{\varphi}^{(\omega^m a)b}$ counts the number of matter multiplets

localised at intersections $(\omega^m a)b$. The correct assignment of the point, at which matter exists, is essential for the correct computation of the holomorphic worldsheet instanton contributions to the Yukawa couplings and other n -point functions [53]. Most notably, there might not exist any matter state at the corner of some triangle formed by three D6-branes at non-vanishing angles since $I_{(\omega^m a)b} + \sum_{i=1}^3 I_{(\omega^m a)b}^{\mathbb{Z}_2^{(i)}} = 0$ (this happened e.g. for the $(\theta^n a)b$ sectors of the Standard Model examples on T^6/\mathbb{Z}'_6 in [41, 2], for which $\tilde{\varphi}^{(\theta^n a)b} = 0$ for $n = 0, 1, 2$ despite intersections of the toroidal three-cycles, cf. table 29 below), and therefore the worldsheet instanton sum for D6-branes on the six-torus [54, 55] cannot be employed, but needs to be refined by taking into account the relative \mathbb{Z}_2 eigenvalues and discrete Wilson lines and displacements of the D6-branes under consideration.

The knowledge of the bifundamental and adjoint matter spectrum at non-trivial angles and the shape of the associated beta function coefficients for $SU(N_a)$ gauge groups,

$$\begin{aligned}
b_{SU(N_a)} &= \underbrace{N_a (-3 + \varphi^{\mathbf{Adj}_a})}_{b_{aa}^A} + \underbrace{\frac{N_a}{2} (\varphi^{\mathbf{Sym}_a} + \varphi^{\mathbf{Anti}_a})}_{b_{aa'}^A} + \underbrace{(\varphi^{\mathbf{Sym}_a} - \varphi^{\mathbf{Anti}_a})}_{b_{aa'}^{\mathcal{M}}} + \underbrace{\sum_{b \neq a} \frac{N_b}{2} (\varphi^{ab} + \varphi^{ab'})}_{\sum_{b \neq a} (b_{ab}^A + b_{ab'}^A)} \\
&\equiv b_{aa}^A + b_{aa'}^A + b_{aa'}^{\mathcal{M}} + \sum_{b \neq a} (b_{ab}^A + b_{ab'}^A),
\end{aligned} \tag{14}$$

is used in the computation of the gauge thresholds in order to determine the absolute normalisation of the annulus amplitudes, cf. section 2.2 below and the detailed discussion in [46]. In (14), we imply the sum over orbifold images in the first index in analogy to (13), e.g. $b_{ab}^A \equiv \sum_{m=0}^{M-1} \tilde{b}_{(\omega^m a)b}^A$ with $\tilde{b}_{(\omega^m a)b}^A$ the contribution to the beta function coefficient from matter localised at the intersections of the orbifold image D6-brane $(\omega^m a)$ with D6-brane b .

The absolute normalisation of the Möbius strip amplitudes for three non-trivial angles is obtained from the amount of antisymmetric and symmetric matter as read off by comparison with the net-chiralities in table 3,

$$\begin{aligned}
\varphi^{\mathbf{Anti}_a} + \varphi^{\mathbf{Sym}_a} &= \sum_{m=0}^{M-1} \left| \frac{I_{(\omega^m a)(\omega^m a)'} + \sum_{i=1}^3 I_{(\omega^m a)(\omega^m a)'}^{\mathbb{Z}_2^{(i)}}}{4} \right| \quad \text{for } T^6/\mathbb{Z}_2 \times \mathbb{Z}_{2M} \text{ with discrete torsion,} \\
\varphi^{\mathbf{Sym}_a} - \varphi^{\mathbf{Anti}_a} &= \sum_{m=0}^{M-1} \hat{c}_{(\omega^m a)}^{\Omega\mathcal{R}} \eta_{\Omega\mathcal{R}} \left| \frac{\tilde{I}_{(\omega^m a)}^{\Omega\mathcal{R}} + \sum_{i=1}^3 \eta_{\mathbb{Z}_2^{(i)}} \tilde{I}_{(\omega^m a)}^{\Omega\mathcal{R}\mathbb{Z}_2^{(i)}}}{4} \right|,
\end{aligned} \tag{15}$$

where $\hat{c}_{(\omega^m a)}^{\Omega\mathcal{R}} = -\text{sgn} \left(\frac{I_{(\omega^m a)(\omega^m a)'} + \sum_{i=1}^3 I_{(\omega^m a)(\omega^m a)'}^{\mathbb{Z}_2^{(i)}}}{\tilde{I}_{(\omega^m a)}^{\Omega\mathcal{R}} + \eta_{\mathbb{Z}_2^{(i)}} \sum_{i=1}^3 \tilde{I}_{(\omega^m a)}^{\Omega\mathcal{R}\mathbb{Z}_2^{(i)}}} \right)$ depends on the relative sign of the

intersection numbers from the annulus and Möbius strip contributions for a given D6-brane image $(\omega^m a)$, and the signs $\eta_{\mathbb{Z}_2^{(i)}}$ are defined in equation (12).

For some vanishing angle, the absolute values of the entries in table 3 do not provide the total amount of matter. The normalisation of the corresponding annulus and Möbius strip amplitudes is instead inferred from a rewritten version of the RR tadpole cancellation conditions displayed in table 4, where the overall normalisation is chosen such that the contributions from three non-trivial angles match with the result derived from the beta function coefficients. More details on the symmetric contraction \star of the three-cycles Π_a

Rewritten RR tadpole cancellation: gauge threshold contributions	
	$0 = \Pi_a \star [\sum_b N_b (\Pi_b + \Pi_{b'}) - 4 \Pi_{O6}]$
T^6	$0 = -\sum_b N_b \sum_{i=1}^3 \left(V_{ab}^{(i)} I_{ab}^{(j \cdot k)} + V_{ab'}^{(i)} I_{ab'}^{(j \cdot k)} \right) + 4 \sum_{i=1}^3 \tilde{V}_a^{\Omega \mathcal{R}, (i)} \tilde{I}_a^{\Omega \mathcal{R}, (j \cdot k)}$
T^6/\mathbb{Z}_3	$0 = \sum_{n=0}^2 \left\{ -\sum_b N_b \sum_{i=1}^3 \left(V_{(\theta^n a)b}^{(i)} I_{(\theta^n a)b}^{(j \cdot k)} + V_{(\theta^n a)b'}^{(i)} I_{(\theta^n a)b'}^{(j \cdot k)} \right) + 4 \sum_{i=1}^3 \tilde{V}_{(\theta^n a)}^{\Omega \mathcal{R}, (i)} \tilde{I}_{(\theta^n a)}^{\Omega \mathcal{R}, (j \cdot k)} \right\}$
T^6/\mathbb{Z}_{2N}	$0 = \sum_{n=0}^{N-1} \left\{ -\sum_b \frac{N_b}{2} \sum_{i=1}^3 \left(V_{(\theta^n a)b}^{(i)} I_{(\theta^n a)b}^{(j \cdot k)} + V_{(\theta^n a)b'}^{(i)} I_{(\theta^n a)b'}^{(j \cdot k)} \right) + 2 \sum_{l=0,2} \sum_{i=1}^3 \tilde{V}_{(\theta^n a)}^{\Omega \mathcal{R} \mathbb{Z}_2^{(l)}, (i)} \tilde{I}_{(\theta^n a)}^{\Omega \mathcal{R} \mathbb{Z}_2^{(l)}, (j \cdot k)} \right\}$ $0 = -\sum_{n=0}^{N-1} \sum_b \frac{N_b}{2} \left(V_{(\theta^n a)b}^{(2)} I_{(\theta^n a)b}^{\mathbb{Z}_2, (1 \cdot 3)} + V_{(\theta^n a)b'}^{(2)} I_{(\theta^n a)b'}^{\mathbb{Z}_2, (1 \cdot 3)} \right)$
$T^6/\mathbb{Z}_2 \times \mathbb{Z}_{2M}$ $\eta = 1$	$0 = \sum_{m=0}^{M-1} \left\{ -\sum_b N_b \sum_{i=1}^3 \left(V_{(\omega^m a)b}^{(i)} I_{(\omega^m a)b}^{(j \cdot k)} + V_{(\omega^m a)b'}^{(i)} I_{(\omega^m a)b'}^{(j \cdot k)} \right) + 2 \sum_{l=0}^3 \sum_{i=1}^3 \tilde{V}_{(\omega^m a)}^{\Omega \mathcal{R} \mathbb{Z}_2^{(l)}, (i)} \tilde{I}_{(\omega^m a)}^{\Omega \mathcal{R} \mathbb{Z}_2^{(l)}, (j \cdot k)} \right\}$
$T^6/\mathbb{Z}_2 \times \mathbb{Z}_{2M}$ $\eta = -1$ for $2M \neq 4$	$0 = \sum_{m=0}^{M-1} \left\{ -\sum_b \frac{N_b}{4} \sum_{i=1}^3 \left(V_{(\omega^m a)b}^{(i)} I_{(\omega^m a)b}^{(j \cdot k)} + V_{(\omega^m a)b'}^{(i)} I_{(\omega^m a)b'}^{(j \cdot k)} \right) + \sum_{l=0}^3 \sum_{i=1}^3 \eta_{\Omega \mathcal{R} \mathbb{Z}_2^{(l)}} \tilde{V}_{(\omega^m a)}^{\Omega \mathcal{R} \mathbb{Z}_2^{(l)}, (i)} \tilde{I}_{(\omega^m a)}^{\Omega \mathcal{R} \mathbb{Z}_2^{(l)}, (j \cdot k)} \right\}$ $0 = -\sum_{m=0}^{M-1} \sum_b \frac{N_b}{4} \sum_{i=1}^3 \left(V_{(\omega^m a)b}^{(i)} I_{(\omega^m a)b}^{\mathbb{Z}_2^{(i)}, (j \cdot k)} + V_{(\omega^m a)b'}^{(i)} I_{(\omega^m a)b'}^{\mathbb{Z}_2^{(i)}, (j \cdot k)} \right)$

Table 4: Rewritten form of the RR tadpole cancellation conditions by means of a symmetric contraction \star of the three-cycles Π_a . For T^6/\mathbb{Z}_{2N} and $T^6/\mathbb{Z}_2 \times \mathbb{Z}_{2M}$ with discrete torsion, the untwisted and twisted tadpoles are cancelled separately. These tadpoles are exactly those which cancel among the different gauge threshold amplitudes, cf. section 2.2.

can be found in appendix A.4 of [40]. Once the absolute normalisation of all amplitudes is determined by combining the known beta function coefficients with tadpole cancellation, the remaining beta function coefficients at some vanishing angle can be cross-checked with

the method of Chan-Paton labels, for a detailed account on T^6/\mathbb{Z}_{2N} backgrounds see appendix A.2 in [40] and on $T^6/\mathbb{Z}_2 \times \mathbb{Z}_{2M}$ with discrete torsion see appendix B.1 in [46].

The explicit expressions for the beta function coefficients allow for very compact expressions for the gauge thresholds due to massive strings, as we will see in the following section.

Since the perturbative formulas for the gauge couplings of $SO(2M_x)$ and $Sp(2M_x)$ gauge groups are very similar to the $SU(N_a)$ case, we briefly comment on the beta function coefficients for these (pseudo)real groups, while the more intricate discussion of anomaly-free $U(1)$ s is relegated to section 2.3. $SO(2M_x)$ and $Sp(2M_x)$ gauge groups are generated by D6_x-branes wrapping three-cycles of the form (10) on the $T^6/\mathbb{Z}_2 \times \mathbb{Z}_{2M}$ background with discrete torsion subject to the necessary condition that they are homologically their own orientifold image,

$$\Pi_x \stackrel{!}{=} \Pi'_x.$$

The sufficient condition requires that these three-cycles are parallel to some O6-plane orbit or perpendicular to it along some four-torus and parallel to it along the remaining two-torus. For the six-torus and T^6/\mathbb{Z}_N orbifolds, the distinction of these two cases has to be made, whereas for $T^6/\mathbb{Z}_2 \times \mathbb{Z}_{2M}$ each O6-plane is perpendicular to another O6-plane. For the latter, in [46] we gave a complete classification of all $\Omega\mathcal{R}$ -invariant three-cycles in dependence of the choice of exotic O6-plane (12) and the shape of untilted or tilted two-tori backgrounds ($b_i = 0$ and $\frac{1}{2}$, respectively). Since this classification is relevant for the examples in section 2.2.5 and in section 4.2, we repeat the result here in table 5. For a

Existence of $\Omega\mathcal{R}$ invariant 3-cycles on $T^6/\mathbb{Z}_2 \times \mathbb{Z}_{2M}$ with discrete torsion	
$\uparrow\uparrow$ to O6-plane	$(\eta_{\mathbb{Z}_2^{(1)}}, \eta_{\mathbb{Z}_2^{(2)}}, \eta_{\mathbb{Z}_2^{(3)}}) \stackrel{!}{=}$
$\Omega\mathcal{R}$	$\left(-(-1)^{2(b_2\sigma^2\tau^2+b_3\sigma^3\tau^3)}, -(-1)^{2(b_1\sigma^1\tau^1+b_3\sigma^3\tau^3)}, -(-1)^{2(b_1\sigma^1\tau_1+b_2\sigma^2\tau^2)} \right)$
$\Omega\mathcal{R}\mathbb{Z}_2^{(1)}$	$\left(-(-1)^{2(b_2\sigma^2\tau^2+b_3\sigma^3\tau^3)}, (-1)^{2(b_1\sigma^1\tau^1+b_3\sigma^3\tau^3)}, (-1)^{2(b_1\sigma^1\tau^1+b_2\sigma^2\tau^2)} \right)$
$\Omega\mathcal{R}\mathbb{Z}_2^{(2)}$	$\left((-1)^{2(b_2\sigma^2\tau^2+b_3\sigma^3\tau^3)}, -(-1)^{2(b_1\sigma^1\tau^1+b_3\sigma^3\tau^3)}, (-1)^{2(b_1\sigma^1\tau^1+b_2\sigma^2\tau^2)} \right)$
$\Omega\mathcal{R}\mathbb{Z}_2^{(3)}$	$\left((-1)^{2(b_2\sigma^2\tau^2+b_3\sigma^3\tau^3)}, (-1)^{2(b_1\sigma^1\tau^1+b_3\sigma^3\tau^3)}, -(-1)^{2(b_1\sigma^1\tau^1+b_2\sigma^2\tau^2)} \right)$

Table 5: Conditions on the existence of $\Omega\mathcal{R}$ invariant rigid three-cycles on $T^6/(\mathbb{Z}_2 \times \mathbb{Z}_{2M} \times \Omega\mathcal{R})$ with discrete torsion for $2M \in \{2, 6, 6'\}$. Their existence depends on the choice $(\eta_{\Omega\mathcal{R}\mathbb{Z}_2^{(i)}})_{i \in \{0 \dots 3\}}$ of some exotic O6-plane and the corresponding sign factors $(\eta_{\mathbb{Z}_2^{(i)}})$ defined in (12), the shape of the two-tori $b_i \in \{0, \frac{1}{2}\}$ as well as the discrete displacements σ^i and Wilson lines τ^i along $T_{(i)}^2$.

classification of $\Omega\mathcal{R}$ -invariant three-cycles on T^6/\mathbb{Z}'_6 see [41], some comments and examples for T^6/\mathbb{Z}_6 can be found in [6, 42], see also appendix A.3 of [40].

The inverse of (the square of) the tree level gauge coupling given below in equation (18) is reduced by the factor one-half, since the orientifold image brane x' does not give a separate contribution. The beta function coefficients for $SO(2M_x)$ and $Sp(2M_x)$ gauge groups read

$$\begin{aligned}
b_{SO/Sp(2M_x)} &= \underbrace{M_x (-3 + \varphi^{\mathbf{Sym}_x} + \varphi^{\mathbf{Anti}_x})}_{b_{xx}^A} + \underbrace{(\varphi^{\mathbf{Sym}_x} - \varphi^{\mathbf{Anti}_x} - 3\xi_x)}_{b_{xx}^{\mathcal{M}}} + \underbrace{\sum_{b \neq x} \frac{N_b}{2} \varphi^{xb}}_{\sum_b b_{xb}^A} \\
&\equiv b_{xx}^A + b_{xx}^{\mathcal{M}} + \sum_b b_{xb}^A \\
&\quad \text{with} \quad \xi_x = \begin{cases} -1 & \text{for } SO(2M_x) \\ 1 & \text{for } Sp(2M_x) \end{cases},
\end{aligned} \tag{16}$$

and by comparison of the sum over bifundamental representations with the analogue in $b_{SU(N_a)}$ in equation (14), one sees that one can automatise the computation by multiplying the beta function coefficient of a hypothetical $SU(M_x)$ gauge factor wrapping the same three-cycle by one-half, i.e. loosely speaking “ $b_{SO/Sp(2M_x)} = \frac{1}{2} b_{SU(M_x)}$ ”. The same relative factor appears in the expansion of the gauge thresholds [40] summarised in the following section.

2.2 $SU(N)$, $SO(2N)$ and $Sp(2N)$ gauge thresholds on fractional and rigid D6-branes

In this section, we briefly review the magnetic background field method in order to compute the gauge thresholds, and we comment on technical simplifications, which lead to compact expressions for each of the bulk, fractional and rigid D6-branes on the different toroidal orbifold backgrounds under consideration. For concreteness, the discussion in this section focusses on $T^6/(\mathbb{Z}_2 \times \mathbb{Z}_{2M} \times \Omega\mathcal{R})$ with discrete torsion, but all necessary ingredients to compute the other backgrounds are contained and the final results stated for every single orbifold background and D6-brane configuration.

The gauge coupling of an $SU(N_a)$ (or $SO(2N_a)$ or $Sp(2N_a)$) gauge factor at energy scale μ is up to one-loop in string perturbation theory given by

$$\frac{8\pi^2}{g_a^2(\mu)} = \frac{8\pi^2}{g_{a,\text{string}}^2} + \frac{b_a}{2} \ln \left(\frac{M_{\text{string}}^2}{\mu^2} \right) + \frac{\Delta_a}{2}, \tag{17}$$

where the tree-level value of (the square of) the gauge coupling is inversely proportional to the length of the three-cycle wrapped by the stack of D6_a-branes defined in equation (4),

$$\frac{4\pi}{g_{a,\text{string}}^2} = \frac{1}{2\sqrt{2}k_a c_a} \frac{M_{\text{Planck}}}{M_{\text{string}}} \prod_{i=1}^3 \sqrt{V_{aa}^{(i)}} \quad \text{with} \quad c_a = \begin{cases} 1 & \text{bulk} \\ 2 & \text{fract.} \\ 4 & \text{rigid} \end{cases} \quad \text{and} \quad k_a = \begin{cases} 1 & SU(N_a) \\ 2 & SO/Sp(2N_a) \end{cases}. \quad (18)$$

The remaining two contributions, the beta function coefficient b_a due to massless strings running in a loop and the gauge threshold Δ_a due to massive strings in the loop, are simultaneously obtained in a CFT computation,

$$b_a \ln \left(\frac{M_{\text{string}}^2}{\mu^2} \right) + \Delta_a = \sum_b \left[\mathcal{T}^A(D6_a, D6_b) + \mathcal{T}^A(D6_a, D6_{b'}) \right] + \mathcal{T}^M(D6_a, O6), \quad (19)$$

where \mathcal{T}^A and \mathcal{T}^M denote the gauge threshold amplitudes with annulus and Möbius strip topology, respectively, and the sum runs over all D6-branes $b = a$ and $b \neq a$ and their orientifold images b' in a given model.

For $T^6/\mathbb{Z}_2 \times \mathbb{Z}_{2M}$ with discrete torsion, the gauge threshold amplitudes consist of two types of sums, on the one hand the untwisted and $\mathbb{Z}_2^{(i)}$ twisted sector contributions in the annulus and cross-cap states of the $\Omega\mathcal{R}$ and $\Omega\mathcal{R}\mathbb{Z}_2^{(i)}$ invariant O6-plane orbits, and on the other hand a sum over orbifold images $(\omega^m a)$ under the \mathbb{Z}_{2M} generator (for $2M \neq 2$) for the D6-brane under consideration,

$$\mathcal{T}^A(D6_a, D6_b) = \sum_{m=0}^{M-1} \left(T_{(\omega^m a)b}^{\mathbf{1}} + \sum_{i=1}^3 T_{(\omega^m a)b}^{\mathbb{Z}_2^{(i)}} \right), \quad \mathcal{T}^M(D6_a, O6) = \sum_{m=0}^{M-1} \left(T_{(\omega^m a)}^{\Omega\mathcal{R}} + \sum_{i=1}^3 T_{(\omega^m a)}^{\Omega\mathcal{R}\mathbb{Z}_2^{(i)}} \right). \quad (20)$$

These amplitudes are obtained from the tree channel vacuum annulus and Möbius strip diagrams

$$\begin{aligned} \mathcal{A}(D6_a, D6_b) &\sim \sum_{\text{sectors}} \int_0^\infty dl \sum_{(\alpha, \beta)} (-1)^{2(\alpha+\beta)} \frac{\vartheta_{[\beta]}^{[\alpha]}(0, 2il)}{\eta^3(2il)} A_{\text{compact}}^{\text{sector}}(\alpha, \beta; \{\phi^{(i)}\}; 2il), \\ \mathcal{M}(D6_a, O6) &\sim \sum_{\text{sectors}} \int_0^\infty dl \sum_{(\alpha, \beta)} (-1)^{2(\alpha+\beta)} \frac{\vartheta_{[\beta]}^{[\alpha]}(0, 2il - \frac{1}{2})}{\eta^3(2il - \frac{1}{2})} M_{\text{compact}}^{\text{sector}}(\alpha, \beta; \{\phi^{(i)}\}; 2il - \frac{1}{2}), \end{aligned} \quad (21)$$

by gauging the non-compact oscillator contributions by a magnetic background field and expanding in a power series of the newly introduced magnetic field. $\alpha, \beta \in \{0, 1/2\}$ denote the different spin structures, and the sum over sectors for the annulus amplitude contains the untwisted ($\mathbf{1}$) and twisted ($\mathbb{Z}_2^{(i)}$ with $i \in \{1, 2, 3\}$) sectors as well as the sum over all

orbifold images of the first D6-brane $(\omega^m a)_{m=0\dots M-1}$. For the Möbius strip, instead of the twist sectors the sum is over the $\Omega\mathcal{R}$ and $\Omega\mathcal{R}\mathbb{Z}_2^{(i)}$ (with $i \in \{1, 2, 3\}$) invariant O6-planes, and again a sum over orbifold images $(\omega^m a)_{m=0\dots M-1}$ is performed. In [40], we had instead written the complete Möbius strip contribution as a sum over all $\Omega\mathcal{R}\theta^n\omega^m$ invariant O6-planes with $n \in \{0, 1\}$ and $m \in \{0 \dots 2M - 1\}$, and we had allocated four different invariances $\Omega\mathcal{R}\theta^p\omega^q$ with $p \in \{0, 1\}$ and $q \in \{-k, -k + M\}$ to a string stretched between D6-branes a and the orientifold image $(\omega^k a')$. These two ways of rewriting the sums give identical results, but the new convention in this article allows us to reduce the discussion to the $T^6/\mathbb{Z}_2 \times \mathbb{Z}_2$ background without and with discrete torsion, when all orbifold images $(\omega^m a)_{m=0\dots M-1}$ are treated as independent D6-branes. By this trick, the gauge threshold contributions to the Möbius strip for three non-vanishing angles can be explicitly rewritten in terms of annulus expressions for the ratios of Gamma functions plus constants and terms linear in the angles, cf. details in appendix A, and the gauge threshold contributions from antisymmetric and symmetric matter take the very simple forms in the last lines of table 9, 12, 10 and 7 for bulk, fractional and rigid D6-branes on T^6 , T^6/\mathbb{Z}_{2N} and $T^6/\mathbb{Z}_2 \times \mathbb{Z}_{2M}$ without and with discrete torsion, respectively.

The passage from the vacuum to the gauge threshold amplitudes boils down to replacing the Jacobi theta functions of the non-compact fermionic contributions in (21) by the second derivative w.r.t. the first argument (for details on the procedure see e.g. [43, 44, 40] and references therein) of the same Jacobi theta functions,

$$\begin{aligned} \mathcal{A}(D6_a, D6_b) &\longrightarrow \mathcal{T}^A(D6_a, D6_b), \\ \frac{\vartheta\left[\begin{smallmatrix} \alpha \\ \beta \end{smallmatrix}\right](0, 2il)}{\eta^3(2il)} &\longrightarrow \frac{\vartheta''\left[\begin{smallmatrix} \alpha \\ \beta \end{smallmatrix}\right](0, 2il)}{\eta^3(2il)}, \end{aligned} \quad (22)$$

while retaining the compact contributions $A_{\text{compact}}^{\text{sector}}(\alpha, \beta; \{\phi^{(i)}\}; 2il)$, and analogously for the amplitudes with Möbius strip topology by replacing the argument $2il \rightarrow 2il - \frac{1}{2}$.

For toroidal orbifold backgrounds, the compact contributions $A_{\text{compact}}^{\text{sector}}(\alpha, \beta; \{\phi^{(i)}\}; 2il)$ and $M_{\text{compact}}^{\text{sector}}(\alpha, \beta; \{\phi^{(i)}\}; 2il - \frac{1}{2})$ are known, see [40] for a complete list on T^6/\mathbb{Z}_{2N} and [43, 44] for results on the six-torus without displacement and Wilson line moduli and [45] for partial results on rigid intersecting D6-branes on $T^6/\mathbb{Z}_2 \times \mathbb{Z}_2$ with discrete torsion. They fall into three classes of supersymmetric angles, $\sum_{i=1}^3 \phi^{(i)} = 0$, with three non-vanishing, one vanishing or three vanishing angles, and into three categories of sectors, the untwisted and $\mathbb{Z}_2^{(i)}$ twisted annulus and the Möbius strips. After transformations of the integrands by means of resummations and Jacobi theta function identities, the gauge threshold amplitudes take the following form for $T^6/\mathbb{Z}_2 \times \mathbb{Z}_{2M}$ with discrete torsion (in the following (i, j, k) are cyclic permutations of $(1, 2, 3)$ whenever they appear simultaneously

in one term):³

1. annulus topology, untwisted sector:

$$\begin{aligned} T_{ab}^{\mathbf{I}}(\phi_{ab}^{(1)}, \phi_{ab}^{(2)}, \phi_{ab}^{(3)}) &= -\frac{N_b}{4} I_{ab} \int_0^\infty dl l^\varepsilon \sum_{i=1}^3 \frac{1}{\pi} \frac{\vartheta_1'}{\vartheta_1}(\phi_{ab}^{(i)}, 2il), \\ T_{ab}^{\mathbf{I}}(0^{(i)}, \phi_{ab}^{(j)}, \phi_{ab}^{(k)}) &= -\frac{N_b}{4} V_{ab}^{(i)} I_{ab}^{(j \cdot k)} \int_0^\infty dl l^\varepsilon \mathcal{L}_{ab}^{(i)}(v_i, V_{ab}^{(i)}; l), \\ T_{ab}^{\mathbf{I}}(0^{(i)}, 0^{(j)}, 0^{(k)}) &= 0. \end{aligned}$$

The first amplitude is $\mathcal{N} = 1$ supersymmetric and depends on the complex structure moduli through the angles (only for the \mathbb{Z}_2 invariant lattice in figure 1, cf. equation (1)), the second amplitude is $\mathcal{N} = 2$ supersymmetric and depends on the Kähler modulus v_i of the two-torus with vanishing relative angle, and the third one preserves $\mathcal{N} = 4$ supersymmetry and hence vanishes.

The dimensionally regularised integrals over the Jacobi theta functions $\vartheta'_\alpha/\vartheta_\alpha(\nu, 2il)$ and lattice contribution $\tilde{\mathcal{L}}^{(i)}(v_i, V^{(i)}; l)$ with parameter $\varepsilon \rightarrow 0$ are given explicitly below.

2. annulus topology, $\mathbb{Z}_2^{(i)}$ twisted sector:

$$\begin{aligned} T_{ab}^{\mathbb{Z}_2^{(i)}}(\phi_{ab}^{(1)}, \phi_{ab}^{(2)}, \phi_{ab}^{(3)}) &= -\frac{N_b}{4} I_{ab}^{\mathbb{Z}_2^{(i)}} \int_0^\infty dl l^\varepsilon \left(\frac{1}{\pi} \frac{\vartheta_1'}{\vartheta_1}(\phi_{ab}^{(i)}, 2il) + \frac{1}{\pi} \frac{\vartheta_4'}{\vartheta_4}(\phi_{ab}^{(j)}, 2il) + \frac{1}{\pi} \frac{\vartheta_4'}{\vartheta_4}(\phi_{ab}^{(k)}, 2il) \right), \\ T_{ab}^{\mathbb{Z}_2^{(i)}}(0^{(i)}, \phi_{ab}^{(j)}, \phi_{ab}^{(k)}) &= -\frac{N_b}{4} V_{ab}^{(i)} I_{ab}^{\mathbb{Z}_2^{(i)}, (j \cdot k)} \int_0^\infty dl l^\varepsilon \mathcal{L}_{ab}^{(i)}(v_i, V_{ab}^{(i)}; l), \\ T_{ab}^{\mathbb{Z}_2^{(i)}}(\phi_{ab}^{(i)}, 0^{(j)}, \phi_{ab}^{(k)}) &= -\frac{N_b}{4} I_{ab}^{\mathbb{Z}_2^{(i)}} \int_0^\infty dl l^\varepsilon \left(\frac{1}{\pi} \frac{\vartheta_1'}{\vartheta_1}(\phi_{ab}^{(i)}, 2il) + \frac{1}{\pi} \frac{\vartheta_4'}{\vartheta_4}(\phi_{ab}^{(k)}, 2il) \right), \\ T_{ab}^{\mathbb{Z}_2^{(i)}}(0^{(i)}, 0^{(j)}, 0^{(k)}) &= -\frac{N_b}{4} V_{ab}^{(i)} I_{ab}^{\mathbb{Z}_2^{(i)}, (j \cdot k)} \int_0^\infty dl l^\varepsilon \mathcal{L}_{ab}^{(i)}(v_i, V_{ab}^{(i)}; l). \end{aligned}$$

The first and third amplitude preserve $\mathcal{N} = 1$ supersymmetry and depend on the complex structure moduli via the angles (cf. comments above on the lattices). The second and fourth amplitude preserve $\mathcal{N} = 2$ supersymmetry and depend on the Kähler modulus v_i of the two-torus where $\mathbb{Z}_2^{(i)}$ acts trivially.

³The annulus and Möbius strip amplitudes for the six-torus and T^6/\mathbb{Z}_N and $T^6/\mathbb{Z}_2 \times \mathbb{Z}_{2M}$ orbifolds without discrete torsions differ in the absolute normalisation, which can be read off by using tables 4 and 3, which contain the contribution to the tadpole and $SU(N_a)$ chiral matter beta function coefficient, respectively. For the six-torus, T^6/\mathbb{Z}_3 and $T^6/\mathbb{Z}_2 \times \mathbb{Z}_{2M}$ without discrete torsion, there are no twisted annulus contributions. The gauge thresholds amplitudes for fractional D6-branes on T^6/\mathbb{Z}_{2N} are explicitly tabulated in the notation of this article in the appendix of [40].

3. Möbius strip topology (the $\Omega\mathcal{R} \equiv \Omega\mathcal{R}\mathbb{Z}_2^{(0)}$ invariant O6-plane is included in the notation by setting $l = 0$):

$$\begin{aligned}
T_a^{\Omega\mathcal{R}\mathbb{Z}_2^{(l)}}(\phi_{a,\Omega\mathcal{R}\mathbb{Z}_2^{(l)}}^{(1)}, \phi_{a,\Omega\mathcal{R}\mathbb{Z}_2^{(l)}}^{(2)}, \phi_{a,\Omega\mathcal{R}\mathbb{Z}_2^{(l)}}^{(3)}) &= \tilde{I}_a^{\Omega\mathcal{R}\mathbb{Z}_2^{(l)}} \int_0^\infty dl l^\varepsilon \sum_{i=1}^3 \frac{1}{\pi} \frac{\vartheta_1'}{\vartheta_1}(\phi_{a,\Omega\mathcal{R}\mathbb{Z}_2^{(l)}}^{(i)}, 2il - \frac{1}{2}), \\
T_a^{\Omega\mathcal{R}\mathbb{Z}_2^{(l)}}(0^{(i)}, \phi_{a,\Omega\mathcal{R}\mathbb{Z}_2^{(l)}}^{(j)}, \phi_{a,\Omega\mathcal{R}\mathbb{Z}_2^{(l)}}^{(k)}) &= \tilde{V}_a^{\Omega\mathcal{R}\mathbb{Z}_2^{(l)},(i)} \tilde{I}_a^{\Omega\mathcal{R}\mathbb{Z}_2^{(l)},(j,k)} \int_0^\infty dl l^\varepsilon \mathcal{L}_{a,\Omega\mathcal{R}\mathbb{Z}_2^{(l)}}^{(i)}(\tilde{v}_i, 2\tilde{V}_a^{\Omega\mathcal{R}\mathbb{Z}_2^{(l)},(i)}; l), \\
T_a^{\Omega\mathcal{R}\mathbb{Z}_2^{(l)}}(0^{(i)}, 0^{(j)}, 0^{(k)}) &= 0.
\end{aligned}$$

The first, second and third amplitude preserve $\mathcal{N} = 1, 2$ and 4 supersymmetry, respectively, and depend on the complex structure moduli via angles, the weighted Kähler modulus \tilde{v}_i or vanish.

The **annulus** amplitudes for non-vanishing angles can be further evaluated using the relations (for $0 < |\nu| < 1$, see e.g. [43–45, 40])

$$\begin{aligned}
\frac{1}{\pi} \int_0^\infty dl l^\varepsilon \frac{\vartheta_\alpha'}{\vartheta_\alpha}(\nu, 2il) &= \delta_{\alpha 1} \cot(\pi\nu) \int_0^\infty dl + \left(\frac{1}{\varepsilon} + \gamma - \ln 2 \right) \left(\frac{\text{sgn}(\nu)}{2} - \nu \right) \\
&\quad - \frac{1}{2} \ln \left(\frac{\Gamma(|\nu|)}{\Gamma(1-|\nu|)} \right)^{\text{sgn}(\nu)} + \delta_{\alpha 4} (\text{sgn}(\nu) - 2\nu) \ln(2) + \mathcal{O}(\varepsilon),
\end{aligned} \tag{23}$$

where the first term on the r.h.s. provides a contribution to the tadpoles in table 4 (remember that $I_{ab} \sum_{i=1}^3 \cot(\pi\phi_{ab}^{(i)}) = \sum_{i=1}^3 V_{ab}^{(i)} I_{ab}^{(j,k)}$), the second one furnishes the contribution to the beta function coefficients (using $I_{ab} \sum_{i=1}^3 \left(\frac{\text{sgn}(\phi_{ab}^{(i)})}{2} - \phi_{ab}^{(i)} \right) = -\frac{|I_{ab}|}{2}$, cf. the absolute values of the terms in table 3) when identifying

$$\ln \left(\frac{M_{\text{string}}}{\mu} \right)^2 \equiv \frac{1}{\varepsilon} + \gamma - \ln 2,$$

and the finite terms in the second line of (23) constitute the contributions to the gauge thresholds due to massive strings.

For $\mathcal{N} = 1$ supersymmetric sectors at three non-trivial angles, the gauge thresholds depend on the complex structure moduli of the two-tori via the relation (1) between the tangent of the angles and ratios of radii (more precisely, only a \mathbb{Z}_2 twist retains the complex structure modulus - a \mathbb{Z}_3 or \mathbb{Z}_4 symmetry extinguishes the modulus, cf. the sole dependence of the angles on torus wrapping numbers in (1)). It should be noted here that the identification of scales might contain a proportionality constant, which must be fixed in section 3 when matching the string and field theoretical one-loop formulas for the gauge couplings.

For one vanishing angle, the integration over the lattice sum for arbitrary displacement ($0 \leq \sigma_{ab}^{(i)} \leq 1$) and Wilson line ($0 \leq \tau_{ab}^{(i)} \leq 1$) moduli [40],

$$\begin{aligned} V_{ab}^{(i)} \int_0^\infty dl l^\varepsilon \mathcal{L}_{ab}^{(i)}(v_i, V_{ab}^{(i)}; l) = & V_{ab}^{(i)} \int_0^\infty dl + \left(\frac{1}{\varepsilon} + \gamma - \ln 2 \right) \delta_{\sigma_{ab}^{(i)}, 0} \delta_{\tau_{ab}^{(i)}, 0} \\ & - \delta_{\sigma_{ab}^{(i)}, 0} \delta_{\tau_{ab}^{(i)}, 0} \Lambda_{0,0}(v_i; V_{ab}^{(i)}) - \left(1 - \delta_{\sigma_{ab}^{(i)}, 0} \delta_{\tau_{ab}^{(i)}, 0} \right) \Lambda(\sigma_{ab}^{(i)}, \tau_{ab}^{(i)}, v_i) \\ & + \mathcal{O}(\varepsilon), \end{aligned} \quad (24)$$

is in the same way split into contributions to the tadpoles and beta function coefficients on the first line and gauge threshold contribution on the second line. This sector with one vanishing angle preserves $\mathcal{N} = 2$ supersymmetry and depends on the Kähler modulus v_i of the two-torus with vanishing angle between the D6-branes. The functions $\Lambda(v_i)$ of this Kähler modulus are slightly differently defined from [40]:

$$\begin{aligned} \Lambda_{0,0}(v; V) &\equiv \ln(2\pi v V \eta^4(iv)), \\ \Lambda(\sigma, \tau, v) &\equiv \ln \left| e^{-\pi\sigma^2 v/4} \frac{\vartheta_1\left(\frac{\tau - i\sigma v}{2}, iv\right)}{\eta(iv)} \right|^2, \end{aligned} \quad (25)$$

in order to make the matching of the beta function coefficients as prefactors for vanishing relative displacements $\vec{\sigma}_{ab}$ or Wilson lines $\vec{\tau}_{ab}$ more obvious. The consistency of the two lattice contributions for $(\sigma, \tau) \rightarrow (0, 0)$ can be checked using the product expansion of the Jacobi-Theta-functions,

$$\begin{aligned} \frac{\vartheta_1(\nu, \tau)}{\eta(\tau)} &= 2 \sin(\pi\nu) q^{\frac{1}{12}} \prod_{n=1}^{\infty} (1 - 2 \cos(2\pi\nu) q^n + q^{2n}) \\ &\xrightarrow{\nu \rightarrow 0} 2\pi\nu \eta^2(\tau) + \mathcal{O}(\nu^2), \end{aligned}$$

together with identifying the divergent factor as the discrete change in the beta function coefficient,

$$\ln \left| e^{-\pi\sigma^2 v/4} 2\pi \frac{\tau - i\sigma v}{2} \right|^2 \stackrel{(\sigma, \tau) \rightarrow (0, 0)}{\approx} - \ln \left(\frac{M_{\text{string}}}{\mu} \right)^2 + \ln(2\pi v V).$$

In section 3, the lattice contributions will be related to the one-loop corrections to the holomorphic gauge kinetic functions and to the Kähler metrics by using the decomposition

$$\begin{aligned} \Lambda_{0,0}(v; V) &= [2 \ln \eta(iv) + c.c.] + \ln(2\pi v V), \\ \Lambda(\sigma, \tau, v) &\equiv \left[\ln \left(e^{-\pi\sigma^2 v/4} \frac{\vartheta_1\left(\frac{\tau - i\sigma v}{2}, iv\right)}{\eta(iv)} \right) + c.c. \right]. \end{aligned} \quad (26)$$

For rigid D6-branes on $T^6/\mathbb{Z}_2 \times \mathbb{Z}_{2M}$ orbifolds with discrete torsion, the relative displacements and Wilson lines $(\sigma_{ab}^{(i)}, \tau_{ab}^{(i)})$ take only discrete values in $\{0, 1\}$, but for bulk D6-branes

on the six-torus or $T^6/\mathbb{Z}_2 \times \mathbb{Z}_{2M}$ without discrete torsion they are continuous open string moduli with values in $[0,1]$ on each two-torus, and for fractional D6-branes on T^6/\mathbb{Z}_{2N} there is one set of such open string moduli associated to the \mathbb{Z}_2 -invariant two-torus.

Using the integrals (23) and (24) of Jacobi-theta functions and Kaluza-Klein and winding sums, all gauge threshold amplitudes with annulus topology can be evaluated explicitly. The complete list of $SU(N_a)$ beta function coefficients from bifundamental and adjoint matter and the gauge threshold contributions from the same representations for all possible configurations of relative angles are given in table 6 for the $T^6/\mathbb{Z}_2 \times \mathbb{Z}_{2M}$ orbifolds with discrete torsion.

$b_{SU(N_a)}$ and gauge thresholds for bifundamental and adjoints: $T^6/\mathbb{Z}_2 \times \mathbb{Z}_{2M}$ with discrete torsion		
$(\phi_{ab}^{(1)}, \phi_{ab}^{(2)}, \phi_{ab}^{(3)})$	$b_{SU(N_a)}^{\text{torsion}} = \sum_b b_{ab}^A + \dots$ $= \sum_b \frac{N_b}{2} \varphi^{ab} + \dots$	$\Delta_{SU(N_a)}^{\text{torsion}} = \sum_b N_b \tilde{\Delta}_{ab}^{\text{torsion}} + \dots$
$(0, 0, 0)$	$-N_b \left(\prod_{n=1}^3 \delta_{\sigma_{ab}^n, 0} \delta_{\tau_{ab}^n, 0} \right) \sum_{i=1}^3 (-1)^{\tau_{ab}^{Z_2^{(i)}}}$	$-\sum_{i=1}^3 \left(-\frac{I_{ab}^{Z_2^{(i)}, (j,k)} N_b}{4} \delta_{\sigma_{ab}^i, 0} \delta_{\tau_{ab}^i, 0} \right) \Lambda_{0,0}(v_i; V_{ab}^{(i)})$ $+ \sum_{i=1}^3 \frac{I_{ab}^{Z_2^{(i)}, (j,k)} N_b}{4} \left(1 - \delta_{\sigma_{ab}^i, 0} \delta_{\tau_{ab}^i, 0} \right) \Lambda(\sigma_{ab}^i, \tau_{ab}^i, v_i)$
$(0, \phi, -\phi)$	$\frac{N_b}{4} \delta_{\sigma_{ab}^1, 0} \delta_{\tau_{ab}^1, 0} \left(I_{ab}^{(2,3)} - I_{ab}^{Z_2^{(1)}, (2,3)} \right)$	$-b_{ab}^A \Lambda_{0,0}(v_1; V_{ab}^{(1)})$ $+ \frac{\{I_{ab}^{(2,3)} + I_{ab}^{Z_2^{(1)}, (2,3)}\} N_b}{4} \left(1 - \delta_{\sigma_{ab}^1, 0} \delta_{\tau_{ab}^1, 0} \right) \Lambda(\sigma_{ab}^1, \tau_{ab}^1, v_1)$ $+ \frac{N_b}{4} \ln(2) \left[\left(I_{ab}^{Z_2^{(2)}} - I_{ab}^{Z_2^{(3)}} \right) (\text{sgn}(\phi) - 2\phi) \right]$
$(\phi^{(1)}, \phi^{(2)}, \phi^{(3)})$ $\sum_{n=1}^3 \phi^{(n)} = 0$	$\frac{N_b}{8} \left(I_{ab} + \text{sgn}(I_{ab}) \sum_{i=1}^3 I_{ab}^{Z_2^{(i)}} \right)$	$b_{ab}^A \text{sgn}(I_{ab}) \sum_{i=1}^3 \ln \left(\frac{\Gamma(\phi_{ab}^{(i)})}{\Gamma(1- \phi_{ab}^{(i)})} \right)^{\text{sgn}(\phi_{ab}^{(i)})}$ $+ \frac{N_b}{4} \ln(2) \left[\sum_{i=1}^3 I_{ab}^{Z_2^{(i)}} \left(\text{sgn}(\phi_{ab}^{(i)}) - 2\phi_{ab}^{(i)} + \text{sgn}(I_{ab}) \right) \right]$

Table 6: Contributions to the $SU(N_a)$ beta function coefficients (middle column) and gauge thresholds (last column) from bifundamental and adjoint matter for all possible supersymmetric configurations, i.e. parallel D6-branes and at one vanishing or three non-vanishing angles, on the $T^6/\mathbb{Z}_2 \times \mathbb{Z}_{2M}$ orbifolds with discrete torsion and $2M \in \{2, 6, 6'\}$. The complete beta function coefficient and gauge threshold are obtained by summing over all $(\omega^m a)b$ sectors, cf. equations (14) and (27). On the orbifolds with discrete torsion, there is no adjoint matter from the aa sector, and for $a \neq b$ at vanishing angles there only exists one non-chiral pair of bifundamental representations for vanishing relative displacements and Wilson lines. For more details on the existence of adjoint matter see section 2.2.4 and table 13. For later convenience of the notation, the beta function coefficient on parallel D6-branes can be decomposed into its contributions from various $\mathbb{Z}_2^{(i)}$ sectors, $b_{ab}^{A,(\vec{0})} \equiv \sum_{i=1}^3 b_{ab}^{A,(i)}$, cf. e.g. table 17.

The complete gauge thresholds $\Delta_{SU(N_a)}$ are obtained by summing over all sectors in the

same way as the beta function coefficients (14), i.e.

$$\Delta_{SU(N_a)} = \sum_b N_b \left(\tilde{\Delta}_{ab} + \tilde{\Delta}_{ab'} \right) + \Delta_{a,\Omega\mathcal{R}} \quad \text{with} \quad \tilde{\Delta}_{ab} = \tilde{\Delta}_{ba}$$

$$\text{and} \quad \tilde{\Delta}_{ab} = \sum_{m=0}^{M-1} \left(\tilde{\Delta}_{(\omega^m a)b}^{\mathbf{I}} + \sum_{i=1}^3 \tilde{\Delta}_{(\omega^m a)b}^{\mathbb{Z}_2^{(i)}} \right), \quad \Delta_{a,\Omega\mathcal{R}} = \sum_{m=0}^{M-1} \left(\Delta_{(\omega^m a)}^{\Omega\mathcal{R}} + \sum_{i=1}^3 \Delta_{(\omega^m a)}^{\Omega\mathcal{R}\mathbb{Z}_2^{(i)}} \right). \quad (27)$$

Analogously to the beta function coefficients for $SO(2M_x)$ or $Sp(2M_x)$ gauge groups in equation (16), the gauge threshold contributions from orthogonal and symplectic gauge groups are given by

$$\Delta_{SO/Sp(2M_x)} = \sum_b N_b \tilde{\Delta}_{xb} + \frac{1}{2} \Delta_{x,\Omega\mathcal{R}},$$

which can be viewed as one-half of the formula for a hypothetical $SU(M_x)$ gauge factor wrapped on the same three-cycle, i.e. “ $\Delta_{SO/Sp(2M_x)} = \frac{1}{2} \Delta_{SU(M_x)}$ ”, see [40] for details.

The $SU(N_a)$ beta function and gauge threshold contributions from bifundamental and adjoint matter on $T^6/\mathbb{Z}_2 \times \mathbb{Z}_{2M}$ with discrete torsion in table 6 can be directly compared to those on the six-torus or T^6/\mathbb{Z}_3 , $T^6/\mathbb{Z}_2 \times \mathbb{Z}_{2M}$ without discrete torsion and T^6/\mathbb{Z}_{2N} orbifolds in tables 8, 10 and 11 below. In section 3, we use these explicit formulas to derive the Kähler metrics, which are universal for all toroidal orbifolds and only depend on the number of non-vanishing angles, as well as the one-loop corrections to the holomorphic gauge kinetic function which also depends on the number of \mathbb{Z}_2 symmetries and the choice of displacement and Wilson line moduli.

For the **Möbius strip** amplitudes, the expansion of the Jacobi theta functions depends on the range of the angle ($0 < |\nu| < \frac{1}{2}$ or $\frac{1}{2} < |\nu| < 1$ with vanishing result for $|\nu| = \frac{1}{2}$, see e.g. [43, 45, 40] and details in appendix A),

$$\begin{aligned} \frac{1}{\pi} \int_0^\infty dl \ell^\varepsilon \frac{\vartheta_1'}{\vartheta_1}(\nu, 2il - \frac{1}{2}) &= \cot(\pi\nu) \int_0^\infty dl + \left(\frac{1}{\varepsilon} + \gamma - \ln 2 \right) \left(\frac{\text{sgn}(\nu) [1 + 2H(|2\nu| - 1)]}{4} - \nu \right) \\ &\quad - \frac{1}{4} \ln \left(\frac{\Gamma(|2\nu| - H(|2\nu| - 1))}{\Gamma(1 - |2\nu| + H(|2\nu| - 1))} \right)^{\text{sgn}(\nu)} + \left[\nu - \frac{\text{sgn}(\nu)}{2} \right] \ln(2) \\ &\quad + \mathcal{O}(\varepsilon), \end{aligned} \quad (28)$$

which is compactly written using the Heaviside step function

$$H(x) = \begin{cases} 1 & x > 0 \\ \frac{1}{2} & x = 0 \\ 0 & x < 0 \end{cases}. \quad (29)$$

The first line of (28) provides again the contribution to the tadpole (using $\tilde{I}_a^{\Omega\mathcal{R}\mathbb{Z}_2^{(l)}} \sum_{i=1}^3 \cot(\phi_{a,\Omega\mathcal{R}\mathbb{Z}_2^{(l)}}^{(i)}) = \sum_{i=1}^3 \tilde{V}_a^{\Omega\mathcal{R}\mathbb{Z}_2^{(l)},(i)} \tilde{I}_a^{\Omega\mathcal{R}\mathbb{Z}_2^{(l)},(j,k)}$) and beta function coefficient, where for later convenience we define the sign factor

$$c_a^{\Omega\mathcal{R}\mathbb{Z}_2^{(l)}} \equiv \left[2 H(|2\phi_{a,\Omega\mathcal{R}\mathbb{Z}_2^{(l)}}^{(k)}| - 1) - 1 \right] \in \{-1, 0, 1\} \quad \text{for } l = 0 \dots 3, \quad (30)$$

where again $\Omega\mathcal{R}\mathbb{Z}_2^{(0)} \equiv \Omega\mathcal{R}$, and the angle $\phi_{a,\Omega\mathcal{R}\mathbb{Z}_2^{(l)}}^{(k)}$ that appears in the definition of the sign $c_a^{\Omega\mathcal{R}\mathbb{Z}_2^{(l)}}$ is the one with maximal absolute value,

$$0 < |\phi_{a,\Omega\mathcal{R}\mathbb{Z}_2^{(l)}}^{(i)}|, |\phi_{a,\Omega\mathcal{R}\mathbb{Z}_2^{(l)}}^{(j)}| < |\phi_{a,\Omega\mathcal{R}\mathbb{Z}_2^{(l)}}^{(k)}| < 1 \quad \text{and} \quad 0 < |\phi_{a,\Omega\mathcal{R}\mathbb{Z}_2^{(l)}}^{(i)}|, |\phi_{a,\Omega\mathcal{R}\mathbb{Z}_2^{(l)}}^{(j)}| < \frac{1}{2},$$

where again (i, j, k) is a cyclic permutation of $(1, 2, 3)$. The contribution to the beta function coefficient from all Möbius amplitudes for a given orbifold invariant D6_a-brane orbit is thus

$$b_{SU(N_a)} \supset \sum_{m=0}^{M-1} \frac{c_{(\omega^m a)}^{\Omega\mathcal{R}} \eta_{\Omega\mathcal{R}} |\tilde{I}_{(\omega^m a)}^{\Omega\mathcal{R}}| + \sum_{i=1}^3 c_{(\omega^m a)}^{\Omega\mathcal{R}\mathbb{Z}_2^{(i)}} \eta_{\Omega\mathcal{R}\mathbb{Z}_2^{(i)}} |\tilde{I}_{(\omega^m a)}^{\Omega\mathcal{R}\mathbb{Z}_2^{(i)}}|}{4},$$

which is identical to the second line of (15), as can be checked on a case-by-case basis, cf. appendix A for details on the various signs $\text{sgn}(\tilde{I}_a^{\Omega\mathcal{R}\mathbb{Z}_2^{(l)}})$ and $c_a^{\Omega\mathcal{R}\mathbb{Z}_2^{(l)}}$ in dependence of the angles.

Finally, the second line on the r.h.s. of equation (28) constitutes the contribution to the gauge threshold. In appendix A, we show in detail that the contribution to the logarithms of Gamma functions from Möbius strips involving any of the four $\Omega\mathcal{R}\mathbb{Z}_2^{(l)}$ invariant O6-planes can be brought to exactly the same form as the annulus contribution from the same D6_a-brane,

$$\begin{aligned} & - \frac{\eta_{\Omega\mathcal{R}\mathbb{Z}_2^{(l)}} \tilde{I}_a^{\Omega\mathcal{R}\mathbb{Z}_2^{(l)}}}{4} \sum_{i=1}^3 \ln \left(\frac{\Gamma(|2\phi_{a,\Omega\mathcal{R}\mathbb{Z}_2^{(l)}}^{(i)}| - H(|2\phi_{a,\Omega\mathcal{R}\mathbb{Z}_2^{(l)}}^{(i)}| - 1))}{\Gamma(1 - |2\phi_{a,\Omega\mathcal{R}\mathbb{Z}_2^{(l)}}^{(i)}| + H(|2\phi_{a,\Omega\mathcal{R}\mathbb{Z}_2^{(l)}}^{(i)}| - 1))} \right)^{\text{sgn}(\phi_{a,\Omega\mathcal{R}\mathbb{Z}_2^{(l)}}^{(i)})} \\ & - \eta_{\Omega\mathcal{R}\mathbb{Z}_2^{(l)}} \tilde{I}_a^{\Omega\mathcal{R}\mathbb{Z}_2^{(l)}} \sum_{i=1}^3 \left[\frac{\text{sgn}(\phi_{a,\Omega\mathcal{R}\mathbb{Z}_2^{(l)}}^{(i)})}{2} - \phi_{a,\Omega\mathcal{R}\mathbb{Z}_2^{(l)}}^{(i)} \right] \ln(2) \\ & = \frac{c_a^{\Omega\mathcal{R}\mathbb{Z}_2^{(l)}} \eta_{\Omega\mathcal{R}\mathbb{Z}_2^{(l)}} |\tilde{I}_a^{\Omega\mathcal{R}\mathbb{Z}_2^{(l)}}|}{4} \text{sgn}(I_{aa'}) \sum_{i=1}^3 \ln \left(\frac{\Gamma(|\phi_{aa'}^{(i)}|)}{\Gamma(1 - |\phi_{aa'}^{(i)}|)} \right)^{\text{sgn}(\phi_{aa'}^{(i)})} + \frac{\eta_{\Omega\mathcal{R}\mathbb{Z}_2^{(l)}} |\tilde{I}_a^{\Omega\mathcal{R}\mathbb{Z}_2^{(l)}}|}{2} \ln(2), \end{aligned} \quad (31)$$

for every $l \in \{0 \dots 3\}$ with $c_a^{\Omega\mathcal{R}\mathbb{Z}_2^{(l)}}$ defined in equation (30). As a result, the annulus and Möbius strip amplitudes from orientifold invariant D6-brane configurations at non-trivial

angles can be summed up to give the simple expression in the last line of table 7 for rigid D6-branes on the $T^6/(\mathbb{Z}_2 \times \mathbb{Z}_{2M} \times \Omega\mathcal{R})$ orientifolds with discrete torsion in which the terms with Gamma functions have the beta function coefficients of the corresponding massless strings in the symmetric and antisymmetric representation as prefactors.

For one vanishing angle between the D6_a-brane and $\Omega\mathcal{R}\mathbb{Z}_2^{(l)}$ invariant O6-plane, the Kaluza-Klein and winding sum of the annulus amplitude in (24) changes by $(v_i, V_{aa'}^{(i)}) \rightarrow (\tilde{v}_i, 2\tilde{V}_a^{\Omega\mathcal{R}\mathbb{Z}_2^{(l)},(i)})$, where the weighted quantities \tilde{v}_i and $\tilde{V}_a^{\Omega\mathcal{R}\mathbb{Z}_2^{(l)},(i)}$ have been introduced in equation (7) and (5), respectively. This leads to the expansion of the Möbius strip contribution to the gauge threshold amplitude for one vanishing angle and arbitrary continuous displacements and Wilson lines (for more details see [40]),

$$\begin{aligned} 2\tilde{V}_a^{\Omega\mathcal{R}\mathbb{Z}_2^{(l)},(i)} \int_0^\infty dl l^\varepsilon \mathcal{L}_{a,\Omega\mathcal{R}\mathbb{Z}_2^{(l)}}^{(i)}(\tilde{v}_i, 2\tilde{V}_a^{\Omega\mathcal{R}\mathbb{Z}_2^{(l)},(i)}; l) = & 2\tilde{V}_a^{\Omega\mathcal{R}\mathbb{Z}_2^{(l)},(i)} \int_0^\infty dl + \left(\frac{1}{\varepsilon} + \gamma - \ln 2 \right) \delta_{\sigma_{aa'},0}^{(i)} \delta_{\tau_{aa'},0}^{(i)} \\ & - \delta_{\sigma_{aa'},0}^{(i)} \delta_{\tau_{aa'},0}^{(i)} \Lambda_{0,0}(\tilde{v}_i; 2\tilde{V}_a^{\Omega\mathcal{R}\mathbb{Z}_2^{(l)},(i)}) \\ & - \left(1 - \delta_{\sigma_{aa'},0}^{(i)} \delta_{\tau_{aa'},0}^{(i)} \right) \Lambda(\sigma_{aa'}^{(i)}, \tau_{aa'}^{(i)}, \tilde{v}_i) + \mathcal{O}(\varepsilon), \end{aligned}$$

where again the tadpole and beta function coefficient are given in the first line and the gauge threshold due to massive strings in the second and third line. For the $T^6/(\mathbb{Z}_2 \times \mathbb{Z}_{2M} \times \Omega\mathcal{R})$ orientifold with discrete torsion, only vanishing relative displacements and Wilson lines $(\sigma_{aa'}^{(i)}, \tau_{aa'}^{(i)}) = (0, 0)$ among orientifold image D6_a and D6_{a'}-branes occur. In this case, it is useful to expand

$$\Lambda_{0,0}(\tilde{v}; 2\tilde{V}) = \Lambda_{0,0}(v; V) + 2 \ln(2) + (4b) \ln \left(\frac{\eta(2iv)}{\vartheta_4(0, 2iv)} \right)$$

into an identical sum $\Lambda_{0,0}(v; V)$ as in the annulus amplitude plus a constant term $2 \ln(2)$ and v -dependent corrections in form of modular functions, which only appear for tilted tori and have to our knowledge only been taken into account in the T^6/\mathbb{Z}_{2N} context in [40] before. The annulus contributions from untwisted and $\mathbb{Z}_2^{(i)}$ twisted sectors aa' strings can now be combined with the Möbius strip contributions from D6_a-branes parallel to some $\Omega\mathcal{R}$ or $\Omega\mathcal{R}\mathbb{Z}_2^{(i)}$ invariant O6-planes, see the first four lines in table 7.

Tables 6 and 7 contain the complete gauge threshold result for all D6-brane configurations (i.e. any intersecting angle, displacement, Wilson line and \mathbb{Z}_2 eigenvalue) on the $T^6/(\mathbb{Z}_2 \times \mathbb{Z}_{2M} \times \Omega\mathcal{R})$ background with discrete torsion. Furthermore, since this background is the technically most challenging one, the complete results for D6-branes on the six-torus or T^6/\mathbb{Z}_3 , the $T^6/\mathbb{Z}_2 \times \mathbb{Z}_{2M}$ orientifold without torsion and T^6/\mathbb{Z}_{2N} can be deduced using the different numerical prefactors on the r.h.s. of table 3 and in table 4. These results are presented in the following sections 2.2.1 to 2.2.3. Together with the discussion of orthogonal

$b_{SU(N_a)}$ and gauge thresholds for (anti)symmetrics: $T^6/\mathbb{Z}_2 \times \mathbb{Z}_{2M}$ with discrete torsion		
$(\phi_{aa'}^{(1)}, \phi_{aa'}^{(2)}, \phi_{aa'}^{(3)})$	$b_{SU(N_a)}^{\text{torsion}} = b_{aa'}^A + b_{aa'}^M + \dots$ $\frac{N_a}{2} (\varphi^{\text{Sym}_a} + \varphi^{\text{Anti}_a}) + (\varphi^{\text{Sym}_a} - \varphi^{\text{Anti}_a}) + \dots$	$\Delta_{SU(N_a)}^{\text{torsion}} = N_a \tilde{\Delta}_{aa'}^{\text{torsion}} + \Delta_{a, \Omega\mathcal{R}}^{\text{torsion}} + \dots$
$(0, 0, 0)$ $\uparrow\uparrow \Omega\mathcal{R}$	$-\frac{N_a}{4} \sum_{i=1}^3 I_{aa'}^{Z_2^{(i)}, (j-k)}$ $-\frac{1}{2} \sum_{i=1}^3 \eta_{\Omega\mathcal{R}Z_2^{(i)}} \tilde{I}_a^{\Omega\mathcal{R}Z_2^{(i)}, (j-k)} $	$-\left(-\frac{N_a}{4} \sum_{i=1}^3 I_{aa'}^{Z_2^{(i)}, (j-k)}\right) \Lambda_{0,0}(v_i, V_{aa'}^{(i)})$ $+\frac{1}{2} \sum_{i=1}^3 \eta_{\Omega\mathcal{R}Z_2^{(i)}} \tilde{I}_a^{\Omega\mathcal{R}Z_2^{(i)}, (j-k)} \Lambda_{0,0}(\tilde{v}_i, 2\tilde{V}_{aa'}^{(i)})$
$(0, 0, 0)$ $\uparrow\uparrow \Omega\mathcal{R}Z_2^{(i)}$	$-\frac{N_a}{4} \sum_{l=1}^3 I_{aa'}^{Z_2^{(l)}, (m-n)}$ $-\frac{1}{2} \left(\eta_{\Omega\mathcal{R}} \tilde{I}_a^{\Omega\mathcal{R}, (j-k)} + \sum_{j \neq i} \eta_{\Omega\mathcal{R}Z_2^{(j)}} \tilde{I}_a^{\Omega\mathcal{R}Z_2^{(j)}, (i-j)} \right)$	$-\left(-\frac{N_a}{4} \sum_{l=1}^3 I_{aa'}^{Z_2^{(l)}, (m-n)}\right) \Lambda_{0,0}(v_l, V_{aa'}^{(l)})$ $+\frac{1}{2} \eta_{\Omega\mathcal{R}} \tilde{I}_a^{\Omega\mathcal{R}, (j-k)} \Lambda_{0,0}(\tilde{v}_i, 2\tilde{V}_{aa'}^{(i)})$ $+\frac{1}{2} \sum_{j \neq i} \eta_{\Omega\mathcal{R}Z_2^{(j)}} \tilde{I}_a^{\Omega\mathcal{R}Z_2^{(j)}, (i-j)} \Lambda_{0,0}(\tilde{v}_k, 2\tilde{V}_{aa'}^{(k)})$
$(0^{(i)}, \phi^{(j)}, \phi^{(k)})$ $\uparrow\uparrow (\Omega\mathcal{R} + \Omega\mathcal{R}Z_2^{(i)})$	$\frac{N_a}{4} \left(I_{aa'}^{(j-k)} - I_{aa'}^{Z_2^{(i)}, (j-k)} \right)$ $-\frac{1}{2} \left(\eta_{\Omega\mathcal{R}} \tilde{I}_a^{\Omega\mathcal{R}, (j-k)} + \eta_{\Omega\mathcal{R}Z_2^{(i)}} \tilde{I}_a^{\Omega\mathcal{R}Z_2^{(i)}, (j-k)} \right)$	$-(b_{aa'}^A + b_{aa'}^M) \Lambda_{0,0}(v_i; V_{aa'}^{(i)}) - (4b_i) b_{aa'}^M \ln \left(\frac{\eta(2iv_i)}{\vartheta_4(0, 2iv_i)} \right)$ $+ \left[\frac{N_b \left(I_{aa'}^{Z_2^{(j)}} - I_{aa'}^{Z_2^{(k)}} \right) (\text{sgn}(\phi_{aa'}^{(j)}) - 2\phi_{aa'}^{(j)})}{4} + \frac{\eta_{\Omega\mathcal{R}Z_2^{(j)}} \tilde{I}_a^{\Omega\mathcal{R}Z_2^{(j)}, (j-k)} + \eta_{\Omega\mathcal{R}Z_2^{(k)}} \tilde{I}_a^{\Omega\mathcal{R}Z_2^{(k)}, (j-k)} }{2} \right] \ln(2)$ $+ \eta_{\Omega\mathcal{R}} \tilde{I}_a^{\Omega\mathcal{R}, (j-k)} + \eta_{\Omega\mathcal{R}Z_2^{(i)}} \tilde{I}_a^{\Omega\mathcal{R}Z_2^{(i)}, (j-k)} $
$(0^{(i)}, \phi^{(j)}, \phi^{(k)})$ $\uparrow\uparrow (\Omega\mathcal{R}Z_2^{(j)} + \Omega\mathcal{R}Z_2^{(k)})$	$\frac{N_a}{4} \left(I_{aa'}^{(j-k)} - I_{aa'}^{Z_2^{(i)}, (j-k)} \right)$ $-\frac{1}{2} \left(\eta_{\Omega\mathcal{R}Z_2^{(j)}} \tilde{I}_a^{\Omega\mathcal{R}Z_2^{(j)}, (j-k)} + \eta_{\Omega\mathcal{R}Z_2^{(k)}} \tilde{I}_a^{\Omega\mathcal{R}Z_2^{(k)}, (j-k)} \right)$	$-(b_{aa'}^A + b_{aa'}^M) \Lambda_{0,0}(v_i; V_{aa'}^{(i)}) - (4b_i) b_{aa'}^M \ln \left(\frac{\eta(2iv_i)}{\vartheta_4(0, 2iv_i)} \right)$ $+ \left[\frac{N_a \left(I_{aa'}^{Z_2^{(j)}} - I_{aa'}^{Z_2^{(k)}} \right) (\text{sgn}(\phi_{aa'}^{(j)}) - 2\phi_{aa'}^{(j)})}{4} + \frac{\eta_{\Omega\mathcal{R}} \tilde{I}_a^{\Omega\mathcal{R}, (j-k)} + \eta_{\Omega\mathcal{R}Z_2^{(i)}} \tilde{I}_a^{\Omega\mathcal{R}Z_2^{(i)}, (j-k)} }{2} \right] \ln(2)$ $+ \eta_{\Omega\mathcal{R}Z_2^{(j)}} \tilde{I}_a^{\Omega\mathcal{R}Z_2^{(j)}, (j-k)} + \eta_{\Omega\mathcal{R}Z_2^{(k)}} \tilde{I}_a^{\Omega\mathcal{R}Z_2^{(k)}, (j-k)} $
$(\phi^{(1)}, \phi^{(2)}, \phi^{(3)})$ $\sum_{n=1}^3 \phi^{(n)} = 0$	$\frac{N_a}{8} \left(I_{aa'} + \text{sgn}(I_{aa'}) \sum_{i=1}^3 I_{aa'}^{Z_2^{(i)}} \right)$ $+\frac{1}{4} \left(c_a^{\Omega\mathcal{R}} \eta_{\Omega\mathcal{R}} \tilde{I}_a^{\Omega\mathcal{R}} + \sum_{i=1}^3 c_a^{\Omega\mathcal{R}Z_2^{(i)}} \eta_{\Omega\mathcal{R}Z_2^{(i)}} \tilde{I}_a^{\Omega\mathcal{R}Z_2^{(i)}} \right)$	$(b_{aa'}^A + b_{aa'}^M) \text{sgn}(I_{aa'}) \sum_{i=1}^3 \ln \left(\frac{\Gamma(\phi_{aa'}^{(i)})}{\Gamma(1- \phi_{aa'}^{(i)})} \right)^{\text{sgn}(\phi_{aa'}^{(i)})}$ $+ \left[\frac{N_a \sum_{i=1}^3 I_{aa'}^{Z_2^{(i)}} (\text{sgn}(\phi_{aa'}^{(i)}) - 2\phi_{aa'}^{(i)} + \text{sgn}(I_{aa'}))}{4} + \sum_{m=0}^3 \frac{\eta_{\Omega\mathcal{R}Z_2^{(m)}} \tilde{I}_a^{\Omega\mathcal{R}Z_2^{(m)}} }{2} \right] \ln(2)$

Table 7: Contributions to $SU(N_a)$ beta function coefficients (middle column) and gauge thresholds (last column) from antisymmetric and symmetric matter on orientifold image D6_a-branes in $T^6/(\mathbb{Z}_2 \times \mathbb{Z}_{2M} \times \Omega\mathcal{R})$ backgrounds with discrete torsion. The special case of vanishing angles and identical three-cycles wrapped by orientifold image D6_{a'}-branes, $\Pi_a = \Pi_{a'}$, leads to orthogonal or symplectic gauge groups and is discussed separately in section 2.2.5, see in particular table 15.

and symplectic gauge factors on each orbifold background in section 2.2.5 and the Abelian gauge groups in section 2.3, this constitutes the most exhaustive possible treatment of all allowed gauge groups on D6-branes and possible factorisable toroidal orbifolds of the type IIA string, which to our knowledge has not been dealt with before.

Building on the complete classification of gauge threshold amplitudes on all factorisable toroidal orbifold backgrounds in this section, the decomposition into the holomorphic gauge kinetic function, Kähler metrics for open string matter fields and the Kähler potential for closed string moduli will be derived in full generality in section 3.

2.2.1 Bulk D6-branes on $T^6/\Omega\mathcal{R}$ and $T^6/(\mathbb{Z}_3 \times \Omega\mathcal{R})$

The gauge thresholds on the six-torus have been computed in [43, 44] for vanishing displacement and Wilson line moduli. We repeat here the results for three non-vanishing angles for completeness. The formulas for one parallel direction with arbitrary continuous Wilson line or displacement in the annulus and Möbius strip contribution have to our

knowledge not been presented before, and also the explicit discussion of orthogonal and symplectic gauge factors in section 2.2.5 and Abelian groups in section 2.3 is presented in this article for the first time.

On the six-torus, open strings on identical D6-branes preserve $\mathcal{N} = 4$ supersymmetry and do not contribute to the gauge thresholds. D6-branes at one vanishing angle on $T^2_{(i)}$ preserve $\mathcal{N} = 2$ supersymmetry and contribute to the Kaluza-Klein and winding sums in (24) which depend on the Kähler modulus v_i , and D6-branes at three angles preserve $\mathcal{N} = 1$ supersymmetry and depend on the complex structure moduli through the angles in (23). There exists only the untwisted annulus amplitude for D6-branes which are not their own orientifold image. The result for all bifundamental and adjoint representations is displayed in table 8. On the T^6/\mathbb{Z}_3 background, the D6-branes also wrap bulk three-cycles,

$b_{SU(N_a)}$ and gauge thresholds for bifundamental and adjoints: T^6 and T^6/\mathbb{Z}_3		
$(\phi_{ab}^{(1)}, \phi_{ab}^{(2)}, \phi_{ab}^{(3)})$	$b_{SU(N_a)}^{\text{torus}} = \sum_b b_{ab}^A + \dots$ $= \sum_b \frac{N_b}{2} \varphi^{ab} + \dots$	$\Delta_{SU(N_a)}^{\text{torus}} = \sum_b N_b \tilde{\Delta}_{ab}^{\text{torus}} + \dots$
$(0, 0, 0)$	—	—
$(0, \phi, -\phi)$	$N_b \delta_{\sigma_{ab}^1, 0} \delta_{\tau_{ab}^1, 0} I_{ab}^{(2,3)} $	$-b_{ab}^A \Lambda_{0,0}(v_1; V_1)$ $-N_b I_{ab}^{(2,3)} \left(1 - \delta_{\sigma_{ab}^1, 0} \delta_{\tau_{ab}^1, 0}\right) \Lambda(\sigma_{ab}^1, \tau_{ab}^1, v_1)$
$(\phi^{(1)}, \phi^{(2)}, \phi^{(3)})$ $\sum_{n=1}^3 \phi^{(n)} = 0$	$\frac{N_b}{2} I_{ab} $	$b_{ab}^A \text{sgn}(I_{ab}) \sum_{i=1}^3 \ln \left(\frac{\Gamma(\phi_{ab}^{(i)})}{\Gamma(1- \phi_{ab}^{(i)})} \right)^{\text{sgn}(\phi_{ab}^{(i)})}$

Table 8: Contributions to the $SU(N_a)$ beta function coefficients and gauge thresholds from open strings in the bifundamental and adjoint representation on the six-torus and the T^6/\mathbb{Z}_3 orbifold with arbitrary continuous displacement and Wilson line moduli $(\sigma_{ab}^i, \tau_{ab}^i)$. Details on adjoint matter contributions are further discussed in section 2.2.4 and table 13.

but when using table 8, the sum over orbifold images in the first index has to be performed,

$$\begin{aligned}
b_{SU(N_a)}^{T^6/\mathbb{Z}_3} &= \sum_{k=0}^2 \left[\sum_b \left(\tilde{b}_{(\theta^k a)b}^{\mathcal{A}} + \tilde{b}_{(\theta^k a)b'}^{\mathcal{A}} \right) + \tilde{b}_{(\theta^k a)(\theta^k a)'}^{\mathcal{M}} \right] \\
&= \sum_{k=0}^2 \left[\sum_{b \neq a} \frac{N_b}{2} \left(\tilde{\varphi}^{(\theta^k a)b} + \tilde{\varphi}^{(\theta^k a)b'} \right) \right] + N_a \sum_{k=1}^2 \tilde{\varphi}^{\mathbf{Adj}_{(\theta^k a)}} \\
&\quad + \sum_{k=0}^2 \left[\frac{N_a}{2} \left(\tilde{\varphi}^{\mathbf{Sym}_{(\theta^k a)}} + \tilde{\varphi}^{\mathbf{Anti}_{(\theta^k a)}} \right) + \left(\tilde{\varphi}^{\mathbf{Sym}_{(\theta^k a)}} - \tilde{\varphi}^{\mathbf{Anti}_{(\theta^k a)}} \right) \right], \\
\Delta_{SU(N_a)}^{T^6/\mathbb{Z}_3} &= \sum_{k=0}^2 \left[\sum_b N_b \left(\tilde{\Delta}_{(\theta^k a)b}^{\text{torus}} + \tilde{\Delta}_{(\theta^k a)b'}^{\text{torus}} \right) + \Delta_{(\theta^k a), \Omega\mathcal{R}}^{\text{torus}} \right],
\end{aligned} \tag{32}$$

where in the second line we used the fact that open aa strings with endpoints on identical bulk D6-branes contribute $\tilde{\varphi}^{\mathbf{Adj}_a} = 3$, which cancels the contribution to the beta function coefficient from the vector multiplet.

There exists only one kind of $\Omega\mathcal{R}$ -invariant O6-plane on the six-torus, and D6-branes parallel to it preserve the full $\mathcal{N} = 4$ supersymmetry, or parallel along one two-torus the $\mathcal{N} = 2$ supersymmetry stated above for bifundamental and adjoint matter. Contrariwise, if the D6-brane is perpendicular to the $\Omega\mathcal{R}$ -invariant O6-plane along one or two tori, the orientifold symmetry breaks half of the supersymmetry. The complete list of $SU(N_a)$ beta function coefficients and gauge threshold corrections due to matter in the symmetric and antisymmetric representations on open strings stretched between orientifold image D6-branes a and a' on the six-torus is given in table 9. For T^6/\mathbb{Z}_3 , the sum over orbifold images $(\theta^k a)$ with $k = 0, 1, 2$ needs to be performed for both the annulus and Möbius strip contributions, see equation (32).

2.2.2 Fractional D6-branes on $T^6/(\mathbb{Z}_2 \times \mathbb{Z}_{2M} \times \Omega\mathcal{R})$ without discrete torsion

D6-branes on the $T^6/\mathbb{Z}_2 \times \mathbb{Z}_{2M}$ orbifolds without discrete torsion only wrap the half-bulk three cycles displayed in table 2. All annulus contributions to the gauge threshold amplitudes thus stem from the untwisted sector, and by comparison with the intersection numbers and rewritten RR tadpole cancellation conditions in tables 3 and 4, the normalisation of the contributions to the $SU(N_a)$ beta function coefficients and gauge thresholds from open strings in the bifundamental or adjoint representation is shown to be identical to the six-torus (up to summation over orbifold images of the first D6-brane index in analogy to equation (13)). The result is listed in the upper part of table 10.

In contrast to the six-torus, there exist four different orbits of $\Omega\mathcal{R}\mathbb{Z}_2^{(l)}$ invariant O6-planes, where for the sake of a compact notation, we set $\Omega\mathcal{R} \equiv \Omega\mathcal{R}\mathbb{Z}_2^{(0)}$ and $l \in \{0 \dots 3\}$. The

$b_{SU(N_a)}$ and gauge thresholds for symmetric and antisymmetric: T^6 and T^6/\mathbb{Z}_3		
$(\phi_{aa'}^{(1)}, \phi_{aa'}^{(2)}, \phi_{aa'}^{(3)})$	$b_{SU(N_a)}^{\text{torus}} = b_{aa'}^{\mathcal{A}} + b_{aa'}^{\mathcal{M}} + \dots$ $= \frac{N_a}{2} (\varphi^{\text{Sym}_a} + \varphi^{\text{Anti}_a}) + (\varphi^{\text{Sym}_a} - \varphi^{\text{Anti}_a}) + \dots$	$\Delta_{SU(N_a)}^{\text{torus}} = N_a \tilde{\Delta}_{aa'}^{\text{torus}} + \Delta_{a,O6}^{\text{torus}} + \dots$
$(0,0,0)$ $\uparrow\uparrow \Omega\mathcal{R}$	—	—
$(0,0,0)$ $\perp \Omega\mathcal{R}$ on $T_j \times T_k$	$-\delta_{\sigma_{aa'},0}^i \delta_{\tau_{aa'},0}^i 2 \tilde{I}_a^{\Omega\mathcal{R},(j-k)} $	$-b_{aa'}^{\mathcal{M}} \Lambda_{0,0}(v_i; V_{aa'}^{(i)}) - (4b_i) b_{aa'}^{\mathcal{M}} \ln\left(\frac{\eta(2iv_i)}{\vartheta_4(0,2iv_i)}\right) - 2 b_{aa'}^{\mathcal{M}} \ln(2)$ $+ 2 \tilde{I}_a^{\Omega\mathcal{R},(j-k)} \left(1 - \delta_{\sigma_{aa'},0}^i \delta_{\tau_{aa'},0}^i\right) \Lambda(\sigma_{aa'}^i, \tau_{aa'}^i, \tilde{v}_i)$
$(0^{(i)}, \phi^{(j)}, \phi^{(k)})$ $\uparrow\uparrow \Omega\mathcal{R}$ on T_i	$\delta_{\sigma_{aa'},0}^i \delta_{\tau_{aa'},0}^i \left\{ N_a I_{aa'}^{(j-k)} - 2 \tilde{I}_a^{\Omega\mathcal{R},(j-k)} \right\}$	$-(b_{aa'}^{\mathcal{A}} + b_{aa'}^{\mathcal{M}}) \Lambda_{0,0}(v_i; V_i) - (4b_i) b_{aa'}^{\mathcal{M}} \ln\left(\frac{\eta(2iv_i)}{\vartheta_4(0,2iv_i)}\right) - 2 b_{aa'}^{\mathcal{M}} \ln(2)$ $- N_a I_{aa'}^{(j-k)} \left(1 - \delta_{\sigma_{aa'},0}^i \delta_{\tau_{aa'},0}^i\right) \Lambda(\sigma_{aa'}^i, \tau_{aa'}^i, v_i)$ $+ 2 \tilde{I}_a^{\Omega\mathcal{R},(j-k)} \left(1 - \delta_{\sigma_{aa'},0}^i \delta_{\tau_{aa'},0}^i\right) \Lambda(\sigma_{aa'}^i, \tau_{aa'}^i, \tilde{v}_i)$
$(0^{(i)}, \phi^{(j)}, \phi^{(k)})$ $\perp \Omega\mathcal{R}$ on T_i	$\delta_{\sigma_{aa'},0}^i \delta_{\tau_{aa'},0}^i N_a I_{aa'}^{(j-k)} $	$-b_{aa'}^{\mathcal{A}} \Lambda_{0,0}(v_i; V_i)$ $- N_a I_{aa'}^{(j-k)} \left(1 - \delta_{\sigma_{aa'},0}^i \delta_{\tau_{aa'},0}^i\right) \Lambda(\sigma_{aa'}^i, \tau_{aa'}^i, v_i)$ $+ 2 \tilde{I}_a^{\Omega\mathcal{R}} \ln(2)$
$(\phi^{(1)}, \phi^{(2)}, \phi^{(3)})$ $\sum_{n=1}^3 \phi^{(n)} = 0$	$\frac{N_a}{2} I_{aa'} + c_a^{\Omega\mathcal{R}} \tilde{I}_a^{\Omega\mathcal{R}} $	$(b_{aa'}^{\mathcal{A}} + b_{aa'}^{\mathcal{M}}) \text{sgn}(I_{aa'}) \sum_{i=1}^3 \ln\left(\frac{\Gamma(\phi_{aa'}^{(i)})}{\Gamma(1- \phi_{aa'}^{(i)})}\right)^{\text{sgn}(\phi_{aa'}^{(i)})}$ $+ 2 \tilde{I}_a^{\Omega\mathcal{R}} \ln(2)$

Table 9: Beta function coefficients and gauge thresholds for $SU(N_a)$ gauge groups from open strings in the symmetric and antisymmetric representation on bulk D6-branes on the six-torus and T^6/\mathbb{Z}_3 . The angles on the first line preserve $\mathcal{N} = 4$, on the second and third line $\mathcal{N} = 2$ and on the last two lines $\mathcal{N} = 1$ supersymmetry. On the first two lines, for vanishing relative displacements and Wilson lines $(\sigma_{aa'}^i, \tau_{aa'}^i) = (0,0)$ along the two-tori (i.e. the D6-branes are on top of or perpendicular to the O6-plane) the gauge group is enhanced to $SO(2N_a)$ and $Sp(2N_a)$, respectively. Details for the orthogonal and symplectic gauge factors are given in section 2.2.5 and table 15.

Möbius strip contributions to the $SU(N_a)$ beta function coefficients and gauge thresholds correspond, up to normalisation and up to the existence of *continuous* displacements and Wilson lines, to those of the $T^6/\mathbb{Z}_2 \times \mathbb{Z}_{2M}$ orbifolds with discrete torsion presented in detail above. From the intersection numbers and rewritten RR tadpole cancellation conditions in tables 3 and 4, it is easy to derive the change of normalisation by a factor of two and the simplification in the signs for only ordinary O6-planes, $\eta_{\Omega\mathcal{R}\mathbb{Z}_2^{(l)}} \equiv 1$ for all $l \in \{0 \dots 3\}$ on orbifolds without discrete torsion. The complete expressions for $SU(N_a)$ beta function coefficients and gauge thresholds due to open strings in the symmetric and antisymmetric representation are listed in the lower part of table 10.

2.2.3 Fractional D6-branes on $T^6/(\mathbb{Z}_{2N} \times \Omega\mathcal{R})$

The beta function coefficients and gauge thresholds for fractional D6-branes on $T^6/(\mathbb{Z}_{2N} \times \Omega\mathcal{R})$ backgrounds have been discussed in detail in [40]. In order to be able to directly compare

$b_{SU(N_a)}$ and gauge thresholds for bifundamental and adjoints: $T^6/\mathbb{Z}_2 \times \mathbb{Z}_{2M}$ without discrete torsion		
$(\phi_{ab}^{(1)}, \phi_{ab}^{(2)}, \phi_{ab}^{(3)})$	$b_{SU(N_a)}^{\text{no torsion}} = \sum_b b_{ab}^A + \dots$ $= \sum_b \frac{N_b}{2} \varphi^{ab} + \dots$	$\Delta_{SU(N_a)}^{\text{no torsion}} = \sum_b N_b \bar{\Delta}_{ab} + \dots$
$(0, 0, 0)$	—	—
$(0, \phi, -\phi)$	$N_b \delta_{\sigma_{ab}^1, 0} \delta_{\tau_{ab}^1, 0} I_{ab}^{(2,3)} $	$-b_{ab}^A \Lambda_{0,0}(v_1; V_{ab}^{(1)})$ $-N_b I_{ab}^{(2,3)} \left(1 - \delta_{\sigma_{ab}^1, 0} \delta_{\tau_{ab}^1, 0}\right) \Lambda(\sigma_{ab}^1, \tau_{ab}^1, v_1)$
$(\phi^{(1)}, \phi^{(2)}, \phi^{(3)})$ $\sum_{n=1}^3 \phi^{(n)} = 0$	$\frac{N_b}{2} I_{ab} $	$b_{ab}^A \text{sgn}(I_{ab}) \sum_{i=1}^3 \ln \left(\frac{\Gamma(\phi_{ab}^{(i)})}{\Gamma(1- \phi_{ab}^{(i)})} \right)^{\text{sgn}(\phi_{ab}^{(i)})}$
$b_{SU(N_a)}$ and gauge thresholds for (anti)symmetrics: $T^6/\mathbb{Z}_2 \times \mathbb{Z}_{2M}$ without discrete torsion		
$(\phi_{aa'}^{(1)}, \phi_{aa'}^{(2)}, \phi_{aa'}^{(3)})$	$b_{SU(N_a)}^{\text{no torsion}} = b_{aa'}^A + b_{aa'}^{\mathcal{M}} + \dots$ $\frac{N_a}{2} (\varphi^{\text{Sym}_a} + \varphi^{\text{Anti}_a}) + (\varphi^{\text{Sym}_a} - \varphi^{\text{Anti}_a}) + \dots$	$\Delta_{SU(N_a)}^{\text{no torsion}} = N_a \bar{\Delta}_{aa'} + \Delta_{a, \Omega \mathcal{R}} + \dots$
$(0, 0, 0)$ $\uparrow \uparrow \Omega \mathcal{R}$	$-\sum_{i=1}^3 \delta_{\sigma_{aa'}^i, 0} \delta_{\tau_{aa'}^i, 0} \tilde{I}_a^{\Omega \mathcal{R} \mathbb{Z}_2^{(i)}, (j,k)} $	$\sum_{i=1}^3 \delta_{\sigma_{aa'}^i, 0} \delta_{\tau_{aa'}^i, 0} \tilde{I}_a^{\Omega \mathcal{R} \mathbb{Z}_2^{(i)}, (j,k)} \Lambda_{0,0}(\tilde{v}_i, 2 \tilde{V}_{aa'}^{(i)})$ $+ \sum_{i=1}^3 \left(1 - \delta_{\sigma_{aa'}^i, 0} \delta_{\tau_{aa'}^i, 0}\right) \tilde{I}_a^{\Omega \mathcal{R} \mathbb{Z}_2^{(i)}, (j,k)} \Lambda(\sigma_{aa'}^i, \tau_{aa'}^i, \tilde{v}_i)$
$(0, 0, 0)$ $\uparrow \uparrow \Omega \mathcal{R} \mathbb{Z}_2^{(i)}$	$-\delta_{\sigma_{aa'}^i, 0} \delta_{\tau_{aa'}^i, 0} \tilde{I}_a^{\Omega \mathcal{R}, (j,k)} $ $-\sum_{j \neq i} \delta_{\sigma_{aa'}^j, 0} \delta_{\tau_{aa'}^j, 0} \tilde{I}_a^{\Omega \mathcal{R} \mathbb{Z}_2^{(j)}, (i,j)} $	$\delta_{\sigma_{aa'}^i, 0} \delta_{\tau_{aa'}^i, 0} \tilde{I}_a^{\Omega \mathcal{R}, (j,k)} \Lambda_{0,0}(\tilde{v}_i, 2 \tilde{V}_{aa'}^{(i)})$ $+ \sum_{j \neq i} \delta_{\sigma_{aa'}^j, 0} \delta_{\tau_{aa'}^j, 0} \tilde{I}_a^{\Omega \mathcal{R} \mathbb{Z}_2^{(j)}, (i,j)} \Lambda_{0,0}(\tilde{v}_j, 2 \tilde{V}_{aa'}^{(j)})$ $+ \left(1 - \delta_{\sigma_{aa'}^i, 0} \delta_{\tau_{aa'}^i, 0}\right) \tilde{I}_a^{\Omega \mathcal{R}, (j,k)} \Lambda(\sigma_{aa'}^i, \tau_{aa'}^i, \tilde{v}_i)$ $+ \sum_{j \neq i} \left(1 - \delta_{\sigma_{aa'}^j, 0} \delta_{\tau_{aa'}^j, 0}\right) \tilde{I}_a^{\Omega \mathcal{R} \mathbb{Z}_2^{(j)}, (i,j)} \Lambda(\sigma_{aa'}^j, \tau_{aa'}^j, \tilde{v}_j)$
$(0_i, \phi_j, \phi_k)_{\phi_k = -\phi_j \neq \pm \frac{1}{2}}$ $\uparrow \uparrow (\Omega \mathcal{R} + \Omega \mathcal{R} \mathbb{Z}_2^{(i)})$ on T_i^2	$\delta_{\sigma_{aa'}^i, 0} \delta_{\tau_{aa'}^i, 0} \left\{ N_a I_{aa'}^{(j,k)} \right.$ $\left. - \tilde{I}_a^{\Omega \mathcal{R}, (j,k)} - \tilde{I}_a^{\Omega \mathcal{R} \mathbb{Z}_2^{(i)}, (j,k)} \right\}$	$-(b_{aa'}^A + b_{aa'}^{\mathcal{M}}) \Lambda_{0,0}(v_i; V_{aa'}^{(i)}) - (4 b_i) b_{aa'}^{\mathcal{M}} \ln \left(\frac{\eta(2iv_i)}{\theta_4(0, 2iv_i)} \right)$ $+ \left(1 - \delta_{\sigma_{aa'}^i, 0} \delta_{\tau_{aa'}^i, 0}\right) \times$ $\times \left(N_a I_{aa'}^{(j,k)} \Lambda(\sigma_{aa'}^i, \tau_{aa'}^i, v_i) + \left[\tilde{I}_a^{\Omega \mathcal{R}, (j,k)} + \tilde{I}_a^{\Omega \mathcal{R} \mathbb{Z}_2^{(i)}, (j,k)} \right] \Lambda(\sigma_{aa'}^i, \tau_{aa'}^i, \tilde{v}_i) \right)$ $+ \left(\tilde{I}_a^{\Omega \mathcal{R} \mathbb{Z}_2^{(j)}} + \tilde{I}_a^{\Omega \mathcal{R} \mathbb{Z}_2^{(k)}} + 2 \delta_{\sigma_{aa'}^i, 0} \delta_{\tau_{aa'}^i, 0} \left\{ \tilde{I}_a^{\Omega \mathcal{R}, (j,k)} + \tilde{I}_a^{\Omega \mathcal{R} \mathbb{Z}_2^{(i)}, (j,k)} \right\} \right) \ln(2)$
$(0_i, \phi_j, \phi_k)_{\phi_k = -\phi_j \neq \pm \frac{1}{2}}$ $\uparrow \uparrow (\Omega \mathcal{R} \mathbb{Z}_2^{(j)} + \Omega \mathcal{R} \mathbb{Z}_2^{(k)})$ on T_i^2	$\delta_{\sigma_{aa'}^i, 0} \delta_{\tau_{aa'}^i, 0} \left\{ N_a I_{aa'}^{(j,k)} \right.$ $\left. - \tilde{I}_a^{\Omega \mathcal{R} \mathbb{Z}_2^{(j)}, (j,k)} - \tilde{I}_a^{\Omega \mathcal{R} \mathbb{Z}_2^{(k)}, (j,k)} \right\}$	$-(b_{aa'}^A + b_{aa'}^{\mathcal{M}}) \Lambda_{0,0}(v_i; V_{aa'}^{(i)}) - (4 b_i) b_{aa'}^{\mathcal{M}} \ln \left(\frac{\eta(2iv_i)}{\theta_4(0, 2iv_i)} \right)$ $+ \left(1 - \delta_{\sigma_{aa'}^i, 0} \delta_{\tau_{aa'}^i, 0}\right) \times$ $\times \left(N_a I_{aa'}^{(j,k)} \Lambda(\sigma_{aa'}^i, \tau_{aa'}^i, v_i) + \left[\tilde{I}_a^{\Omega \mathcal{R} \mathbb{Z}_2^{(j)}, (j,k)} + \tilde{I}_a^{\Omega \mathcal{R} \mathbb{Z}_2^{(k)}, (j,k)} \right] \Lambda(\sigma_{aa'}^i, \tau_{aa'}^i, \tilde{v}_i) \right)$ $+ \left(\tilde{I}_a^{\Omega \mathcal{R}} + \tilde{I}_a^{\Omega \mathcal{R} \mathbb{Z}_2^{(i)}} + 2 \delta_{\sigma_{aa'}^i, 0} \delta_{\tau_{aa'}^i, 0} \left\{ \tilde{I}_a^{\Omega \mathcal{R} \mathbb{Z}_2^{(j)}, (j,k)} + \tilde{I}_a^{\Omega \mathcal{R} \mathbb{Z}_2^{(k)}, (j,k)} \right\} \right) \ln(2)$
$(\phi^{(1)}, \phi^{(2)}, \phi^{(3)})$ $\sum_{n=1}^3 \phi^{(n)} = 0$	$\frac{N_a}{2} I_{aa'} $ $+ \frac{c_{\Omega \mathcal{R}}}{2} \tilde{I}_a^{\Omega \mathcal{R}} + \sum_{i=1}^3 \frac{c_{\Omega \mathcal{R} \mathbb{Z}_2^{(i)}}}{2} \tilde{I}_a^{\Omega \mathcal{R} \mathbb{Z}_2^{(i)}} $	$(b_{aa'}^A + b_{aa'}^{\mathcal{M}}) \text{sgn}(I_{aa'}) \sum_{i=1}^3 \ln \left(\frac{\Gamma(\phi_{aa'}^{(i)})}{\Gamma(1- \phi_{aa'}^{(i)})} \right)^{\text{sgn}(\phi_{aa'}^{(i)})}$ $+ \sum_{m=0}^3 \tilde{I}_a^{\Omega \mathcal{R} \mathbb{Z}_2^{(m)}} \ln(2)$

Table 10: $SU(N_a)$ beta function coefficients and gauge thresholds for half-bulk D6-branes on $T^6/(\mathbb{Z}_2 \times \mathbb{Z}_{2M} \times \Omega \mathcal{R})$ without discrete torsion. In the last line, the notation is shortened by setting $\Omega \mathcal{R} \mathbb{Z}_2^{(0)} \equiv \Omega \mathcal{R}$. A stack of D6-branes on top of some O6-plane with vanishing relative displacements and Wilson lines of the orientifold image D6-branes everywhere, $(\vec{\sigma}_{aa'}, \vec{\tau}_{aa'}) = (0, 0)$, leads to an $Sp(2N_a)$ gauge group and is further discussed in section 2.2.5 and table 15. The contributions from adjoint matter are scrutinised in section 2.2.4 and table 13.

with the other factorisable orbifolds in this article and for the decomposition into holomorphic gauge kinetic function and Kähler metrics, we rewrite the results for bifundamental and adjoint matter in table 11 as sums of the untwisted and $\mathbb{Z}_2 \equiv \mathbb{Z}_2^{(2)}$ twisted annulus amplitudes and re-express the gauge thresholds by using the known form of the associated beta function coefficients.

The $SU(N_a)$ beta function coefficients and gauge thresholds for antisymmetric and symmetric matter on $T^6/(\mathbb{Z}_{2N} \times \Omega \mathcal{R})$ are given in table 12 in a greatly simplified form compared to [40], i.e. we have factorised out the beta function coefficients as prefactors of

$b_{SU(N_a)}$ and gauge thresholds for bifundamentals and adjoints: T^6/\mathbb{Z}_{2N} with $\mathbb{Z}_2 \equiv \mathbb{Z}_2^{(2)}$		
$(\phi_{ab}^{(1)}, \phi_{ab}^{(2)}, \phi_{ab}^{(3)})$	$b_{SU(N_a)}^{\mathbb{Z}_2} = \sum_b b_{ab}^A + \dots$ $= \sum_b \frac{N_b}{2} \varphi^{ab} + \dots$	$\Delta_{SU(N_a)}^{\mathbb{Z}_{2N}} = N_b \tilde{\Delta}_{ab} + \dots$
$(0, 0, 0)$	$-\frac{I_{ab}^{\mathbb{Z}_2, (1,3)} N_b}{2} \delta_{\sigma_{ab}^2, 0} \delta_{\tau_{ab}^2, 0}$	$-b_{ab}^A \Lambda_{0,0}(v_2; V_{ab}^{(2)})$ $+ \frac{I_{ab}^{\mathbb{Z}_2, (1,3)} N_b}{2} \left(1 - \delta_{\sigma_{ab}^2, 0} \delta_{\tau_{ab}^2, 0}\right) \Lambda(\sigma_{ab}^2, \tau_{ab}^2, v_2)$
$(\phi, -\phi, 0)$	$\frac{N_b}{2} \delta_{\sigma_{ab}^3, 0} \delta_{\tau_{ab}^3, 0} I_{ab}^{(1,2)} $	$-b_{ab}^A \Lambda_{0,0}(v_3; V_{ab}^{(3)})$ $-\frac{N_b}{2} I_{ab}^{(1,2)} \left(1 - \delta_{\sigma_{ab}^3, 0} \delta_{\tau_{ab}^3, 0}\right) \Lambda(\sigma_{ab}^3, \tau_{ab}^3, v_3)$ $-\frac{N_b I_{ab}^{\mathbb{Z}_2}}{2} (\text{sgn}(\phi) - 2\phi) \ln(2)$
$(\phi, 0, -\phi)$	$\frac{N_b}{2} \delta_{\sigma_{ab}^2, 0} \delta_{\tau_{ab}^2, 0} \left(I_{ab}^{(1,3)} - I_{ab}^{\mathbb{Z}_2, (1,3)}\right)$	$-b_{ab}^A \Lambda_{0,0}(v_2; V_{ab}^{(2)})$ $-\frac{N_b}{2} \left\{ I_{ab}^{(1,3)} - I_{ab}^{\mathbb{Z}_2, (1,3)}\right\} \left(1 - \delta_{\sigma_{ab}^2, 0} \delta_{\tau_{ab}^2, 0}\right) \Lambda(\sigma_{ab}^2, \tau_{ab}^2, v_2)$
$(0, \phi, -\phi)$	$\frac{N_b}{2} \delta_{\sigma_{ab}^1, 0} \delta_{\tau_{ab}^1, 0} I_{ab}^{(2,3)} $	$-b_{ab}^A \Lambda_{0,0}(v_1; V_{ab}^{(1)})$ $-\frac{N_b}{2} I_{ab}^{(2,3)} \left(1 - \delta_{\sigma_{ab}^1, 0} \delta_{\tau_{ab}^1, 0}\right) \Lambda(\sigma_{ab}^1, \tau_{ab}^1, v_1)$ $+\frac{N_b I_{ab}^{\mathbb{Z}_2}}{2} (\text{sgn}(\phi) - 2\phi) \ln(2)$
$(\phi^{(1)}, \phi^{(2)}, \phi^{(3)})$ with $\sum_{k=1}^3 \phi^{(k)} = 0$	$\frac{N_b}{4} (I_{ab} + \text{sgn}(I_{ab}) I_{ab}^{\mathbb{Z}_2})$	$b_{ab}^A \text{sgn}(I_{ab}) \sum_{i=1}^3 \ln \left(\frac{\Gamma(\phi_{ab}^{(i)})}{\Gamma(1- \phi_{ab}^{(i)})} \right)^{\text{sgn}(\phi_{ab}^{(i)})}$ $+ \frac{N_b}{2} I_{ab}^{\mathbb{Z}_2} \left(\text{sgn}(I_{ab}) + \text{sgn}(\phi_{ab}^{(2)}) - 2\phi_{ab}^{(2)} \right) \ln(2)$

Table 11: $SU(N_a)$ beta function coefficients and gauge thresholds from bifundamental and adjoint matter on fractional D6-branes on the T^6/\mathbb{Z}_{2N} orbifold. The $\mathbb{Z}_2 \equiv \mathbb{Z}_2^{(2)}$ subgroup is chosen to leave the second two-torus invariant. The entries on the first and third line preserve $\mathcal{N} = 2$ supersymmetry, all other entries have only $\mathcal{N} = 1$. Details on adjoint matter are discussed in section 2.2.4 and table 13.

gauge thresholds and used the relation (31) for the logarithms of Gamma functions in the Möbius strip contributions.

2.2.4 Example I: the adjoints of $SU(N_a)$

In order to further evaluate the amount of adjoint matter on each factorisable toroidal orbifold background, we can use the fact, that the toroidal intersection numbers of orbifold

$b_{SU(N_a)}$ and gauge thresholds for symmetric and antisymmetric: T^6/\mathbb{Z}_{2N} with $\mathbb{Z}_2 \equiv \mathbb{Z}_2^{(2)}$		
$(\phi_{aa'}^{(1)}, \phi_{aa'}^{(2)}, \phi_{aa'}^{(3)})$	$b_{SU(N_a)}^{\mathbb{Z}_{2N}} = b_{aa'}^A + b_{aa'}^M + \dots =$ $\frac{N_a}{2} (\varphi^{\text{Sym}}_a + \varphi^{\text{Antia}}) + (\varphi^{\text{Sym}}_a - \varphi^{\text{Antia}}) + \dots$	$\Delta_{SU(N_a)}^{\mathbb{Z}_{2N}} = N_a \bar{\Delta}_{aa'} + \Delta_{a,O6} + \dots$
$(0, 0, 0)$ $\uparrow\uparrow \Omega\mathcal{R}$	$-\delta_{\sigma^2,0} \delta_{\tau^2,0} \times$ $\left(\frac{N_a I_{aa'}^{\mathbb{Z}_2, (1,3)}}{2} + \tilde{I}_a^{\Omega\mathcal{R}\mathbb{Z}_2, (1,3)} \right)$	$-(b_{aa'}^A + b_{aa'}^M) \Lambda_{0,0}(v_2; V_{aa'}^{(2)}) - (4b_2) b_{aa'}^M \ln \left(\frac{\eta(2iv_2)}{\vartheta_4(0, 2iv_2)} \right) - 2b_{aa'}^M \ln(2)$ $+ \left(1 - \delta_{\sigma^2,0} \delta_{\tau^2,0} \right) \left[\frac{I_{aa'}^{\mathbb{Z}_2, (1,3)} N_a}{2} \Lambda(\sigma_{aa'}^2, \tau_{aa'}^2, v_2) + \tilde{I}_a^{\Omega\mathcal{R}\mathbb{Z}_2, (1,3)} \Lambda(\sigma_{aa'}^2, \tau_{aa'}^2, \tilde{v}_2) \right]$
$(0, 0, 0)$ $\uparrow\uparrow \Omega\mathcal{R}\mathbb{Z}_2^{(2)}$	$-\delta_{\sigma^2,0} \delta_{\tau^2,0} \times$ $\left(\frac{N_a I_{aa'}^{\mathbb{Z}_2, (1,3)}}{2} + \tilde{I}_a^{\Omega\mathcal{R}, (1,3)} \right)$	$-(b_{aa'}^A + b_{aa'}^M) \Lambda_{0,0}(v_2; V_{aa'}^{(2)}) - (4b_2) b_{aa'}^M \ln \left(\frac{\eta(2iv_2)}{\vartheta_4(0, 2iv_2)} \right) - 2b_{aa'}^M \ln(2)$ $+ \left(1 - \delta_{\sigma^2,0} \delta_{\tau^2,0} \right) \left[\frac{I_{aa'}^{\mathbb{Z}_2, (1,3)} N_a}{2} \Lambda(\sigma_{aa'}^2, \tau_{aa'}^2, v_2) + \tilde{I}_a^{\Omega\mathcal{R}, (1,3)} \Lambda(\sigma_{aa'}^2, \tau_{aa'}^2, \tilde{v}_2) \right]$
$(0, 0, 0)$ $\perp \Omega\mathcal{R}$ on $T_1 \times T_2$	$-\left(\frac{N_a I_{aa'}^{\mathbb{Z}_2, (1,3)} \delta_{\sigma^2,0} \delta_{\tau^2,0}}{2} \right.$ $\left. + \tilde{I}_a^{\Omega\mathcal{R}, (1,2)} + \tilde{I}_a^{\Omega\mathcal{R}\mathbb{Z}_2, (2,3)} \right)$	$-b_{aa'}^A \Lambda_{0,0}(v_2; V_{aa'}^{(2)}) + \tilde{I}_a^{\Omega\mathcal{R}, (1,2)} \Lambda_{0,0}(\tilde{v}_3; 2\tilde{V}_{aa'}^{(3)}) + \tilde{I}_a^{\Omega\mathcal{R}\mathbb{Z}_2, (2,3)} \Lambda_{0,0}(\tilde{v}_1; 2\tilde{V}_{aa'}^{(1)})$ $+ \frac{I_{aa'}^{\mathbb{Z}_2, (1,3)} N_a}{2} \left(1 - \delta_{\sigma^2,0} \delta_{\tau^2,0} \right) \Lambda(\sigma_{aa'}^2, \tau_{aa'}^2, v_2)$
$(0, 0, 0)$ $\perp \Omega\mathcal{R}$ on $T_2 \times T_3$	$-\left(\frac{N_a I_{aa'}^{\mathbb{Z}_2, (1,3)} \delta_{\sigma^2,0} \delta_{\tau^2,0}}{2} \right.$ $\left. + \tilde{I}_a^{\Omega\mathcal{R}, (2,3)} + \tilde{I}_a^{\Omega\mathcal{R}\mathbb{Z}_2, (1,2)} \right)$	$-b_{aa'}^A \Lambda_{0,0}(v_2; V_{aa'}^{(2)}) + \tilde{I}_a^{\Omega\mathcal{R}, (2,3)} \Lambda_{0,0}(\tilde{v}_1; 2\tilde{V}_{aa'}^{(1)}) + \tilde{I}_a^{\Omega\mathcal{R}\mathbb{Z}_2, (1,2)} \Lambda_{0,0}(\tilde{v}_3; 2\tilde{V}_{aa'}^{(3)})$ $+ \frac{I_{aa'}^{\mathbb{Z}_2, (1,3)} N_a}{2} \left(1 - \delta_{\sigma^2,0} \delta_{\tau^2,0} \right) \Lambda(\sigma_{aa'}^2, \tau_{aa'}^2, v_2)$
$(\phi, -\phi, 0)$ $\uparrow\uparrow \Omega\mathcal{R}$ on T_3	$\frac{N_a}{2} I_{aa'}^{(1,2)} - \tilde{I}_a^{\Omega\mathcal{R}, (1,2)} $	$-(b_{aa'}^A + b_{aa'}^M) \Lambda_{0,0}(v_3; V_{aa'}^{(3)}) - (4b_3) b_{aa'}^M \ln \left(\frac{\eta(2iv_3)}{\vartheta_4(0, 2iv_3)} \right)$ $+ \left(-\frac{N_a I_{aa'}^{\mathbb{Z}_2}}{2} (\text{sgn}(\phi) - 2\phi) + \tilde{I}_a^{\Omega\mathcal{R}\mathbb{Z}_2} + 2 \tilde{I}_a^{\Omega\mathcal{R}, (1,2)} \right) \ln(2)$
$(\phi, -\phi, 0)$ $\perp \Omega\mathcal{R}$ on T_3	$\frac{N_a}{2} I_{aa'}^{(1,2)} - \tilde{I}_a^{\Omega\mathcal{R}\mathbb{Z}_2, (1,2)} $	$-(b_{aa'}^A + b_{aa'}^M) \Lambda_{0,0}(v_3; V_{aa'}^{(3)}) - (4b_3) b_{aa'}^M \ln \left(\frac{\eta(2iv_3)}{\vartheta_4(0, 2iv_3)} \right)$ $+ \left(-\frac{N_a I_{aa'}^{\mathbb{Z}_2}}{2} (\text{sgn}(\phi) - 2\phi) + \tilde{I}_a^{\Omega\mathcal{R}} + 2 \tilde{I}_a^{\Omega\mathcal{R}\mathbb{Z}_2, (1,2)} \right) \ln(2)$
$(\phi, 0, -\phi)_{\phi \neq \pm \frac{1}{2}}$ $\uparrow\uparrow (\Omega\mathcal{R} + \Omega\mathcal{R}\mathbb{Z}_2^{(2)})$ on T_2	$\delta_{\sigma^2,0} \delta_{\tau^2,0} \left[\frac{N_a (I_{aa'}^{(1,3)} - I_{aa'}^{\mathbb{Z}_2, (1,3)})}{2} \right.$ $\left. - \tilde{I}_a^{\Omega\mathcal{R}, (1,3)} - \tilde{I}_a^{\Omega\mathcal{R}\mathbb{Z}_2, (1,3)} \right]$	$-(b_{aa'}^A + b_{aa'}^M) \Lambda_{0,0}(v_2; V_{aa'}^{(2)}) - (4b_2) b_{aa'}^M \ln \left(\frac{\eta(2iv_2)}{\vartheta_4(0, 2iv_2)} \right)$ $+ \left(1 - \delta_{\sigma^2,0} \delta_{\tau^2,0} \right) \times \left[\frac{N_a (I_{aa'}^{(1,2)} + I_{aa'}^{\mathbb{Z}_2, (1,3)})}{2} \Lambda(\sigma_{aa'}^2, \tau_{aa'}^2, v_2) \right.$ $\left. - \left(\tilde{I}_a^{\Omega\mathcal{R}, (1,3)} + \tilde{I}_a^{\Omega\mathcal{R}\mathbb{Z}_2, (1,3)} \right) \Lambda(\sigma_{aa'}^2, \tau_{aa'}^2, \tilde{v}_2) \right]$ $- 2b_{aa'}^M \ln(2)$
$(\phi, 0, -\phi)_{\phi \neq \pm \frac{1}{2}}$ $\perp (\Omega\mathcal{R} + \Omega\mathcal{R}\mathbb{Z}_2^{(2)})$ on T_2	$\frac{N_a (I_{aa'}^{(1,3)} - I_{aa'}^{\mathbb{Z}_2, (1,3)})}{2} \delta_{\sigma^2,0} \delta_{\tau^2,0}$	$-b_{aa'}^A \Lambda_{0,0}(v_2; V_{aa'}^{(2)})$ $+ \frac{N_a (I_{aa'}^{(1,2)} + I_{aa'}^{\mathbb{Z}_2, (1,3)})}{2} \left(1 - \delta_{\sigma^2,0} \delta_{\tau^2,0} \right) \Lambda(\sigma_{aa'}^2, \tau_{aa'}^2, v_2)$ $+ (\tilde{I}_a^{\Omega\mathcal{R}} + \tilde{I}_a^{\Omega\mathcal{R}\mathbb{Z}_2}) \ln(2)$
$(0, \phi, -\phi)$ $\uparrow\uparrow \Omega\mathcal{R}$ on T_1	$\frac{N_a}{2} I_{aa'}^{(2,3)} - \tilde{I}_a^{\Omega\mathcal{R}, (2,3)} $	$-(b_{aa'}^A + b_{aa'}^M) \Lambda_{0,0}(v_1; V_{aa'}^{(1)}) - (4b_1) b_{aa'}^M \ln \left(\frac{\eta(2iv_1)}{\vartheta_4(0, 2iv_1)} \right)$ $+ \left(\frac{N_a I_{aa'}^{\mathbb{Z}_2}}{2} (\text{sgn}(\phi) - 2\phi) + \tilde{I}_a^{\Omega\mathcal{R}\mathbb{Z}_2} + 2 \tilde{I}_a^{\Omega\mathcal{R}, (2,3)} \right) \ln(2)$
$(0, \phi, -\phi)$ $\perp \Omega\mathcal{R}$ on T_1	$\frac{N_a}{2} I_{aa'}^{(2,3)} - \tilde{I}_a^{\Omega\mathcal{R}\mathbb{Z}_2, (2,3)} $	$-(b_{aa'}^A + b_{aa'}^M) \Lambda_{0,0}(v_1; V_{aa'}^{(1)}) - (4b_1) b_{aa'}^M \ln \left(\frac{\eta(2iv_1)}{\vartheta_4(0, 2iv_1)} \right)$ $+ \left(\frac{N_a I_{aa'}^{\mathbb{Z}_2}}{2} (\text{sgn}(\phi) - 2\phi) + \tilde{I}_a^{\Omega\mathcal{R}} + 2 \tilde{I}_a^{\Omega\mathcal{R}\mathbb{Z}_2, (2,3)} \right) \ln(2)$
$(\phi^{(1)}, \phi^{(2)}, \phi^{(3)})$ $0 < \phi^{(i)} , \phi^{(j)} \leq \phi^{(k)} < 1$ $\text{sgn}(\phi^{(i)}) = \text{sgn}(\phi^{(j)})$ $\neq \text{sgn}(\phi^{(k)})$	$\frac{N_a (I_{aa'} + \text{sgn}(I_{aa'}) I_{aa'}^{\mathbb{Z}_2})}{2}$ $+ \frac{c_a^{\Omega\mathcal{R}} \tilde{I}_a^{\Omega\mathcal{R}} + c_a^{\Omega\mathcal{R}\mathbb{Z}_2} \tilde{I}_a^{\Omega\mathcal{R}\mathbb{Z}_2} }{2}$	$(b_{aa'}^A + b_{aa'}^M) \text{sgn}(I_{aa'}) \sum_{i=1}^3 \ln \left(\frac{\Gamma(\phi^{(i)})}{\Gamma(1 - \phi^{(i)})} \right) \text{sgn}(\phi^{(i)})$ $+ \left(\frac{N_a I_{aa'}^{\mathbb{Z}_2}}{2} (\text{sgn}(I_{aa'}) + \text{sgn}(\phi_{aa'}^{(2)}) - 2\phi_{aa'}^{(2)}) + \tilde{I}_a^{\Omega\mathcal{R}} + \tilde{I}_a^{\Omega\mathcal{R}\mathbb{Z}_2} \right) \ln(2)$

Table 12: $SU(N_a)$ beta function coefficients and gauge thresholds from symmetric and antisymmetric matter on $T^6/(\mathbb{Z}_{2N} \times \Omega\mathcal{R})$. If the D6_a-brane is parallel or perpendicular to one of the O6-planes with vanishing relative displacement and Wilson line, $(\sigma_{aa'}^2, \tau_{aa'}^2) = (0, 0)$, along the \mathbb{Z}_2 invariant two-torus $T_{(2)}^2$, the gauge group is enhanced to $Sp(2N_a)$, cf. section 2.2.5 and table 15.

image D6-branes for every single case can be derived using the relations (2),

$$\begin{aligned}
T^6/\mathbb{Z}_3: \quad I_{(\theta a)a} &= -I_{(\theta^2 a)a} = -\prod_{i=1}^3 [(n_a^i)^2 + n_a^i m_a^i + (m_a^i)^2], \\
T^6/\mathbb{Z}_4: \quad I_{(\theta a)a} &= -0^{(2)} \cdot \prod_{i=1,3} [(n_a^i)^2 + (m_a^i)^2], \\
T^6/\mathbb{Z}_6: \quad I_{(\theta a)a} &= -I_{(\theta^2 a)a} = \prod_{i=1}^3 [(n_a^i)^2 + n_a^i m_a^i + (m_a^i)^2], \\
T^6/\mathbb{Z}'_6: \quad I_{(\theta a)a} &= I_{(\theta^2 a)a} = -0^{(3)} \cdot \prod_{i=1,2} [(n_a^i)^2 + n_a^i m_a^i + (m_a^i)^2], \\
T^6/\mathbb{Z}_2 \times \mathbb{Z}_4: \quad I_{(\omega a)a} &= -0^{(1)} \cdot \prod_{i=2,3} [(n_a^i)^2 + (m_a^i)^2], \\
T^6/\mathbb{Z}_2 \times \mathbb{Z}_6: \quad I_{(\omega a)a} &= I_{(\omega^2 a)a} = -0^{(1)} \cdot \prod_{i=2,3} [(n_a^i)^2 + n_a^i m_a^i + (m_a^i)^2],
\end{aligned} \tag{33}$$

and the explicit expressions for the contributions to the gauge thresholds are obtained from the relative angles, which are given by $2\pi\vec{v}$ and $2\pi\vec{w}$ for T^6/\mathbb{Z}_{2N} and $T^6/\mathbb{Z}_2 \times \mathbb{Z}_{2M}$ orbifolds, respectively, with the shift vectors listed in table 1. The results for all factorisable toroidal orbifold backgrounds are compared in table 13.

One can directly read off from table 13 that the aa -sector on the six-torus, T^6/\mathbb{Z}_3 and $T^6/\mathbb{Z}_2 \times \mathbb{Z}_{2M}$ without discrete torsion preserves $\mathcal{N} = 4$ supersymmetry (i.e. there exist three matter multiplets in the adjoint representation) and therefore does not contribute to the beta function coefficient and gauge threshold. The aa -sector on T^6/\mathbb{Z}_{2N} preserves only $\mathcal{N} = 2$ and on $T^6/\mathbb{Z}_2 \times \mathbb{Z}_{2M}$ with discrete torsion $\mathcal{N} = 1$ supersymmetry, which corresponds to one and no adjoint matter multiplet, respectively, as well as a non-vanishing gauge threshold which depends on the Kähler moduli v_i via the Kaluza-Klein and winding sums in the first line of (25) for both $\mathcal{N} = 1, 2$. This completes the classification of open strings transforming in the adjoint representation on the six-torus and the $T^6/\mathbb{Z}_2 \times \mathbb{Z}_2$ orbifolds without and with discrete torsion.

The T^6/\mathbb{Z}_4 and $T^6/\mathbb{Z}_2 \times \mathbb{Z}_4$ orbifolds have one sector $(\theta a)a$ or $(\omega a)a$, respectively, of intersections of orbifold image D6-branes which can provide additional adjoint matter. While on T^6/\mathbb{Z}_4 the (non)existence of matter depends on the \mathbb{Z}_2 invariance of the intersection point of the $D6_{(\theta a)}$ - and $D6_a$ -brane and the combination of discrete displacements and Wilson lines $(\sigma_a^i, \tau_a^i)_{i \in \{1,3\}}$ along the directions where \mathbb{Z}_2 acts non-trivially, on $T^6/\mathbb{Z}_2 \times \mathbb{Z}_4$ there exists always one adjoint matter multiplet per intersection of orbifold image $D6_{(\omega a)}$ - and $D6_a$ -branes. In both cases, the gauge threshold contribution is due to massive strings at the same intersection points and consists of a Kaluza-Klein and winding sum along the two-torus where the orbifold images D6-branes are parallel to each other.

On the T^6/\mathbb{Z}_N orbifolds with $N \in \{3, 6, 6'\}$ as well as the $T^6/\mathbb{Z}_2 \times \mathbb{Z}_{2M}$ orbifolds with $2M \in \{6, 6'\}$, the $(\theta a)a$ and $(\theta^2 a)a$ [or $(\omega a)a$ and $(\omega^2 a)a$] sectors are paired up to provide the two helicity states and scalar degrees of freedom of one massless chiral multiplet with a given \mathbb{Z}_2 transformation behaviour per intersection. The contributions from adjoints at intersections of orbifold images in table 13 can be classified along two different lines: on T^6/\mathbb{Z}_6' and $T^6/\mathbb{Z}_2 \times \mathbb{Z}_6$ there is one vanishing angle leading to a Kähler modulus dependence of the gauge threshold along this two torus, whereas for T^6/\mathbb{Z}_3 , T^6/\mathbb{Z}_6 and $T^6/\mathbb{Z}_2 \times \mathbb{Z}_6$ the orbifold images intersect non-trivially along all three tori and the Gamma functions can be evaluated explicitly at the intersection angles, cf. table 14. On the other hand, the T^6/\mathbb{Z}_3 and $T^6/\mathbb{Z}_2 \times \mathbb{Z}_{2M}$ orbifolds without discrete torsion only have contributions from the untwisted annulus amplitude to the gauge thresholds, and the beta function coefficient appears as a global prefactor, whereas the T^6/\mathbb{Z}_{2N} and $T^6/\mathbb{Z}_2 \times \mathbb{Z}_{2M}$ orbifolds with discrete torsion ($2N, 2M \in \{6, 6'\}$) have \mathbb{Z}_2 twisted annulus amplitudes contributing to the gauge threshold. Since in the latter case, the beta function coefficient cannot be factored out of

the gauge thresholds, we conclude that (some of) the massive open string modes transform differently from the massless modes under the \mathbb{Z}_2 transformations.

2.2.5 Example 2: (anti)symmetric matter of $SO(2M_x)$ and $Sp(2M_x)$ gauge groups

The orientifold invariant D6-branes on the six-torus, T^6/\mathbb{Z}_3 and $T^6/\mathbb{Z}_2 \times \mathbb{Z}_{2M}$ orbifolds without discrete torsion wrap bulk three-cycles which are either parallel or perpendicular (along some four-torus) to some O6-plane. For T^6/\mathbb{Z}_{2N} and $T^6/\mathbb{Z}_2 \times \mathbb{Z}_{2M}$ orbifolds with discrete torsion, in addition the exceptional contributions to the fractional or rigid three-cycles have to be mapped to themselves in order to obtain orientifold invariant three-cycles. A classification of these three-cycles for the T^6/\mathbb{Z}'_6 background is given in [41], [6, 42] contain some examples and comments for T^6/\mathbb{Z}_6 and some explicit examples on these two orbifolds are discussed in appendix A.3 of [40]; finally for $T^6/\mathbb{Z}_2 \times \mathbb{Z}_{2M}$ with discrete torsion the complete classification in table 5 is reproduced from [46]; for T^6/\mathbb{Z}_4 there exists to our knowledge no discussion of $\Omega\mathcal{R}$ invariant fractional D6-branes.

The beta function coefficients and gauge thresholds from the xx sector of orientifold invariant $D6_x$ -branes on all factorisable toroidal orbifolds background are listed in table 15 together with the amount of supersymmetry preserved by the $D6_x$ -brane and the type of gauge group and matter content from the xx -sector.

While the gauge group and matter content from the xx -sector is independent of the background lattice orientations - but the bulk wrapping numbers and discrete Wilson lines and displacements of an invariant three-cycle depend on the lattice - the matter content at intersections of orbifold image $D6_{(\theta^k x)}$ -branes depends on the $\Omega\mathcal{R}$ -invariance of the intersection points and therefore the background lattice. Some examples on T^6/\mathbb{Z}_6 and T^6/\mathbb{Z}'_6 are given in appendix A.3 of [40]. A complete analysis is time-consuming and at this point not very illuminating, but we have given the fully generic prescription for evaluating examples in the previous sections, and for T^6/\mathbb{Z}'_6 the examples of $Sp(2)_c$ and $Sp(6)_{h_3}$ gauge groups perpendicular and parallel along $T^2_{(2)}$ to the O6-planes, respectively, are evaluated in section 5.

2.3 Comments on anomaly-free $U(1)$ gauge groups

For $U(1)_a \subset U(N_a)$ gauge couplings, the normalisation of the tree level gauge coupling (18) changes compared to the non-Abelian $SU(N_a) \subset U(N_a)$ factor (see e.g. [56, 2]),

$$\frac{1}{g_{U(1)_a, \text{tree}}^2} = \frac{2N_a}{g_{a, \text{tree}}^2}, \quad (34)$$

and for massless linear combinations of Abelian gauge factors, $U(1)_X = \sum_i x_i U(1)_i$, the tree level gauge coupling is a sum of contributions from different D6_i-branes,

$$\frac{1}{g_X^2} = \sum_i x_i^2 \frac{1}{g_{U(1)_i}^2}. \quad (35)$$

At one-loop, the beta function coefficient contains the same factor $2N_a$ compared to the $SU(N_a)$ case, and adjoint matter of $U(N_a)$ is uncharged under $U(1)_a$, whereas symmetric and antisymmetric matter has twice the charge of states transforming in the fundamental representation. The result for a single (unphysical) $U(1)_a$ gauge factor,

$$\begin{aligned} b_{U(1)_a} &= 2 N_a \left(\underbrace{N_a (\varphi^{\text{Sym}_a} + \varphi^{\text{Anti}_a})}_{2 b_{aa'}^A} + \underbrace{(\varphi^{\text{Sym}_a} - \varphi^{\text{Anti}_a})}_{b_{aa'}^M} + \underbrace{\sum_{b \neq a} \frac{N_b}{2} (\varphi^{ab} + \varphi^{ab'})}_{\sum_{b \neq a} (b_{ab}^A + b_{ab'}^A)} \right) \\ &\equiv 2 N_a \left(2 b_{aa'}^A + b_{aa'}^M + \sum_{b \neq a} (b_{ab}^A + b_{ab'}^A) \right), \end{aligned} \quad (36)$$

can be directly compared to the $SU(N_a)$ beta function coefficient in (14).

For massless $U(1)_X$ factors, the beta function coefficient consists of a sum over the beta function coefficients per D6_i-brane plus corrections from bifundamental matter on two such D6-branes [2],

$$b_{U(1)_X} = \sum_i x_i^2 b_{U(1)_i} + 2 \sum_{i < j} N_i N_j x_i x_j \left(-\varphi^{ij} + \varphi^{ij'} \right). \quad (37)$$

Also the gauge threshold corrections to a single $U(1)_a$ factor due to massive strings running in the loop can be expressed in terms of the building blocks $\tilde{\Delta}$ for the $SU(N_a)$ case [46],

$$\begin{aligned} \Delta_{U(1)_a} &= 2 N_a \left(2 N_a \tilde{\Delta}_{aa'} + \Delta_{a, \Omega \mathcal{R}} + \sum_{b \neq a} N_b (\tilde{\Delta}_{ab} + \tilde{\Delta}_{ab'}) \right) \\ &= 2 N_a \left(\Delta_{SU(N_a)} + N_a (\tilde{\Delta}_{aa'} - \tilde{\Delta}_{aa}) \right), \end{aligned} \quad (38)$$

and finally the gauge thresholds for massless linear combinations $U(1)_X$ are given by

$$\Delta_{U(1)_X} = \sum_i x_i^2 \Delta_{U(1)_i} + 4 \sum_{i < j} N_i N_j x_i x_j \left(-\tilde{\Delta}_{ij} + \tilde{\Delta}_{ij'} \right). \quad (39)$$

This completes the necessary input data for deriving the holomorphic gauge kinetic function of Abelian gauge factors, which are included in the general discussion in the following section.

3 Kähler metrics, Kähler potential and holomorphic gauge kinetic function at one loop

In the previous section, the corrections to the gauge couplings were computed via string one-loop amplitudes leading to formula (17). In field theory, the gauge couplings are given by [57, 58]

$$\begin{aligned} \frac{8\pi^2}{g_a^2(\mu)} = & 8\pi^2 \Re(f_a) + \frac{b_a}{2} \ln \left(\frac{M_{\text{Planck}}^2}{\mu^2} \right) + \frac{b_a + 2 C_2(\mathbf{Adj}_a)}{2} \mathcal{K} \\ & + C_2(\mathbf{Adj}_a) \ln[g_a^{-2}(\mu^2)] - \sum_a C_2(\mathbf{R}_a) \ln \det K_{\mathbf{R}_a}(\mu^2), \end{aligned} \quad (40)$$

where f_a is the holomorphic gauge kinetic function, $K_{\mathbf{R}_a}$ the Kähler metric of the representation \mathbf{R}_a under the gauge group and $C_2(\mathbf{R}_a)$ the quadratic Casimir with $\mathbf{R}_a \in \{(\mathbf{N}_a, \overline{\mathbf{N}}_b), (\mathbf{N}_a, \mathbf{N}_b), \mathbf{Anti}_a, \mathbf{Sym}_a, \mathbf{Adj}_a\}$ (or some complex conjugate) of $U(N_a) \times U(N_b)$ for D-brane models, and $SO(2M_x)$ or $Sp(2M_x)$ in case of orientifold invariant D-branes. \mathcal{K} denotes the Kähler potential and b_a the beta function coefficient of the gauge group $G_a \in \{SU(N_a), SO(2M_a), Sp(2M_a), U(1)_a\}$.

3.1 Tree level gauge kinetic function

The holomorphic gauge kinetic function and Kähler metrics are obtained by matching the expressions (17) and (40) stepwise, namely first at tree level,

$$\frac{1}{g_{a,\text{tree}}^2} = \frac{(2\pi)^{3/2}}{c_a k_a} \left(S \prod_{l=1}^3 U_l \right)^{1/4} \prod_{i=1}^3 \sqrt{V_{aa}^{(i)}} \stackrel{!}{=} \Re(f_a^{\text{tree}}), \quad (41)$$

where $h_{21}^{\text{bulk}} = 3$ has been used and S and U_l are the four dimensional dilaton and bulk complex structure moduli defined in equation (48) below. Modifications for $h_{21}^{\text{bulk}} = 1, 0$ are

discussed in section 3.2.2 below. The factor $\prod_{i=1}^3 \sqrt{V_{aa}^{(i)}}$, which is the ratio of the three-cycle volume to the square root of the total compact volume and depends on the ratios of two-torus radii (cf. the definition in equation (4)), reduces to a holomorphic expression of the complex structure moduli upon supersymmetry as follows. A generic three-cycle can be decomposed into orientifold even and odd components,

$$\Pi_a = \sum_{i=0}^{h_{21}} \left(\tilde{X}_a^i \Pi_i^{\text{even}} + \tilde{Y}_a^i \Pi_i^{\text{odd}} \right), \quad \Pi_{a'} = \sum_{i=0}^{h_{21}} \left(\tilde{X}_a^i \Pi_i^{\text{even}} - \tilde{Y}_a^i \Pi_i^{\text{odd}} \right), \quad (42)$$

and in terms of the corresponding wrapping numbers $(\tilde{X}_a^i, \tilde{Y}_a^i)$, the bulk supersymmetry conditions can be cast into the form

$$\sum_{i=0}^{h_{21}^{\text{bulk}}} \tilde{Y}_a^i f_i(r_k) = 0, \quad \sum_{i=0}^{h_{21}^{\text{bulk}}} \tilde{X}_a^i g_i(r_k) > 0, \quad (43)$$

where $f_i(r_k)$ and $g_i(r_k)$ are functions of the ratio of radii r_k of the three two-tori $T_{(k)}^2$ that can be rewritten in terms of linear dependences on the dilaton and bulk complex structure moduli, cf. equation (48) below. For a suitable choice of the global prefactor in the functions $f_i(r_k)$ and $g_i(r_k)$, one can show on a case-by-case basis that the $(\text{length})^2$ of the bulk three-cycles can be written as

$$\prod_{i=1}^3 V_{aa}^{(i)} = \left[\sum_{i=0}^{h_{21}^{\text{bulk}}} \tilde{X}_a^i g_i(r_k) \right]^2 + \left[\sum_{i=0}^{h_{21}^{\text{bulk}}} \tilde{Y}_a^i f_i(r_k) \right]^2, \quad (44)$$

where the second term drops out due to supersymmetry and the first term is the square of a holomorphic function which is linear in the dilaton and bulk complex structure moduli and depends on the choice of the orbifold and orientifold invariant background lattice. At this point, we discuss the six-torus and its T^6/\mathbb{Z}_2 and $T^6/\mathbb{Z}_2 \times \mathbb{Z}_2$ orbifolds in detail, while the orbifolds T^6/\mathbb{Z}_4 and $T^6/\mathbb{Z}_2 \times \mathbb{Z}_4$ as well as T^6/\mathbb{Z}'_6 and $T^6/\mathbb{Z}_2 \times \mathbb{Z}_6$ with one bulk complex structure modulus each and T^6/\mathbb{Z}_6 and $T^6/\mathbb{Z}_2 \times \mathbb{Z}'_6$ without bulk complex structures are relegated to appendix B.1 to B.3.

For arbitrary untilted **a**-type and tilted **b**-type lattices ($b_i \in \{0, \frac{1}{2}\}$), the $\Omega\mathcal{R}$ -even and odd bulk three cycles on $T^6/\mathbb{Z}_2 \times \mathbb{Z}_2$ are given by (with (i, j, k) cyclic permutations of $(1, 2, 3)$),

see e.g. [59, 8, 46])

$$\begin{aligned}
\Pi_0^{\text{even}} &= \left(\prod_{i=1}^3 \frac{1}{1-b_i} \right) \left(\Pi_{135} - \sum_{i=1}^3 b_i \Pi_{2i;2j-1;2k-1} + \sum_{k=1}^3 b_i b_j \Pi_{2i;2j;2k-1} - b_1 b_2 b_3 \Pi_{246} \right), \\
\Pi_i^{\text{even}} &= \frac{1}{1-b_i} \left(\Pi_{2i-1;2j;2k} - b_i \Pi_{246} \right), \\
\Pi_0^{\text{odd}} &= \Pi_{246}, \\
\Pi_i^{\text{odd}} &= \frac{1}{(1-b_j)(1-b_k)} \left(\Pi_{2i;2j-1;2k-1} - b_j \Pi_{2i;2j;2k-1} - b_k \Pi_{2i;2j-1;2k} + b_j b_k \Pi_{246} \right),
\end{aligned} \tag{45}$$

with non-vanishing intersection numbers

$$\Pi_K^{\text{even}} \circ \Pi_L^{\text{odd}} = -4 \left(\prod_{i=1}^3 \frac{1}{1-b_i} \right) \delta_{KL} \quad \text{for} \quad K, L \in \{0 \dots 3\}.$$

The coefficients of orientifold even and odd bulk three-cycles are as usual given by (see e.g. [59, 8])

$$\begin{aligned}
\tilde{X}_a^0 &\equiv \prod_{i=1}^3 n_a^i, & \tilde{X}_a^i &\equiv n_a^i (m_a^j + b_j n_a^j) (m_a^k + b_k n_a^k), \\
\tilde{Y}_a^0 &\equiv \prod_{i=1}^3 (m_a^i + b_i n_a^i), & \tilde{Y}_a^i &\equiv (m_a^i + b_i n_a^i) n_a^j n_a^k,
\end{aligned} \tag{46}$$

and the bulk supersymmetry conditions read

$$\tilde{Y}_a^0 - \sum_{i=1}^3 \frac{1}{r_j r_k} \tilde{Y}_a^i = 0, \quad \tilde{X}_a^0 - \sum_{i=1}^3 (r_j r_k) \tilde{X}_a^i > 0, \tag{47}$$

which leads to the expression for the (length)² of a bulk three-cycle

$$\begin{aligned}
\prod_{i=1}^3 V_{aa}^{(i)} &= \prod_{i=1}^3 \frac{1}{r_i} ((n_a^i)^2 + r_i^2 (m_a^i + b_i n_a^i)^2) \\
&= \frac{1}{(r_1 r_2 r_3)} \left[\left(\tilde{X}_a^0 - \sum_{i=1}^3 (r_j r_k) \tilde{X}_a^i \right)^2 + (r_1 r_2 r_3)^2 \left(\tilde{Y}_a^0 - \sum_{i=1}^3 \frac{1}{r_j r_k} \tilde{Y}_a^i \right)^2 \right] \\
&\stackrel{\text{SUSY}}{=} \left(\frac{1}{\sqrt{r_1 r_2 r_3}} \tilde{X}_a^0 - \sum_{i=1}^3 \sqrt{\frac{r_j r_k}{r_i}} \tilde{X}_a^i \right)^2,
\end{aligned}$$

where on the second line, the identities $\tilde{X}_a^0 \tilde{X}_a^i = \tilde{Y}_a^j \tilde{Y}_a^k$ and $\tilde{Y}_a^0 \tilde{Y}_a^i = \tilde{X}_a^j \tilde{X}_a^k$ have been used. In terms of the notation in equations (43) and (44), the functions are $f(r_1, r_2, r_3) =$

$\left(\sqrt{r_1 r_2 r_3}, -\sqrt{\frac{r_i}{r_j r_k}}\right)$ and $\vec{g}(r_1, r_2, r_3) = \left(\frac{1}{\sqrt{r_1 r_2 r_3}}, -\sqrt{\frac{r_j r_k}{r_i}}\right)$ for $T^6/\mathbb{Z}_2 \times \mathbb{Z}_2$ with (i, j, k) cyclic permutations of $(1, 2, 3)$.

Defining the four dimensional field theoretical dilaton and complex structure moduli fields at tree level via the ratios of radii and the stringy dilaton $e^{\phi_4} = \frac{e^{\phi_{10}}}{\sqrt{v_1 v_2 v_3}}$,

$$S \sim \frac{e^{-\phi_4}}{\sqrt{r_1 r_2 r_3}}, \quad U_i \sim e^{-\phi_4} \sqrt{\frac{r_j r_k}{r_i}}, \quad (48)$$

the gauge couplings for supersymmetric D6-branes thus take the form

$$\Re(f_{SU(N_a)}^{\text{tree}}) \stackrel{!}{=} \frac{1}{g_{a,\text{tree}}^2} \sim \frac{1}{k_a c_a} \left(S \tilde{X}_a^0 - \sum_{i=1}^3 U_i \tilde{X}_a^i \right) \quad \text{on } T^6/(\mathbb{Z}_2 \times \mathbb{Z}_2 \times \Omega\mathcal{R}), \quad (49)$$

with the constants c_a and k_a related to the type of D6-brane and gauge group, respectively, as defined in equation (18).

Other toroidal orbifolds have a reduced number of bulk complex structures due to some underlying \mathbb{Z}_3 or \mathbb{Z}_4 symmetry leading to similar expressions as (49) for the tree level holomorphic gauge kinetic function with the sum running over $h_{21}^{\text{bulk}} = 1, 0$. The corresponding modifications are discussed in section 3.2.2 below.

3.2 One-loop results for T^6 and T^6/\mathbb{Z}_2 and $T^6/\mathbb{Z}_2 \times \mathbb{Z}_2$ with $\eta = \pm 1$

The one-loop corrections to both formulas (17) and (40) can be decomposed according to the open string sectors with identical ($a = b$) or different endpoints ($a \neq b$), cf. the decomposition of gauge thresholds in (27). The case $a \neq b$ also includes orbifold ($b = (\theta^k a)$ or $(\omega^k a)$) and orientifold ($b = (\theta^k a')$ or $(\omega^k a')$) image D6-branes. The following discussion focuses on $SU(N_a)$ gauge groups on the $T^6/\mathbb{Z}_2 \times \mathbb{Z}_2$ orientifolds without and with discrete torsion as well as the six-torus and $T^4/\mathbb{Z}_2 \times T^2$. This covers all cases of bulk, fractional and rigid D6-branes. Additional \mathbb{Z}_3 or \mathbb{Z}_4 symmetries lead to a reduced number of bulk complex structures and thus a modified universal global prefactor $f(S, U_i)$ of the open string Kähler metrics as detailed in section 3.2.2 below. Comments on other types of gauge groups $SO(2M)$, $Sp(2M)$ and $U(1)_X$ are given in section 3.3 and 3.4, respectively.

- Strings with endpoints on identical branes aa provide the vector multiplet in the adjoint representation of $SU(N_a)$ and three, one or no chiral multiplet in the adjoint representation, i.e. $\varphi^{\text{Adj}_a} = 3, 1, 0$ for $T^6/\mathbb{Z}_2 \times \mathbb{Z}_2$ without torsion, $T_{(1,3)}^4/\mathbb{Z}_2 \times T_{(2)}^2$ and $T^6/\mathbb{Z}_2 \times \mathbb{Z}_2$ with discrete torsion, respectively.

The result from the one-loop string computation needs to be matched by all those field theory contributions describing the dynamics of the same fields,

$$\begin{aligned} \frac{b_{aa}^A}{2} \ln \left(\frac{M_{\text{string}}}{\mu} \right)^2 + \frac{N_a \tilde{\Delta}_{aa}}{2} &\stackrel{!}{=} \frac{b_{aa}^A}{2} \ln \left(\frac{M_{\text{Planck}}}{\mu} \right)^2 + \frac{b_{aa}^A + 2C_2(\mathbf{Adj}_a)}{2} \mathcal{K} + \\ &+ C_2(\mathbf{Adj}_a) \ln [g_a^{-2}(\mu^2)] - \sum_{i=1}^{\varphi^{\mathbf{Adj}_a}} C_2(\mathbf{Adj}_a) \ln K_{\mathbf{Adj}_a}^{(i)} \\ &+ 8\pi^2 \Re(\delta_a f_{SU(N_a)}^{1\text{-loop}}), \end{aligned}$$

where $f_{SU(N_a)}^{1\text{-loop}} = f_{SU(N_a)}^{\text{tree}} + \sum_b \delta_b f_{SU(N_a)}^{1\text{-loop}}$ constitutes the perturbatively exact result for the holomorphic gauge kinetic function and the terms $C_2(\mathbf{Adj}_a) (\mathcal{K} + \ln [g_a^{-2}(\mu^2)])$ on the r.h.s. only occur for the case of identical D6-branes. The beta function coefficients and gauge thresholds for the aa sector are given in table 13. The Kähler metrics for the adjoint matter multiplets on identical D6-branes are derived in an iterative procedure since we explicitly insert the tree level gauge coupling in the logarithm on the r.h.s. and only take into account the Kähler potential for the bulk closed string moduli and the dilaton,

$$\begin{aligned} 0 &\stackrel{!}{=} \frac{-3 + \varphi^{\mathbf{Adj}_a}}{2} \left[\ln \left(\frac{M_{\text{Planck}}}{M_{\text{string}}} \right)^2 + \mathcal{K}_{\text{bulk}} \right] + \mathcal{K}_{\text{bulk}} + \ln [g_{a,\text{tree}}^{-2}] \\ &- \sum_{i=1}^{\varphi^{\mathbf{Adj}_a}} \ln K_{\mathbf{Adj}_a}^{(i)} + \frac{8\pi^2}{N_a} \Re(\delta_a f_{SU(N_a)}^{1\text{-loop}}) - \frac{\tilde{\Delta}_{aa}}{2}, \end{aligned} \quad (50)$$

where the value of the quadratic Casimir of the adjoint representation, $C_2(\mathbf{Adj}_a) = 2N_a C_2(\mathbf{N}_a) = N_a$, has been inserted.

Using the form of tree level gauge coupling in equation (41) and the definition of the dilaton and bulk complex structure moduli in (48) together with the standard ansatz for the Kähler potential for the closed string bulk fields,

$$\mathcal{K}_{\text{bulk}} = -\ln S - \sum_{i=1}^3 \ln U_i - \sum_{i=1}^3 \ln v_i, \quad (51)$$

the first line in (50) can be rewritten as (with $k_a = 1$ for $SU(N_a)$)

$$\begin{aligned} &\frac{-3 + \varphi^{\mathbf{Adj}_a}}{2} \left[\ln \left(\frac{M_{\text{Planck}}}{M_{\text{string}}} \right)^2 + \mathcal{K}_{\text{bulk}} \right] + \mathcal{K}_{\text{bulk}} + \ln [g_{a,\text{tree}}^{-2}] \\ &= \frac{-3 + \varphi^{\mathbf{Adj}_a}}{2} \left[\ln (S \prod_{i=1}^3 U_i)^{1/2} - \ln (S \prod_{i=1}^3 U_i v_i) \right] - \ln (S \prod_{i=1}^3 U_i v_i) \\ &\quad + \ln \left[(S \prod_{i=1}^3 U_i)^{1/4} \frac{(2\pi)^{3/2} \prod_{i=1}^3 \sqrt{V_{aa}^{(i)}}}{c_a} \right] \\ &= -\frac{\varphi^{\mathbf{Adj}_a}}{4} \ln (S \prod_{i=1}^3 U_i) + \frac{1 - \varphi^{\mathbf{Adj}_a}}{2} \ln (\prod_{i=1}^3 v_i) + \ln \left(\frac{(2\pi)^{3/2} \prod_{i=1}^3 \sqrt{V_{aa}^{(i)}}}{c_a} \right). \end{aligned} \quad (52)$$

In order to rewrite the second line in (50), the gauge threshold contributions can be read off from table 13,

$$\frac{\tilde{\Delta}_{aa}}{2} = \frac{2}{c_a} \begin{cases} 0 & T^6 \text{ and } T^6/\mathbb{Z}_2 \times \mathbb{Z}_{2M} \text{ with } \eta = 1 \\ \Lambda_{0,0}(v_2; V_{aa}^{(2)}) & T^6/\mathbb{Z}_{2N} \\ \sum_{i=1}^3 \Lambda_{0,0}(v_i; V_{aa}^{(i)}) & T^6/\mathbb{Z}_2 \times \mathbb{Z}_{2M} \text{ with } \eta = -1 \end{cases},$$

with the lattice sums defined in (25) and $c_a = 1, 2, 4$ for bulk, fractional and rigid D6-branes, respectively. With the ansatz for the Kähler metrics analogous to the six-torus [44] (with (ijk) cyclic permutations of (123) and i the index associated to the continuous displacement and Wilson line modulus on $T_{(i)}^2$),

$$K_{\mathbf{Adj}_a}^{(i)} = \frac{\sqrt{2\pi}}{c_a} \frac{f(S, U_l)}{v_i} \sqrt{\frac{V_{aa}^{(j)} V_{aa}^{(k)}}{V_{aa}^{(i)}}} \quad \text{with} \quad f(S, U_l) = \left(S \prod_{l=1}^3 U_l \right)^{-1/4}, \quad (53)$$

and the one-loop contribution to the holomorphic gauge kinetic function,

$$\delta_a f_{SU(N_a)}^{1\text{-loop}} = \frac{N_a}{\pi^2 c_a} \times \begin{cases} 0 & T^6 \text{ and } T^6/\mathbb{Z}_2 \times \mathbb{Z}_{2M} \text{ with } \eta = 1 \\ \ln \eta(iv_2) & T^6/\mathbb{Z}_{2N} \\ \sum_{i=1}^3 \ln \eta(iv_i) & T^6/\mathbb{Z}_2 \times \mathbb{Z}_{2M} \text{ with } \eta = -1 \end{cases}, \quad (54)$$

the second line of (50) can be recast for the various torus and orbifold backgrounds as follows.

– On T^6 and $T^6/\mathbb{Z}_2 \times \mathbb{Z}_2$ without discrete torsion, the second line reads

$$\begin{aligned} & - \sum_{i=1}^{\varphi^{\mathbf{Adj}_a}} \ln K_{\mathbf{Adj}_a}^{(i)} + \frac{8\pi^2}{N_a} \Re(\delta_a f_{SU(N_a)}^{1\text{-loop}}) - \frac{\tilde{\Delta}_{aa}}{2} \\ & = - \ln \left[\frac{(2\pi)^{3/2} \sqrt{V_{aa}^{(1)} V_{aa}^{(2)} V_{aa}^{(3)}}}{c_a^3 v_1 v_2 v_3 (S \prod_{l=1}^3 U_l)^{3/4}} \right] + \emptyset + \emptyset \\ & = - \ln \frac{(2\pi)^{3/2} \sqrt{\prod_{i=1}^3 V_{aa}^{(i)}}}{c_a^3} + \ln \left(\prod_{i=1}^3 v_i \right) + \frac{3}{4} \ln \left(S \prod_{l=1}^3 U_l \right), \end{aligned}$$

and exactly cancels the first line (52) of (50) since $c_a = 1$ for toroidal three-cycles, $k_a = 1$ for $SU(N_a)$ gauge groups and because there exist three adjoint multiplets, $\varphi^{\mathbf{Adj}_a} = 3$, related to the continuous displacement and Wilson line moduli per two-torus. The ansatz for the bulk Kähler potential (51), adjoint Kähler metrics on identical D6-branes (53) and one-loop contribution to the holomorphic gauge kinetic function (54) are thus mutually consistent.

- On $T^4_{(1,3)}/\mathbb{Z}_2 \times T^2_{(2)}$, there exists one adjoint multiplet, $\varphi^{\mathbf{Adj}_a} = 1$, related to the Wilson line and displacement modulus on the two-torus $T^2_{(2)}$ without \mathbb{Z}_2 twist, and the gauge threshold receives lattice sum contributions from this two-torus,

$$\begin{aligned}
& - \sum_{i=1}^{\varphi^{\mathbf{Adj}_a}} \ln K_{\mathbf{Adj}_a}^{(i)} + \frac{8\pi^2}{N_a} \Re(\delta_a f_{SU(N_a)}^{1-\text{loop}}) - \frac{\tilde{\Delta}_{aa}}{2} \\
& = - \ln \left[\frac{\sqrt{2\pi}}{c_a v_2 (S \prod_{l=1}^3 U_l)^{1/4}} \sqrt{\frac{V_{aa}^{(1)} V_{aa}^{(3)}}{V_{aa}^{(2)}}} \right] + \frac{8}{c_a} \ln \eta(iv_2) - \frac{2}{c_a} [4 \ln \eta(iv_2) + \ln (2\pi v_2 V_{aa}^{(2)})] \\
& = \frac{1}{4} \ln \left(S \prod_{l=1}^3 U_l \right) - \ln \frac{(2\pi)^{3/2} \prod_{i=1}^3 \sqrt{V_{aa}^{(i)}}}{c_a}.
\end{aligned}$$

Due to $c_a = 2$ for fractional D6-branes on orbifolds with one \mathbb{Z}_2 (sub)symmetry and $k_a = 1$ for $SU(N_a)$, the ansatz for the bulk Kähler potential (51) and Kähler metrics (53) and holomorphic gauge kinetic function (54) are again mutually consistent.

- On $T^6/\mathbb{Z}_2 \times \mathbb{Z}_2$ with discrete torsion, the aa sector does not contain any chiral multiplet, $\varphi_{\mathbf{Adj}_a} = 0$, due to the discrete character of the displacements and Wilson lines, and with $c_a = 4$ for rigid D6-branes on orbifolds with $\mathbb{Z}_2 \times \mathbb{Z}_2$ (sub)symmetry and discrete torsion,

$$\begin{aligned}
& - \sum_{i=1}^{\varphi^{\mathbf{Adj}_a}} \ln K_{\mathbf{Adj}_a}^{(i)} + \frac{8\pi^2}{N_a} \Re(\delta_a f_{SU(N_a)}^{1-\text{loop}}) - \frac{\tilde{\Delta}_{aa}}{2} \\
& = \emptyset + \frac{8}{c_a} \sum_{i=1}^3 \ln \eta(iv_i) - \frac{2}{c_a} \sum_{i=1}^3 [4 \ln \eta(iv_i) + \ln (2\pi v_i V_{aa}^{(i)})] \\
& = -\frac{1}{2} \ln \left(\prod_{i=1}^3 v_i \right) - \ln \left((2\pi)^{3/2} \prod_{i=1}^3 \sqrt{V_{aa}^{(i)}} \right),
\end{aligned}$$

the second line of (50) cancels the first line (52) as expected.

This completes the discussion of the aa sector for the six-torus and its orbifolds $T^4/\mathbb{Z}_2 \times T^2$ and $T^6/\mathbb{Z}_2 \times \mathbb{Z}_2$ without and with discrete torsion. Changes due to the existence of a reduced number of bulk complex structure moduli on other toroidal orbifolds amount to modifications in the prefactor $f(S, U_l)$ in (53) and changes in the prefactors of the dilaton and bulk complex structure contributions to the Kähler potential (51) as discussed in section 3.2.2.

- For strings with endpoints on two different D6-branes a and b and $b \neq (\omega^k a), (\omega^l a')$ for any k, l , the generic form of matching the string and field theory calculation is

simpler since the term $C_2(\mathbf{Adj}_a) (\mathcal{K} + \ln[g_a^{-2}(\mu)^2])$ has already been taken care of in the aa sector,

$$\begin{aligned} \frac{b_{ab}^A}{2} \ln \left(\frac{M_{\text{string}}}{\mu} \right)^2 + \frac{N_a \tilde{\Delta}_{ab}}{2} &\stackrel{!}{=} \frac{b_{ab}^A}{2} \ln \left(\frac{M_{\text{Planck}}}{\mu} \right)^2 + \frac{b_{ab}^A}{2} \mathcal{K} + \\ &- \sum_{i=1}^{\varphi(\mathbf{N}_a, \overline{\mathbf{N}}_b)} N_b C_2(\mathbf{N}_a) \ln K_{(\mathbf{N}_a, \overline{\mathbf{N}}_b)}^{(i)} + 8\pi^2 \Re(\delta_b f_{SU(N_a)}^{1-\text{loop}}). \end{aligned}$$

Using the value $C_2(\mathbf{N}_a) = \frac{1}{2}$ for the quadratic Casimir of the fundamental representation, this matching condition can be rewritten as

$$\begin{aligned} 0 &\stackrel{!}{=} \frac{b_{ab}^A}{2} \left(\ln \left(\frac{M_{\text{Planck}}}{M_{\text{string}}} \right)^2 + \mathcal{K}_{\text{bulk}} \right) - \sum_{i=1}^{\varphi(\mathbf{N}_a, \overline{\mathbf{N}}_b)} \frac{N_b}{2} \ln K_{(\mathbf{N}_a, \overline{\mathbf{N}}_b)}^{(i)} + 8\pi^2 \Re(\delta_b f_{SU(N_a)}^{1-\text{loop}}) - \frac{\Delta_{ab}}{2} \\ &= -\frac{b_{ab}^A}{2} \ln \left[\left(S \prod_{i=1}^3 U_i \right)^{1/2} \left(\prod_{i=1}^3 v_i \right) \right] - \sum_{i=1}^{\varphi(\mathbf{N}_a, \overline{\mathbf{N}}_b)} \frac{N_b}{2} \ln K_{(\mathbf{N}_a, \overline{\mathbf{N}}_b)}^{(i)} + 8\pi^2 \Re(\delta_b f_{SU(N_a)}^{1-\text{loop}}) - \frac{\Delta_{ab}}{2}, \end{aligned} \tag{55}$$

where on the second line the relation of the mass scales in terms of the dilaton and bulk complex structure moduli defined in (48) as well as the bulk Kähler potential (51) have been used. For the six-torus considered in [44], all multiplets in a given representations are on equal footing, and the sum over logarithms of Kähler metrics on the second line of (55) boils down to $-b_{ab}^A \ln K_{(\mathbf{N}_a, \overline{\mathbf{N}}_b)}$. Since on the six-torus, also the gauge thresholds from open strings in the bifundamental representation in table 8 have the beta function coefficient b_{ab}^A as a global prefactor, the Kähler metrics can be read off in a straight forward manner. For orbifolds containing some $\mathbb{Z}_2^{(i)}$ symmetry, the gauge thresholds contain additional terms proportional to $I_{ab}^{\mathbb{Z}_2^{(i)}}$ times the angle $\phi_{ab}^{(i)}$ plus constants consisting of sign factors as displayed in tables 6 and 11 for bifundamental and adjoint matter, and terms proportional to the intersection numbers with the O6-planes for symmetric or antisymmetric matter on any torus or orbifold background as displayed in tables 7, 9, 10 and 12. We will first determine the Kähler metrics from the terms proportional to the beta function coefficients and argue further below that all the additional terms enter the one-loop corrections to the gauge kinetic functions. This leads to Kähler metrics which only depend on the (non-)vanishing of the angles, but are universal for all orbifold backgrounds and all (bifundamental, adjoint, symmetric, antisymmetric) matter representations. The non-trivial information on the background and matter representations is encoded in the beta function coefficients and modifies the one-loop contributions to the holomorphic gauge kinetic function.

The gauge threshold corrections from ab sectors computed in section 2 and the corresponding open string Kähler metrics and corrections to the holomorphic gauge kinetic functions fall into two distinct classes:

1. The D6-branes a and b under consideration are parallel along at least one two-torus. This includes the case with completely parallel D6-branes with different choices of \mathbb{Z}_2 eigenvalues, displacements or Wilson lines on T^6/\mathbb{Z}_{2N} and $T^6/\mathbb{Z}_2 \times \mathbb{Z}_2$ with discrete torsion. Following the argumentation of [44], the functional dependence of the Kähler metrics on the bulk moduli and the (length)² $V_{ab}^{(i)}$ on the two-torus $T_{(i)}^2$ where the branes are parallel is given by (with (ijk) a cyclic permutation of (123))

$$K_{(\mathbf{N}_a, \mathbf{N}_b)}^{(i)} = f(S, U_l) \sqrt{\frac{2\pi V_{ab}^{(i)}}{v_j v_k}}, \quad (56)$$

where $f(S, U_l)$ is defined in (53). The generic form of the functional dependence can be seen from the fact that beta function coefficient b_{ab}^A for one vanishing angle indeed appears in front of the lattice sums in tables 6, 10, 8 and 11 for $T^6/\mathbb{Z}_2 \times \mathbb{Z}_{2M}$ with and without discrete torsion, the six-torus and T^6/\mathbb{Z}_{2N} , respectively. On T^6/\mathbb{Z}_{2N} , the case of parallel D6-branes is of exactly the same type, whereas for $T^6/\mathbb{Z}_2 \times \mathbb{Z}_{2M}$ with discrete torsion the beta function coefficient needs to be decomposed into three contributions, reflecting the fact that the three different kinds of possible non-chiral bifundamental matter pairs correspond to the two-torus label i or in other words to opposite $\mathbb{Z}_2^{(j)}$ and $\mathbb{Z}_2^{(k)}$ and identical $\mathbb{Z}_2^{(i)}$ eigenvalues. Our present result is in contrast to [45], where the expression (53) was proposed also for bifundamental matter. However, in the derivation of (53) the term $C_2(\mathbf{Adj}_a)(\mathcal{K} + \ln[g_a^{-2}(\mu^2)])$ was assigned to the aa sector, and it cannot be again used for the ab contributions. The Kähler metrics for bifundamental matter on parallel or intersecting D6-branes in various toroidal orbifold backgrounds are summarised in table 16.

The one-loop contributions to the holomorphic gauge kinetic function from ab sectors, which depend on the two-torus volumes v_i , can be straightforwardly read off from the lattice sums in tables 6, 10, 8 and 11 for the various cases of open strings with endpoints on different D6-branes a and b , and the result is summarised in table 17. In the presence of some \mathbb{Z}_2 symmetry, the gauge threshold for D6-branes parallel along $T_{(i)}^2$ and at angles along $T_{(j)}^2 \times T_{(k)}^2$ contains additional terms

$$\Delta_{SU(N_a)} \supset -\frac{N_b}{c_a} \sum_{l=j,k} I_{ab}^{\mathbb{Z}_2^{(l)}} \left(2\phi_{ab}^{(l)} - \text{sgn}(\phi_{ab}^{(l)}) \right) \ln 2, \quad (57)$$

cf. tables 6 and 11 for $T^6/\mathbb{Z}_2 \times \mathbb{Z}_{2M}$ with discrete torsion and T^6/\mathbb{Z}_{2N} , respectively, where in the latter case $I_{ab}^{\mathbb{Z}_2^{(l)}} \equiv 0$ for $l \neq 2$. It is tempting to assign the terms (57) to some dependence of the Kähler metrics on the \mathbb{Z}_2 transformation properties of the matter localisations. However, it is possible to have (57) non-vanishing, while there is no massless matter state in the corresponding ab sector as discussed below for examples with three non-vanishing angles in the Standard Model on T^6/\mathbb{Z}'_6 . The term (57) is thus interpreted as an angle-dependent one-loop contribution to the holomorphic gauge kinetic function $\delta_b f_{SU(N_a)}^{\text{1-loop}}(\phi_{ab}^{(i)})$,

$$\Re \left(\delta_b f_{SU(N_a)}^{\text{1-loop}}(\phi_{ab}^{(i)}) \right) = -\frac{N_b}{16\pi^2 c_a} \sum_{l=j,k} I_{ab}^{\mathbb{Z}_2^{(l)}} \left(2\phi_{ab}^{(l)} - \text{sgn}(\phi_{ab}^{(l)}) \right) \ln 2, \quad (58)$$

which implicitly depends on the complex structure moduli through $\arctan(\phi_{ab}^{(l)}) \sim r_l$.

2. If the D6-branes are at angles on all three tori, the gauge threshold computation provides the functional dependence, cf. e.g. [44],

$$K_{(\mathbf{N}_a, \bar{\mathbf{N}}_b)} = f(S, U_l) \sqrt{\prod_{i=1}^3 \frac{1}{v_i} \left(\frac{\Gamma(|\phi_{ab}^{(i)}|)}{\Gamma(1 - |\phi_{ab}^{(i)}|)} \right)^{-\frac{\text{sgn}(\phi_{ab}^{(i)})}{\text{sgn}(I_{ab})}}}, \quad (59)$$

for all toroidal orbifold backgrounds, where all angles are chosen in the range $0 < |\phi_{ab}^{(i)}| < 1$ and obey the bulk supersymmetry condition $\sum_{i=1}^3 \phi_{ab}^{(i)} = 0$, and $f(S, U_l)$ has been defined in (53). The sign factor $\text{sgn}(I_{ab})$ in the exponential is essential for obtaining the same Kähler potential from the computations of the ab and its inverse ba sector and has to our knowledge not properly been taken into account before. The comparison of all bifundamental Kähler metrics is given in table 16.

The dependence on the two-torus volumes v_i is fully contained in the Kähler metrics (59), and there is no v_i dependent contribution to the holomorphic gauge kinetic functions. In the presence of \mathbb{Z}_2 symmetries, however, the gauge threshold contains additional terms proportional to the intersection angles $\phi_{ab}^{(i)}$,

$$\Delta_{SU(N_a)} \supset -\frac{N_b}{c_a} \sum_{i=1}^3 I_{ab}^{\mathbb{Z}_2^{(i)}} \left(2\phi_{ab}^{(i)} - \text{sgn}(\phi_{ab}^{(i)}) - \text{sgn}(I_{ab}) \right) \ln 2, \quad (60)$$

cf. tables 6 and 11. These terms have the identical shape as (57) for one vanishing angle along $T_{(i)}^2$ when taking into account that this leads to $\text{sgn}(I_{ab}) = 0$ and $I_{ab}^{\mathbb{Z}_2^{(i)}} = 0$. The case of the six-torus and the $T^6/\mathbb{Z}_2 \times \mathbb{Z}_{2M}$ orbifolds without torsion can be formally included by setting $I_{ab}^{\mathbb{Z}_2^{(i)}} \equiv 0$ for all i . Taking a look at the Standard Model example on T^6/\mathbb{Z}'_6 in table 29 reveals that there are

no massless states in the $xy \in \{a(\theta^k b)_{k=0,1,2}, a(\theta c), c(\theta^2 d)\}$ sectors, while the angles $\phi_{xy}^{(2)}$ in table 29 and intersection numbers $I_{xy}^{\mathbb{Z}_2^{(2)}}$ listed explicitly in [40] are non-vanishing. The term (60) can thus not be assigned to a change in the normalisation of Kähler metrics due to different matter localisations, but in complete analogy to (58) for one vanishing angle, it is instead interpreted as an angle dependent one-loop correction to the holomorphic gauge kinetic function,

$$\Re \left(\delta_b f_{SU(N_a)}^{1\text{-loop}}(\phi_{ab}^{(i)}) \right) = -\frac{N_b}{16\pi^2 c_a} \sum_{i=1}^3 I_{ab}^{\mathbb{Z}_2^{(i)}} \left(2\phi_{ab}^{(i)} - \text{sgn}(\phi_{ab}^{(i)}) - \text{sgn}(I_{ab}) \right) \ln 2, \quad (61)$$

which can be formally taken to hold for all supersymmetric configurations with vanishing or non-vanishing angles upon setting \mathbb{Z}_2 invariant intersection numbers or sign factors to zero as described above.

- At the intersection of orbifold image D6-branes a and $(\omega^k a)$, the matter states transform in the adjoint representation. The matching in equation (55) needs to be modified by using the corresponding quadratic Casimir, $C_2(\mathbf{Adj}_a) = N_a$,

$$0 \stackrel{!}{=} -\frac{b_{(\omega^k a)a}^A + b_{(\omega^{-k} a)a}^A}{2} \ln \left[\left(S \prod_{i=1}^3 U_i \right)^{1/2} \left(\prod_{i=1}^3 v_i \right) \right] - \sum_{i=1}^{\varphi \mathbf{Adj}_a} N_a \ln K_{(\mathbf{Adj}_a)}^{(i)} \quad (62)$$

$$+ 8\pi^2 \Re([\delta_{(\theta^k a)} + \delta_{(\theta^{-k} a)}] f_{SU(N_a)}^{1\text{-loop}}) - \frac{\Delta_{(\theta^k a)a} + \Delta_{(\theta^{-k} a)a}}{2},$$

where we have used that for orbifolds other than T^6/\mathbb{Z}_4 or $T^6/\mathbb{Z}_2 \times \mathbb{Z}_4$, the two degrees of freedom of a complex boson or Weyl fermion in the adjoint representation stem from the combination of one sector $(\theta^k a)a$ plus its inverse $(\theta^{-k} a)a$. As used in table 13, the gauge threshold and beta function contributions from inverse sectors are identical, $\Delta_{(\theta^k a)a} = \Delta_{(\theta^{-k} a)a}$ and $b_{(\omega^k a)a}^A = b_{(\omega^{-k} a)a}^A$, which means that the factor of two in the quadratic Casimir of the adjoint in (62) compared to the bifundamental in (55) is absorbed by the combination of inverse sectors, and therefore the Kähler metrics and v_i dependent loop corrections to the holomorphic gauge kinetic function are identical to those of bifundamentals at some non-vanishing intersection angles in tables 16 and 17. Also the angle dependent loop corrections to the holomorphic gauge kinetic function match (61).

- Last but not least, for orientifold image D6-branes a and a' the symmetric and antisymmetric representations \mathbf{Sym}_a and \mathbf{Anti}_a of $SU(N_a)$ have to be taken into

account,

$$\begin{aligned}
0 &\stackrel{!}{=} \frac{b_{aa'}^{\mathcal{A}} + b_{aa'}^{\mathcal{M}}}{2} \left[\ln \left(\frac{M_{\text{Planck}}}{M_{\text{string}}} \right)^2 + \mathcal{K}_{\text{bulk}} \right] - \sum_{i=1}^{\varphi_{\text{Anti}a}} \frac{N_a - 2}{2} \ln K_{\text{Anti}a}^{(i)} - \sum_{j=1}^{\varphi_{\text{Sym}a}} \frac{N_a + 2}{2} \ln K_{\text{Sym}a}^{(j)} \\
&\quad + 8\pi^2 \Re(\delta_{a'} f_{U(1)_a}^{1-\text{loop}}) - \frac{\Delta_{aa'} + \Delta_{a,\Omega\mathcal{R}}}{2} \\
&= - \frac{b_{aa'}^{\mathcal{A}} + b_{aa'}^{\mathcal{M}}}{2} \ln \left[\left(S \prod_{i=1}^3 U_i \right)^{1/2} \left(\prod_{i=1}^3 v_i \right) \right] - \frac{N_a}{2} \left(\sum_{i=1}^{\varphi_{\text{Anti}a}} \ln K_{\text{Anti}a}^{(i)} + \sum_{j=1}^{\varphi_{\text{Sym}a}} \ln K_{\text{Sym}a}^{(j)} \right) \\
&\quad - \left(\sum_{j=1}^{\varphi_{\text{Sym}a}} \ln K_{\text{Sym}a}^{(j)} - \sum_{i=1}^{\varphi_{\text{Anti}a}} \ln K_{\text{Anti}a}^{(i)} \right) + 8\pi^2 \Re(\delta_{a'} f_{SU(N_a)}^{1-\text{loop}}) - \frac{\Delta_{aa'} + \Delta_{a,\Omega\mathcal{R}}}{2},
\end{aligned} \tag{63}$$

where on the last two lines the Kähler metrics have been grouped into contributions from the annulus diagram with global prefactor $\frac{N_a}{2}$ and those from the Möbius strip without this factor. The gauge threshold contributions in tables 7, 9, 10 and 12 can be brought to a global form depending on the number of non-vanishing angles, where our notation is adopted to the $T^6/(\mathbb{Z}_2 \times \mathbb{Z}_{2M} \times \Omega\mathcal{R})$ orientifold with discrete torsion, and modifications for other torus and orbifold backgrounds boil down to setting some constants to zero. While for rigid D6-branes, the relative displacements and Wilson lines vanish identically, i.e. $\delta_{\sigma_{aa'},0}^i \delta_{\tau_{aa'},0}^i \equiv 1$ (cf. table 7), we keep the notation such that fractional and bulk D6-branes are taken into account in the following as well.

- D6-brane parallel to some $\Omega\mathcal{R}\mathbb{Z}_2^{(m)}$ plane with $m \in \{0 \dots 3\}$ on $T^6/\mathbb{Z}_2 \times \mathbb{Z}_{2M}$ with discrete torsion and $a \neq a'$ due to the exceptional three-cycles contribute

$$\begin{aligned}
\frac{\Delta_{aa'} + \Delta_{a,\Omega\mathcal{R}}}{2} &= - \frac{1}{2} \sum_{i=1}^3 \left(b_{aa'}^{\mathcal{A},(i)} \Lambda_{0,0}(v_i; V_{aa'}^{(i)}) + b_{aa'}^{\mathcal{M},(i)} \Lambda_{0,0}(\tilde{v}_i; 2\tilde{V}_{aa'}^{(i)}) \right) \\
&\quad - \frac{1}{2} \sum_{i=1}^3 \left(1 - \delta_{\sigma_{aa'},0}^i \delta_{\tau_{aa'},0}^i \right) \left(\tilde{b}_{aa'}^{\mathcal{A},(i)} \Lambda(\sigma_{aa'}^i, \tau_{aa'}^i, v_i) + \tilde{b}_{aa'}^{\mathcal{M},(i)} \Lambda(\sigma_{aa'}^i, \tau_{aa'}^i, \tilde{v}_i) \right)
\end{aligned} \tag{64}$$

to the gauge threshold, cf. table 7. This is modified for other backgrounds as follows:

- * T^6 : The annulus amplitude preserves $\mathcal{N} = 4$ supersymmetry with $b_{aa'}^{\mathcal{A},(i)} \equiv 0$ for $i = 1, 2, 3$. For the Möbius strip two cases need to be distinguished, cf. table 9.
 - If the D6-brane a is parallel to the $\Omega\mathcal{R}$ plane, also the Möbius strip contribution preserves $\mathcal{N} = 4$ and consequently $b_{aa'}^{\mathcal{M},(i)} \equiv 0$ for all i . For $(\vec{\sigma}_{aa'}, \vec{\tau}_{aa'}) = (\vec{0}, \vec{0})$, the gauge group is enhanced to $SO(2N_a)$, cf.

tables 15 and 19, otherwise the symmetric and antisymmetric matter states receive a mass, and the matching condition (63) is trivially fulfilled.

- If the D6-brane a is parallel to some $\Omega\mathcal{R}\mathbb{Z}_2^{(m)}$ plane with $m \in \{1, 2, 3\}$, the Möbius strip amplitude only preserves $\mathcal{N} = 2$ supersymmetry, i.e. $b_{aa'}^{\mathcal{M},(m)} \neq 0$ and $b_{aa'}^{\mathcal{M},(n)} \equiv 0 \equiv b_{aa'}^{\mathcal{M},(p)}$, where (m, n, p) is a cyclic permutation of $(1, 2, 3)$. The gauge group is of $U(N_a)$ type for $(\sigma_{aa'}^m, \tau_{aa'}^m) \neq (0, 0)$ and $Sp(2M_a)$ otherwise, cf. tables 15 and 19.
- * T^6/\mathbb{Z}_{2N} : The annulus amplitude is $\mathcal{N} = 2$ supersymmetric with $b_{aa'}^{\mathcal{A},(1)} \equiv 0 \equiv b_{aa'}^{\mathcal{A},(3)}$. For $(\sigma_{aa'}^2, \tau_{aa'}^2) = (0, 0)$ the gauge group is of $Sp(2N_a)$ type, cf. tables 15 and 19, and $U(N_a)$ otherwise. The Möbius strip amplitude belongs to one of the two cases, cf. table 12.
 - For $m \in \{0, 2\}$ the Möbius strip amplitude preserves the same $\mathcal{N} = 2$ supersymmetry, i.e. $b_{aa'}^{\mathcal{M},(1)} \equiv 0 \equiv b_{aa'}^{\mathcal{M},(3)}$.
 - For $m \in \{1, 3\}$ the Möbius strip amplitude is only $\mathcal{N} = 1$ supersymmetric with $b_{aa'}^{\mathcal{M},(2)} \equiv 0$ but $b_{aa'}^{\mathcal{M},(1)}, b_{aa'}^{\mathcal{M},(3)} \neq 0$ and $b_{aa'}^{\mathcal{A},(2)} \neq 0$, and the Wilson lines and displacements on $T_{(1)}^2 \times T_{(3)}^2$ only take discrete values, i.e. $\sigma_{aa'}^1 = \tau_{aa'}^1 = \sigma_{aa'}^3 = \tau_{aa'}^3 = 0$.
- * $T^6/\mathbb{Z}_2 \times \mathbb{Z}_{2M}$ without discrete torsion: The annulus amplitude is (up to normalisation) identical to T^6 with $b_{aa'}^{\mathcal{A},(i)} \equiv 0$ for $i = 1, 2, 3$, cf. 10.

On the $T^6/\mathbb{Z}_2 \times \mathbb{Z}_{2M}$ orbifold with discrete torsion, all displacements and Wilson lines are discrete, i.e. $(\vec{\sigma}_{aa'}, \vec{\tau}_{aa'}) = (\vec{0}, \vec{0})$, and therefore the second line in (64) vanishes.

The two-torus volume v_i dependent one-loop contributions to the holomorphic gauge kinetic functions are now easily read off as displayed in the first two rows of table 18. The Kähler metrics for symmetric or antisymmetric matter take the form

$$K_{\mathbf{Anti}_a}^{(i)} = f(S, U_l) \sqrt{\frac{2\pi V_{aa'}^{(i)}}{v_j v_k}} \quad \text{for vanishing angles,} \quad (65)$$

which is identical to the one for bifundamental matter on parallel D6-branes (56). Here we have used the fact that the beta function coefficients in tables 7, 9, 10 and 12 can be evaluated on a case-by case basis for vanishing angles leading to

$$(\varphi^{\mathbf{Anti}_a}, \varphi^{\mathbf{Sym}_a}) = \begin{cases} (2, 0) & T^6/\mathbb{Z}_2 \times \mathbb{Z}_{2M} \text{ with } \eta = -1 \\ (4, 0) & T^6/\mathbb{Z}_{2N} \end{cases}.$$

In all other cases, the symmetric or antisymmetric matter is either massive due to some non-vanishing displacement or Wilson line, or the gauge group is enhanced to $SO(2N_a)$ or $Sp(2N_a)$ as discussed in section 2.2.5.

The gauge threshold contains a constant contribution which we assign to the holomorphic gauge kinetic function,

$$\Re(\delta_{a'} f_{SU(N_a)}^{1\text{-loop}}(c)) = \begin{cases} \frac{1}{2\pi^2} \ln \frac{2(v_1 v_3 V_{aa'}^{(1)} V_{aa'}^{(3)})^{1/4}}{\sqrt{v_2 V_{aa'}^{(2)}}} & T^6/\mathbb{Z}_{2N} \text{ and } a \perp \Omega\mathcal{R} \text{ on } T_{(2)}^2 \\ -\frac{b_{aa'}^{\mathcal{M}}}{8\pi^2} \ln 2 = \begin{cases} \frac{1}{4\pi^2} \ln 2 & T^6/\mathbb{Z}_2 \times \mathbb{Z}_{2M} \text{ with } \eta = -1 \\ \frac{1}{2\pi^2} \ln 2 & T^6/\mathbb{Z}_{2N} \text{ and } a \uparrow\uparrow \Omega\mathcal{R} \text{ on } T_{(2)}^2 \\ 0 & \text{otherwise} \end{cases} \end{cases}, \quad (66)$$

where in a slight abuse of notation we have included a logarithmic dependence on the two-torus volumes for T^6/\mathbb{Z}_{2N} and $a \perp \Omega\mathcal{R}$ along $T_{(2)}^2$. All other dependences on these variables are contained in the usual Dedekind eta and Jacobi theta functions.

- A D6-brane parallel to some $\Omega\mathcal{R}\mathbb{Z}_2^{(m)}$ and $\Omega\mathcal{R}\mathbb{Z}_2^{(n)}$ plane with $m, n \in \{0 \dots 3\}$ along one two-torus $T_{(i)}^2$ and at non-trivial angles on the remaining four-torus (with (m, n, p, q) some cyclic permutation of $(0, 1, 2, 3)$) contributes the following to the gauge thresholds,

$$\begin{aligned} \frac{\Delta_{aa'} + \Delta_{a, \Omega\mathcal{R}}}{2} = & -\frac{1}{2} \left(b_{aa'}^{\mathcal{A}} \Lambda_{0,0}(v_i; V_{aa'}^{(i)}) + b_{aa'}^{\mathcal{M}} \Lambda_{0,0}(\tilde{v}_i; 2\tilde{V}_{aa'}^{(i)}) \right) \\ & -\frac{1}{2} \left(1 - \delta_{\sigma_{aa'}, 0}^i \delta_{\tau_{aa'}, 0}^i \right) \left(\tilde{b}_{aa'}^{\mathcal{A}} \Lambda(\sigma_{aa'}^i, \tau_{aa'}^i, v_i) + \tilde{b}_{aa'}^{\mathcal{M}} \Lambda(\sigma_{aa'}^i, \tau_{aa'}^i, \tilde{v}_i) \right) \\ & + \left[-\frac{N_a}{2} \sum_{l \neq i} \frac{I_{aa'}^{\mathbb{Z}_2^{(l)}}}{c_a} \left(2\phi_{aa'}^{(l)} - \text{sgn}(\phi_{aa'}^{(l)}) \right) + \frac{\eta_{\Omega\mathcal{R}\mathbb{Z}_2^{(p)}} |\tilde{I}_a^{\Omega\mathcal{R}\mathbb{Z}_2^{(p)}}| + \eta_{\Omega\mathcal{R}\mathbb{Z}_2^{(q)}} |\tilde{I}_a^{\Omega\mathcal{R}\mathbb{Z}_2^{(q)}}|}{c_a} \right] \ln 2. \end{aligned} \quad (67)$$

The second line is again absent for rigid D6-branes on $T^6/\mathbb{Z}_2 \times \mathbb{Z}_{2M}$ with discrete torsion, cf. table 7, while other orbifold backgrounds have the following simplifications.

- * T^6 : there is no contribution from \mathbb{Z}_2 fixed points, i.e. $I_{aa'}^{\mathbb{Z}_2^{(l)}} \equiv 0$ for $l \in \{1, 2, 3\}$, and only one regular O6-plane exists, i.e. $\eta_{\Omega\mathcal{R}} \equiv 1$ and $\eta_{\Omega\mathcal{R}\mathbb{Z}_2^{(l)}} \equiv 0$ for all $l \in \{1, 2, 3\}$. Two cases need to be distinguished, cf. table 9.
 - For the D6-branes parallel to the $\Omega\mathcal{R}$ -plane along $T_{(i)}^2$, the two contributions $b_{aa'}^{\mathcal{A}}$ and $b_{aa'}^{\mathcal{M}}$ to the beta function coefficients are non-vanishing, but $\eta_{\Omega\mathcal{R}\mathbb{Z}_2^{(p)}} |\tilde{I}_a^{\Omega\mathcal{R}\mathbb{Z}_2^{(p)}}| + \eta_{\Omega\mathcal{R}\mathbb{Z}_2^{(q)}} |\tilde{I}_a^{\Omega\mathcal{R}\mathbb{Z}_2^{(q)}}| = 0$.

- For the D6-branes perpendicular to the $\Omega\mathcal{R}$ -plane along $T_{(i)}^2$, the Möbius strip contribution to the beta function vanishes, $b_{aa'}^{\mathcal{M}} = 0$, but the intersections with the O6-planes contribute a constant to the gauge threshold, $\eta_{\Omega\mathcal{R}\mathbb{Z}_2^{(p)}} |\tilde{I}_a^{\Omega\mathcal{R}\mathbb{Z}_2^{(p)}}| + \eta_{\Omega\mathcal{R}\mathbb{Z}_2^{(q)}} |\tilde{I}_a^{\Omega\mathcal{R}\mathbb{Z}_2^{(q)}}| = |\tilde{I}_a^{\Omega\mathcal{R}}| + |\tilde{I}_a^{\Omega\mathcal{R}\mathbb{Z}_2^{(2)}}|$.
- * T^6/\mathbb{Z}_{2N} : only $\mathbb{Z}_2^{(2)}$ forms a subgroup of \mathbb{Z}_{2N} , i.e. $I_{aa'}^{\mathbb{Z}_2^{(1)}} \equiv 0 \equiv I_{aa'}^{\mathbb{Z}_2^{(3)}}$, and only two regular O6-planes exist, i.e. $\eta_{\Omega\mathcal{R}} \equiv 1 \equiv \eta_{\Omega\mathcal{R}\mathbb{Z}_2^{(2)}}$ and $\eta_{\Omega\mathcal{R}\mathbb{Z}_2^{(1)}} \equiv 0 \equiv \eta_{\Omega\mathcal{R}\mathbb{Z}_2^{(3)}}$. Three cases have to be distinguished, cf. table 12.
 - If the D6-branes are parallel to the $\Omega\mathcal{R}$ -plane along $T_{(2)}^2$, the constant term from the O6-plane intersections vanishes, $\eta_{\Omega\mathcal{R}\mathbb{Z}_2^{(p)}} |\tilde{I}_a^{\Omega\mathcal{R}\mathbb{Z}_2^{(p)}}| + \eta_{\Omega\mathcal{R}\mathbb{Z}_2^{(q)}} |\tilde{I}_a^{\Omega\mathcal{R}\mathbb{Z}_2^{(q)}}| = 0$.
 - For the D6-branes perpendicular to the $\Omega\mathcal{R}$ -plane along $T_{(2)}^2$, the Möbius strip does not contribute to the beta function, $b_{aa'}^{\mathcal{M}} = 0$, but the O6-plane intersections contribute to the gauge threshold, $\eta_{\Omega\mathcal{R}\mathbb{Z}_2^{(p)}} |\tilde{I}_a^{\Omega\mathcal{R}\mathbb{Z}_2^{(p)}}| + \eta_{\Omega\mathcal{R}\mathbb{Z}_2^{(q)}} |\tilde{I}_a^{\Omega\mathcal{R}\mathbb{Z}_2^{(q)}}| = |\tilde{I}_a^{\Omega\mathcal{R}}|$.
 - If the stack of D6-branes is parallel or perpendicular to the $\Omega\mathcal{R}$ -plane along $T_{(i)}^2$ with $i \in \{1, 3\}$, the displacement and Wilson line only take discrete values, i.e. $\delta_{\sigma_{aa'}, 0} \delta_{\tau_{aa'}, 0} = 1$, and only one of the O6-plane intersections contributes, $\eta_{\Omega\mathcal{R}\mathbb{Z}_2^{(p)}} |\tilde{I}_a^{\Omega\mathcal{R}\mathbb{Z}_2^{(p)}}| + \eta_{\Omega\mathcal{R}\mathbb{Z}_2^{(q)}} |\tilde{I}_a^{\Omega\mathcal{R}\mathbb{Z}_2^{(q)}}| = |\tilde{I}_a^{\Omega\mathcal{R}\mathbb{Z}_2^{(2)}}|$ or $|\tilde{I}_a^{\Omega\mathcal{R}}|$ for parallel or perpendicular to $\Omega\mathcal{R}$, respectively.
- * $T^6/\mathbb{Z}_2 \times \mathbb{Z}_{2M}$ without torsion: as for T^6 there is no fixed point contribution, i.e. $I_{aa'}^{\mathbb{Z}_2^{(l)}} \equiv 0$ for all l , and all O6-planes are regular, i.e. $\eta_{\Omega\mathcal{R}} \equiv 1 \equiv \eta_{\Omega\mathcal{R}\mathbb{Z}_2^{(l)}}$ for all l , cf. table 10.

The v_i dependent contributions to the holomorphic gauge kinetic function from this sector are displayed in the third and fourth row in table 18 for all orbifolds under consideration. The functional dependence of the Kähler metrics in this sector is identical to (65),

$$K_{\mathbf{Anti}_a/\mathbf{Sym}_a}^{(i)} = f(S, U_l) \sqrt{\frac{2\pi V_{aa'}^{(i)}}{v_j v_k}} \quad \text{for one vanishing angle,} \quad (68)$$

and additionally there is an angle dependent contribution identical to (58) plus a constant contribution to the holomorphic gauge kinetic function,

$$\begin{aligned} \Re \left(\delta_{a'} f_{SU(N_a)}^{1\text{-loop}}(\phi_{ab}^{(i)}) \right) = & \frac{1}{8\pi^2 c_a} \left(-\frac{N_a}{2} \sum_{l=j,k} I_{aa'}^{\mathbb{Z}_2^{(l)}} \left(2\phi_{aa'}^{(l)} - \text{sgn}(\phi_{aa'}^{(l)}) \right) \right. \\ & \left. + \eta_{\Omega\mathcal{R}\mathbb{Z}_2^{(p)}} |\tilde{I}_a^{\Omega\mathcal{R}\mathbb{Z}_2^{(p)}}| + \eta_{\Omega\mathcal{R}\mathbb{Z}_2^{(q)}} |\tilde{I}_a^{\Omega\mathcal{R}\mathbb{Z}_2^{(q)}}| \right). \end{aligned} \quad (69)$$

This formula holds again for all torus and orbifold backgrounds when setting some of the intersection numbers to zero as detailed above. Examples with non-vanishing (69) and no massless matter are given by the dd' and $d(\theta^2 d')$ sectors of the Standard Model on T^6/\mathbb{Z}'_6 in table 29, supporting again the correct assignment of the terms to the holomorphic gauge kinetic function.

- If the stack of D6-branes is at three non-trivial angles to the O6-planes, the gauge threshold computation gives

$$\begin{aligned} \frac{\Delta_{aa'} + \Delta_{a,\Omega\mathcal{R}}}{2} = & -\frac{b_{aa'}^A + b_{aa'}^{\mathcal{M}}}{2} \sum_{i=1}^3 \ln \left(\frac{\Gamma(|\phi_{aa'}^{(i)}|)}{\Gamma(1 - |\phi_{aa'}^{(i)}|)} \right)^{-\frac{\text{sgn}(\phi_{aa'}^{(i)})}{\text{sgn}(I_{aa'})}} \\ & + \left[-\frac{N_a}{2} \sum_{i=1}^3 \frac{I_{aa'}^{\mathbb{Z}_2^{(i)}}}{c_a} \left(2\phi_{aa'}^{(i)} - \text{sgn}(\phi_{aa'}^{(i)}) - \text{sgn}(I_{aa'}) \right) + \sum_{m=0}^3 \frac{\eta_{\Omega\mathcal{R}\mathbb{Z}_2^{(m)}} |\tilde{I}_z^{\Omega\mathcal{R}\mathbb{Z}_2^{(m)}}|}{c_a} \right] \ln 2. \end{aligned} \quad (70)$$

This formula holds for all toroidal orbifold backgrounds discussed in this article, provided the vanishing of some \mathbb{Z}_2 fixed or orientifold invariant intersection points is taken into account as detailed for the case of one vanishing angle.

The sectors with three non-trivial angles do not contribute to the v_i -dependent part of the holomorphic gauge kinetic function. The Kähler metrics for symmetric and antisymmetric matter at aa' intersections are given by

$$K_{\text{Anti}_a/\text{Sym}_a} = f(S, U_l) \sqrt{\prod_{i=1}^3 \frac{1}{v_i} \left(\frac{\Gamma(|\phi_{aa'}^{(i)}|)}{\Gamma(1 - |\phi_{aa'}^{(i)}|)} \right)^{-\frac{\text{sgn}(\phi_{aa'}^{(i)})}{\text{sgn}(I_{aa'})}}}, \quad (71)$$

and the additional angle-dependent and constant terms in the gauge threshold (70) are assigned to the loop-correction to the holomorphic gauge kinetic function,

$$\begin{aligned} \Re \left(\delta_{a'} f_{SU(N_a)}^{\text{1-loop}}(\phi_{aa'}^{(i)}) \right) = & \frac{1}{8\pi^2 c_a} \left(-\frac{N_a}{2} \sum_{i=1}^3 I_{aa'}^{\mathbb{Z}_2^{(i)}} \left(2\phi_{aa'}^{(i)} - \text{sgn}(\phi_{aa'}^{(i)}) - \text{sgn}(I_{aa'}) \right) \right. \\ & \left. + \sum_{m=0}^3 \eta_{\Omega\mathcal{R}\mathbb{Z}_2^{(m)}} |\tilde{I}_a^{\Omega\mathcal{R}\mathbb{Z}_2^{(m)}}| \right) \ln 2. \end{aligned} \quad (72)$$

The case with one vanishing angle (69) can again be included by noticing that some of the intersection numbers vanish.

For later comparison with the case of a single $U(1)_a \subset U(N_a)$ factor in section 3.4.1, we can formally decompose the one-loop correction to the holomorphic gauge kinetic function

from the sector aa' into its annulus and Möbius strip contributions,

$$\delta_{a'} f_{SU(N_a)}^{1\text{-loop}} \equiv \delta_{a'} f_{SU(N_a)}^{1\text{-loop}, \mathcal{A}} + \delta_{a'} f_{SU(N_a)}^{1\text{-loop}, \mathcal{M}}. \quad (73)$$

The complete list of such v_i -dependent contributions for any torus or orbifold background considered in this article is listed in table 18. In the angle plus constant term (72), the annulus and Möbius strip contributions correspond to the first and second line, respectively.

3.2.1 Complexification and one-loop redefinition of the closed string moduli

Complexification of moduli by axions

The ansatz for the tree level gauge kinetic function (18) and gauge threshold amplitudes (19) uses the geometric moduli only. However, the $\mathcal{N} = 1$ field theory depends on the complexifications of the dilaton S and complex structures U_l and Kähler moduli v_i ,

$$S^c = S + i \xi_0, \quad U_l^c = U_l + i \xi_l, \quad T_i^c = v_i + i b_i, \quad (74)$$

with the RR axions $\xi_{L,L=0\dots h_{21}} = \int_{L^{\text{th}} - \mathcal{R} \text{ even } 3\text{-cycle}} C_3$ and the NSNS axions $b_{i,i=1\dots h_{11}} = \int_{i^{\text{th}} - \mathcal{R} \text{ odd } 2\text{-cycle}} B_2$, see [60] for the derivation of IIA orientifolds on smooth Calabi-Yau spaces and Appendix A of [46] for the evaluation of the closed string spectrum on all type IIA toroidal orbifolds considered here.

The rewritten form (26) of the lattice sums and the transformation of Dedekind eta and Jacobi theta functions under complex conjugation,

$$\overline{\eta(\tau)} = \eta(-\bar{\tau}), \quad \overline{\vartheta_i(\nu, \tau)} = \vartheta_i(\bar{\nu}, -\bar{\tau}) \quad i = 1 \dots 4,$$

justifies the ansatz, e.g. [61, 45], to replace the moduli by their complexifications in the tree-level and all one-loop corrections to the holomorphic gauge kinetic functions in equations (49), (81) and (82) and tables 17 and 18, if at the same time the displacement and Wilson line moduli are paired into complex scalars,

$$\Sigma_a^i = \sigma_a^i + i \frac{\tau_a^i}{v_i}, \quad (75)$$

leading to the complexification $-i \frac{T_i^c \Sigma_{ab}^i}{2}$ of the argument $\frac{\tau_{ab}^i - i \sigma_{ab}^i}{2}$ of the Jacobi theta function $\vartheta_1(\frac{\tau_{ab}^i - i \sigma_{ab}^i}{2}, i v_i)$ in the one-loop contributions to the holomorphic gauge kinetic functions from D6-branes with some non-vanishing relative displacement or Wilson line.

One-loop field redefinitions

In type IIA compactifications, the four dimensional dilaton and complex structure moduli

participate in the generalised Green-Schwarz mechanism for anomalous $U(1)$ gauge factors. This leads to one-loop redefinitions of the field theory expressions,

$$S \rightarrow S + \delta_{GS} S, \quad U_l \rightarrow U_l + \delta_{GS} U_l, \quad (76)$$

under gauge transformations of the anomalous (massive) Abelian gauge factors. This field redefinition cannot be seen in the matching of gauge thresholds computed by CFT methods with the standard $\mathcal{N} = 1$ supergravity expressions above. There exist different proposals for the field redefinitions in the literature, which we discuss below.

- In [61, 45], it was proposed that the one-loop redefinitions are given by

$$\delta_{GS} S = \mp \frac{1}{16\pi^2 c_a} \sum_b N_b \tilde{Y}_b^0 \sum_{i=1}^3 \phi_b^{(i)} \ln v_i, \quad \delta_{GS} U_l = \pm \frac{1}{16\pi^2 c_a} \sum_b N_b \tilde{Y}_b^l \sum_{i=1}^3 \phi_b^{(i)} \ln v_i, \quad (77)$$

with the orientifold odd three-cycle wrapping numbers \tilde{Y}_b^l defined in equation (42), providing a mixing with the bulk Kähler moduli. It was furthermore argued that the angle dependent contributions (61) to the holomorphic gauge kinetic function might be the result of a one-loop redefinition of exceptional complex structure moduli. We were unable to reproduce the proposed transformations for the toroidal orbifolds considered in this article for the following reasons.

1. The derivation of these transformations relies on chiral matter only existing at three intersection angles and consequently the same type of Kähler metrics (59) with different angles as arguments for all chiral states. However, in the presence of \mathbb{Z}_2 symmetries, additional chiral matter states can arise at one vanishing intersection angle with a different shape of the Kähler metrics (56). A prominent example of this kind are two generations of right-handed quarks from the ac sector in the T^6/\mathbb{Z}'_6 example in table 29 versus the third generation from the $a(\theta^2 c)$ sector below.
2. For orbifolds with \mathbb{Z}_3 or \mathbb{Z}_4 subsymmetry, the bulk three-cycle wrapping numbers are sums of toroidal wrapping numbers over all images $(\omega^k a)$ of a . While the net-intersection number for exceptional three-cycles is given by $\frac{1}{c_a} \sum_{m=0}^{M-1} I_{(\omega^m a)b}^{\mathbb{Z}_2^{(i)}}$, cf. table 3, the angle dependent one-loop contribution to the gauge thresholds (60) requires to simultaneously transform the angles $\phi_{(\omega^m a)b}^{(i)} = \phi_{(\omega^m a)b}^{(i)} - 2\pi m w_i \bmod 1$. This is in contradiction to factorising out the bulk wrapping numbers in (77), especially since $\phi_{x(\omega^k y)}^{(2)} = 0$ occurs for some orbifold images $(\omega^k y)$, e.g. for $x(\omega^k y) \in \{b(\theta^2 d), cd, bd'\}$ of the T^6/\mathbb{Z}'_6 example in section 5.

3. The combination of \tilde{Y}_b^l times the angle $\phi_b^{(i)}$ in (77) leads to identical expressions for orientifold image D6-branes b and b' with opposite $U(1)$ charges. However, the anomaly of some Abelian gauge factor is in direct correspondence to the chirality of the massless states and thus also the signs of the corresponding $U(1)$ charges.

In conclusion, the proposed field redefinitions (77) cannot apply to toroidal orbifolds with \mathbb{Z}_2 subsectors or non-trivial orbifold image cycles, and are therefore also likely to not occur for the six-torus, for which already a contradiction concerning chirality arises.

- In [1], the one-loop field redefinitions are expressed as

$$\delta_{GS} S = \lambda_S \sum_b N_b \tilde{Y}_b^0 \Lambda^{(b)}, \quad \delta_{GS} U_l = \lambda_l \sum_b N_b \tilde{Y}_b^l \Lambda^{(b)}, \quad (78)$$

in terms of the gauge transformation parameters $\Lambda^{(b)}$ of anomalous massive $U(1)_b$ gauge factors, where λ_S, λ_l are normalisation constants which depend on the chiral spectrum. They are encoded in the anomaly matrix with components [1],

$$C_{ab} = \frac{1}{4\pi^2} \text{tr}(Q_a^2 Q_b), \quad C_{aa} = \frac{1}{12\pi^2} \text{tr}(Q_a^3), \quad (79)$$

which is computed from the chiral spectrum in table 3 on the left hand side. The expressions (78) are consistent with summations over orbifold image D6-branes as well as with the distinction of orientifold image D6-branes with opposite $U(1)$ charge assignments.

We give the anomaly matrices for all examples on $T^6/\mathbb{Z}_2 \times \mathbb{Z}_2$ with discrete torsion and on T^6/\mathbb{Z}_6' in the corresponding sections, but leave the evaluation of the constants λ_S, λ_l to the interested reader since gauge transformations of anomalous $U(1)$ s are not relevant for the perturbative treatment of the effective action performed in this article.

3.2.2 Modifications for T^6/\mathbb{Z}_{2N} and $T^6/\mathbb{Z}_2 \times \mathbb{Z}_{2M}$ with $\eta = \pm 1$ and $h_{21}^{\text{bulk}} = 0, 1$

In section 3.1, the holomorphic gauge kinetic function at tree level was derived for $h_{21}^{\text{bulk}} = 3$, which is valid for the six-torus and its orbifolds T^6/\mathbb{Z}_2 and $T^6/\mathbb{Z}_2 \times \mathbb{Z}_2$ with and without discrete torsion. All other orbifolds in table 1 have a reduced number of bulk complex structures due to some \mathbb{Z}_3 or \mathbb{Z}_4 subsymmetry.

As detailed in appendix B, the T^6/\mathbb{Z}'_6 and $T^6/\mathbb{Z}_2 \times \mathbb{Z}_6$ orbifolds project out two of the three bulk complex structure moduli yielding the modified definitions of the field theoretical dilaton and complex structure,

$$S \sim \frac{e^{-\phi_4}}{\sqrt{r}}, \quad U \sim e^{-\phi_4} \sqrt{r}, \quad (80)$$

where r is the ratio of radii on the one two-torus where only a \mathbb{Z}_2 symmetry acts. This leads to the relation

$$\Re(f_{SU(N_a)}^{\text{tree}}) \stackrel{!}{=} \frac{1}{g_{a,\text{tree}}^2} \sim \frac{1}{k_a c_a} \left(S \tilde{X}_a^0 - U \tilde{X}_a^1 \right) \quad \text{on } T^6/(\mathbb{Z}'_6 \times \Omega\mathcal{R}) \text{ and } T^6/(\mathbb{Z}_2 \times \mathbb{Z}_6 \times \Omega\mathcal{R}), \quad (81)$$

with the bulk wrapping numbers $\tilde{X}_a^0, \tilde{X}_a^1$ for all six inequivalent lattices given in table 34 of appendix B.2. The corresponding results for T^6/\mathbb{Z}_4 and $T^6/\mathbb{Z}_2 \times \mathbb{Z}_4$ with also one bulk complex structure modulus are given in appendix B.1, table 33.

The T^6/\mathbb{Z}_6 and $T^6/\mathbb{Z}_2 \times \mathbb{Z}'_6$ orbifolds have no bulk complex structure modulus, $S \sim e^{-\phi_4}$, and thus

$$\Re(f_{SU(N_a)}^{\text{tree}}) \stackrel{!}{=} \frac{1}{g_{a,\text{tree}}^2} \sim \frac{1}{k_a c_a} S \tilde{X}_a^0 \quad \text{on } T^6/(\mathbb{Z}_6 \times \Omega\mathcal{R}) \text{ and } T^6/(\mathbb{Z}_2 \times \mathbb{Z}'_6 \times \Omega\mathcal{R}), \quad (82)$$

with \tilde{X}_a^0 listed in table 35 in appendix B.3 for the different background lattices.

At one-loop, the ratio of the mass scales $M_{\text{Planck}}/M_{\text{string}} \sim e^{-\phi_4}$ is recovered by replacing the product of bulk moduli in (53) as follows,

$$f(S, U_l) = \left(S \prod_{l=1}^{h_{21}^{\text{bulk}}} U_l \right)^{-\alpha/4} \quad \text{with } \alpha = \begin{cases} 1 & h_{21}^{\text{bulk}} = 3 \\ 2 & 1 \\ 4 & 0 \end{cases}. \quad (83)$$

The matching of the one-loop field and string theory results for the gauge coupling with the terms involving the Kähler potential requires the simultaneous replacement

$$\mathcal{K}_{\text{bulk}} = -\alpha \ln S - \alpha \sum_{l=1}^{h_{21}^{\text{bulk}}} \ln U_l - \sum_{i=1}^3 \ln v_i. \quad (84)$$

Both modifications (83) and (84) can also be understood from the fact that for r_2, r_3 fixed constants, the definition (48) of the bulk complex structures and dilaton on the factorisable six-torus leads to $S \propto U_1$ and $U_2 \propto U_3$. If also r_1 is a fixed constant, all four moduli are related, $S \propto U_1 \propto U_2 \propto U_3$. Inserting these relations in (53) and (51) leads to the exponent α in (83) and (84), respectively.

3.3 Kähler metrics and holomorphic gauge kinetic functions for $SO(2M)$ and $Sp(2M)$

For D6-branes which are their own orientifold images, $x = x'$, the quadratic Casimir of the adjoint representation in equation (40) is given by $C_2(\mathbf{Adj}_x) = M_x + \xi_x$, where $\xi_x = \pm 1$ for $Sp(2M_x)$ and $SO(2M_x)$, respectively. With the beta function coefficients given by (16) and the multiplicities of symmetric and antisymmetric representations listed in table 15, the matching of the string and field theory computation reads

$$\begin{aligned}
0 \stackrel{!}{=} & -\frac{M_x(-3 + \varphi^{\mathbf{Sym}_x} + \varphi^{\mathbf{Anti}_x}) + (\varphi^{\mathbf{Sym}_x} - \varphi^{\mathbf{Anti}_x} - 3\xi_x)}{2} \ln \left[\left(S \prod_{i=1}^3 U_i \right)^{1/2} \prod_{j=1}^3 v_j \right] \\
& + (M_x + \xi_x) \ln \left[\left(S \prod_{i=1}^3 U_i \right)^{-3/4} \frac{(2\pi)^{3/2} \prod_{i=1}^3 \sqrt{V_{xx}^{(i)}}}{(\prod_{k=1}^3 v_k) c_x k_x} \right] - \varphi^{\mathbf{Anti}_x} (M_x - 1) \ln K_{\mathbf{Anti}_x} \\
& - \varphi^{\mathbf{Sym}_x} (M_x + 1) \ln K_{\mathbf{Sym}_x} + 8\pi^2 \Re(\delta_x f_{SO/Sp(2M_x)}^{1\text{-loop}}) - \frac{M_x \tilde{\Delta}_{xx} + \Delta_{x,\Omega\mathcal{R}}/2}{2},
\end{aligned} \tag{85}$$

where the relations for the mass scales, bulk Kähler potential and tree level gauge couplings have been inserted. The matching condition can be evaluated on a case-by case basis, for which the result is summarised in table 19. The derivation requires a distinction of the following cases.

- For T^6 and T^6/\mathbb{Z}_3 , two cases need to be distinguished.
 - For $x \uparrow\uparrow \Omega\mathcal{R}$, one has $(\xi_x, \varphi^{\mathbf{Sym}_x}, \varphi^{\mathbf{Anti}_x}) = (-1, 0, 3)$ with vanishing gauge threshold correction, $\frac{M_x \tilde{\Delta}_{xx} + \Delta_{x,\Omega\mathcal{R}}/2}{2} = 0$, due to the underlying $\mathcal{N} = 4$ supersymmetry. The string to field theory matching condition reduces to (with $c_x = 1$ for bulk D6-branes and $k_x = 2$ for $SO(2M_x)$)

$$0 \stackrel{!}{=} (M_x - 1) \ln \left[\left(S \prod_{i=1}^3 U_i \right)^{-3/4} \frac{(2\pi)^{3/2} \prod_{i=1}^3 \sqrt{V_{xx}^{(i)}}}{2 (\prod_{k=1}^3 v_k)} \right] - 3(M_x - 1) \ln K_{\mathbf{Anti}_x}, \tag{86}$$

from which the Kähler metrics of the antisymmetrics are inferred,

$$K_{\mathbf{Anti}_x}^{(i)} = \left(S \prod_{l=1}^3 U_l \right)^{-1/4} \frac{(2\pi)^{1/2}}{2^{1/3} c_x v_i} \sqrt{\frac{V_{xx}^{(j)} V_{xx}^{(k)}}{V_{xx}^{(i)}}} \quad \text{with} \quad (ijk) = (123) \text{ cyclic}. \tag{87}$$

Due to $\mathcal{N} = 4$, there is no one-loop contribution to the holomorphic gauge kinetic function.

- For $x \perp \Omega\mathcal{R}$ along some $T_{(j,k)}^4$, the parameters are $(\xi_x, \varphi^{\mathbf{Sym}_x}, \varphi^{\mathbf{Anti}_x}) = (1, 1, 2)$ and the gauge threshold $\frac{M_x \tilde{\Delta}_{xx} + \Delta_{x, \Omega\mathcal{R}}/2}{2} = 2 \Lambda_{0,0}(\tilde{v}_i; 2\tilde{V}_{xx}^{(i)})$ stems from the O6-plane breaking $\mathcal{N} = 4$ to $\mathcal{N} = 2$ supersymmetry. The terms proportional to M_x in (85) are consistent with the normalisation (87) of the Kähler metrics for both antisymmetric and symmetric representations, and the remaining constants are assigned to $\delta_x f_{Sp(2M_x)}^{1\text{-loop}}$, cf. table 19.
- For T^6/\mathbb{Z}_{2N} , again two distinct cases exist.
 - For $x \uparrow\uparrow \Omega\mathcal{R}$ or $\Omega\mathcal{R}\mathbb{Z}_2^{(2)}$, one has the constants $(\xi_x, \varphi^{\mathbf{Sym}_x}, \varphi^{\mathbf{Anti}_x}) = (1, 1, 0)$ and the gauge threshold contribution $\frac{M_x \tilde{\Delta}_{xx} + \Delta_{x, \Omega\mathcal{R}}/2}{2} = M_x \Lambda_{0,0}(v_2; V_{xx}^{(2)}) + \Lambda_{0,0}(\tilde{v}_2; 2\tilde{V}_{xx}^{(2)})$ from an $\mathcal{N} = 2$ supersymmetric sector. The contribution to the holomorphic gauge kinetic function and the Kähler metric are displayed in table 19.
 - For $x \perp \Omega\mathcal{R}$ along $T_{(2)}^2$, the parameters are $(\xi_x, \varphi^{\mathbf{Sym}_x}, \varphi^{\mathbf{Anti}_x}) = (1, 0, 1)$ and the gauge threshold $\frac{M_x \tilde{\Delta}_{xx} + \Delta_{x, \Omega\mathcal{R}}/2}{2} = M_x \Lambda_{0,0}(v_2; V_{xx}^{(2)}) + \sum_{i=1,3} \Lambda_{0,0}(\tilde{v}_i; 2\tilde{V}_{xx}^{(i)})$ belong to an $\mathcal{N} = 1$ supersymmetric sector, cf. table 19 for the Kähler metric and contribution to the holomorphic gauge kinetic function.
- For $T^6/\mathbb{Z}_2 \times \mathbb{Z}_{2M}$ without torsion, the parameters $(\xi_x, \varphi^{\mathbf{Sym}_x}, \varphi^{\mathbf{Anti}_x}) = (1, 0, 3)$ and $\frac{M_x \tilde{\Delta}_{xx} + \Delta_{x, \Omega\mathcal{R}}/2}{2} = \sum_{i=1}^3 \Lambda_{0,0}(\tilde{v}_i; 2\tilde{V}_{xx}^{(i)})$ belong to an $\mathcal{N} = 1$ supersymmetric sector, cf. the penultimate line in table 19 for the field theory result.
- For $T^6/\mathbb{Z}_2 \times \mathbb{Z}_{2M}$ with discrete torsion the parameters are $(\xi_x, \varphi^{\mathbf{Sym}_x}, \varphi^{\mathbf{Anti}_x}) = (1, 0, 0)$ and the gauge threshold reads $\frac{M_x \tilde{\Delta}_{xx} + \Delta_{x, \Omega\mathcal{R}}/2}{2} = \frac{M_x}{2} \sum_{i=1}^3 \Lambda_{0,0}(v_i; V_{xx}^{(i)}) + \frac{1}{2} \sum_{i=1}^3 \Lambda_{0,0}(\tilde{v}_i; 2\tilde{V}_{xx}^{(i)})$. The sector is $\mathcal{N} = 1$ supersymmetric without massless matter. The assignment of all constants to the holomorphic gauge kinetic function $\delta_x f_{Sp(2M_x)}^{1\text{-loop}}$ on the last line in table 19 is unique - in contrast to those cases which contain both, some Kähler metric and contribution to $\delta f^{1\text{-loop}}$.

In summary, the Kähler metrics for antisymmetric and symmetric matter from the xx sector of orientifold invariant D6-branes have the universal shape (87), and the one-loop contribution to the holomorphic gauge kinetic function has the same global prefactor $1/c_x$ as at tree level. The powers of 2 in the annulus contribution stem from the factor $\ln(1/c_x k_x)$ in the logarithm of the tree level gauge coupling, while the powers of 2 in the Möbius strip contribution to $\delta_x f_{Sp(2M_x)}^{1\text{-loop}}$ can be traced back to a combination of $\ln(1/c_x k_x)$ with $\ln 4$ per lattice sum $\Lambda_{0,0}(\tilde{v}_i; 2\tilde{V}_{xx}^{(i)})$.

The present discussion covers only the xx sector of orientifold invariant D6-branes. The $x(\omega^k x)$ sectors require a discussion of the transformation properties of the intersection

points under the orbifold and orientifold projection. Since the latter depend on the choice of the background lattice, a complete case-by-case study goes beyond the scope of this article. The branes c and h_3 in the Standard Model example on T^6/\mathbb{Z}'_6 with gauge groups $Sp(2)_c$ and $Sp(6)_{h_3}$ are of the type $c \uparrow\uparrow \Omega\mathcal{R}$ and $h_3 \perp \Omega\mathcal{R}$ on $T^2_{(2)}$ discussed in this section, and in section 5 details on the $x(\omega^k x)$ sectors are given for these two examples.

3.4 Gauge kinetic functions for anomaly-free $U(1)$ s

Abelian gauge symmetries are ubiquitous in D-brane models, they appear as anomaly-free linear combinations in the physical hyper charge and $B - L$ symmetry and provide kinetic mixing in the open string sector [62, 63] as well as with the closed string RR photons, thereby providing candidates for a ‘dark photon’, see e.g. [29] and references therein. Anomalous $U(1)$ symmetries remain as global symmetries in perturbation theory which can be broken non-perturbatively by instanton effects, see e.g. [64–66] for D2-instantons in D6-brane models. The kinetic mixing happens at the one-loop level, and we derive here the perturbatively exact holomorphic gauge kinetic functions for a single $U(1)_a$ on a stack of D6 $_a$ -branes and for an anomaly-free linear combination $U(1)_X$ from various stacks of D6-branes in section 3.4.1 and 3.4.2, respectively.

3.4.1 Holomorphic gauge kinetic function for a single $U(1)$ factor

The generic formula (40) for the field theoretical gauge coupling at one loop is modified for a single $U(1)_a \subset U(N_a)$ gauge factor by replacing the quadratic Casimir by the product of the dimension of the representation times the (charge)²,

$$C_2(\mathbf{R}_a) \rightarrow Q_a^2 \dim(\mathbf{R}_a) \quad \text{with} \quad Q_a = \begin{cases} 0 \\ 1 \\ 2 \end{cases} \quad \text{and} \quad \dim(\mathbf{R}_a) = \begin{cases} N_a^2 & \mathbf{R}_a = (\mathbf{Adj}_a) \\ N_a N_b & (\mathbf{N}_a, \bar{\mathbf{N}}_b) \\ \frac{N_a(N_a \pm 1)}{2} & (\mathbf{Sym}_a / \mathbf{Anti}_a) \end{cases}, \quad (88)$$

and the corresponding beta function coefficient is given in equation (36) in section 2.3. The holomorphic gauge kinetic function at tree level is encoded in equation (34),

$$f_{U(1)_a}^{\text{tree}} = 2N_a f_{SU(N_a)}^{\text{tree}}, \quad (89)$$

and the one-loop contributions to the holomorphic gauge kinetic function are included in the gauge threshold (38) for a single $U(1)_a$ gauge factor. The matching of the result of the one-loop string computation with the field theory formula is decomposed into open string sectors analogously to the $SU(N_a)$ case.

- aa strings with endpoints on identical D6-branes neither contribute to the beta function coefficient (36) nor the gauge threshold (38), and since $Q_a = 0$ for matter in the adjoint representation \mathbf{Adj}_a of $U(N_a)$ this matches the expected vanishing contribution to the field theory result. This argument applies also to strings ending on orbifold image D6-branes a and $(\omega^k a)$.
- Strings with endpoints on different D6-branes a and b with $b \neq (\omega^k a'), (\omega^k a)$ contribute $2N_a$ times the result of the string calculation of the $SU(N_a)$ case to the beta function coefficient (36) and gauge threshold (38) of $U(1)_a$. Since on the field theory side, the quadratic Casimir is replaced by the charge of a fundamental representation, $N_b C_2(\mathbf{N}_a) = \frac{N_b}{2} \rightarrow N_a N_b$, the matching (55) in the ab sector of $SU(N_a)$ is reproduced by $U(1)_a$, and the Kähler metrics for bifundamental representations in table 16 are recovered. The one-loop contributions to the holomorphic gauge kinetic function of $U(1)_a$ are given by,

$$\delta_b f_{U(1)_a}^{1\text{-loop}} = 2N_a \delta_b f_{SU(N_a)}^{1\text{-loop}} \quad \text{for } b \neq (\omega^k a'), (\omega^k a), \quad (90)$$

with the one-loop corrections to the holomorphic gauge kinetic function of $SU(N_a)$ presented in table 17 for any orbifold considered in this article.

- For strings with endpoints on orientifold image D6-branes a and a' , the contributions from the annulus and Möbius strip diagrams have to be taken into account separately. Due to the $U(1)_a$ charge $Q_a = 2$ of symmetric and antisymmetric representations of $U(N_a)$, the annulus contributes $4N_a$ times the $SU(N_a)$ annulus result to the beta function coefficient and gauge threshold, while the Möbius strip contributes $2N_a$ times the $SU(N_a)$ Möbius strip result, cf. equations (36) and (38). The one-loop contribution to the holomorphic gauge kinetic function from the aa' sector is thus given by

$$\begin{aligned} \delta_{a'} f_{U(1)_a}^{1\text{-loop}} &\equiv \delta_{a'} f_{U(1)_a}^{1\text{-loop}, \mathcal{A}} + \delta_{a'} f_{U(1)_a}^{1\text{-loop}, \mathcal{M}} \\ &= 4N_a \delta_{a'} f_{SU(N_a)}^{1\text{-loop}, \mathcal{A}} + 2N_a \delta_{a'} f_{SU(N_a)}^{1\text{-loop}, \mathcal{M}}, \end{aligned} \quad (91)$$

where the individual annulus and Möbius strip contributions to the $SU(N_a)$ case can be read off from table 18. The result can be checked explicitly by comparing the

matching for the string and field theoretic computations for the $U(1)_a$ case,

$$\begin{aligned}
0 \stackrel{!}{=} & 2N_a \left\{ \frac{2b_{aa'}^{\mathcal{A}} + b_{aa'}^{\mathcal{M}}}{2} \left[\ln \left(\frac{M_{\text{Planck}}}{M_{\text{string}}} \right)^2 + \mathcal{K}_{\text{bulk}} \right] \right. \\
& - N_a \left(\sum_{i=1}^{\varphi_{\text{Anti}_a}} \ln K_{\text{Anti}_a}^{(i)} + \sum_{i=1}^{\varphi_{\text{Sym}_a}} \ln K_{\text{Sym}_a}^{(i)} \right) - \left(\sum_{i=1}^{\varphi_{\text{Sym}_a}} \ln K_{\text{Sym}_a}^{(i)} - \sum_{i=1}^{\varphi_{\text{Anti}_a}} \ln K_{\text{Anti}_a}^{(i)} \right) \\
& \left. + 8\pi^2 \Re(\delta_{a'} f_{U(1)_a}^{1\text{-loop}}) - \frac{2N_a (2\Delta_{aa'} + \Delta_{a,\Omega\mathcal{R}})}{2} \right\},
\end{aligned} \tag{92}$$

with the $SU(N_a)$ case in (63).

The total one-loop correction to the holomorphic gauge kinetic function of a single (not necessarily anomaly-free) $U(1)_a$ factor can be summarised as follows,

$$\begin{aligned}
\delta_{\text{total}} f_{U(1)_a}^{1\text{-loop}} & \equiv \delta_{a'} f_{U(1)_a}^{1\text{-loop}} + \sum_{b \neq a, a'} \delta_b f_{U(1)_a}^{1\text{-loop}} \\
& = 2N_a \left(2\delta_{a'} f_{SU(N_a)}^{1\text{-loop}, \mathcal{A}} + \delta_{a'} f_{SU(N_a)}^{1\text{-loop}, \mathcal{M}} + \sum_{b \neq a, a'} \delta_b f_{SU(N_a)}^{1\text{-loop}} \right).
\end{aligned} \tag{93}$$

This form will serve as a basic building block for the anomaly-free linear combination of several individual Abelian gauge factors in the following section.

3.4.2 Gauge kinetic function for anomaly-free linear combinations of $U(1)$ s

Anomaly-free massless Abelian gauge factors $U(1)_X$ such as the hyper charge or $B-L$ symmetry are typically linear combinations of several $U(1)_i \subset U(N_i)$ factors, $U(1)_X = \sum_i x_i U(1)_i$, with charge assignments

$$Q_X = \sum_i x_i Q_{U(1)_i}. \tag{94}$$

The tree level gauge coupling (35) in section 2.3 leads to the holomorphic gauge kinetic function at tree-level,

$$f_{U(1)_X}^{\text{tree}} = \sum_i x_i^2 f_{U(1)_i}^{\text{tree}}, \tag{95}$$

with $f_{U(1)_i}^{\text{tree}}$ given in (89), and the beta function coefficients (37) and gauge threshold corrections (39) contain the analogous summation over contributions from each single $U(1)_i$ factor weighted by x_i^2 plus mixed terms proportional to $x_i x_j$ with $i < j$ that arise at one

loop. The matching of string and field theory expressions is simplified by rewriting the sum over Kähler metrics analogously,

$$\begin{aligned}
\sum_{\mathbf{R}_a} Q_{X, \mathbf{R}_a}^2 \dim(\mathbf{R}_a) \ln K_{\mathbf{R}_a} &= \sum_{i < j} N_i N_j \left[(x_i - x_j)^2 \ln K_{(\mathbf{N}_i, \overline{\mathbf{N}}_j)} + (x_i + x_j)^2 \ln K_{(\mathbf{N}_i, \mathbf{N}_j)} \right] \\
&\quad + \sum_i 2N_i x_i^2 \left[(N_i - 1) \ln K_{\mathbf{Anti}_i} + (N_i + 1) \ln K_{\mathbf{Sym}_i} \right] \\
&= \sum_i x_i^2 N_i \left(\sum_{j \neq i} N_j \left[\ln K_{(\mathbf{N}_i, \overline{\mathbf{N}}_j)} + \ln K_{(\mathbf{N}_i, \mathbf{N}_j)} \right] \right. \\
&\quad \left. + 2N_i (\ln K_{\mathbf{Anti}_i} + \ln K_{\mathbf{Sym}_i}) + 2 (\ln K_{\mathbf{Sym}_i} - \ln K_{\mathbf{Anti}_i}) \right) \\
&\quad + 2 \sum_{i < j} N_i N_j x_i x_j \left[-\ln K_{(\mathbf{N}_i, \overline{\mathbf{N}}_j)} + \ln K_{(\mathbf{N}_i, \mathbf{N}_j)} \right],
\end{aligned} \tag{96}$$

where the sum on the third and fourth line exactly matches the single $U(1)_i$ contributions from the beta function coefficient and gauge threshold. The complete one-loop correction to the holomorphic gauge kinetic function of the linear combination $U(1)_X$ takes the form

$$\delta_{\text{total}} f_{U(1)_X}^{1\text{-loop}} = \sum_i x_i^2 \delta_{\text{total}} f_{U(1)_i}^{1\text{-loop}} + 4 \sum_{i < j} x_i x_j N_i \left(-\delta_j f_{SU(N_i)}^{1\text{-loop}} + \delta_{j'} f_{SU(N_i)}^{1\text{-loop}} \right), \tag{97}$$

where in the sum over $i < j$, we have used the fact that $\tilde{\Delta}_{ij} = \tilde{\Delta}_{ji}$, cf. e.g. [43–45, 40], and therefore $N_i N_j \tilde{\Delta}_{ij} = N_i \Delta_{ij} = N_j \Delta_{ji}$, which carries over to the holomorphic part as $N_i \delta_j f_{U(1)_i}^{1\text{-loop}} = N_j \delta_i f_{U(1)_j}^{1\text{-loop}}$. The total one-loop correction to the holomorphic gauge kinetic function has been defined in (93) for a single $U(1)_i$, and the individual contributions are given in table 17 and 18 for all orbifold backgrounds considered in this paper.

This completes the discussion of massless and massive Abelian gauge factors. An example of the massless $B - L$ symmetry in the Standard Model on T^6/\mathbb{Z}'_6 is given in section 5.

4 Example on $T^6/\mathbb{Z}_2 \times \mathbb{Z}_2$: Magnetised D9-branes vs. D6-branes at angles

Up to now, we have shown that our results for the gauge thresholds, Kähler metrics and holomorphic gauge kinetic functions of bulk, fractional and rigid D6-branes fit - up to subtleties in the one-loop field redefinitions of the dilaton and complex structure moduli and the extra terms from \mathbb{Z}_2 fixed and orientifold invariant points in the holomorphic gauge kinetic function at one loop - with those existing in the literature for the six-torus

and $T^6/\mathbb{Z}_2 \times \mathbb{Z}_2$ without torsion with vanishing displacement and Wilson line moduli [43, 61] and the partial results on $T^6/\mathbb{Z}_2 \times \mathbb{Z}_2$ with discrete torsion [45]. In this section, we further test the consistency of our results for rigid D6-branes in Type IIA string theory on $T^6/(\mathbb{Z}_2 \times \mathbb{Z}_2 \times \Omega\mathcal{R})$ with discrete torsion by matching with the T-dual D9- and D5-brane models in Type IIB string theory on $T^6/(\mathbb{Z}_2 \times \mathbb{Z}_2 \times \Omega)$ without torsion that were introduced in [1]. We find that, using rigid D6-branes at $\mathbb{Z}_2 \times \mathbb{Z}_2$ singularities, the gauge groups of the T-dual rigid D5-branes are of $U(N)$ type, which can be related to the $Sp(2N)$ groups in [1] by a recombination of rigid orientifold image D6-branes to fractional D6-branes stuck at one type of \mathbb{Z}_2 singularity only.

The correspondence of our notation with the one by Angelantonj *et al.* [1] is displayed in table 20: the T-dual of the exotic $O5_3$ -plane is the $\Omega\mathcal{R}\mathbb{Z}_2^{(3)}$ invariant exotic O6-plane, and the discrete choices of fixed point contributions correspond to displacements σ^i away from the origin of the two-torus $T_{(i)}^2$. Discrete Wilson lines are not taken into account in these examples.

For the bulk three-cycles on $T^6/\mathbb{Z}_2 \times \mathbb{Z}_2$, the notation is given in section 3.1 in formulas (45) to (47) with $b_1 = b_2 = b_3 = 0$ for the **aaa**-torus. For vanishing discrete Wilson lines, the exceptional three-cycles can be written as

$$\Pi_{\mathbb{Z}_2^{(k)}} = (-1)^{\tau_a^{\mathbb{Z}_2^{(k)}}} \sum_{\alpha\beta \in F_k^a} \left(n_a^k \varepsilon_{\alpha\beta}^{(k)} + m_a^k \tilde{\varepsilon}_{\alpha\beta}^{(k)} \right),$$

where F_k^a denotes the sets of $\mathbb{Z}_2^{(k)}$ fixed points on $T_{(i)}^2 \times T_{(j)}^2$ through which the toroidal three-cycles pass. The inclusion of discrete Wilson lines introduces additional relative signs among the different fixed point contributions, see [46] for details, but this possibility will be neglected in the following. For the given choice of an exotic O6-plane $\Omega\mathcal{R}\mathbb{Z}_2^{(3)}$, the overall three-cycle of the O6-planes is given by (remember the number $N_{O6} = 8$ of parallel O6-planes on the **aaa**-torus),

$$\Pi_{O6} = 2 \left(\Pi_{135}^{\text{bulk}} - \Pi_{146}^{\text{bulk}} - \Pi_{236}^{\text{bulk}} + \Pi_{245}^{\text{bulk}} \right),$$

and the exceptional three-cycles transform under the orientifold symmetry on the **aaa**-torus as follows

$$(\varepsilon_{\beta\gamma}^{(1)}, \tilde{\varepsilon}_{\beta\gamma}^{(1)}) \xrightarrow{\Omega\mathcal{R}} (-\varepsilon_{\beta\gamma}^{(1)}, \tilde{\varepsilon}_{\beta\gamma}^{(1)}), \quad (\varepsilon_{\alpha\gamma}^{(2)}, \tilde{\varepsilon}_{\alpha\gamma}^{(2)}) \xrightarrow{\Omega\mathcal{R}} (-\varepsilon_{\alpha\gamma}^{(2)}, \tilde{\varepsilon}_{\alpha\gamma}^{(2)}), \quad (\varepsilon_{\alpha\beta}^{(3)}, \tilde{\varepsilon}_{\alpha\beta}^{(3)}) \xrightarrow{\Omega\mathcal{R}} (\varepsilon_{\alpha\beta}^{(3)}, -\tilde{\varepsilon}_{\alpha\beta}^{(3)}), \quad (98)$$

where each $\mathbb{Z}_2^{(i)}$ fixed point $\alpha\beta \in T_{(j)}^2 \times T_{(k)}^2$ remains inert on the **aaa**-torus. In other words, the orientifold projection on the bulk and exceptional three-cycles on the **aaa**-torus is fixed completely by

$$(n_a^i, m_a^i) \xrightarrow{\Omega\mathcal{R}} (n_a^i, -m_a^i), \quad (\tau_a^{\mathbb{Z}_2^{(1)}}, \tau_a^{\mathbb{Z}_2^{(2)}}, \tau_a^{\mathbb{Z}_2^{(3)}}) \xrightarrow{\Omega\mathcal{R}} (\tau_a^{\mathbb{Z}_2^{(1)}} + 1, \tau_a^{\mathbb{Z}_2^{(2)}} + 1, \tau_a^{\mathbb{Z}_2^{(3)}}). \quad (99)$$

The supersymmetry conditions on the bulk three-cycles are given in equation (47). Supersymmetry of the rigid three-cycle implies that only exceptional three-cycles in a certain set $\{F_k^a\}_{k=1,2,3}$ of points traversed by the bulk three-cycle contribute, for more details see appendix C.

The bulk RR tadpole cancellation condition for an exotic $\Omega\mathcal{R}\mathbb{Z}_2^{(3)}$ -plane and the **aaa**-torus can be brought to the form,

$$\sum_x N_x \vec{X}_x = 16 (1, -1, -1, 1)^T,$$

while the exceptional contributions to the RR tadpoles have to cancel solely among the rigid D6-branes,

$$\sum_x N_x m_x^i \sum_{\alpha\beta \in F_x^i} \tilde{\varepsilon}_{\alpha\beta}^{(i)} = 0 \quad \text{for } i = 1, 2, \quad \sum_x N_x n_x^3 \sum_{\alpha\beta \in F_x^3} \varepsilon_{\alpha\beta}^{(3)} = 0.$$

Net-chiralities are computed via the intersection numbers of rigid three-cycles,

$$\begin{aligned} \Pi_a^{\text{rigid}} \circ \Pi_b^{\text{rigid}} &= -\frac{1}{4} \left(\vec{X}_a \cdot \vec{Y}_b - \vec{Y}_a \cdot \vec{X}_b + \sum_{i=1}^3 (-1)^{\tau_{ab}^{\mathbb{Z}_2^{(i)}}} I_{ab}^{(i)} \sum_{\substack{\alpha_a \beta_a \in F_a^i \\ \alpha_b \beta_b \in F_b^i}} \delta_{\alpha_a \alpha_b} \delta_{\beta_a \beta_b} \right) \equiv -\frac{1}{4} \left(I_{ab} + \sum_{i=1}^3 I_{ab}^{\mathbb{Z}_2^{(i)}} \right), \\ \Pi_a^{\text{rigid}} \circ \Pi_{O6} &= 2 \vec{Y}_a \cdot \vec{X}_{O6} \equiv -\frac{1}{4} \sum_{i=0}^3 \eta_{\Omega\mathcal{R}\mathbb{Z}_2^{(i)}} \tilde{I}_a^{\Omega\mathcal{R}\mathbb{Z}_2^{(i)}}, \end{aligned}$$

where the first line holds for vanishing discrete Wilson lines. For orientifold image D6-branes a and $b = a'$, the sum over fixed points gives $\sum_{\substack{\alpha_a \beta_a \in F_a^i \\ \alpha_b \beta_b \in F_{a'}^i}} \delta_{\alpha_a \alpha_b} \delta_{\beta_a \beta_b} = 4$, and the differences in $\mathbb{Z}_2^{(i)}$ eigenvalues due to the orientifold projection are given in (99).

The non-chiral part of the spectrum is computed from the beta function coefficients in tables 6 and 7. For all examples, the individual (toroidal and $\mathbb{Z}_2^{(i)}$ fixed point) intersection numbers are given in appendix C.

4.1 Examples 1 and 2 by Angelantonj *et al.* revisited

4.1.1 Example 1

The T-dual to the first magnetised D9-brane example in [1] contains four rigid D6-branes wrapping the same bulk three-cycle but with all four possible different combinations of

$\mathbb{Z}_2^{(i)}$ eigenvalues. The D6-brane configuration is displayed in table 21. The explicit rigid three-cycles are given in equation (120) of appendix C.1. The bulk RR tadpole cancellation condition requires $N_{a_i} = 4$ for $i = 1 \dots 4$, and net-chiralities are given by the intersection numbers of the rigid D6-branes,

$$\begin{aligned}\Pi_{a_i} \circ \Pi_{a_j} &= 0, \\ \Pi_{a_i} \circ \Pi'_{a_j} &= -2 \left(1 + (-1)^{\mathbb{Z}_2^{(1)} a_i a_j} \delta_{(\sigma^2 \sigma^3)_{a_i a_j}, 0} + (-1)^{\mathbb{Z}_2^{(2)} a_i a_j} \delta_{(\sigma^1 \sigma^3)_{a_i a_j}, 0} + (-1)^{\mathbb{Z}_2^{(3)} a_i a_j} \delta_{(\sigma^1 \sigma^2)_{a_i a_j}, 0} \right) \\ &= \begin{cases} -8 & a_i = a_j \\ 0 & a_i \neq a_j \end{cases} \quad \text{with} \quad (\vec{\sigma}_{a_i a_j}) = (\vec{0}), \\ \Pi_{a_i} \circ \Pi_{O6} &= -8,\end{aligned}$$

where on the second line we abbreviated $\delta_{(\sigma^m \sigma^n)_{a_i a_j}, 0} \equiv \delta_{\sigma_{a_i a_j}^m, 0} \delta_{\sigma_{a_i a_j}^n, 0}$. The individual toroidal and $\mathbb{Z}_2^{(i)}$ invariant intersection numbers are displayed in table 38 of appendix C.1 and can be checked for consistency with the net-chiralities. As a result, the gauge group $\prod_{i=1}^4 U(4)_{a_i}$ arises with the complete (chiral + non-chiral) massless matter spectrum consisting of non-chiral pairs of bifundamentals in the $a_i a_{j, j>i}$ sectors plus eight antisymmetric representations per D6-brane stack as listed in table 22, which matches with the original spectrum of [1] upon renaming of the D6-branes and their orientifold images,

$$(a_1, a_2, a_3, a_4)_{\text{here}} \simeq (a, \bar{a}, b', \bar{b}')_{\text{Angelantonj et al.}} \quad (100)$$

The anomaly matrix matches as expected the result reported in [1],

$$(C_{a_i a_j}) = \frac{32}{\pi^2} \begin{pmatrix} -1 & 0 & 0 & 0 \\ 0 & -1 & 0 & 0 \\ 0 & 0 & -1 & 0 \\ 0 & 0 & 0 & -1 \end{pmatrix},$$

up to re-labelling of the $\Omega\mathcal{R}$ images (b', \bar{b}') as (a_3, a_4) .

The Kähler metrics and v_i dependent one-loop contributions to the holomorphic gauge kinetic function $\delta_y f_{SU(4)_{a_1}}^{1\text{-loop}}$ with $y \in \{a_j, a'_j\}$ of the first gauge factor are given in table 23. The complete v_i -dependent one-loop contribution to $SU(4)_{a_1}$,

$$\delta_{\text{total}} f_{SU(4)_{a_1}}^{1\text{-loop}}(v_i) = \sum_{j=1}^4 \delta_{a_j} f_{SU(4)_{a_1}}^{1\text{-loop}}(v_i) = 0,$$

vanishes due to cancellations between $j = 1$ and $j = 2, 3, 4$. In accord with [1], the perturbative holomorphic gauge kinetic function is given by its tree-level value,

$$f_{SU(4)_{a_1}}^{1\text{-loop}} = f_{SU(4)_{a_1}}^{\text{tree}} + \text{const} \sim S + U_1 + U_2 - U_3 + \text{const}.$$

The additional angle dependent terms on the first line in (61) and (72) drop out upon summation, $\sum_{j=1}^4 I_{a_1 a'_j}^{\mathbb{Z}_2^{(k)}} = 0$ for any $k \in \{1, 2, 3\}$, as can be read off from the individual \mathbb{Z}_2 invariant intersection numbers in table 38 upon using the relative \mathbb{Z}_2 eigenvalues in table 37 of appendix C.1. The constant term consisting of the intersection numbers with O6-planes listed in table 38 gives

$$\text{const} = \frac{1}{2\pi^2} \ln 2.$$

This completes the discussion of the perturbatively exact holomorphic gauge kinetic function for $SU(4)_{a_1}$. The constant factor was to our knowledge not included in [1].

The Kähler metrics in table 23 for the complete massless spectrum have not been computed in [1] and are, to our knowledge, listed here for the first time.

4.1.2 Comments on example 2

The second example in [1] relies on the same rigid D6-branes as the previous example, where the gauge group is partially broken by vevs of some bifundamental representations as follows: each gauge factor is decomposed as $U(4)_{a_i} \rightarrow U(2)_{a_i} \times \widetilde{U(2)}_{a_i}$ with the splitting of the corresponding representations.

$$\begin{aligned} & \frac{U(4)_{a_i} \rightarrow U(2)_{a_i} \times \widetilde{U(2)}_{a_i}}{\mathbf{16}_{\text{Adj}} \rightarrow (\mathbf{4}_{\text{Adj}}, \mathbf{1}) + (\mathbf{1}, \mathbf{4}_{\text{Adj}}) + [(\mathbf{2}, \overline{\mathbf{2}}) + c.c.]} \\ & \mathbf{4} \rightarrow (\mathbf{2}, \mathbf{1}) + (\mathbf{1}, \mathbf{2}) \\ & \mathbf{6}_{\text{Anti}} \rightarrow (\mathbf{1}_{\text{Anti}}, \mathbf{1}) + (\mathbf{1}, \mathbf{1}_{\text{Anti}}) + (\mathbf{2}, \mathbf{2}) \\ & \mathbf{10}_{\text{Sym}} \rightarrow (\mathbf{3}_{\text{Sym}}, \mathbf{1}) + (\mathbf{1}, \mathbf{3}_{\text{Sym}}) + (\mathbf{2}, \mathbf{2}) \end{aligned}$$

Under this decomposition, the representations in table 22 split as,

$$\begin{aligned} & \frac{\prod_{i=1}^4 U(4)_{a_i} \rightarrow \left(\prod_{i=1}^4 U(2)_{a_i} \right) \times \left(\prod_{i=1}^4 \widetilde{U(2)}_{a_i} \right)}{(\mathbf{16}_{\text{Adj}}, \mathbf{1}, \mathbf{1}, \mathbf{1}) \rightarrow (\mathbf{4}_{\text{Adj}}, \mathbf{1}, \mathbf{1}, \mathbf{1}; \mathbf{1}, \mathbf{1}, \mathbf{1}, \mathbf{1}) + (\mathbf{1}, \mathbf{1}, \mathbf{1}, \mathbf{1}; \mathbf{4}_{\text{Adj}}, \mathbf{1}, \mathbf{1}, \mathbf{1}) + [(2, 1, 1, 1; \overline{2}, 1, 1, 1) + c.c.]} \\ & (\mathbf{4}, \overline{\mathbf{4}}, \mathbf{1}, \mathbf{1}) \rightarrow (\mathbf{2}, \overline{\mathbf{2}}, \mathbf{1}, \mathbf{1}; \mathbf{1}, \mathbf{1}, \mathbf{1}, \mathbf{1}) + (2, 1, 1, 1; \mathbf{1}, \overline{2}, 1, 1) + (1, \overline{2}, 1, 1; 2, 1, 1, 1) + (1, 1, 1, 1; 2, \overline{2}, 1, 1) \\ & (\overline{\mathbf{6}}_{\text{Anti}}, \mathbf{1}, \mathbf{1}, \mathbf{1}) \rightarrow (\mathbf{1}_{\text{Anti}}, \mathbf{1}, \mathbf{1}, \mathbf{1}; \mathbf{1}, \mathbf{1}, \mathbf{1}, \mathbf{1}) + (\mathbf{1}, \mathbf{1}, \mathbf{1}, \mathbf{1}; \mathbf{1}_{\text{Anti}}, \mathbf{1}, \mathbf{1}, \mathbf{1}) + (\overline{\mathbf{2}}, \mathbf{1}, \mathbf{1}, \mathbf{1}; \overline{\mathbf{2}}, \mathbf{1}, \mathbf{1}, \mathbf{1}) \end{aligned}$$

and the last four gauge factors are broken to the diagonal one, $\left(\prod_{i=1}^4 \widetilde{U(2)}_{a_i}\right) \rightarrow \widetilde{U(2)}_{\text{diag}}$, by giving suitable vevs to bifundamental matter states. The states which have to survive the projection in order to reproduce the spectrum of the second example in [1] are highlighted in bold letters in table 24. The vevs are chosen such that the diagonal Abelian gauge factor $\widetilde{U(2)}_{\text{diag}}$ effectively wraps a bulk three-cycle.

4.2 Example 3 by Angelantonj *et al.* revisited

The third example in [1] has three different kinds of D6-branes a_i , b_j and c_k with $i \in \{1 \dots 4\}$ and $j, k \in \{1, 2\}$. The explicit bulk and fixed point configurations are given in table 25, and the bulk RR tadpoles cancel for $N_{a_i} = 2$, $N_{b_j} = N_{c_k} = 4$.⁴ In contrast to the four unitary times four symplectic gauge factor listed in [1], it turns out that the full gauge group on rigid D6-branes consists of eight unitary gauge factors,

$$\left(\prod_{i=1}^4 U(2)_{a_i}\right) \times \left(\prod_{i=1}^2 U(4)_{b_i}\right) \times \left(\prod_{i=1}^2 U(4)_{c_i}\right),$$

as can be explicitly verified by close inspection of the exceptional parts of the three-cycles Π_{b_j} , Π_{c_k} and their orientifold images given in (121) and (122) in appendix C.2. Table 5 also shows that for the present choice of exotic O6-plane with $(\eta_{\mathbb{Z}_2^{(1)}}, \eta_{\mathbb{Z}_2^{(2)}}, \eta_{\mathbb{Z}_2^{(3)}}) = (1, 1, -1)$ on the **aaa**-torus, i.e. $b_1 = b_2 = b_3 = 0$, all orientifold invariant rigid three-cycles will have their bulk parts parallel to the $\Omega\mathcal{R}\mathbb{Z}_2^{(3)}$ invariant O6-plane, whereas the $D6_{b_j}$ are parallel to the $\Omega\mathcal{R}$ -invariant plane and the $D6_{c_k}$ -branes are parallel to the $\Omega\mathcal{R}\mathbb{Z}_2^{(1)}$ -invariant plane. The symplectic gauge factors [1] arise by recombination processes of orientifold image D6-branes as detailed further below.

⁴In table 10 of [1]v3, only bifundamental matter in $a_i a_j$ sectors with $(i, j) = (1, 2)$ and $(3, 4)$ is listed, for which a matching of the spectrum requires a discrete displacement $(\vec{\sigma}_{a_j, j=3,4}) = (1, 0, 0)$ along $T_{(1)}^2$, and correspondingly not only the beta function coefficients $b_{a_1 a_j, j \in \{3,4\}}^A = 0$ in the analogon to table 27 vanish, but also the one-loop gauge threshold contributions $\delta_{a_j, j \in \{3,4\}} \text{f}_{SU(2)_{a_1}}^{\text{1-loop}}(v_j)$ leading in total to a non-vanishing one-loop contribution $\sum_{j=1}^4 \delta_{a_j} \text{f}_{SU(2)_{a_1}}^{\text{1-loop}}(v_i) = \frac{1}{2\pi} \sum_{i=2}^3 \ln \eta(iv_i)$. The displacement $(\vec{\sigma}_{a_i, i \in \{3,4\}}) = (1, 0, 0)$ modifies also the $a_i b_j$ and $a_i c_j$ sectors for $i \in \{3, 4\}$ in table 26 and the corresponding entries in the anomaly-matrix (101) as follows: the $a_i b_j$ sectors contribute $(\mathbf{1}, \mathbf{1}, \bar{\mathbf{2}}, \mathbf{1}; \mathbf{4}, \mathbf{1}; \mathbf{1}, \mathbf{1}) + (\mathbf{1}, \mathbf{1}, \bar{\mathbf{2}}, \mathbf{1}; \mathbf{1}, \mathbf{4}; \mathbf{1}, \mathbf{1}) + (\mathbf{1}, \mathbf{1}, \mathbf{1}, \bar{\mathbf{2}}; \mathbf{1}, \mathbf{4}; \mathbf{1}, \mathbf{1}) + (\mathbf{1}, \mathbf{1}, \mathbf{1}, \bar{\mathbf{2}}; \mathbf{4}, \mathbf{1}; \mathbf{1}, \mathbf{1})$ and the $a_i c_j$ sectors $(\mathbf{1}, \mathbf{1}, \bar{\mathbf{2}}, \mathbf{1}; \mathbf{1}, \mathbf{1}; \mathbf{4}, \mathbf{1}) + (\mathbf{1}, \mathbf{1}, \bar{\mathbf{2}}, \mathbf{1}; \mathbf{1}, \mathbf{1}; \mathbf{1}, \mathbf{4}) + (\mathbf{1}, \mathbf{1}, \mathbf{1}, \bar{\mathbf{2}}; \mathbf{1}, \mathbf{1}; \mathbf{1}, \mathbf{4}) + (\mathbf{1}, \mathbf{1}, \mathbf{1}, \bar{\mathbf{2}}; \mathbf{1}, \mathbf{1}; \mathbf{4}, \mathbf{1})$ to the massless spectrum, and the associated anomaly matrix entries read $\begin{pmatrix} C_{a_3 b_1} & C_{a_3 b_2} \\ C_{a_4 b_1} & C_{a_4 b_2} \end{pmatrix} = - \begin{pmatrix} C_{b_1 a_3} & C_{b_1 a_4} \\ C_{b_2 a_3} & C_{b_2 a_4} \end{pmatrix} = \begin{pmatrix} C_{a_3 c_1} & C_{a_3 c_2} \\ C_{a_4 c_1} & C_{a_4 c_2} \end{pmatrix} = - \begin{pmatrix} C_{c_1 a_3} & C_{c_1 a_4} \\ C_{c_2 a_3} & C_{c_2 a_4} \end{pmatrix} = \begin{pmatrix} \frac{1}{2} & \frac{1}{2} \\ \frac{1}{2} & \frac{1}{2} \end{pmatrix}$. However, as communicated to me by some authors of [1], the spectrum in table 10 of [1]v3 belongs to a D-brane configuration without any discrete displacement and Wilson line parameters turned on, and the missing states in the $a_i a_j$ sector with $i \in \{1, 2\}$ and $j \in \{3, 4\}$ can be found in table 2 of [67].

The net-chiralities are obtained from the following intersection numbers,

$$\begin{aligned}
\Pi_{a_i} \circ \Pi_{a_j} &= \Pi_{b_i} \circ \Pi_{b_j} = \Pi_{c_i} \circ \Pi_{c_j} = \Pi_{c_i} \circ \Pi_{O6} = \Pi_{c_j} \circ \Pi_{O6} = 0, \\
\Pi_{a_i} \circ \Pi_{b_j} &= \frac{1}{2} \left(-1 + (-1)^{\tau_{a_i b_j}^{\mathbb{Z}_2^{(1)}}} + \left[(-1)^{\tau_{a_i b_j}^{\mathbb{Z}_2^{(2)}}} - (-1)^{\tau_{a_i b_j}^{\mathbb{Z}_2^{(3)}}} \right] \delta_{\sigma_{a_i b_j}^1, 0} \right) \\
&= \begin{cases} 0 & (-1)^{\tau_{a_i b_j}^{\mathbb{Z}_2^{(k)}}} = (+, +, +), (+, -, -) \\ -1 + \delta_{\sigma_{a_i b_j}^1, 0} & (-, +, -) \\ -1 - \delta_{\sigma_{a_i b_j}^1, 0} & (-, -, +) \end{cases} , \\
\Pi_{a_i} \circ \Pi_{c_j} &= \frac{1}{2} \left(-1 + (-1)^{\tau_{a_i c_j}^{\mathbb{Z}_2^{(1)}}} + \left[-(-1)^{\tau_{a_i c_j}^{\mathbb{Z}_2^{(2)}}} + (-1)^{\tau_{a_i c_j}^{\mathbb{Z}_2^{(3)}}} \right] \delta_{\sigma_{a_i c_j}^1, 0} \right) \\
&= \begin{cases} 0 & (-1)^{\tau_{a_i c_j}^{\mathbb{Z}_2^{(k)}}} = (+, +, +), (+, -, -) \\ -1 - \delta_{\sigma_{a_i c_j}^1, 0} & (-, +, -) \\ -1 + \delta_{\sigma_{a_i c_j}^1, 0} & (-, -, +) \end{cases} , \\
\Pi_{b_i} \circ \Pi_{c_j} &= \frac{\delta_{\sigma_{b_i c_j}^1, 0}}{2} \left(-(-1)^{\tau_{b_i c_j}^{\mathbb{Z}_2^{(2)}}} + (-1)^{\tau_{b_i c_j}^{\mathbb{Z}_2^{(3)}}} \right) = \delta_{\sigma_{b_i c_j}^1, 0} \times \begin{cases} -1 & (-1)^{\tau_{b_i c_j}^{\mathbb{Z}_2^{(k)}}} = (-, +, -) \\ 0 & (+, +, +), (+, -, -) \\ 1 & (-, -, +) \end{cases} , \\
\Pi_{a_i} \circ \Pi'_{a_j} &= -2 \left(2 + 2(-1)^{\tau_{a_i a_j}^{\mathbb{Z}_2^{(1)}}} \delta_{(\sigma^2 + \sigma^3)_{a_i a_j}, 0} + (-1)^{\tau_{a_i a_j}^{\mathbb{Z}_2^{(2)}}} \delta_{(\sigma^1 + \sigma^3)_{a_i a_j}, 0} + (-1)^{\tau_{a_i a_j}^{\mathbb{Z}_2^{(3)}}} \delta_{(\sigma^1 + \sigma^2)_{a_i a_j}, 0} \right) \\
&= \begin{cases} -12 & (-1)^{\tau_{a_i a_j}^{\mathbb{Z}_2^{(i)}}} = (+, +, +) \text{ and } \sigma_{a_i a_j}^1 = \sigma_{a_i a_j}^2 = \sigma_{a_i a_j}^3 = 0 \\ -4 & (+, -, -) \text{ and } \sigma_{a_i a_j}^1 = \sigma_{a_i a_j}^2 = \sigma_{a_i a_j}^3 = 0 \\ 0 & (-, +, -), (-, -, +) \text{ and } \sigma_{a_i a_j}^2 = \sigma_{a_i a_j}^3 = 0 \end{cases} ,
\end{aligned}$$

$$\Pi_{a_i} \circ \Pi_{O6} = -12,$$

and the full matter spectrum is computed using the individual torus and $\mathbb{Z}_2^{(i)}$ invariant intersection numbers in table 39 of appendix C.2. It consists of different kinds of bifundamental and antisymmetric matter representations as listed in table 26.

Since the rigid b_i and c_j -branes do support the symplectic gauge factors listed in [1] before recombination to fractional non-rigid orientifold invariant D6-branes, it is not surprising that the matter spectrum presented here does not fully agree with the literature. The $a_i a_j$, $a_i a'_j$, $a_i b_j$, $a_i b'_j$, $a_i c_j$ and $a_i c'_j$ sectors match with [1] (up to the conjugate representation on

all a_3 and a_4 branes just like in the first example and up to the complex instead of real representations on b_j and c_j). The multiplicities in all $b_i b_j$, $b_i b'_j$, $c_i c_j$ and $c_i c'_j$ sectors are by a factor of two bigger than those given in [1], which is consistent with the following breaking pattern of the gauge groups upon the recombination of two rigid to two fractional to a single bulk D6-brane along path (a), where the spectrum in [1] corresponds to

$U(4)_{c_1} \times U(4)_{c_2}$ $c_i c_j : \quad [(\mathbf{1}, \mathbf{1}, \mathbf{1}, \mathbf{1}; \mathbf{1}, \mathbf{1}; \mathbf{4}, \overline{\mathbf{4}}) + c.c.]$ $c_i c'_j : \quad [(\mathbf{1}, \mathbf{1}, \mathbf{1}, \mathbf{1}; \mathbf{1}, \mathbf{1}; \mathbf{4}, \mathbf{4}) +$ $\quad + (\mathbf{1}, \mathbf{1}, \mathbf{1}, \mathbf{1}; \mathbf{1}, \mathbf{1}; \mathbf{6}_{\text{Anti}}, \mathbf{1}) +$ $\quad + (\mathbf{1}, \mathbf{1}, \mathbf{1}, \mathbf{1}; \mathbf{1}, \mathbf{1}; \mathbf{1}, \mathbf{6}_{\text{Anti}}) + c.c.]$	$\xrightarrow{(1b)}$	$U(4)_{\tilde{C}}$ $\tilde{C}\tilde{C} : \quad [(\mathbf{1}, \mathbf{1}, \mathbf{1}, \mathbf{1}; \mathbf{1}, \mathbf{1}; \mathbf{6}_{\text{Anti}}) + c.c.]$
$(1a) \downarrow$		$\downarrow (2b)$
$Sp(4)_{\tilde{c}_1} \times Sp(4)_{\tilde{c}_2}$ $\tilde{c}_i \tilde{c}_i : \quad (\mathbf{1}, \mathbf{1}, \mathbf{1}, \mathbf{1}; \mathbf{1}, \mathbf{1}; \mathbf{6}_{\text{Anti}}, \mathbf{1})$ $\quad + (\mathbf{1}, \mathbf{1}, \mathbf{1}, \mathbf{1}; \mathbf{1}, \mathbf{1}; \mathbf{1}, \mathbf{6}_{\text{Anti}})$ $\tilde{c}_1 \tilde{c}_2 : \quad 2 \times (\mathbf{1}, \mathbf{1}, \mathbf{1}, \mathbf{1}; \mathbf{1}, \mathbf{1}; \mathbf{4}, \mathbf{4})$	$\xrightarrow{(2a)}$	$Sp(4)_C$ $CC : \quad (\mathbf{1}, \mathbf{1}, \mathbf{1}, \mathbf{1}; \mathbf{1}, \mathbf{1}; \mathbf{6}_{\text{Anti}})$

performing step (1a) on the spectrum in table 26 by recombining $\Pi_{\tilde{c}_i} = \Pi_{c_i} + \Pi_{c'_i}$. Performing instead step (1b) with $\Pi_{\tilde{C}} = \Pi_{c_1} + \Pi_{c_2}$ or $\Pi_{\tilde{C}} = \Pi_{c_1} + \Pi_{c'_2}$ leads to fractional D6-branes along $T^2_{(1)} \times \left(T^4_{(2,3)}/\mathbb{Z}_2^{(1)}\right)$ which are T-dual to the well-known fractional D5-branes in [68, 69]. Finally step (2a) or (2b) leads to a pure bulk D6-brane wrapping $\Pi_C = \sum_{i=1}^2 (\Pi_{c_i} + \Pi_{c'_i})$, which is the T-dual to a D5-brane at an arbitrary position in the bulk. The discussion for the recombination of the b_i -branes follows the same lines with the T-duality directions chosen along the $\Re(z_{2i-1})$ axes instead of the $\Im(z_{2i})$ axes above.

The spectrum in table 26 satisfies all consistency checks involving net-chiralities and the cancellation of the eight different $U(N_x)^3$ anomalies. Details on the match to [1] are given in appendix C.2 based on a close inspection of the rigid three-cycles and RR tadpole cancellation conditions in the presence of an exotic $\Omega\mathcal{R}\mathbb{Z}_2^{(3)}$ -plane.

The anomaly matrix with entries defined in (79) reads

$$\left(\begin{array}{c|c|c} C_{a_i a_j} & C_{a_i b_j} & C_{a_i c_j} \\ \hline C_{b_i a_j} & C_{b_i b_j} & C_{b_i c_j} \\ \hline C_{c_i a_j} & C_{c_i b_j} & C_{c_i c_j} \end{array} \right) = \frac{4}{\pi^2} \left(\begin{array}{cccc|cc|cc} -3 & -1 & 0 & 0 & -1 & 0 & -1 & 0 \\ -1 & -3 & 0 & 0 & 0 & -1 & 0 & -1 \\ 0 & 0 & -3 & -1 & 0 & 1 & 1 & 0 \\ 0 & 0 & -1 & -3 & 1 & 0 & 0 & 1 \\ \hline -1 & 0 & 0 & -1 & 0 & 0 & -1 & 1 \\ 0 & -1 & -1 & 0 & 0 & 0 & 1 & -1 \\ \hline -1 & 0 & -1 & 0 & -1 & 1 & 0 & 0 \\ 0 & -1 & 0 & -1 & 1 & -1 & 0 & 0 \end{array} \right), \quad (101)$$

and the $a_i a_j$ sectors in the upper left corner agree with the complete anomaly matrix in [1], whereas the other entries appear here since we consider the gauge group $(\prod_{i=1}^2 U(4)_{b_i}) \times (\prod_{j=1}^2 U(4)_{c_j})$ before the breaking to $(\prod_{i=1}^2 Sp(4)_{b_i}) \times (\prod_{j=1}^2 Sp(4)_{c_j})$.

The Kähler metrics and the v_i -dependent one-loop contributions to the holomorphic gauge kinetic function $\delta_y f_{SU(2)_{a_1}}^{1\text{-loop}}(v_i)$ involving brane a_1 are listed in table 27. The tree-level value of the holomorphic gauge kinetic functions for the a_i branes,

$$f_{SU(2)_{a_i}}^{\text{tree}} \sim S + U_1 + 2U_2 - 2U_3,$$

agrees with [1].

The holomorphic gauge kinetic function for a_1 in this example does not receive a v_i -moduli dependent one-loop correction due to the cancellation from all a_i sectors,

$$\delta_{\text{total}} f_{SU(2)_{a_1}}^{1\text{-loop}} = \sum_{j=1}^4 \delta_{a_j} f_{SU(2)_{a_1}}^{1\text{-loop}}(v_i) + \text{const} = \text{const},$$

in agreement with [1]. The Kähler metrics for matter with $SU(2)_{a_1}$ charge in table 27 are to our knowledge given here for the first time.

The angle dependent contributions in (61) and (72) again sum to zero,

$$\sum_{j=1}^4 I_{a_1 a'_j}^{\mathbb{Z}_2^{(k)}} = \sum_{j=1}^4 I_{a_1 b_j}^{\mathbb{Z}_2^{(k)}} = \sum_{j=1}^4 I_{a_1 c_j}^{\mathbb{Z}_2^{(k)}} = 0 \quad \text{for } k = 1, 2, 3,$$

and the constant factor due to the intersections with O6-planes is twice the one from example 1,

$$\text{const} = \frac{1}{\pi^2} \ln 2,$$

as can be seen by comparing the individual intersection numbers for the present model in table 39 with those of example 1 in table 38. This completes the discussion of the open string Kähler metrics with charge under the $D6_{a_1}$ -brane and perturbatively exact holomorphic gauge kinetic function for the same D6-brane.

5 Example on T^6/\mathbb{Z}'_6 : the Standard Model on fractional D6-branes

On the T^6/\mathbb{Z}'_6 orbifold background, each torus three-cycle has three orbifold images. This leads to a sum over these images when computing the holomorphic gauge kinetic function, and matter states with identical charges can be localised at intersections of different orbifold images and thereby have distinct Kähler metrics. This happens e.g. for the various quark families in the Standard Model on T^6/\mathbb{Z}'_6 presented in [41, 2], for which the gauge thresholds have been computed in [40]. More model building on the same orbifold background can be found e.g. in [70–72]. In this section, we will give some examples for the decomposition into Kähler metrics for matter charged under the QCD stack $SU(3)_a$ or the ‘leptonic’ stack $U(1)_d$ as well as for the perturbatively exact holomorphic gauge kinetic function $f_{SU(3)_a}$ along the generic prescription in section 3.2 with modifications for $h_{21}^{\text{bulk}} = 1$ discussed in section 3.2.2. We will furthermore discuss two examples of orientifold invariant D6-branes, one parallel and the other perpendicular to the $\Omega\mathcal{R}$ plane as classified in section 3.3, and finally we will use the framework of section 3.4 and present the complete perturbatively exact holomorphic gauge kinetic functions for the single $U(1)_a$ and $U(1)_d$ factors as well as for the anomaly-free combination $U(1)_{B-L} = \frac{1}{3}U(1)_a + U(1)_d$.

The D6-brane configuration is displayed in table 28. In order to compute the Kähler metrics for D6-branes intersecting at three non-vanishing angles, it is useful to note the following values of ratios of Gamma functions (cf. table 14),

$$\prod_{i=1}^3 \left(\frac{\Gamma(|\phi_{xy}^{(i)}|)}{\Gamma(1 - |\phi_{xy}^{(i)}|)} \right)^{-\frac{\text{sgn}(\phi_{xy}^{(i)})}{\text{sgn}(I_{xy})}} = \begin{cases} \frac{25}{2} & (\vec{\phi}_{xy}) = \pm(\frac{1}{6}, \frac{1}{6}, -\frac{1}{3}) \\ 8 & \pm(\frac{1}{3}, \frac{1}{3}, -\frac{2}{3}) \\ 10 & \pm(\frac{1}{6}, \frac{1}{3}, -\frac{1}{2}) \end{cases},$$

which occur in the model. Since the Kähler metrics are independent of the chirality, each value holds for both orientations of angles. This is assured by the factor $\text{sgn}(I_{xy})$ in the exponent. The relative angles, beta function coefficients and Kähler metrics related to branes a and d , which include those for all quarks and leptons, are listed in table 29 as typical examples.

In contrast to the Standard Model on the six-torus, e.g. [73], or the $T^6/\mathbb{Z}_2 \times \mathbb{Z}_2$ orbifold, e.g. [4, 3, 8], particle generations can arise at intersections of various orbifold image D6-branes. As an example, the ac sector provides two generations of right-handed quarks with Kähler metric $K_{(\bar{3},1)} = f(S,U) \sqrt{\frac{4\pi}{\sqrt{3}v_2v_3}}$ at vanishing angle on $T_{(1)}^2$, while the $a(\theta^2c)$ sector provides the third right-handed quark generation with Kähler metric $K_{(\bar{3},1)} = f(S,U) \sqrt{\frac{10}{v_1v_2v_3}}$ at three non-trivial angles. The size of the physical Yukawa couplings is thus not only governed by the triangular worldsheets contributing to the holomorphic factor [54, 55], but also by the values of the Kähler metrics. For matter localised at some intersection with one vanishing angle, e.g. $\phi_{ac}^{(1)} = 0$, the Kähler metric depends only on the volume of the remaining four-torus, e.g. v_2v_3 for the ac sector. This makes it possible to obtain Yukawa hierarchies by choosing unisotropic two-tori. More details for the interplay of these various effects will be given in [53].

The holomorphic tree-level gauge couplings for $SU(3)_a$, the anomalous $U(1)_a$ and $U(1)_d$ and the massless linear combination $U(1)_{B-L}$ read

$$f_{SU(3)_a}^{\text{tree}} = \text{const.} \cdot U, \quad f_{U(1)_a}^{\text{tree}} = \text{const.} \cdot 6U, \quad f_{U(1)_d}^{\text{tree}} = \text{const.} \cdot 6U, \quad f_{U(1)_{B-L}}^{\text{tree}} = \text{const.} \cdot \frac{20}{3}U, \quad (102)$$

with the definition of the bulk complex structure U on T^6/\mathbb{Z}'_6 given in (80) and the constant identical for all four gauge groups. These gauge factors do at tree level not depend on the dilaton S , as can be seen from the corresponding bulk wrapping numbers in table 28.

The basic building blocks for the one-loop contributions to the holomorphic gauge kinetic functions of the strong interactions, $f_{SU(3)_a}^{1\text{-loop}}$, as well as the (anomalous and unphysical) single $U(1)$ charges, $f_{U(1)_a}^{1\text{-loop}}$ and $f_{U(1)_d}^{1\text{-loop}}$, and their physical linear combination $U(1)_{B-L} = \frac{1}{3}U(1)_a + U(1)_d$, $f_{U(1)_{B-L}}^{1\text{-loop}}$, are listed in table 30. For $SU(3)_a$, summing up all contributions we obtain the two-torus volume v_i dependent one-loop correction,

$$\begin{aligned} \delta_{\text{total}} f_{SU(3)_a}^{1\text{-loop}}(v_i) &= \sum_{k=0}^2 \sum_{y=a,a',b,b',c,d,d',h_3} \delta_{(\theta^k y)} f_{SU(3)_a}^{1\text{-loop}}(v_i) \\ &= \frac{1}{2\pi^2} \left(\ln \eta(i\tilde{v}_1) - \ln \eta(iv_1) \right) - \frac{2}{\pi^2} \ln \eta(iv_3) - \frac{3}{4\pi^2} \ln \left(e^{-\pi v_3/4} \frac{\vartheta_1\left(\frac{1-iv_3}{2}, iv_3\right)}{\eta(iv_3)} \right), \end{aligned} \quad (103)$$

and the ‘constant’ contribution is given by

$$\delta_{\text{total}} f_{SU(3)_a}^{1\text{-loop}}(c) = \frac{1}{2\pi^2} \ln \left[2^{15/8} \left(\frac{\sqrt{3}r v_1 v_3}{v_2^2} \right)^{1/4} \right]. \quad (104)$$

The dependence on two-torus volumes in the ‘constant’ factor arises because the stack a is of the special type discussed in section 3.2 perpendicular to the $\Omega\mathcal{R}$ invariant O6-plane

orbit along $T_{(2)}^2 \times T_{(3)}^2$. The one-loop correction (103) is a rather short expression compared to the ones for $U(1)_d$ and $U(1)_{B-L}$ below since the third two-torus is of **a**-type, which allows to combine the lattice sums from annulus and Möbius strip.

For the single (anomalous) $U(1)_a$ and $U(1)_d$ gauge factors summing up the generic one-loop contributions (93) gives

$$\begin{aligned} \delta_{\text{total}} f_{U(1)_a}^{\text{1-loop}}(v_i) &= 6 \times \left(\delta_{\text{total}} f_{SU(3)_a}^{\text{1-loop}}(v_i) + \sum_{k=0}^2 \delta_{(\theta^k a')} f_{SU(3)_a}^{\text{1-loop}, \mathcal{A}}(v_i) - \sum_{k=0}^2 \delta_{(\theta^k a)} f_{SU(3)_a}^{\text{1-loop}}(v_i) \right) \\ &= \frac{3}{\pi^2} \left(\ln \eta(i\tilde{v}_1) - \ln \eta(iv_1) \right) - \frac{18}{\pi^2} \ln \eta(iv_2) \\ &\quad - \frac{12}{\pi^2} \ln \eta(iv_3) - \frac{9}{2\pi^2} \ln \left(e^{-\pi v_3/4} \frac{\vartheta_1\left(\frac{1-iv_3}{2}, iv_3\right)}{\eta(iv_3)} \right), \end{aligned} \quad (105)$$

and

$$\begin{aligned} \delta_{\text{total}} f_{U(1)_d}^{\text{1-loop}}(v_i) &= 2 \times \left(\sum_{k=0}^2 \sum_{y \neq d} \delta_{(\theta^{-k} y)} f_{SU(1)_d}^{\text{1-loop}}(v_i) + \sum_{k=0}^2 \delta_{(\theta^{-k} d')} f_{SU(1)_d}^{\text{1-loop}, \mathcal{A}}(v_i) \right) \\ &= -\frac{3}{2\pi^2} \ln \left(e^{-\pi v_1/4} \frac{\vartheta_1\left(\frac{-iv_1}{2}, iv_1\right)}{\eta(iv_1)} \right) - \delta_{\sigma_{cd}^2, 0} \delta_{\tau_{cd}^2, 0} \times \frac{1}{\pi^2} \ln \eta(iv_2) \\ &\quad - \frac{1}{\pi^2} \left(\delta_{\sigma_{bd}^2, 0} \delta_{\tau_{bd}^2, 0} + \delta_{\sigma_{bd'}^2, 0} \delta_{\tau_{bd'}^2, 0} \right) \ln \eta(iv_2) \\ &\quad - \frac{1}{\pi^2} (1 - \delta_{\sigma_{bd}^2, 0} \delta_{\tau_{bd}^2, 0}) \ln \left(e^{-\pi(\sigma_{bd}^2)^2 v_2/4} \frac{\vartheta_1\left(\frac{\tau_{bd}^2 - i\sigma_{bd}^2 v_2}{2}, iv_2\right)}{\eta(iv_2)} \right) \\ &\quad - \frac{1}{2\pi^2} (1 - \delta_{\sigma_{bd'}^2, 0} \delta_{\tau_{bd'}^2, 0}) \ln \left(e^{-\pi(\sigma_{bd'}^2)^2 v_2/4} \frac{\vartheta_1\left(\frac{\tau_{bd'}^2 - i\sigma_{bd'}^2 v_2}{2}, iv_2\right)}{\eta(iv_2)} \right) \\ &\quad - \frac{1}{2\pi^2} (1 - \delta_{\sigma_{cd}^2, 0} \delta_{\tau_{cd}^2, 0}) \ln \left(e^{-\pi(\sigma_{cd}^2)^2 v_2/4} \frac{\vartheta_1\left(\frac{\tau_{cd}^2 - i\sigma_{cd}^2 v_2}{2}, iv_2\right)}{\eta(iv_2)} \right) \\ &\quad + \delta_{\sigma_{dd'}^2, 0} \delta_{\tau_{dd'}^2, 0} \times \frac{2}{\pi} (-\ln \eta(iv_2) + \ln \eta(i\tilde{v}_2)) \\ &\quad - (1 - \delta_{\sigma_{dd'}^2, 0} \delta_{\tau_{dd'}^2, 0}) \frac{1}{\pi^2} \times \left[\ln \left(e^{-\pi(\sigma_{dd'}^2)^2 v_2/4} \frac{\vartheta_1\left(\frac{\tau_{dd'}^2 - i\sigma_{dd'}^2 v_2}{2}, iv_2\right)}{\eta(iv_2)} \right) \right. \\ &\quad \quad \left. - \ln \left(e^{-\pi(\sigma_{dd'}^2)^2 \tilde{v}_2/4} \frac{\vartheta_1\left(\frac{\tau_{dd'}^2 - i\sigma_{dd'}^2 \tilde{v}_2}{2}, i\tilde{v}_2\right)}{\eta(i\tilde{v}_2)} \right) \right] \\ &\quad - \frac{9}{\pi^2} \ln \eta(iv_3) - \frac{9}{\pi^2} \ln \left(e^{-\pi v_3/4} \frac{\vartheta_1\left(\frac{1-iv_3}{2}, iv_3\right)}{\eta(iv_3)} \right). \end{aligned} \quad (106)$$

The lengthy expression for the latter is due to the continuous relative displacements and

Wilson lines for all D6-branes along $T_{(2)}^2$, which are crucial for making non-chiral matter massive and for breaking $Sp(2)_c \rightarrow U(1)_c$. The Kähler metrics for massless matter depend only on the relative intersection angles and are thus not changed under this gauge symmetry breaking. This means in particular that right-handed up- and down-type quarks as well as Higgses in the present example will have pairwise identical Kähler metrics.

The $U(1)$ anomaly matrix (79) has the form

$$\begin{pmatrix} C_{aa} & C_{ab} & C_{ad} \\ C_{ba} & C_{bb} & C_{bd} \\ C_{da} & C_{db} & C_{dd} \end{pmatrix} = \frac{1}{2\pi^2} \begin{pmatrix} 0 & 9 & 0 \\ 9 & 0 & -3 \\ 0 & 9 & 0 \end{pmatrix}$$

before the breaking of $Sp(2)_c \rightarrow U(1)_c$. The fact that this matrix has rank two is in agreement with the existence of a massless $U(1)_{B-L} = \frac{1}{3}U(1)_a + U(1)_d$ gauge group, for which the v_i dependent one-loop corrections to the holomorphic gauge kinetic function are given by

$$\begin{aligned} \delta_{\text{total}} f_{U(1)_{B-L}}^{\text{1-loop}}(v_i) &= \frac{1}{9} \delta_{\text{total}} f_{U(1)_a}^{\text{1-loop}}(v_i) + \delta_{\text{total}} f_{U(1)_d}^{\text{1-loop}}(v_i) + 4 \left(-\delta_d f_{SU(3)_a}^{\text{1-loop}}(v_i) + \delta_{d'} f_{SU(3)_a}^{\text{1-loop}}(v_i) \right) \\ &= \frac{1}{3\pi^2} \left(\ln \eta(i\tilde{v}_1) - \ln \eta(iv_1) \right) - \frac{3}{2\pi^2} \ln \left(e^{-\pi v_1/4} \frac{\vartheta_1\left(\frac{-iv_1}{2}, iv_1\right)}{\eta(iv_1)} \right) \\ &\quad - \frac{1}{\pi^2} \left(\delta_{\sigma_{bd}^2,0} \delta_{\tau_{bd}^2,0} + \delta_{\sigma_{bd'}^2,0} \delta_{\tau_{bd'}^2,0} + 2 \right) \ln \eta(iv_2) \\ &\quad - \frac{1}{\pi^2} (1 - \delta_{\sigma_{bd}^2,0} \delta_{\tau_{bd}^2,0}) \ln \left(e^{-\pi(\sigma_{bd}^2)^2 v_2/4} \frac{\vartheta_1\left(\frac{\tau_{bd}^2 - i\sigma_{bd}^2 v_2}{2}, iv_2\right)}{\eta(iv_2)} \right) \\ &\quad - \frac{1}{2\pi^2} (1 - \delta_{\sigma_{bd'}^2,0} \delta_{\tau_{bd'}^2,0}) \ln \left(e^{-\pi(\sigma_{bd'}^2)^2 v_2/4} \frac{\vartheta_1\left(\frac{\tau_{bd'}^2 - i\sigma_{bd'}^2 v_2}{2}, iv_2\right)}{\eta(iv_2)} \right) \\ &\quad - \delta_{\sigma_{cd}^2,0} \delta_{\tau_{cd}^2,0} \times \frac{1}{\pi^2} \ln \eta(iv_2) - \frac{1}{2\pi^2} (1 - \delta_{\sigma_{cd}^2,0} \delta_{\tau_{cd}^2,0}) \ln \left(e^{-\pi(\sigma_{cd}^2)^2 v_2/4} \frac{\vartheta_1\left(\frac{\tau_{cd}^2 - i\sigma_{cd}^2 v_2}{2}, iv_2\right)}{\eta(iv_2)} \right) \\ &\quad + \delta_{\sigma_{dd'}^2,0} \delta_{\tau_{dd'}^2,0} \times \frac{2}{\pi} (-\ln \eta(iv_2) + \ln \eta(i\tilde{v}_2)) \\ &\quad - (1 - \delta_{\sigma_{dd'}^2,0} \delta_{\tau_{dd'}^2,0}) \frac{1}{\pi^2} \times \left[\ln \left(e^{-\pi(\sigma_{dd'}^2)^2 v_2/4} \frac{\vartheta_1\left(\frac{\tau_{dd'}^2 - i\sigma_{dd'}^2 v_2}{2}, iv_2\right)}{\eta(iv_2)} \right) \right. \\ &\quad \quad \left. - \ln \left(e^{-\pi(\sigma_{dd'}^2)^2 \tilde{v}_2/4} \frac{\vartheta_1\left(\frac{\tau_{dd'}^2 - i\sigma_{dd'}^2 \tilde{v}_2}{2}, i\tilde{v}_2\right)}{\eta(i\tilde{v}_2)} \right) \right] \\ &\quad - \frac{31}{3\pi^2} \ln \eta(iv_3) - \frac{19}{2\pi^2} \ln \left(e^{-\pi v_3/4} \frac{\vartheta_1\left(\frac{1-iv_3}{2}, iv_3\right)}{\eta(iv_3)} \right), \end{aligned} \tag{107}$$

following the prescription (97) for the one-loop contributions. The ‘constant’ one-loop contributions are given by

$$\begin{aligned}\delta_{\text{total}} f_{U(1)_a}^{1\text{-loop}}(c) &= \frac{3}{4\pi^2} \ln \left[2^{11/2} \sqrt{3} \frac{v_1 v_3}{v_2^2} r \right], \\ \delta_{\text{total}} f_{U(1)_d}^{1\text{-loop}}(c) &= \frac{3}{2\pi^2} \ln 2, \\ \delta_{\text{total}} f_{U(1)_{B-L}}^{1\text{-loop}}(c) &= \frac{1}{12\pi^2} \ln \left[2^{47/2} \sqrt{3} \frac{v_1 v_3}{v_2^2} r \right],\end{aligned}\tag{108}$$

where again the explicit v_i dependence arises from the special $\Omega\mathcal{R}$ invariance of the $a(\theta a')$ sector.

The Kähler metrics for the symmetric representation in the cc sector of $Sp(2)_c$ and the antisymmetric representation in the $h_3 h_3$ sector of $Sp(6)_{h_3}$ can be read off from table 19 with the $(\text{length})^2$ values of the three-cycles per two-torus listed in table 28,

$$K_{\text{Sym}_c}^{cc} = f(S, U_l) \frac{\sqrt{2\pi}}{2^{4/3} v_2} \frac{1}{\sqrt{3r}}, \quad K_{\text{Anti}_{h_3}}^{h_3 h_3} = f(S, U_l) \frac{\sqrt{2\pi}}{2^{4/3} v_2} \sqrt{r}.\tag{109}$$

There exist three more antisymmetric representations of $Sp(2)_c$ at the intersections of orbifold images $c(\theta^k c)_{k=1,2}$ and one antisymmetric representation of $Sp(6)_{h_3}$ at the intersection $h_3(\theta^k h_3)_{k=1,2}$ with Kähler metrics

$$K_{\text{Anti}_c}^{c(\theta^k c)} = f(S, U_l) \sqrt{\frac{2\pi}{r v_1 v_2}}, \quad K_{\text{Anti}_{h_3}}^{h_3(\theta^k h_3)} = f(S, U_l) \sqrt{\frac{2\pi r}{v_1 v_2}}.\tag{110}$$

It is again obvious that the Kähler metrics of states in the same representation Anti_{h_3} but at different intersections of orbifold images D6-branes, $h_3 h_3$ and $h_3(\theta^k h_3)_{k=1,2}$, differ in their two-torus volume v_i dependence. This completes our discussion of examples for the non-trivial structure of D6-brane configurations and the corresponding Kähler metrics and holomorphic gauge kinetic functions.

6 Conclusions and Outlook

In this article, we completed the derivation of the perturbatively exact holomorphic gauge kinetic function and the Kähler metrics in the $\mathcal{N} = 1$ supergravity formulation via open string gauge threshold one-loop computations for all factorisable toroidal orbifolds taking into account all possible configurations of vanishing or non-vanishing intersection angles and continuous or discrete Wilson line and displacement moduli per two-torus. The at

first complicated and lengthy formulas are considerably simplified by rewriting them in terms of dependences on beta function coefficients whenever possible. The Kähler metrics for adjoint matter on identical D6-branes in (53) depend on the kind of wrapped bulk, fractional or rigid three-cycle, whereas all other Kähler metrics in table 16 only depend on the intersection angles and have an universal shape for all orbifold backgrounds on factorisable tori considered here. The perturbatively exact holomorphic gauge kinetic functions on the other hand depend on both the number of \mathbb{Z}_2 symmetries of the orbifold background and the relative position of the D6-branes with respect to the O6-planes as compared in tables 17 and 18 for the part depending on the Kähler moduli. In addition, we found a one-loop correction to the gauge kinetic function for fractional and rigid D6-branes in (61) depending on the complex structure moduli and a constant contribution in (66) and the second line of (72) due to the intersection with O6-planes, both of which have to our knowledge not been properly appreciated before in the transformation to the supergravity basis. All results are given in terms of real geometric bulk moduli with their complexifications by axions explained in section 3.2.1, where we also briefly discuss some contradicting statements in the literature concerning one-loop field redefinitions of the bulk moduli under gauge transformations of anomalous massive Abelian groups. The field theory of chiral matter at one vanishing angle has to our knowledge not been analysed before, neither in the intersecting D6-brane nor its T-dual magnetised D-brane language, but it is of crucial importance for model building, as we have discussed in an example with Standard Model spectrum on T^6/\mathbb{Z}'_6 , due to the possible hierarchical structure of the associated Kähler metrics for unisotropic choices of the two-torus volumes. Moreover, we have corrected here the formula for bifundamental matter on parallel D6-branes compared to the literature [45], which assigned the one of the adjoints also to bifundamentals. In the context of symplectic gauge groups, we found a subtle ambiguity related to the assignment of constants to the Kähler metrics or gauge kinetic functions, which might be resolved by a complementary computation of scattering amplitudes along the lines derived for the six-torus in [74, 11]. It also remains to be seen how the field theory formulas generalise to non-factorisable orbifolds.

We proceeded to present some examples, first on $T^6/\mathbb{Z}_2 \times \mathbb{Z}_2$ with discrete torsion, where a detailed analysis of the rigid D6-brane geometry underlying the T-dual of a magnetised D9/D5-brane model in [1] was performed and the corresponding Kähler metrics presented for the first time. As a second class of examples, we computed the Kähler metrics for matter charged under the QCD or the ‘leptonic’ stack in the Standard Model with hidden sector on T^6/\mathbb{Z}'_6 , providing an explicit example for a different Kähler metric of the last right-handed quark generation compared to the first two with a possible hierarchy if the volume of the first two-torus differs considerably from the other two. In the course of the computation we also found that in contrast to our previous statements [40] the non-chiral

antisymmetric pair on parallel orientifold image D6-branes charged under $SU(3)_a$ cannot acquire a mass by a parallel displacement.

Further directions of research will on the one hand include the application of the complete field theory results to the existing Standard Model vacua on T^6/\mathbb{Z}'_6 while combining with worldsheet instanton contributions to the Yukawa couplings [53] along the lines derived for the six-torus in [54, 55], and with non-perturbative D-instanton contributions [66], and the search for new models on rigid D6-branes in $T^6/\mathbb{Z}_2 \times \mathbb{Z}_{2M}$ backgrounds with discrete torsion [46] which is currently under way. In this context it will be interesting to analyse if there exist explicit models which are compatible with a low string scale, $M_{\text{string}} \sim \text{TeV}$, as proposed in [75–78].

On the other hand, the explicit formulas for one-loop mixing of a single $U(1)$ in (93) and linearly combined massless $U(1)$ s in (97) open up new possibilities for studying the kinetic mixing of the observable Standard Model $U(1)$ with some dark Z' photon, possibly including also the recently investigated RR photons [29]; the classification of the one-loop holomorphic gauge kinetic functions in tables 17 and 18 with beta function coefficients as prefactors might also be useful for extrapolating to compactifications on smooth Calabi-Yau spaces, and last but not least it will be interesting to investigate if phenomenologically appealing spectra on D-branes are destabilised by instantons as studied e.g. in [79] for a simpler toy model.

Acknowledgements

The work of G. H. is partially supported by the “Research Center Elementary Forces and Mathematical Foundations” (EMG) at the Johannes Gutenberg-Universität Mainz.

The author thanks Carlo Angelantonj and especially Emilian Dudas for valuable correspondences concerning the correct matching with the T-dual to the D9/D5-brane model [1] discussed in section 4.2 in this article.

Beta function coefficients $b_{SU(N_a)}$ and gauge thresholds $\Delta_{SU(N_a)}$ for the adjoints			
k	$(\vec{\phi}_{(\theta^k a)_a})$ or $\theta \leftrightarrow \omega$	$b_{SU(N_a)} = \sum_k b_{(\theta^k a)_a}^A + \dots$ $= N_a(-3 + \sum_k \varphi^{\text{Adj}_{a,k}}) + \dots$	$\Delta_{SU(N_a)} = N_a \sum_k \tilde{\Delta}_{(\theta^k a)_a} + \dots$
T^6 and T^6/\mathbb{Z}_3			
0	(0, 0, 0)	—	—
1 + 2	$\mp(\frac{1}{3}, -\frac{2}{3}, \frac{1}{3})$	$N_a I_{(\theta a)_a} $	$-6 b_{(\theta a)_a} \ln(2)$
T^6/\mathbb{Z}_{2N}			
0	(0, 0, 0)	$-2 N_a$	$2 N_a \Lambda_{0,0}(v_2; V_{aa}^{(2)})$
T^6/\mathbb{Z}_4			
1	$(\frac{1}{2}, 0, -\frac{1}{2})$	$\frac{N_a \left(I_{(\theta a)_a}^{(1,3)} - I_{(\theta a)_a}^{\mathbb{Z}_2, (1,3)} \right)}{2}$	$-b_{(\theta a)_a}^A \Lambda_{0,0}(v_2; V_{aa}^{(2)})$
T^6/\mathbb{Z}_6			
1 + 2	$\pm(\frac{1}{3}, -\frac{2}{3}, \frac{1}{3})$	$\frac{N_a \left(I_{(\theta a)_a} + \text{sgn}(I_{(\theta a)_a}) \cdot I_{(\theta a)_a}^{\mathbb{Z}_2} \right)}{2}$	$-\left(6 b_{(\theta a)_a}^A + \frac{2 N_a I_{(\theta a)_a}^{\mathbb{Z}_2}}{3} \right) \ln(2)$
T^6/\mathbb{Z}'_6			
1 + 2	$\pm(\frac{1}{3}, -\frac{1}{3}, 0)$	$N_a I_{(\theta a)_a}^{(1,2)} $	$-2 b_{(\theta a)_a}^A \Lambda_{0,0}(v_3; V_{aa}^{(3)}) - N_a \frac{I_{(\theta a)_a}^{\mathbb{Z}_2}}{3} \ln(2)$
$T^6/\mathbb{Z}_2 \times \mathbb{Z}_{2M}$ without discrete torsion			
0	(0, 0, 0)	—	—
$T^6/\mathbb{Z}_2 \times \mathbb{Z}_4$ without and with discrete torsion			
1	$(0, \frac{1}{2}, -\frac{1}{2})$	$N_a I_{(\omega a)_a}^{(2,3)} $	$-b_{(\omega a)_a}^A \Lambda_{0,0}(v_1; V_{aa}^{(1)})$
$T^6/\mathbb{Z}_2 \times \mathbb{Z}_6$ without discrete torsion			
1 + 2	$\pm(0, \frac{1}{3}, -\frac{1}{3})$	$2 N_a I_{(\omega a)_a}^{(2,3)} $	$-2 b_{(\omega a)_a}^A \Lambda_{0,0}(v_1; V_{aa}^{(1)})$
$T^6/\mathbb{Z}_2 \times \mathbb{Z}'_6$ without discrete torsion			
1 + 2	$\pm(-\frac{2}{3}, \frac{1}{3}, \frac{1}{3})$	$N_a I_{(\omega a)_a} $	$-6 b_{(\omega a)_a}^A \ln(2)$
$T^6/\mathbb{Z}_2 \times \mathbb{Z}_{2M}$ with discrete torsion			
0	(0, 0, 0)	$-3 N_a$	$N_a \sum_{i=1}^3 \Lambda_{0,0}(v_i; V_{aa}^{(i)})$
$T^6/\mathbb{Z}_2 \times \mathbb{Z}_6$ with discrete torsion			
1 + 2	$\pm(0, \frac{1}{3}, -\frac{1}{3})$	$\frac{N_a \left(I_{(\omega a)_a}^{(2,3)} - I_{(\omega a)_a}^{\mathbb{Z}_2, (2,3)} \right)}{2}$	$-2 b_{(\omega a)_a}^A \Lambda_{0,0}(v_1; V_{aa}^{(1)}) + \frac{N_a I_{(\omega a)_a}^{\mathbb{Z}_2}}{6} \ln(2)$
$T^6/\mathbb{Z}_2 \times \mathbb{Z}'_6$ with discrete torsion			
1 + 2	$\pm(-\frac{2}{3}, \frac{1}{3}, \frac{1}{3})$	$\frac{N_a \left(I_{(\omega a)_a} + \text{sgn}(I_{(\omega a)_a}) \sum_{i=1}^3 I_{(\omega a)_a}^{\mathbb{Z}_2^{(i)}} \right)}{4}$	$\left(-6 b_{(\omega a)_a}^A + \frac{N_a}{3} \sum_{i=1}^3 I_{(\omega a)_a}^{\mathbb{Z}_2^{(i)}} \right) \ln(2)$

Table 13: $SU(N_a)$ beta function coefficients and gauge thresholds due to massless and massive open strings transforming in the adjoint representation for all factorisable toroidal orbifold backgrounds. The toroidal intersection numbers are given in equation (33). The corresponding Kähler metrics for adjoints on identical D6-branes are given in equation (53), while those at intersections of orbifold images $(\omega^k a)_a$ have the same form as the Kähler metrics for bifundamental matter in table 16. Similarly, the v_i dependent one-loop contributions to the holomorphic gauge kinetic

ϕ	1/6	1/3	1/2	2/3	5/6
$\frac{\Gamma(\phi)}{\Gamma(1-\phi)}$	5	2	1	$\frac{1}{2}$	$\frac{1}{5}$

Table 14: Ratios of Gamma functions for special values of intersection angles commonly appearing in D6-brane models on toroidal orbifolds.

Beta function coefficients and gauge thresholds for $SO(2M_x)$ and $Sp(2M_x)$				
$(\phi_{xx'}^{(1)}, \phi_{xx'}^{(2)}, \phi_{xx'}^{(3)})$	$b_{SO/Sp(2M_x)} = b_{xx'}^A + b_{xx'}^M + \dots$	$\Delta_{SO(2M_x)} = M_x \tilde{\Delta}_{xx'} + \frac{1}{2} \Delta_{x, \Omega \mathcal{R}} + \dots$	SUSY	(exotic O-plane) gauge group + matter
T^6 and T^6/\mathbb{Z}_3				
$(0, 0, 0)$ $\uparrow\uparrow \Omega \mathcal{R}$	—	—	$\mathcal{N} = 4$	$SO(2M_x)$ +3 Adj _x
$(0, 0, 0)$ $\perp \Omega \mathcal{R}$ on $T_{(j)}^2 \times T_{(k)}^2$	−4	$4 \Lambda_{0,0}(v_i, V_{xx'}^{(i)}) + 8 \ln(2) + 16 b_i \ln\left(\frac{\eta(2iv_i)}{\vartheta_4(0, 2iv_i)}\right)$	$\mathcal{N} = 2$	$Sp(2M_x)$ + Sym _x +2 Anti _x
T^6/\mathbb{Z}_{2N}				
$(0, 0, 0)$ $\uparrow\uparrow \Omega \mathcal{R}$ or $\Omega \mathcal{R} \mathbb{Z}_2^{(2)}$	$-2M_x - 2$	$(2M_x + 2) \Lambda_{0,0}(v_2, V_{xx'}^{(2)}) + 4 \ln(2) + 8 b_2 \ln\left(\frac{\eta(2iv_2)}{\vartheta_4(0, 2iv_2)}\right)$	$\mathcal{N} = 2$	$Sp(2M_x)$ + Sym _x
$(0, 0, 0)$ $\perp \Omega \mathcal{R}$ and $\Omega \mathcal{R} \mathbb{Z}_2^{(2)}$ on $T_{(2)}^2$	$-2M_x - 4$	$2M_x \Lambda_{0,0}(v_2, V_{xx'}^{(2)}) + 2 \sum_{i=1,3} \Lambda_{0,0}(v_i, V_{xx'}^{(i)}) + 8 \ln(2) + 8 \sum_{i=1,3} b_i \ln\left(\frac{\eta(2iv_i)}{\vartheta_4(0, 2iv_i)}\right)$	$\mathcal{N} = 1$	$Sp(2M_x)$ + Anti _x
$T^6/\mathbb{Z}_2 \times \mathbb{Z}_{2M}$ without discrete torsion				
$(0, 0, 0)$	−6	$2 \sum_{i=1}^3 \Lambda_{0,0}(v_i, V_{xx'}^{(i)}) + 12 \ln(2) + 8 \sum_{i=1}^3 b_i \ln\left(\frac{\eta(2iv_i)}{\vartheta_4(0, 2iv_i)}\right)$	$\mathcal{N} = 1$	$Sp(2M_x)$ +3 Anti _x
$T^6/\mathbb{Z}_2 \times \mathbb{Z}_{2M}$ with discrete torsion				
$(0, 0, 0)$ $\uparrow\uparrow \Omega \mathcal{R} \mathbb{Z}_2^{(k)}$ $k = 0 \dots 3$	$-3M_x - 3$	$\sum_{i=1}^3 (M_x + 1) \Lambda_{0,0}(v_i, V_{xx'}^{(i)}) + 6 \ln(2) + 4 \sum_{i=1}^3 b_i \ln\left(\frac{\eta(2iv_i)}{\vartheta_4(0, 2iv_i)}\right)$	$\mathcal{N} = 1$	$(\eta_{\Omega \mathcal{R} \mathbb{Z}_2^{(k)}} = -1)$ $Sp(2M_x)$

Table 15: Beta function coefficients and gauge thresholds for D6_x-branes which are their own orientifold image D6_{x'}. The amount of supersymmetry preserved for each D6-brane is given in the fourth column, and in the last column the type of (pseudo)real gauge group and matter content from the xx -sector is given. The special intersection numbers with O6-planes (6) have been inserted. Additional matter in the symmetric or antisymmetric representation generically exists at the intersection of orbifold image D6-branes, but a systematic case-by-case study for any orbifold and lattice orientation goes beyond the scope of this article. An example for each of the two distinct classes of $Sp(2N_x)$ groups on the **ABa** lattice on T^6/\mathbb{Z}'_6 is presented in section 5.

Kähler metrics for bifundamental matter $(\mathbf{N}_a, \overline{\mathbf{N}}_b)$ on various orbifolds			
$(\phi_{ab}^{(1)}, \phi_{ab}^{(2)}, \phi_{ab}^{(3)})$	T^6 and $T^6/\mathbb{Z}_2 \times \mathbb{Z}_{2M}$ without torsion	T^6/\mathbb{Z}_{2N}	$T^6/\mathbb{Z}_2 \times \mathbb{Z}_{2M}$ with discrete torsion
$(0, 0, 0)$	—	$f(S, U_l) \sqrt{\frac{2\pi V_{ab}^{(2)}}{v_1 v_3}}$	$f(S, U_l) \sqrt{\frac{2\pi V_{ab}^{(i)}}{v_j v_k}}$ $(ijk) \simeq (1, 2, 3)$ cyclic
$(0^{(i)}, \phi^{(j)}, \phi^{(k)})$ $\phi^{(j)} = -\phi^{(k)}$	$f(S, U_l) \sqrt{\frac{2\pi V_{ab}^{(i)}}{v_j v_k}}$		
$(\phi^{(1)}, \phi^{(2)}, \phi^{(3)})$ $\sum_{i=1}^3 \phi^{(i)} = 0$	$f(S, U_l) \sqrt{\prod_{i=1}^3 \frac{1}{v_i} \left(\frac{\Gamma(\phi_{ab}^{(i)})}{\Gamma(1- \phi_{ab}^{(i)})} \right)^{-\frac{\text{sgn}(\phi_{ab}^{(i)})}{\text{sgn}(I_{ab})}}}$		

Table 16: Comparison of the Kähler metrics for bifundamental matter. The functional dependence of the Kähler metrics is solely determined by the number of vanishing angles and the assignment of multiplets to the two-torus $T_{(i)}^2$ where the D6-branes are parallel, independently of the orbifold background. For two or three intersection angles, the Kähler metrics of adjoint matter at orbifold intersections have the same shape, whereas the Kähler metrics for adjoint matter on identical D6-branes differ and are given by (53).

1-loop contribution to the gauge kinetic function $\delta_b f_{SU(N_a)}^{1\text{-loop}}(v_i)$ from bifundamental sectors on various orbifolds			
$(\phi_{ab}^{(1)}, \phi_{ab}^{(2)}, \phi_{ab}^{(3)})$	T^6 and $T^6/\mathbb{Z}_2 \times \mathbb{Z}_{2M}$ without torsion	T^6/\mathbb{Z}_{2N}	$T^6/\mathbb{Z}_2 \times \mathbb{Z}_{2M}$ with discrete torsion
$(0, 0, 0)$	—	$ \begin{aligned} & -\frac{b_{ab}^A}{4\pi^2} \ln \eta(iv_2) \\ & -\frac{\tilde{b}_{ab}^A}{8\pi^2} (1 - \delta_{\sigma_{ab}^2, 0} \delta_{\tau_{ab}^2, 0}) \times \\ & \times \ln \left(e^{-\pi(\sigma_{ab}^2)^2 v_2/4} \frac{\vartheta_1(\frac{\tau_{ab}^2 - i\sigma_{ab}^2 v_2}{2}, iv_2)}{\eta(iv_2)} \right) \end{aligned} $	$ \begin{aligned} & -\sum_{i=1}^3 \frac{b_{ab}^{A,(i)}}{4\pi^2} \ln \eta(iv_i) \\ & -\sum_{i=1}^3 \frac{\tilde{b}_{ab}^{A,(i)}}{8\pi^2} (1 - \delta_{\sigma_{ab}^i, 0} \delta_{\tau_{ab}^i, 0}) \times \\ & \times \ln \left(e^{-\pi(\sigma_{ab}^i)^2 v_i/4} \frac{\vartheta_1(\frac{\tau_{ab}^i - i\sigma_{ab}^i v_i}{2}, iv_i)}{\eta(iv_i)} \right) \end{aligned} $
$(0^{(i)}, \phi^{(j)}, \phi^{(k)})_{\phi^{(j)} = -\phi^{(k)}}$	$-\frac{b_{ab}^A}{4\pi^2} \ln \eta(iv_i) - \frac{\tilde{b}_{ab}^A}{8\pi^2} (1 - \delta_{\sigma_{ab}^i, 0} \delta_{\tau_{ab}^i, 0}) \ln \left(e^{-\pi(\sigma_{ab}^i)^2 v_i/4} \frac{\vartheta_1(\frac{\tau_{ab}^i - i\sigma_{ab}^i v_i}{2}, iv_i)}{\eta(iv_i)} \right)$	—	
$(\phi^{(1)}, \phi^{(2)}, \phi^{(3)})$			

Table 17: Comparison of the two-torus volume v_i dependent one-loop contributions $\delta_b f_{SU(N_a)}^{1\text{-loop}}(v_i)$ to the holomorphic gauge kinetic function from bifundamental and adjoint sectors. The corresponding beta-function coefficients are given in the second column of table 8 for the six-torus, table 10 for $T^6/\mathbb{Z}_2 \times \mathbb{Z}_{2M}$ without discrete torsion, table 11 for T^6/\mathbb{Z}_{2N} and table 6 for $T^6/\mathbb{Z}_2 \times \mathbb{Z}_{2M}$ with discrete torsion. The contributions from adjoint matter at intersection of orbifold images are of the same form, whereas those on identical D6-branes differ and are given in (54).

Comparison of one-loop contribution to the gauge kinetic function $\delta_a f_{SU(N_a)}^{1\text{-loop}}(v_i)$ from (anti)symmetric sectors on various orbifolds				
$(\phi_{aa'}^{(1)}, \phi_{aa'}^{(2)}, \phi_{aa'}^{(3)})$	T^6	$T^6/\mathbb{Z}_2 \times \mathbb{Z}_{2M}$ without torsion	T^6/\mathbb{Z}_{2N}	$T^6/\mathbb{Z}_2 \times \mathbb{Z}_{2M}$ with discrete torsion
$(0, 0, 0)$ $\uparrow\uparrow \Omega\mathcal{R}$	—	$-\sum_{i=1}^3 \frac{b_{aa'}^{M_i(i)}}{4\pi^2} \ln \eta(i\tilde{v}_i)$ $-\sum_{i=1}^3 \left[\frac{\tilde{b}_{aa'}^{M_i(i)}}{8\pi^2} (1 - \delta_{\sigma^i}^{aa'} \delta_{aa',0}^{i,i}) \times \right.$ $\left. \times \ln \left(e^{-\pi(\sigma^i)^2 \tilde{v}_i/4} \frac{\vartheta_1(\frac{\tau^i - i\sigma^i}{2} \frac{\tilde{v}_i}{i\tilde{v}_i})}{\eta(i\tilde{v}_i)} \right) \right]$	$-\frac{b_{aa'}^{M_i(i)}}{4\pi^2} \ln \eta(i\tilde{v}_2) - \frac{b_{aa'}^{M_i(i)}}{4\pi^2} \ln \eta(i\tilde{v}_2)$ $-(1 - \delta_{\sigma^2}^{aa'} \delta_{aa',0}^{2,2}) \times$ $\left[\frac{\tilde{b}_{aa'}^{M_i(i)}}{8\pi^2} \ln \left(e^{-\pi(\sigma^2)^2 \tilde{v}_2/4} \frac{\vartheta_1(\frac{\tau^2 - i\sigma^2}{2} \frac{i\tilde{v}_2}{i\tilde{v}_2})}{\eta(i\tilde{v}_2)} \right) \right.$ $\left. + \frac{\tilde{b}_{aa'}^{M_i(i)}}{8\pi^2} \ln \left(e^{-\pi(\sigma^2)^2 \tilde{v}_2/4} \frac{\vartheta_1(\frac{\tau^2 - i\sigma^2}{2} \frac{\tilde{v}_2}{i\tilde{v}_2})}{\eta(i\tilde{v}_2)} \right) \right]$	$-\sum_{i=1}^3 \frac{b_{aa'}^{A_i(i)}}{4\pi^2} \ln \eta(i\tilde{v}_i)$ $-\sum_{i=1}^3 \frac{b_{aa'}^{M_i(i)}}{4\pi^2} \ln \eta(i\tilde{v}_i)$
$(0, 0, 0)$ $\uparrow\uparrow \Omega\mathcal{R}\mathbb{Z}_2^{(i)}$	$-\frac{b_{aa'}^{M_i(i)}}{4\pi^2} \ln \eta(i\tilde{v}_i)$ $-\frac{\tilde{b}_{aa'}^{M_i(i)}}{8\pi^2} (1 - \delta_{\sigma^i}^{aa'} \delta_{aa',0}^{i,i}) \times$ $\times \ln \left(e^{-\pi(\sigma_{aa'}^i)^2 \tilde{v}_i/4} \frac{\vartheta_1(\frac{\tau^i - i\sigma_{aa'}^i}{2} \frac{\tilde{v}_i}{i\tilde{v}_i})}{\eta(i\tilde{v}_i)} \right)$	same as $\uparrow\uparrow \Omega\mathcal{R}$	$\boxed{i=2} :$ same as $\uparrow\uparrow \Omega\mathcal{R}$ $\boxed{i=1, 3} :$ $\frac{-\frac{b_{aa'}^{M_i(i)}}{4\pi^2} \ln \eta(i\tilde{v}_2)}{-\frac{b_{aa'}^{M_i(i)}}{4\pi^2} \ln \eta(i\tilde{v}_1) - \frac{b_{aa'}^{M_i(i)}}{4\pi^2} \ln \eta(i\tilde{v}_3)}$	same as $\uparrow\uparrow \Omega\mathcal{R}$
$(0^{(i)}, \phi^{(j)}, \phi^{(k)})$ $\uparrow\uparrow (\Omega\mathcal{R} + \Omega\mathcal{R}\mathbb{Z}_2^{(i)})$	$-\frac{b_{aa'}^{M_i(i)}}{4\pi^2} \ln \eta(i\tilde{v}_i)$ $-\frac{\tilde{b}_{aa'}^{M_i(i)}}{8\pi^2} (1 - \delta_{\sigma^i}^{aa'} \delta_{aa',0}^{i,i}) \ln \left(e^{-\pi(\sigma_{aa'}^i)^2 \tilde{v}_i/4} \frac{\vartheta_1(\frac{\tau^i - i\sigma_{aa'}^i}{2} \frac{\tilde{v}_i}{i\tilde{v}_i})}{\eta(i\tilde{v}_i)} \right)$ $-\frac{\tilde{b}_{aa'}^{M_i(i)}}{8\pi^2} (1 - \delta_{\sigma^i}^{aa'} \delta_{aa',0}^{i,i}) \ln \left(e^{-\pi(\sigma_{aa'}^i)^2 \tilde{v}_i/4} \frac{\vartheta_1(\frac{\tau^i - i\sigma_{aa'}^i}{2} \frac{\tilde{v}_i}{i\tilde{v}_i})}{\eta(i\tilde{v}_i)} \right)$	$-\frac{b_{aa'}^{M_i(i)}}{4\pi^2} \ln \eta(i\tilde{v}_i) - \frac{b_{aa'}^{M_i(i)}}{4\pi^2} \ln \eta(i\tilde{v}_i)$ $-\frac{\tilde{b}_{aa'}^{M_i(i)}}{8\pi^2} (1 - \delta_{\sigma^i}^{aa'} \delta_{aa',0}^{i,i}) \ln \left(e^{-\pi(\sigma_{aa'}^i)^2 \tilde{v}_i/4} \frac{\vartheta_1(\frac{\tau^i - i\sigma_{aa'}^i}{2} \frac{\tilde{v}_i}{i\tilde{v}_i})}{\eta(i\tilde{v}_i)} \right)$ $-\frac{\tilde{b}_{aa'}^{M_i(i)}}{8\pi^2} (1 - \delta_{\sigma^i}^{aa'} \delta_{aa',0}^{i,i}) \ln \left(e^{-\pi(\sigma_{aa'}^i)^2 \tilde{v}_i/4} \frac{\vartheta_1(\frac{\tau^i - i\sigma_{aa'}^i}{2} \frac{\tilde{v}_i}{i\tilde{v}_i})}{\eta(i\tilde{v}_i)} \right)$	$\boxed{i=2} :$ same as $(0, 0, 0) \uparrow\uparrow \Omega\mathcal{R}$ $\boxed{i=1, 3} :$ $\frac{-\frac{b_{aa'}^{M_i(i)}}{4\pi^2} \ln \eta(i\tilde{v}_i) - \frac{b_{aa'}^{M_i(i)}}{4\pi^2} \ln \eta(i\tilde{v}_i)}{-\frac{b_{aa'}^{M_i(i)}}{4\pi^2} \ln \eta(i\tilde{v}_1) - \frac{b_{aa'}^{M_i(i)}}{4\pi^2} \ln \eta(i\tilde{v}_3)}$	$-\frac{b_{aa'}^{A_i(i)}}{4\pi^2} \ln \eta(i\tilde{v}_i)$ $-\frac{b_{aa'}^{M_i(i)}}{4\pi^2} \ln \eta(i\tilde{v}_i)$
$(0^{(i)}, \phi^{(j)}, \phi^{(k)})$ $\uparrow\uparrow (\Omega\mathcal{R}\mathbb{Z}_2^{(j)} + \Omega\mathcal{R}\mathbb{Z}_2^{(k)})$	$-\frac{b_{aa'}^{M_i(i)}}{4\pi^2} \ln \eta(i\tilde{v}_i)$ $-\frac{\tilde{b}_{aa'}^{M_i(i)}}{8\pi^2} (1 - \delta_{\sigma^i}^{aa'} \delta_{aa',0}^{i,i}) \times$ $\times \ln \left(e^{-\pi(\sigma_{aa'}^i)^2 \tilde{v}_i/4} \frac{\vartheta_1(\frac{\tau^i - i\sigma_{aa'}^i}{2} \frac{\tilde{v}_i}{i\tilde{v}_i})}{\eta(i\tilde{v}_i)} \right)$	same as $\uparrow\uparrow (\Omega\mathcal{R} + \Omega\mathcal{R}\mathbb{Z}_2^{(i)})$	$\boxed{i=2} :$ $-\frac{b_{aa'}^{A_i(i)}}{4\pi^2} \ln \eta(i\tilde{v}_2)$ $\boxed{i=1, 3} :$ same as $\uparrow\uparrow (\Omega\mathcal{R} + \Omega\mathcal{R}\mathbb{Z}_2^{(i)})$	same as $\uparrow\uparrow (\Omega\mathcal{R} + \Omega\mathcal{R}\mathbb{Z}_2^{(i)})$
$(\phi^{(1)}, \phi^{(2)}, \phi^{(3)})$	—	—	—	—

Table 18: Comparison of the two-torus volume v_i dependent one-loop contributions $\delta_a f_{SU(N_a)}^{1\text{-loop}}(v_i)$ to the holomorphic gauge kinetic function from (anti)symmetric sectors. The corresponding beta-function coefficients are given in the second column of table 9 for the six-torus, table 10 for $T^6/\mathbb{Z}_2 \times \mathbb{Z}_{2M}$ without torsion, table 12 for T^6/\mathbb{Z}_{2N} and table 7 for $T^6/\mathbb{Z}_2 \times \mathbb{Z}_{2M}$ with discrete torsion. For the six-torus, the three non-trivial cases are identical since $b_{aa'}^A = 0$ for $(0, 0, 0) \uparrow\uparrow \Omega\mathcal{R}\mathbb{Z}_2^{(i)}$ and $b_{aa'}^M = 0$ for $(0^{(i)}, \phi^{(j)}, \phi^{(k)}) \uparrow\uparrow (\Omega\mathcal{R}\mathbb{Z}_2^{(j)} + \Omega\mathcal{R}\mathbb{Z}_2^{(k)})$, cf. table 9. Similarly, for T^6/\mathbb{Z}_{2N} the case $(0^{(i)}, \phi^{(j)}, \phi^{(k)}) \uparrow\uparrow (\Omega\mathcal{R}\mathbb{Z}_2^{(j)} + \Omega\mathcal{R}\mathbb{Z}_2^{(k)})$ is identical to $(0^{(i)}, \phi^{(j)}, \phi^{(k)}) \uparrow\uparrow (\Omega\mathcal{R} + \Omega\mathcal{R}\mathbb{Z}_2^{(i)})$ since $b_{aa'}^M \equiv 0$ for the former, cf. table 12.

1-loop gauge kinetic functions and Kähler metrics for $SO(2M_x)$ and $Sp(2M_x)$			
$(\phi_{xx'}^{(1)}, \phi_{xx'}^{(2)}, \phi_{xx'}^{(3)})$	SUSY	$\delta_x \mathbf{f}_{SO/Sp(2M_x)}^{1\text{-loop}}$	$K_{\mathbf{Anti}_x}^{(i)}, K_{\mathbf{Sym}_x}^{(i)}$
T^6 and T^6/\mathbb{Z}_3			
$(0, 0, 0)$ $\uparrow\uparrow \Omega\mathcal{R}$	$\mathcal{N} = 4$	—	$K_{\mathbf{Anti}_x}^{(i), i=1,2,3} = f(S, U_l) \frac{(2\pi)^{1/2}}{2^{1/3} v_i} \sqrt{\frac{V_{xx}^{(j)} V_{xx}^{(k)}}{V_{xx}^{(i)}}}$
$(0, 0, 0)$ $\perp \Omega\mathcal{R}$ on $T_{(j)}^2 \times T_{(k)}^2$	$\mathcal{N} = 2$	$\frac{1}{\pi^2} \ln(2^{2/3} \eta(i\tilde{v}_i))$	$K_{\mathbf{Sym}_x}^{(i)} = f(S, U_l) \frac{\sqrt{2\pi}}{2^{1/3} v_i} \sqrt{\frac{V_{xx}^{(j)} V_{xx}^{(k)}}{V_{xx}^{(i)}}}$ $K_{\mathbf{Anti}_x}^{(j)} = f(S, U_l) \frac{\sqrt{2\pi}}{2^{1/3} v_j} \sqrt{\frac{V_{xx}^{(i)} V_{xx}^{(k)}}{V_{xx}^{(j)}}}$ $K_{\mathbf{Anti}_x}^{(k)} = f(S, U_l) \frac{\sqrt{2\pi}}{2^{1/3} v_k} \sqrt{\frac{V_{xx}^{(i)} V_{xx}^{(j)}}{V_{xx}^{(k)}}}$
T^6/\mathbb{Z}_{2N}			
$(0, 0, 0)$ $\uparrow\uparrow \Omega\mathcal{R}$ or $\Omega\mathcal{R}\mathbb{Z}_2^{(2)}$	$\mathcal{N} = 2$	$\frac{1}{2\pi^2} \left(M_x \ln(2^{1/6} \eta(iv_2)) + \ln(2^{2/3} \eta(i\tilde{v}_2)) \right)$	$K_{\mathbf{Sym}_x}^{(2)} = f(S, U_l) \frac{\sqrt{2\pi}}{2^{4/3} v_2} \sqrt{\frac{V_{xx}^{(1)} V_{xx}^{(3)}}{V_{xx}^{(2)}}}$
$(0, 0, 0)$ $\perp \Omega\mathcal{R}$ and $\Omega\mathcal{R}\mathbb{Z}_2^{(2)}$ on $T_{(2)}^2$	$\mathcal{N} = 1$	$\frac{1}{2\pi^2} \left(M_x \ln(2^{1/6} \eta(iv_2)) + \sum_{j=1,3} \ln(2^{11/12} \eta(i\tilde{v}_j)) \right)$	$K_{\mathbf{Anti}_x}^{(2)} = f(S, U_l) \frac{\sqrt{2\pi}}{2^{4/3} v_2} \sqrt{\frac{V_{xx}^{(1)} V_{xx}^{(3)}}{V_{xx}^{(2)}}}$
$T^6/\mathbb{Z}_2 \times \mathbb{Z}_{2M}$ without discrete torsion			
$(0, 0, 0)$	$\mathcal{N} = 1$	$\frac{1}{2\pi^2} \left(M_x \ln 2^{-1/2} + \sum_{i=1}^3 \ln(2\eta(i\tilde{v}_i)) \right)$	$K_{\mathbf{Anti}_x}^{(i), i=1,2,3} = f(S, U_l) \frac{\sqrt{2\pi}}{2^{4/3} v_i} \sqrt{\frac{V_{xx}^{(j)} V_{xx}^{(k)}}{V_{xx}^{(i)}}}$
$T^6/\mathbb{Z}_2 \times \mathbb{Z}_{2M}$ with discrete torsion			
$(0, 0, 0)$ $\uparrow\uparrow \Omega\mathcal{R}\mathbb{Z}_2^{(k)}$ $k = 0 \dots 3$	$\mathcal{N} = 1$	$\frac{1}{4\pi^2} \left(M_x \sum_{i=1}^3 \ln(\sqrt{2}\eta(iv_i)) + \sum_{i=1}^3 \ln(2\eta(i\tilde{v}_i)) \right)$	—

Table 19: One-loop contributions to the holomorphic gauge kinetic functions and Kähler metrics from the xx sector of orientifold invariant D6-branes with $SO(2M_x)$ (T^6 and $x \uparrow\uparrow \Omega\mathcal{R}$) or $Sp(2M_x)$ (otherwise) gauge factors. In all cases with non-vanishing $\delta_x \mathbf{f}_{Sp(2M_x)}^{1\text{-loop}}$ and $K_{\mathbf{Anti}_x/\mathbf{Sym}_x}^{(j)}$ for some j , there is an ambiguity of assigning constants, which has been fixed here by requiring the (up to the normalisation factor $1/c_x$) identical form (87) for all Kähler metrics.

Comparison of magnetised D9-branes and intersecting D6-branes on $T^6/\mathbb{Z}_2 \times \mathbb{Z}_2$		
Angelantonj et al.	T-duality \Leftrightarrow	this article
no B -field		aaa -torus
g, f, h	Orbifold generators	$\mathbb{Z}_2^{(1)}(\omega), \mathbb{Z}_2^{(2)}(\theta\omega), \mathbb{Z}_2^{(3)}(\theta)$
$O9$	O-planes	$\Omega\mathcal{R}(\eta_{\Omega\mathcal{R}} = 1)$
$O5_1(\epsilon_1 = 1)$		$\Omega\mathcal{R}\mathbb{Z}_2^{(1)}(\eta_{\Omega\mathcal{R}\mathbb{Z}_2^{(1)}} = 1)$
$O5_2(\epsilon_2 = 1)$		$\Omega\mathcal{R}\mathbb{Z}_2^{(2)}(\eta_{\Omega\mathcal{R}\mathbb{Z}_2^{(2)}} = 1)$
$O5_3(\epsilon_3 = -1)$	exotic O-plane	$\Omega\mathcal{R}\mathbb{Z}_2^{(3)}(\eta_{\Omega\mathcal{R}\mathbb{Z}_2^{(3)}} = -1)$
$H_a^{(i)} = \frac{m_a^i}{n_a^i R_1^{(i)} R_2^{(i)}}$	Magnetic Flux \Leftrightarrow Angle	$\tan(\pi\phi_a^{(i)}) = \frac{m_a^i R_2^{(i)}}{n_a^i R_1^{(i)}}$
S	Dilaton	S
T_i (Kähler)	Bulk moduli	U_i (Complex structures)
U_i (Complex structures)		T_i (Kähler)
M_i^l (Kähler)	Except. moduli	W_i^l (Complex structures)
$\left. \begin{array}{l} (X_1^{a_i}, X_2^{a_i}, X_3^{a_i}) \in \\ \{(1, 1, 1), (1, -1, -1)\} \end{array} \right\}$	$\left. \begin{array}{l} \text{D-branes} \\ \mathbb{Z}_2 \text{ eigenvalues} \end{array} \right\}$	$\left\{ \begin{array}{l} \left((-1)^{\tau_{a_i}^{\mathbb{Z}_2^{(1)}}}, (-1)^{\tau_{a_i}^{\mathbb{Z}_2^{(2)}}}, (-1)^{\tau_{a_i}^{\mathbb{Z}_2^{(3)}}} \right) \\ \in \{(+, +, +), (+, -, -)\} \end{array} \right\}$
$\epsilon_l^{(a)} \in \{0, 1\}$	fixed point choices	$\left\{ \begin{array}{l} \sigma_a^i \in \{0, 1\} \text{ (displacements)} \\ \tau_a^i \equiv 0 \text{ (no Wilson lines)} \end{array} \right\}$

Table 20: Comparison of the notation for magnetised D9- and D5-branes on $T^6/(\mathbb{Z}_2 \times \mathbb{Z}_2 \times \Omega)$ without discrete torsion in [1] and the T-dual D6-branes at angles on the untitled **aaa**-torus of the $T^6/(\mathbb{Z}_2 \times \mathbb{Z}_2 \times \Omega\mathcal{R})$ background with discrete torsion.

T-dual D6-brane configurations of examples 1 & 2 on $T^6/\mathbb{Z}_2 \times \mathbb{Z}_2$							
D6 _x -brane	$(\vec{\phi}_x)$	Torus wrappings $(n_x^1, m_x^1; n_x^2, m_x^2; n_x^3, m_x^3)$	$(\vec{X}_x); (\vec{Y}_x)$	$(\vec{\sigma}_x)$	$(-1)^{\tau_x^2}$	$(\vec{\tau}_x)$	(\vec{V}_{xx})
a_1 a_2 a_3 a_4	$(\phi^{(1)}, \phi^{(2)}, \phi^{(3)})$ $\sum_{i=1}^3 \phi^{(i)} = 0$	$(1, 1; 1, 1; 1, -1)$	$\begin{pmatrix} 1 \\ -1 \\ -1 \\ 1 \end{pmatrix}; \begin{pmatrix} -1 \\ 1 \\ 1 \\ -1 \end{pmatrix}$	$(\vec{0})$	$(+++)$ $(+- -)$ $(-+ -)$ $(-- +)$	$(\vec{0})$	$\begin{pmatrix} \frac{1}{r_1} + r_1 \\ \frac{1}{r_2} + r_2 \\ \frac{1}{r_3} + r_3 \end{pmatrix}$
a'_1 a'_2 a'_3 a'_4	$(-\phi^{(1)}, -\phi^{(2)}, -\phi^{(3)})$	$(1, -1; 1, -1; 1, 1)$	$\begin{pmatrix} 1 \\ -1 \\ -1 \\ 1 \end{pmatrix}; \begin{pmatrix} 1 \\ -1 \\ -1 \\ 1 \end{pmatrix}$	$(\vec{0})$	$(-- +)$ $(-+ -)$ $(+ - -)$ $(+++)$	$(\vec{0})$	$\begin{pmatrix} \frac{1}{r_1} + r_1 \\ \frac{1}{r_2} + r_2 \\ \frac{1}{r_3} + r_3 \end{pmatrix}$

Table 21: The four stacks of D6-branes a_i on $T^6/\mathbb{Z}_2 \times \mathbb{Z}_2$ with discrete torsion which give the T-dual to the first magnetised D9-brane model in [1]. The bulk RR tadpoles cancel for $N_{a_1} = \dots N_{a_4} = 4$ resulting in the gauge group $\prod_{i=1}^4 U(4)_{a_i}$. The three-cycles are supersymmetric if the complex structure on the last two-torus is related to the other two by $r_3 = \frac{r_1+r_2}{1-r_1r_2}$.

Massless matter spectrum of Ex. 1 on $T^6/\mathbb{Z}_2 \times \mathbb{Z}_2$ with gauge group $\prod_{i=1}^4 U(4)_{a_i}$	
$a_i a_j$	$[(4, \bar{4}, 1, 1) + (1, 1, 4, \bar{4}) + (4, 1, \bar{4}, 1) + (1, 4, 1, \bar{4}) + (4, 1, 1, \bar{4}) + (1, 4, \bar{4}, 1) + c.c.]$
$a_i a'_j$	$+8 \times [(\bar{6}_{\text{Anti}}, 1, 1, 1) + (1, \bar{6}_{\text{Anti}}, 1, 1) + (1, 1, \bar{6}_{\text{Anti}}, 1) + (1, 1, 1, \bar{6}_{\text{Anti}})]$

Table 22: The matter spectrum of the first example with magnetised D9-branes on $T^6/\mathbb{Z}_2 \times \mathbb{Z}_2$ without torsion in [1] is (up to the renaming of D-branes, cf. (100)) correctly reproduced by the T-dual configuration of intersecting rigid D6-branes on $T^6/\mathbb{Z}_2 \times \mathbb{Z}_2$ with discrete torsion given in table 21. The left column shows the sector from which the representations arise.

Example 1 on $T^6/\mathbb{Z}_2 \times \mathbb{Z}_2$: Kähler metrics and gauge kinetic functions involving brane a_1				
y	$(\vec{\phi}_{a_1 y})$	$b_{a_1 y}^A$	$K_{(a_1, \bar{N}_y)}$	$\delta_y f_{SU(4)_{a_1}}^{\text{1-loop}}(v_i)$
a_1	$(0, 0, 0)$	-12	$-$	$\sum_{i=1}^3 \frac{1}{\pi^2} \ln \eta(iv_i)$
$a_{j,j>1}$	$(0, 0, 0)$	4	$f(S, U_l) \sqrt{\frac{2\pi(\frac{1}{r_1} + r_1)}{v_2 v_3}}$ $f(S, U_l) \sqrt{\frac{2\pi(\frac{1}{r_2} + r_2)}{v_1 v_3}}$ $f(S, U_l) \sqrt{\frac{2\pi(\frac{1}{r_3} + r_3)}{v_1 v_2}}$	$-\frac{1}{\pi^2} \ln \eta(iv_1) \quad j=2$ $-\frac{1}{\pi^2} \ln \eta(iv_2) \quad 3$ $-\frac{1}{\pi^2} \ln \eta(iv_3) \quad 4$
a'_1	$(-2\phi^{(1)}, -2\phi^{(2)}, -2\phi^{(3)})$	$b_{a_1 a'_1}^A + b_{a_1 a'_1}^M$ $= 16 - 8$	$K_{\text{Anti}_{a_1}} = \frac{f(S, U_l)}{\sqrt{v_1 v_2 v_3}} \times$ $\sqrt{\frac{\Gamma(2\phi^{(1)})\Gamma(2\phi^{(2)})\Gamma(1-2\phi^{(1)}-2\phi^{(2)})}{\Gamma(1-2\phi^{(1)})\Gamma(1-2\phi^{(2)})\Gamma(2\phi^{(1)}+2\phi^{(2)})}}$	$-$
$a'_{j,j>1}$	$(-2\phi^{(1)}, -2\phi^{(2)}, -2\phi^{(3)})$	0	$-$	$-$

Table 23: Relative angles, beta function coefficients, Kähler metrics and v_i dependent one-loop contributions to the holomorphic gauge kinetic function involving D6-brane a_1 of example 1 on $T^6/\mathbb{Z}_2 \times \mathbb{Z}_2$ with discrete torsion, which is T-dual to the first magnetised D9-brane example in [1]. The bifundamental representations arise on parallel D6-branes whereas the antisymmetric matter states arise at three non-vanishing intersections.

Gauge breaking from example 1 to 2 on $T^6/\mathbb{Z}_2 \times \mathbb{Z}_2$		
$\prod_{i=1}^4 U(4)_{a_i} \rightarrow$		$(\prod_{i=1}^4 U(2)_{a_i}) \times \widetilde{U(2)}_{\text{diag}}$
$a_i a_j$	$[(4, \bar{4}, 1, 1) + (1, 1, 4, \bar{4}) + c.c.]$ $+ [(4, 1, \bar{4}, 1) + (1, 4, 1, \bar{4}) + c.c.]$ $+ [(4, 1, 1, \bar{4}) + (1, 4, \bar{4}, 1) + c.c.]$	$[(2, \bar{2}, 1, 1; 1) + (1, 1, 2, \bar{2}; 1) + c.c.]$ $+ [(2, 1, \bar{2}, 1; 1) + (1, 2, 1, \bar{2}; 1) + c.c.]$ $+ [(2, 1, 1, \bar{2}; 1) + (1, 2, \bar{2}, 1; 1) + c.c.]$
$a_i a'_j$	$+8 \times [(\bar{6}_{\text{Anti}}, 1, 1, 1) + (1, \bar{6}_{\text{Anti}}, 1, 1)]$ $+8 \times [(1, 1, \bar{6}_{\text{Anti}}, 1) + (1, 1, 1, \bar{6}_{\text{Anti}})]$	$+8 \times [(\bar{1}_{\text{Anti}}, 1, 1, 1; 1) + (1, \bar{1}_{\text{Anti}}, 1, 1; 1)]$ $+8 \times [(\bar{2}, 1, 1, 1; \bar{2}) + (1, \bar{2}, 1, 1; \bar{2})]$ $+16 \times (1, 1, 1, 1; \bar{1}_{\text{Anti}})$ $+8 \times [(1, 1, \bar{1}_{\text{Anti}}, 1; 1) + (1, 1, 1, \bar{1}_{\text{Anti}}; 1)]$ $+8 \times [(1, 1, \bar{2}, 1; \bar{2}) + (1, 1, 1, \bar{2}; \bar{2})]$ $+16 \times (1, 1, 1, 1; \bar{1}_{\text{Anti}})$

Table 24: The matter representations in the second example of [1] on $T^6/\mathbb{Z}_2 \times \mathbb{Z}_2$ originate from giving vevs to some bifundamental representations in example 1. On the r.h.s., the spectrum in bold letters corresponds to the one listed in [1].

T-dual D6-brane configurations of example 3 on $T^6/\mathbb{Z}_2 \times \mathbb{Z}_2$							
D6 _x -brane	$(\vec{\phi}_x)$	Torus wrappings $(n_x^1, m_x^1, n_x^2, m_x^2, n_x^3, m_x^3)$	$(\vec{X}_x); (\vec{Y}_x)$	$(\vec{\sigma}_x)$	$(-1)^{\tau_x^{\mathbb{Z}_2}}$	$(\vec{\tau}_x)$	(\vec{V}_{xx})
a_1 a_2 a_3 a_4	$(\phi^{(1)}, \phi^{(2)}, \phi^{(3)})$ $\sum_{i=1}^3 \phi^{(i)} = 0$	$(1, 2; 1, 1; 1, -1)$	$\begin{pmatrix} 1 \\ -1 \\ -2 \\ 2 \end{pmatrix}; \begin{pmatrix} -2 \\ 2 \\ 1 \\ -1 \end{pmatrix}$	$(\vec{0})$	$(+++)$ $(+--)$ $(-+-)$ $(---)$	$(\vec{0})$	$\begin{pmatrix} \frac{1}{r_1} + 4r_1 \\ \frac{1}{r_2} + r_2 \\ \frac{1}{r_3} + r_3 \end{pmatrix}$
a'_1 a'_2 a'_3 a'_4	$(-\phi^{(1)}, -\phi^{(2)}, -\phi^{(3)})$	$(1, -2; 1, -1; 1, 1)$	$\begin{pmatrix} 1 \\ -1 \\ -2 \\ 2 \end{pmatrix}; \begin{pmatrix} 2 \\ -2 \\ -1 \\ 1 \end{pmatrix}$	$(\vec{0})$	$(--+)$ $(-+-)$ $(+--)$ $(+++)$	$(\vec{0})$	$\begin{pmatrix} \frac{1}{r_1} + 4r_1 \\ \frac{1}{r_2} + r_2 \\ \frac{1}{r_3} + r_3 \end{pmatrix}$
b_1 b_2	$(0, 0, 0)$	$(1, 0; 1, 0; 1, 0)$	$\begin{pmatrix} 1 \\ 0 \\ 0 \\ 0 \end{pmatrix}; \begin{pmatrix} 0 \\ 0 \\ 0 \\ 0 \end{pmatrix}$	$(\vec{0})$	$(+++)$ $(+--)$	$(\vec{0})$	$\begin{pmatrix} \frac{1}{r_1} \\ \frac{1}{r_2} \\ \frac{1}{r_3} \end{pmatrix}$
$b'_2 (\equiv b_3)$ $b'_1 (\equiv b_4)$	$(0, 0, 0)$	$(1, 0; 1, 0; 1, 0)$	$\begin{pmatrix} 1 \\ 0 \\ 0 \\ 0 \end{pmatrix}; \begin{pmatrix} 0 \\ 0 \\ 0 \\ 0 \end{pmatrix}$	$(\vec{0})$	$(-+-)$ $(--+)$	$(\vec{0})$	$\begin{pmatrix} \frac{1}{r_1} \\ \frac{1}{r_2} \\ \frac{1}{r_3} \end{pmatrix}$
c_1 c_2	$(0, \frac{1}{2}, -\frac{1}{2})$	$(1, 0; 0, 1; 0, -1)$	$\begin{pmatrix} 0 \\ -1 \\ 0 \\ 0 \end{pmatrix}; \begin{pmatrix} 0 \\ 0 \\ 0 \\ 0 \end{pmatrix}$	$(\vec{0})$	$(+++)$ $(+--)$	$(\vec{0})$	$\begin{pmatrix} \frac{1}{r_1} \\ r_2 \\ r_3 \end{pmatrix}$
$c'_1 (\equiv c_3)$ $c'_2 (\equiv c_4)$	$(0, \frac{1}{2}, -\frac{1}{2})$	$(1, 0; 0, 1; 0, -1)$	$\begin{pmatrix} 0 \\ -1 \\ 0 \\ 0 \end{pmatrix}; \begin{pmatrix} 0 \\ 0 \\ 0 \\ 0 \end{pmatrix}$	$(\vec{0})$	$(-+-)$ $(--+)$	$(\vec{0})$	$\begin{pmatrix} \frac{1}{r_1} \\ r_2 \\ r_3 \end{pmatrix}$

Table 25: The eight stacks of D6-branes a_i , b_j , c_k and their orientifold images which are T-dual to the third magnetised D9/D5-brane model of [1]. A close inspection of the rigid three-cycles reveals that none of the D6-brane can be chosen to be orientifold invariant. RR tadpole cancellation leads to the gauge group $\left(\prod_{i=1}^4 U(2)_{a_i}\right) \times \left(\prod_{j=1}^2 U(4)_{b_j}\right) \times \left(\prod_{k=1}^2 U(4)_{c_k}\right)$, and the matter spectrum matches the one in [1] with corrections in [67] taken into account. For the D6 _{c_j} -branes, the orientifold image D-branes listed here have a different shape $(\vec{\tau}_{c'_j}^{\mathbb{Z}_2}) = (\vec{\tau}_{c_j}^{\mathbb{Z}_2}) + (1, 0, 1)$ because we performed a simultaneous sign-flip of the toroidal wrapping numbers on $T_{(2)}^2 \times T_{(3)}^2$ for the sake of a more compact notation. The $\left(\prod_{j=1}^2 Sp(4)_{b_j}\right) \times \left(\prod_{k=1}^2 Sp(4)_{c_k}\right)$ gauge group in [1] is obtained after recombination of orientifold image D6-branes $b_j + b'_j$ and $c_k + c'_k$ as detailed in the text. Supersymmetry requires the relation $r_3 = \frac{2r_1+r_2}{1-2r_1r_2}$ for the shapes of the three two-tori.

Matter spectrum of Ex. 3 on $T^6/\mathbb{Z}_2 \times \mathbb{Z}_2$ with gauge group $(\prod_{i=1}^4 U(2)_{a_i}) \times (\prod_{j=1}^2 U(4)_{b_j}) \times (\prod_{k=1}^2 U(4)_{c_k})$	
$a_i a_j$	$[(2, \bar{2}, 1, 1, 1, 1, 1, 1) + (1, 1, 2, \bar{2}, 1, 1, 1, 1) + (2, 1, \bar{2}, 1, 1, 1, 1, 1) + (1, 2, 1, \bar{2}, 1, 1, 1, 1) + (2, 1, 1, \bar{2}, 1, 1, 1, 1) + (1, 2, \bar{2}, 1, 1, 1, 1, 1) + c.c.]$ $+4 \times [(\bar{2}, \bar{2}, 1, 1, 1, 1, 1, 1) + (1, 1, \bar{2}, \bar{2}, 1, 1, 1, 1)]$ $+12 \times [(1_{\text{Anti}}, 1, 1, 1, 1, 1, 1, 1) + (1, 1_{\text{Anti}}, 1, 1, 1, 1, 1, 1) + (1, 1, 1_{\text{Anti}}, 1, 1, 1, 1, 1) + (1, 1, 1, 1_{\text{Anti}}, 1, 1, 1, 1)]$
$a_i b_j$	$+2 \times (1, 1, \bar{2}, 1, 1, 4, 1, 1) + 2 \times (1, 1, 1, \bar{2}, 4, 1, 1, 1)$
$a_i b'_j$	$+2 \times [(\bar{2}, 1, 1, 1, \bar{4}, 1, 1, 1) + (1, \bar{2}, 1, 1, 1, \bar{4}, 1, 1)]$
$a_i c_j$	$+2 \times (1, 1, \bar{2}, 1, 1, 4, 1) + 2 \times (1, 1, 1, \bar{2}, 1, 1, 4)$
$a_i c'_j$	$+2 \times [(\bar{2}, 1, 1, 1, 1, \bar{4}, 1) + (1, \bar{2}, 1, 1, 1, 1, \bar{4})]$
$b_i b_j$	$+ [(1, 1, 1, 1, 4, \bar{4}, 1, 1) + c.c.]$
$b_i b'_j$	$+ [(1, 1, 1, 1, 4, 4, 1, 1) + (1, 1, 1, 1, 6_{\text{Anti}}, 1, 1, 1) + (1, 1, 1, 1, 1, 6_{\text{Anti}}, 1, 1) + c.c.]$
$b_i c_j$	$+\emptyset$
$b_i c'_j$	$+(1, 1, 1, 1, 4, 1, 1, 4) + (1, 1, 1, 1, 1, 4, 4, 1) + (1, 1, 1, 1, \bar{4}, 1, \bar{4}, 1) + (1, 1, 1, 1, 1, \bar{4}, 1, \bar{4})$
$c_i c_j$	$+ [(1, 1, 1, 1, 1, 1, 4, \bar{4}) + c.c.]$
$c_i c'_j$	$+ [(1, 1, 1, 1, 1, 1, 4, 4) + (1, 1, 1, 1, 1, 1, 6_{\text{Anti}}, 1) + (1, 1, 1, 1, 1, 1, 1, 6_{\text{Anti}}) + c.c.]$

Table 26: The complete massless matter spectrum on intersecting rigid D6-branes on $T^6/\mathbb{Z}_2 \times \mathbb{Z}_2$ with discrete torsion which is T-dual to the magnetised D9/D5-brane example 3 in [1] including the corrections in [67]. The spectra match up to reordering and complex conjugation of all a_3 and a_4 states and upon the recombination of the $D6_{b_j}$ and $D6_{c_j}$ -branes with their orientifold images to the reduced gauge group $(\prod_{j=1}^2 Sp(4)_{b_j}) \times (\prod_{k=1}^2 Sp(4)_{c_k})$ as discussed in the text.

Example 3 on $T^6/\mathbb{Z}_2 \times \mathbb{Z}_2$: Kähler metrics and gauge kinetic functions involving brane a_1				
y	$(\vec{\phi}_{a_1 y})$	$b_{a_1 y}^A$	$K_{(4_{a_1}, \bar{\mathbf{K}}_y)}$	$\delta_y f_{SU(2)_{a_1}}^{1\text{-loop}}(v_i)$
a_1	$(0, 0, 0)$	-6	$-$	$\sum_{i=1}^3 \frac{1}{2\pi^2} \ln \eta(iv_i)$
$a_{j,j=2,3,4}$	$(0, 0, 0)$	2	$f(S, U_l) \sqrt{\frac{2\pi \left(\frac{1}{r_j-1} + 4r_j-1 \right)}{v_j \bmod 3 \ v_{j+1} \bmod 3}}$	$-\frac{1}{2\pi^2} \ln \eta(iv_{j-1})$
a'_1	$(-2\phi^{(1)}, -2\phi^{(2)}, -2\phi^{(3)})$	$b_{ay}^A + b_{ay}^M$ $= 12 - 12$	$K_{\text{Anti}a} = \frac{f(S, U_l)}{\sqrt{v_1 v_2 v_3}} \times \sqrt{\frac{\Gamma(2\phi^{(1)}) \Gamma(2\phi^{(2)}) \Gamma(1-2 \phi^{(3)})}{\Gamma(1-2\phi^{(1)}) \Gamma(1-2\phi^{(2)}) \Gamma(2 \phi^{(3)})}}$	$-$
a'_2	$(-2\phi^{(1)}, -2\phi^{(2)}, -2\phi^{(3)})$	4	$\frac{f(S, U_l)}{\sqrt{v_1 v_2 v_3}} \sqrt{\frac{\Gamma(2\phi^{(1)}) \Gamma(2\phi^{(2)}) \Gamma(1-2 \phi^{(3)})}{\Gamma(1-2\phi^{(1)}) \Gamma(1-2\phi^{(2)}) \Gamma(2 \phi^{(3)})}}$	$-$
$a'_{j,j=3,4}$	$(-2\phi^{(1)}, -2\phi^{(2)}, -2\phi^{(3)})$	0	$-$	$-$
$b_{k,k=1,2,2'}$	$(-\phi^{(1)}, -\phi^{(2)}, -\phi^{(3)})$	0	$-$	$-$
b'_1	$(-\phi^{(1)}, -\phi^{(2)}, -\phi^{(3)})$	4	$\frac{f(S, U_l)}{\sqrt{v_1 v_2 v_3}} \sqrt{\frac{\Gamma(\phi^{(1)}) \Gamma(\phi^{(2)}) \Gamma(1- \phi^{(3)})}{\Gamma(1-\phi^{(1)}) \Gamma(1-\phi^{(2)}) \Gamma(\phi^{(3)})}}$	$-$
$c_{l,l=1,2,2'}$	$(-\phi^{(1)}, \frac{1}{2} - \phi^{(2)}, -\frac{1}{2} - \phi^{(3)})$	0	$-$	$-$
c'_1	$(-\phi^{(1)}, \frac{1}{2} - \phi^{(2)}, -\frac{1}{2} - \phi^{(3)})$	4	$\frac{f(S, U_l)}{\sqrt{v_1 v_2 v_3}} \sqrt{\frac{\Gamma(\phi^{(1)}) \Gamma(\frac{1}{2}-\phi^{(2)}) \Gamma(\frac{1}{2}+ \phi^{(3)})}{\Gamma(1-\phi^{(1)}) \Gamma(\frac{1}{2}+\phi^{(2)}) \Gamma(\frac{1}{2}- \phi^{(3)})}}$	$-$

Table 27: Relative angles, beta function coefficients, Kähler metrics and two-torus volume v_i dependent one-loop contributions to the holomorphic gauge kinetic function involving D6-brane a_1 of example 3 on $T^6/\mathbb{Z}_2 \times \mathbb{Z}_2$ with discrete torsion.

D6-brane configuration for the SM with hidden sector $Sp(6)_{h_3}$ on T^6/\mathbb{Z}'_6							
D6 _x -brane	$(\vec{\phi}_x)$	Torus wrappings (n_x^i, m_x^i)	$(\vec{X}_x); (\vec{Y}_x) =$ $\left(\frac{P_x+Q_x}{2}; \left(-\frac{U_x+V_x}{2}, \frac{Q_x-P_x}{2}\right)\right)$	(σ_x^1, σ_x^3)	$(-1)^{\tau_x^2}$	(τ_x^1, τ_x^3)	(\vec{V}_{xx})
a	$(-\frac{1}{3}, -\frac{1}{6}, \frac{1}{2})$	$(1, -1; 1, 0; 0, 1)$	$\begin{pmatrix} 0 \\ -1 \end{pmatrix}; \begin{pmatrix} 0 \\ 0 \end{pmatrix}$	$(1; 1)$	$(+)$	$(1, 1)$	$\begin{pmatrix} \frac{2}{\sqrt{3}} \\ \frac{2}{\sqrt{3}} \\ r \end{pmatrix}$
h_3				$(0, 0)$	$(+)$	$(1, 0)$	
b	$(\frac{1}{6}, -\frac{1}{3}, \frac{1}{6})$	$(1, 1; 2, -1; 1, 1)$	$\begin{pmatrix} \frac{3}{2} \\ -\frac{3}{2} \end{pmatrix}; \begin{pmatrix} -\frac{3}{2} \\ -\frac{3}{2} \end{pmatrix}$	$(1, 0)$	$(-)$	$(1, 0)$	$\begin{pmatrix} 2\sqrt{3} \\ 2\sqrt{3} \\ \frac{1}{r} + r \end{pmatrix}$
c	$(-\frac{1}{3}, \frac{1}{3}, 0)$	$(1, -1; -1, 2; 1, 0)$	$\begin{pmatrix} 1 \\ 0 \end{pmatrix}; \begin{pmatrix} 0 \\ 0 \end{pmatrix}$	$(1, 1)$	$(+)$	$(1, 1)$	$\begin{pmatrix} \frac{2}{\sqrt{3}} \\ 2\sqrt{3} \\ \frac{1}{r} \end{pmatrix}$
d	$(\frac{1}{6}, \frac{1}{3}, -\frac{1}{2})$	$(1, 1; 1, -2; 0, 1)$	$\begin{pmatrix} 0 \\ -3 \end{pmatrix}; \begin{pmatrix} 0 \\ 0 \end{pmatrix}$	$(0, 1)$	$(+)$	$(1, 1)$	$\begin{pmatrix} 2\sqrt{3} \\ 2\sqrt{3} \\ r \end{pmatrix}$

Table 28: Geometrical setup of the supersymmetric Standard Model example with hidden sector $Sp(6)_{h_3}$ on the **ABa** lattice in the T^6/\mathbb{Z}'_6 background [41, 2, 40]. Brane b preserves supersymmetry for the ratio of radii on the **a**-type $T^2_{(3)}$ torus $r = 1/\sqrt{3}$. Details on the exceptional cycles and intersection numbers are given in [41, 2, 40].

Angles, beta function coefficients and Kähler metrics for D6-branes a and d of the SM on T^6/\mathbb{Z}'_6									
Brane a									
y	$(\vec{\phi}_{ay})$	b_{ay}^A	$K_{(\mathbf{3}_a, \bar{\mathbf{N}}_y)}$	$(\vec{\phi}_{a(\theta y)})$	$b_{a(\theta y)}^A$	$K_{(\mathbf{3}_a, \bar{\mathbf{N}}_y)}$	$(\vec{\phi}_{a(\theta^2 y)})$	$b_{a(\theta^2 y)}^A$	$K_{(\mathbf{3}_a, \bar{\mathbf{N}}_y)}$
a	$(0, 0, 0)$	-6	$K_{\text{Adj}_a} = \sqrt{\frac{\pi r}{2}} \frac{f(S, U)}{v_2}$	$\pm(\frac{1}{3}, -\frac{1}{3}, 0)$	3	$K_{\text{Adj}_a} = f(S, U) \sqrt{\frac{2\pi r}{v_1 v_2}}$			
a'	$(-\frac{1}{3}, \frac{1}{3}, 0)$	$b_{aa'}^A + b_{aa'}^M = \frac{3}{2} - 1$	$K_{\text{Anti}_a} = f(S, U) \sqrt{\frac{2\pi r}{v_1 v_2}}$	$(0, 0, 0)$	$b_{a(\theta a')}^A + b_{a(\theta a')}^M = 6 - 4 = 2$	$K_{\text{Anti}_a} = f(S, U) \sqrt{\frac{4\pi}{\sqrt{3} v_1 v_3}}$	$(\frac{1}{3}, -\frac{1}{3}, 0)$	$b_{a(\theta^2 a')}^A + b_{a(\theta^2 a')}^M = \frac{3}{2} - 1$	$K_{\text{Anti}_a} = f(S, U) \sqrt{\frac{2\pi r}{v_1 v_2}}$
b	$(\frac{1}{2}, -\frac{1}{6}, -\frac{1}{3})$	0	$-$	$(-\frac{1}{6}, \frac{1}{2}, -\frac{1}{3})$	0	$-$	$(\frac{1}{6}, \frac{1}{6}, -\frac{1}{3})$	0	$-$
b'	$(\frac{1}{6}, -\frac{1}{2}, \frac{1}{3})$	2	$f(S, U) \sqrt{\frac{10}{v_1 v_2 v_3}}$	$(-\frac{1}{2}, \frac{1}{6}, \frac{1}{3})$	2	$f(S, U) \sqrt{\frac{10}{v_1 v_2 v_3}}$	$(-\frac{1}{6}, -\frac{1}{6}, \frac{1}{3})$	1	$f(S, U) \sqrt{\frac{25}{2 v_1 v_2 v_3}}$
c	$(0, \frac{1}{2}, -\frac{1}{2})$	2	$f(S, U) \sqrt{\frac{4\pi}{\sqrt{3} v_2 v_3}}$	$(\frac{1}{3}, \frac{1}{6}, -\frac{1}{2})$	0	$-$	$(-\frac{1}{3}, -\frac{1}{6}, \frac{1}{2})$	1	$f(S, U) \sqrt{\frac{10}{v_1 v_2 v_3}}$
d	$(\frac{1}{2}, -\frac{1}{2}, 0)$	2	$f(S, U) \sqrt{\frac{2\pi r}{v_1 v_2}}$	$(-\frac{1}{6}, \frac{1}{6}, 0)$	$\frac{1}{2}$	$f(S, U) \sqrt{\frac{2\pi r}{v_1 v_2}}$	$(\frac{1}{6}, -\frac{1}{6}, 0)$	$\frac{1}{2}$	$f(S, U) \sqrt{\frac{2\pi r}{v_1 v_2}}$
d'	$(\frac{1}{6}, -\frac{1}{6}, 0)$	$\frac{1}{2}$	$f(S, U) \sqrt{\frac{2\pi r}{v_1 v_2}}$	$(\frac{1}{2}, -\frac{1}{2}, 0)$	2	$f(S, U) \sqrt{\frac{2\pi r}{v_1 v_2}}$	$(-\frac{1}{6}, \frac{1}{6}, 0)$	$\frac{1}{2}$	$f(S, U) \sqrt{\frac{2\pi r}{v_1 v_2}}$
h_3	$(0, 0, 0)$	0	$-$	$(\frac{1}{3}, -\frac{1}{3}, 0)$	$3 \cdot 0_3$	$-$	$(-\frac{1}{3}, \frac{1}{3}, 0)$	$3 \cdot 0_3$	$-$
Brane d									
x	$(\vec{\phi}_{xd})$	b_{dx}^A	$K_{(\mathbf{N}_x, \bar{\mathbf{I}}_d)}$	$(\vec{\phi}_{x(\theta d)})$	$b_{(\theta d)x}^A$	$K_{(\mathbf{N}_x, \bar{\mathbf{I}}_d)}$	$(\vec{\phi}_{x(\theta^2 d)})$	$b_{(\theta^2 d)x}^A$	$K_{(\mathbf{N}_x, \bar{\mathbf{I}}_d)}$
b	$(0, -\frac{1}{3}, \frac{1}{3})$	$3 \cdot 0_1$	$-$	$(\frac{1}{3}, -\frac{2}{3}, \frac{1}{3})$	6	$f(S, U) \sqrt{\frac{8}{v_1 v_2 v_3}}$	$(-\frac{1}{3}, 0, \frac{1}{3})$	4	$f(S, U) \sqrt{\frac{4\pi\sqrt{3}}{v_1 v_3}}$
c	$(\frac{1}{2}, 0, -\frac{1}{2})$	2	$f(S, U) \sqrt{\frac{4\pi\sqrt{3}}{v_1 v_3}}$	$(-\frac{1}{6}, -\frac{1}{3}, \frac{1}{2})$	3	$f(S, U) \sqrt{\frac{10}{v_1 v_2 v_3}}$	$(\frac{1}{6}, \frac{1}{3}, -\frac{1}{2})$	0	$-$
h_3	$(\frac{1}{2}, -\frac{1}{2}, 0)$	$24 \cdot 0_3$	$-$	$(-\frac{1}{6}, \frac{1}{6}, 0)$	$6 \cdot 0_3$	$-$	$(\frac{1}{6}, -\frac{1}{6}, 0)$	$6 \cdot 0_3$	$-$
x	$(\vec{\phi}_{xd'})$	$b_{d'x}^A$	$K_{(\mathbf{N}_x, \bar{\mathbf{I}}_d)}$	$(\vec{\phi}_{x(\theta d')})$	$b_{(\theta d')x}^A$	$K_{(\mathbf{N}_x, \bar{\mathbf{I}}_d)}$	$(\vec{\phi}_{x(\theta^2 d')})$	$b_{(\theta^2 d')x}^A$	$K_{(\mathbf{N}_x, \bar{\mathbf{I}}_d)}$
b	$(-\frac{1}{3}, 0, \frac{1}{3})$	2	$f(S, U) \sqrt{\frac{4\pi\sqrt{3}}{v_1 v_3}}$	$(0, -\frac{1}{3}, \frac{1}{3})$	$3 \cdot 0_1$	$-$	$(\frac{1}{3}, -\frac{2}{3}, \frac{1}{3})$	3	$f(S, U) \sqrt{\frac{8}{v_1 v_2 v_3}}$
d'	$(-\frac{1}{3}, \frac{1}{3}, 0)$	$2b_{dd'}^A + b_{dd'}^M = 9 - 9 = 0$	$-$	$(0, 0, 0)$	$2b_{d(\theta d')}^A + b_{d(\theta d')}^M = 4 - 4 = 0$	$-$	$(\frac{1}{3}, -\frac{1}{3}, 0)$	$2b_{d(\theta^2 d')}^A + b_{d(\theta^2 d')}^M = 9 - 9 = 0$	$-$

Table 29: Relative angles, beta function coefficients and Kähler metrics for matter charged under $U(3)_a$ or $U(1)_d$ of the Standard Model example with hidden $Sp(6)_{h_3}$ on T^6/\mathbb{Z}'_6 [2]. This includes all left- and right-handed quarks at $a(\theta^k b')$ and $a(\theta^k c)$ intersections, respectively, and leptons at $b(\theta^k d^{(\prime)})$ and $c(\theta^k d^{(\prime)})$ intersections. The beta function coefficients $b_{(\theta^k d)_a}^A$ and $b_{a(\theta^k d)}^A$ with reversed lower indices differ by the global factor $N_a/N_d = 3$, i.e. $(b_{(\theta^k d)_a}^A)_{k=1,2,3} = (6, \frac{3}{2}, \frac{3}{2})$ and $(b_{a(\theta^k d)}^A)_{k=1,2,3} = (\frac{3}{2}, 6, \frac{3}{2})$. The corresponding v_i dependent one-loop contributions to the holomorphic gauge kinetic functions $\delta_y \mathbf{f}_{SU(3)_a}^{1\text{-loop}}(v_i)$ and $\delta_x \mathbf{f}_{SU(1)_d}^{1\text{-loop}}(v_i)$ are given in table 30.

1-loop contributions to the holomorphic gauge kinetic function $\delta_y \mathbf{f}_{SU(3)_a}^{1\text{-loop}}(v_i)$ for the SM on T^6/\mathbb{Z}'_6			
y	$\delta_y \mathbf{f}_{SU(3)_a}^{1\text{-loop}}(v_i)$	$\delta_{(\theta y)} \mathbf{f}_{SU(3)_a}^{1\text{-loop}}(v_i)$	$\delta_{(\theta^2 y)} \mathbf{f}_{SU(3)_a}^{1\text{-loop}}(v_i)$
a	$\frac{3}{2\pi^2} \ln \eta(iv_2)$	$-\frac{3}{4\pi^2} \ln \eta(iv_3)$	
a'	$-\frac{1}{8\pi^2} \ln \eta(iv_3)$	$-\frac{3}{2\pi^2} \ln \eta(iv_2)$ $+\frac{1}{2\pi^2} \ln \eta(i\tilde{v}_1) + \frac{1}{2\pi^2} \ln \eta(iv_3)$	$-\frac{1}{8\pi^2} \ln \eta(iv_3)$
b	—	—	—
b'	—	—	—
c	$-\frac{1}{2\pi^2} \ln \eta(iv_1)$	—	—
d	$-\frac{1}{2\pi^2} \ln \eta(iv_3)$	$-\frac{1}{8\pi^2} \ln \eta(iv_3)$	$-\frac{1}{8\pi^2} \ln \eta(iv_3)$
d'	$-\frac{1}{8\pi^2} \ln \eta(iv_3)$	$-\frac{1}{2\pi^2} \ln \eta(iv_3)$	$-\frac{1}{8\pi^2} \ln \eta(iv_3)$
h_3	—	$-\frac{3}{8\pi^2} \ln \left(e^{-\pi v_3/4} \frac{\vartheta_1(\frac{1-i\tilde{v}_3}{2}, i\tilde{v}_3)}{\eta(i\tilde{v}_3)} \right)$	$-\frac{3}{8\pi^2} \ln \left(e^{-\pi v_3/4} \frac{\vartheta_1(\frac{1-i\tilde{v}_3}{2}, i\tilde{v}_3)}{\eta(i\tilde{v}_3)} \right)$
1-loop contributions to the auxiliary holomorphic gauge kinetic function $\delta_x \mathbf{f}_{SU(1)_d}^{1\text{-loop}}$			
x	$\delta_x \mathbf{f}_{SU(1)_d}^{1\text{-loop}}(v_i)$	$\delta_{(\theta^{-1}x)} \mathbf{f}_{SU(1)_d}^{1\text{-loop}}(v_i)$	$\delta_{(\theta^{-2}x)} \mathbf{f}_{SU(1)_d}^{1\text{-loop}}(v_i)$
b	$-\frac{3}{8\pi^2} \ln \left(e^{-\pi v_1/4} \frac{\vartheta_1(\frac{-i\tilde{v}_1}{2}, i\tilde{v}_1)}{\eta(i\tilde{v}_1)} \right)$	—	$-\delta_{\sigma_{bd}^2,0} \delta_{\tau_{bd}^2,0} \times \frac{1}{\pi^2} \ln \eta(iv_2)$ $-\frac{1}{2\pi^2} (1 - \delta_{\sigma_{bd}^2,0} \delta_{\tau_{bd}^2,0}) \times$ $\times \ln \left(e^{-\pi(\sigma_{bd}^2)^2 v_2/4} \frac{\vartheta_1(\frac{\tau_{bd}^2 - i\sigma_{bd}^2 v_2}{2}, i\tilde{v}_2)}{\eta(i\tilde{v}_2)} \right)$
b'	$-\delta_{\sigma_{bd'}^2,0} \delta_{\tau_{bd'}^2,0} \times \frac{1}{2\pi^2} \ln \eta(iv_2)$ $-\frac{1}{4\pi^2} (1 - \delta_{\sigma_{bd'}^2,0} \delta_{\tau_{bd'}^2,0}) \times$ $\times \ln \left(e^{-\pi(\sigma_{bd'}^2)^2 v_2/4} \frac{\vartheta_1(\frac{\tau_{bd'}^2 - i\sigma_{bd'}^2 v_2}{2}, i\tilde{v}_2)}{\eta(i\tilde{v}_2)} \right)$	$-\frac{3}{8\pi^2} \ln \left(e^{-\pi v_1/4} \frac{\vartheta_1(\frac{-i\tilde{v}_1}{2}, i\tilde{v}_1)}{\eta(i\tilde{v}_1)} \right)$	—
c	$-\delta_{\sigma_{cd}^2,0} \delta_{\tau_{cd}^2,0} \times \frac{1}{2\pi^2} \ln \eta(iv_2)$ $-\frac{1}{4\pi^2} (1 - \delta_{\sigma_{cd}^2,0} \delta_{\tau_{cd}^2,0}) \times$ $\times \ln \left(e^{-\pi(\sigma_{cd}^2)^2 v_2/4} \frac{\vartheta_1(\frac{\tau_{cd}^2 - i\sigma_{cd}^2 v_2}{2}, i\tilde{v}_2)}{\eta(i\tilde{v}_2)} \right)$	—	—
h_3	$-\frac{3}{\pi^2} \ln \left(e^{-\pi v_3/4} \frac{\vartheta_1(\frac{1-i\tilde{v}_3}{2}, i\tilde{v}_3)}{\eta(i\tilde{v}_3)} \right)$	$-\frac{3}{4\pi^2} \ln \left(e^{-\pi v_3/4} \frac{\vartheta_1(\frac{1-i\tilde{v}_3}{2}, i\tilde{v}_3)}{\eta(i\tilde{v}_3)} \right)$	$-\frac{3}{4\pi^2} \ln \left(e^{-\pi v_3/4} \frac{\vartheta_1(\frac{1-i\tilde{v}_3}{2}, i\tilde{v}_3)}{\eta(i\tilde{v}_3)} \right)$
d'	$\frac{9}{8\pi^2} \ln \eta(iv_3)$	$\delta_{\sigma_{dd'}^2,0} \delta_{\tau_{dd'}^2,0} \times \left(-\frac{1}{2\pi^2} \ln \eta(iv_2) + \frac{1}{\pi^2} \ln \eta(i\tilde{v}_2) \right)$ $-(1 - \delta_{\sigma_{dd'}^2,0} \delta_{\tau_{dd'}^2,0}) \times$ $\times \left[\frac{1}{4\pi^2} \ln \left(e^{-\pi(\sigma_{dd'}^2)^2 v_2/4} \frac{\vartheta_1(\frac{\tau_{dd'}^2 - i\sigma_{dd'}^2 v_2}{2}, i\tilde{v}_2)}{\eta(i\tilde{v}_2)} \right) \right]$ $-\frac{1}{2\pi^2} \ln \left(e^{-\pi(\sigma_{dd'}^2)^2 \tilde{v}_2/4} \frac{\vartheta_1(\frac{\tau_{dd'}^2 - i\sigma_{dd'}^2 \tilde{v}_2}{2}, i\tilde{v}_2)}{\eta(i\tilde{v}_2)} \right)$	$\frac{9}{8\pi^2} \ln \eta(iv_3)$

Table 30: Two-torus volume v_i dependent one-loop contributions to the holomorphic gauge kinetic functions involving branes a and d . The total gauge kinetic function $\mathbf{f}_{SU(3)_a}^{1\text{-loop}}$ is given in the text. The auxiliary formal expressions $\delta_x \mathbf{f}_{SU(1)_d}^{1\text{-loop}}(v_i)$ are basic building blocks for the holomorphic gauge kinetic functions of the single $U(1)_d$ gauge factor $\mathbf{f}_{U(1)_d}^{1\text{-loop}}$ and the massless $U(1)_{B-L}$ group $\mathbf{f}_{U(1)_{B-L}}^{1\text{-loop}}$.

A Reformulations of the Möbius strip contributions to the gauge thresholds

In [40], we had derived the shape of the finite part of the r.h.s. of equation (28) as

$$-\frac{1}{4} \ln \left\{ \frac{\Gamma(|\nu|)^{\text{sgn}(\nu)}}{\Gamma(1-|\nu|)^{\text{sgn}(\nu)}} \cdot \frac{\Gamma(\nu + \frac{1}{2} - \text{sgn}(\nu)H(|\nu| - \frac{1}{2}))}{\Gamma(-\nu + \frac{1}{2} + \text{sgn}(\nu)H(|\nu| - \frac{1}{2}))} \right\} - \text{sgn}(\nu) \frac{1 - 2H(|2\nu| - 1)}{4} \ln(2),$$

which becomes zero for $\nu = \pm \frac{1}{2}$.

Using the Gamma function identity

$$\Gamma(z)\Gamma(z + \frac{1}{2}) = \sqrt{2\pi} 2^{-2z+\frac{1}{2}} \Gamma(2z),$$

the finite terms can be evaluated for the four ranges $-1 < \nu < -\frac{1}{2}$, $-\frac{1}{2} < \nu < 0$, $0 < \nu < \frac{1}{2}$ and $\frac{1}{2} < \nu < 1$ separately. The result is as given in (28), i.e.

$$-\frac{1}{4} \ln \left(\frac{\Gamma(|2\nu| - H(|2\nu| - 1))}{\Gamma(1 - |2\nu| + H(|2\nu| - 1))} \right)^{\text{sgn}(\nu)} + \left[\nu - \frac{\text{sgn}(\nu)}{2} \right] \ln(2), \quad (111)$$

see also [45] for $|\nu| < \frac{1}{2}$. Defining

$$X_{aa'}^{(n)} \equiv \ln \left(\frac{\Gamma(|\phi_{aa'}^{(n)}|)}{\Gamma(1 - |\phi_{aa'}^{(n)}|)} \right)^{\text{sgn}(\phi_{aa'}^{(n)})},$$

$$X_{a, \Omega\mathcal{R}\mathbb{Z}_2^{(l)}}^{(n)} \equiv \ln \left(\frac{\Gamma(\nu_{a, \Omega\mathcal{R}\mathbb{Z}_2^{(l)}}^{(n)})}{\Gamma(1 - \nu_{a, \Omega\mathcal{R}\mathbb{Z}_2^{(l)}}^{(n)})} \right)^{\text{sgn}(\phi_{a, \Omega\mathcal{R}\mathbb{Z}_2^{(l)}}^{(n)})} \quad \text{with} \quad \nu_{a, \Omega\mathcal{R}\mathbb{Z}_2^{(l)}}^{(n)} \equiv |2\phi_{a, \Omega\mathcal{R}\mathbb{Z}_2^{(l)}}^{(n)}| - H(|2\phi_{a, \Omega\mathcal{R}\mathbb{Z}_2^{(l)}}^{(n)}| - 1),$$

with $n \in \{1, 2, 3\}$ the two-torus index and $l \in \{0 \dots 3\}$, where $l = 0$ corresponds to the $\Omega\mathcal{R}$ invariant O6-plane, and the Heaviside step function $H(x)$ as defined in equation (29), we show that

$$X_{a, \Omega\mathcal{R}\mathbb{Z}_2^{(l)}}^{(n)} = X_{aa'}^{(n)} \quad \text{for all} \quad l \in \{0 \dots 3\} \quad (112)$$

for all $\mathcal{N} = 1$ supersymmetric D6-brane configurations at non-trivial angles. Equation (31) furthermore uses the relation among the different sign factors,

$$c_a^{\Omega\mathcal{R}\mathbb{Z}_2^{(l)}} \cdot \text{sgn}(I_a^{\Omega\mathcal{R}\mathbb{Z}_2^{(l)}}) \cdot \text{sgn}(I_{aa'}) = -1, \quad (113)$$

which we also show here on a case-by-case basis.

Without loss of generality, the angles $\phi_a^{(n)} \equiv -\phi_{a,\Omega\mathcal{R}}^{(n)}$ w.r.t. the $\Omega\mathcal{R}$ invariant O6-plane can be chosen in the range

$$0 < |\phi_{a,\Omega\mathcal{R}}^{(i)}|, |\phi_{a,\Omega\mathcal{R}}^{(j)}| < |\phi_{a,\Omega\mathcal{R}}^{(k)}| < 1 \quad \text{and} \quad 0 < |\phi_{a,\Omega\mathcal{R}}^{(i)}|, |\phi_{a,\Omega\mathcal{R}}^{(j)}| < \frac{1}{2} \quad (114)$$

with $\text{sgn}(\phi_{a,\Omega\mathcal{R}}^{(i)}) = \text{sgn}(\phi_{a,\Omega\mathcal{R}}^{(j)}) = -\text{sgn}(\phi_{a,\Omega\mathcal{R}}^{(k)})$,

with (i, j, k) a cyclic permutation of $(1, 2, 3)$. For the largest (absolute value of an) angle, three different ranges have to be considered: $0 < |\phi_{a,\Omega\mathcal{R}}^{(k)}| < \frac{1}{2}$ or $|\phi_{a,\Omega\mathcal{R}}^{(k)}| = \frac{1}{2}$ or $\frac{1}{2} < |\phi_{a,\Omega\mathcal{R}}^{(k)}| < 1$.

We first show that $X_{a,\Omega\mathcal{R}}^{(n)} = X_{aa'}^{(n)}$: The angles $\phi_{aa'}^{(n)}$ between orientifold image branes $D6_a$ and $D6'_a$ in the range $0 < |\phi_{aa'}^{(n)}| < 1$, where we do not further constrain the two smaller angles as in (114), are given as follows:

1. for $0 < |\phi_{a,\Omega\mathcal{R}}^{(k)}| < \frac{1}{2}$: the angles between orientifold image D6-branes and those between D6-brane and $\Omega\mathcal{R}$ invariant O6-plane are related by $\phi_{aa'}^{(n)} = 2\phi_{a,\Omega\mathcal{R}}^{(n)}$ for all $n \in \{1, 2, 3\}$. The equality (112) is obviously fulfilled.

The sign factor (30) of the Möbius strip contribution to the beta function coefficient takes the value $c_a^{\Omega\mathcal{R}} = -1$, and since $\text{sgn}(I_a^{\Omega\mathcal{R}}) = \text{sgn}(I_{aa'})$ equation (113) is fulfilled.

2. for $|\phi_{a,\Omega\mathcal{R}}^{(k)}| = \frac{1}{2}$: there are two different possibilities of shifting the angles $(\phi_{aa'}^{(n)})$ such that they are in the denoted range:

$$(\phi_{aa'}^{(i)}, \phi_{aa'}^{(j)}, \phi_{aa'}^{(k)}) = (2\phi_{a,\Omega\mathcal{R}}^{(i)}, 2\phi_{a,\Omega\mathcal{R}}^{(j)}, 0) - \begin{cases} (\text{sgn}(\phi_{a,\Omega\mathcal{R}}^{(i)}), 0, 0) \\ (0, \text{sgn}(\phi_{a,\Omega\mathcal{R}}^{(j)}), 0) \end{cases}$$

and $(\text{sgn}(\phi_{aa'}^{(i)}), \text{sgn}(\phi_{aa'}^{(j)})) = \begin{cases} (-\text{sgn}(\phi_{a,\Omega\mathcal{R}}^{(i)}), \text{sgn}(\phi_{a,\Omega\mathcal{R}}^{(j)})) \\ (\text{sgn}(\phi_{a,\Omega\mathcal{R}}^{(i)}), -\text{sgn}(\phi_{a,\Omega\mathcal{R}}^{(j)})) \end{cases},$

where the shift $\phi_{aa'}^{(k)} = 2\phi_{a,\Omega\mathcal{R}}^{(k)} - \text{sgn}(\phi_{a,\Omega\mathcal{R}}^{(k)}) = 0$ has already been performed. It is now easy to see that the Möbius strip contributions to the logarithm of Gamma functions from all three angles cancel out, and the annulus amplitude contributes a Kaluza-Klein and winding sum along the two-torus $T_{(k)}^2$, where $D6_a$ and $D6'_a$ are parallel to each other and perpendicular to the $\Omega\mathcal{R}$ invariant O6-plane.

The constant (30) for the Möbius strip contribution to the beta function coefficient vanishes, $c_a^{\Omega\mathcal{R}} = 0$.

3. for $\frac{1}{2} < |\phi_{a,\Omega\mathcal{R}}^{(k)}| < 1$, there exist the three different shifts of the angles $(\phi_{aa'}^{(n)})$ displayed in table 31, which lead to identical expressions for $X_{a,\Omega\mathcal{R}}^{(n)}$ and coincide with $X_{aa'}^{(n)}$, as

Angles of a $D6_a$ -brane with the $\Omega\mathcal{R}$ -invariant O6-plane and its image $D6_{a'}$ -brane	
$(\phi_{aa'}^{(i)}, \phi_{aa'}^{(j)}, \phi_{aa'}^{(k)})$	$(\text{sgn}(\phi_{aa'}^{(i)}), \text{sgn}(\phi_{aa'}^{(j)}), \text{sgn}(\phi_{aa'}^{(k)}))$
$(2\phi_{a,\Omega\mathcal{R}}^{(i)}, 2\phi_{a,\Omega\mathcal{R}}^{(j)}, 2\phi_{a,\Omega\mathcal{R}}^{(k)} + \text{sgn}(\phi_{a,\Omega\mathcal{R}}^{(k)}) \cdot (1, 1, -2))$	$(-\text{sgn}(\phi_{a,\Omega\mathcal{R}}^{(i)}), -\text{sgn}(\phi_{a,\Omega\mathcal{R}}^{(j)}), -\text{sgn}(\phi_{a,\Omega\mathcal{R}}^{(k)}))$
$(2\phi_{a,\Omega\mathcal{R}}^{(i)}, 2\phi_{a,\Omega\mathcal{R}}^{(j)}, 2\phi_{a,\Omega\mathcal{R}}^{(k)} + \text{sgn}(\phi_{a,\Omega\mathcal{R}}^{(k)}) \cdot (1, 0, -1))$	$(-\text{sgn}(\phi_{a,\Omega\mathcal{R}}^{(i)}), \text{sgn}(\phi_{a,\Omega\mathcal{R}}^{(j)}), \text{sgn}(\phi_{a,\Omega\mathcal{R}}^{(k)}))$
$(2\phi_{a,\Omega\mathcal{R}}^{(i)}, 2\phi_{a,\Omega\mathcal{R}}^{(j)}, 2\phi_{a,\Omega\mathcal{R}}^{(k)} + \text{sgn}(\phi_{a,\Omega\mathcal{R}}^{(k)}) \cdot (0, 1, -1))$	$(\text{sgn}(\phi_{a,\Omega\mathcal{R}}^{(i)}), -\text{sgn}(\phi_{a,\Omega\mathcal{R}}^{(j)}), \text{sgn}(\phi_{a,\Omega\mathcal{R}}^{(k)}))$

Table 31: Relation among the angles $(\phi_{aa'}^{(n)})$ of orientifold image $D6_a$ and $D6_{a'}$ branes and the angles $(\phi_{a,\Omega\mathcal{R}}^{(n)})$ w.r.t. the $\Omega\mathcal{R}$ invariant O6-plane for the maximal (absolute value of the) angle $|\phi_{a,\Omega\mathcal{R}}^{(k)}| > \frac{1}{2}$. The shifts, e.g. $\phi_{aa'}^{(i)} = 2\phi_{a,\Omega\mathcal{R}}^{(i)} - \text{sgn}(\phi_{a,\Omega\mathcal{R}}^{(i)})$ on the first and second line, ensure that $|\phi_{aa'}^{(n)}| < 1$ for all n .

can be checked on a case-by-case basis.

The sign (30) of the Möbius strip contribution to the beta function coefficient is $c_a^{\Omega\mathcal{R}} = 1$, and since in table 31 we show that $\text{sgn}(I_a^{\Omega\mathcal{R}}) = -\text{sgn}(I_{aa'})$ the signs satisfy the relation (113).

Now we show for definiteness that the relation (112) is fulfilled for the $\Omega\mathcal{R}\mathbb{Z}_2^{(2)}$ invariant O6-plane and the maximal angle (more precisely the maximal absolute value) on any of the three two-tori. The relation between the angles of a given $D6_a$ -brane w.r.t. to the $\Omega\mathcal{R}$ and $\Omega\mathcal{R}\mathbb{Z}_2^{(2)}$ invariant O6-planes are displayed in table 32. For all five distinct configurations of angles, one can read off that $X_{a,\Omega\mathcal{R}\mathbb{Z}_2^{(2)}}^{(n)} = X_{a,\Omega\mathcal{R}}^{(n)}$, which combined with the already demonstrated equality $X_{a,\Omega\mathcal{R}}^{(n)} = X_{aa'}^{(n)}$ gives the desired result. From table 32, one can also read off that $c_a^{\Omega\mathcal{R}\mathbb{Z}_2^{(2)}} \cdot \text{sgn}(\tilde{I}_a^{\Omega\mathcal{R}\mathbb{Z}_2^{(2)}}) = c_a^{\Omega\mathcal{R}} \cdot \text{sgn}(\tilde{I}_a^{\Omega\mathcal{R}})$ for all $\mathcal{N} = 1$ supersymmetric configuration of three non-vanishing angles, which implies that the relation (113) of signs is fulfilled for the $\Omega\mathcal{R}\mathbb{Z}_2^{(2)}$ -invariant O6-plane. The case $|\phi_{a,\Omega\mathcal{R}}^{(k)}| = \frac{1}{2}$ does not contribute to the logarithms of Gamma functions since this angle implies that two of the $\Omega\mathcal{R}\mathbb{Z}_2^{(l)}$ -invariant O6-planes are parallel and the other two perpendicular to the $D6_a$ -brane along $T_{(k)}^6$. This completes the proof for all T^6/\mathbb{Z}_{2N} orientifolds.

The remaining two cases $l \in \{1, 3\}$ for $T^6/\mathbb{Z}_2 \times \mathbb{Z}_{2M}$ orientifolds without and with discrete torsion are obtained from the $\Omega\mathcal{R}\mathbb{Z}_2^{(2)}$ case by permutation of the two-torus indices.

Angles of a D6 _a -brane with the $\Omega\mathcal{R}$ - and $\Omega\mathcal{R}\mathbb{Z}_2^{(2)}$ -invariant O6-planes			
	$(\vec{\phi}_{a,\Omega\mathcal{R}\mathbb{Z}_2^{(2)}})$	$\text{sgn}(\vec{\phi}_{a,\Omega\mathcal{R}\mathbb{Z}_2^{(2)}})$	$c_a^{\Omega\mathcal{R}\mathbb{Z}_2^{(2)}}$
$\text{sgn}(\phi_{a,\Omega\mathcal{R}}^{(1)}) = \text{sgn}(\phi_{a,\Omega\mathcal{R}}^{(3)})$ $ \phi_{a,\Omega\mathcal{R}}^{(n)} < \frac{1}{2}$ for all n $ \phi_{a,\Omega\mathcal{R}}^{(2)} > \frac{1}{2}$	$(\vec{\phi}_{a,\Omega\mathcal{R}}) + \text{sgn}(\phi_{a,\Omega\mathcal{R}}^{(2)}) \cdot (\frac{1}{2}, -1, \frac{1}{2})$ $ \phi_{a,\Omega\mathcal{R}\mathbb{Z}_2^{(2)}}^{(2)} > \frac{1}{2}$ $ \phi_{a,\Omega\mathcal{R}\mathbb{Z}_2^{(2)}}^{(n)} < \frac{1}{2}$ for all n	$-\text{sgn}(\vec{\phi}_{a,\Omega\mathcal{R}})$	1 -1
$\text{sgn}(\phi_{a,\Omega\mathcal{R}}^{(1)}) \neq \text{sgn}(\phi_{a,\Omega\mathcal{R}}^{(3)})$ $ \phi_{a,\Omega\mathcal{R}}^{(n)} < \frac{1}{2}$ for all n	$(\vec{\phi}_{a,\Omega\mathcal{R}}) + \text{sgn}(\phi_{a,\Omega\mathcal{R}}^{(3)}) \cdot (\frac{1}{2}, 0, -\frac{1}{2})$ $ \phi_{a,\Omega\mathcal{R}\mathbb{Z}_2^{(2)}}^{(n)} < \frac{1}{2}$ for all n	$(-\text{sgn}(\phi_{a,\Omega\mathcal{R}}^{(1)}), \text{sgn}(\phi_{a,\Omega\mathcal{R}}^{(2)}), -\text{sgn}(\phi_{a,\Omega\mathcal{R}}^{(3)}))$	-1
$ \phi_{a,\Omega\mathcal{R}}^{(3)} > \frac{1}{2}$		$(-\text{sgn}(\phi_{a,\Omega\mathcal{R}}^{(1)}), \text{sgn}(\phi_{a,\Omega\mathcal{R}}^{(2)}), \text{sgn}(\phi_{a,\Omega\mathcal{R}}^{(3)}))$	
$ \phi_{a,\Omega\mathcal{R}}^{(1)} > \frac{1}{2}$		$(\text{sgn}(\phi_{a,\Omega\mathcal{R}}^{(1)}), \text{sgn}(\phi_{a,\Omega\mathcal{R}}^{(2)}), -\text{sgn}(\phi_{a,\Omega\mathcal{R}}^{(3)}))$	

Table 32: Relation between angles $(\phi_{a,\Omega\mathcal{R}\mathbb{Z}_2^{(2)}}^{(n)})$ of a D6_a-brane with the $\Omega\mathcal{R}\mathbb{Z}_2^{(2)}$ invariant O6-plane and the angles $(\phi_{a,\Omega\mathcal{R}}^{(n)})$ of the same D6_a-brane with the $\Omega\mathcal{R}$ invariant O6-plane. The first column lists the five inequivalent shapes of the angles $(\phi_{a,\Omega\mathcal{R}}^{(n)})$, the explicit expressions for $(\phi_{a,\Omega\mathcal{R}\mathbb{Z}_2^{(2)}}^{(n)})$ in terms of shifts of the former angles are given in the second column with classification of the maximal angle, and their sign relative to the one of $(\phi_{a,\Omega\mathcal{R}}^{(n)})$ is given in the third column. The last column lists the sign factor $c_a^{\Omega\mathcal{R}\mathbb{Z}_2^{(2)}}$ that appears in the beta function coefficient.

B Tree level gauge couplings for various orbifolds

B.1 The T^6/\mathbb{Z}_4 and $T^6/\mathbb{Z}_2 \times \mathbb{Z}_4$ orientifolds

The geometry of the $T^6/(\mathbb{Z}_4 \times \Omega\mathcal{R})$ orientifold has been discussed in detail in [80], and the $T^6/(\mathbb{Z}_2 \times \mathbb{Z}_4 \times \Omega\mathcal{R})$ orientifolds with and without discrete torsion in [46], see also [7, 81]. A generic bulk three-cycle takes the form

$$\begin{aligned}
\Pi^{\text{bulk}} &= P \rho_1 + Q \rho_2 + U \rho_3 + V \rho_4, \\
\text{with } P &\equiv n^1 X, \quad Q \equiv m^1 Y, \quad U \equiv -m^1 X, \quad V \equiv n^1 Y, \\
\text{and } X &\equiv n^2 n^3 - m^2 m^3, \quad Y \equiv n^2 m^3 + m^2 n^3,
\end{aligned} \tag{115}$$

where the expansion in terms of one-cycle wrapping numbers (n^i, m^i) applies to the $T^6/\mathbb{Z}_2 \times \mathbb{Z}_4$ case and T^6/\mathbb{Z}_4 is obtained by permutation of two-torus indices, cf. table 1. The non-vanishing intersection numbers of the basic cycles ρ_i are given by

$$\rho_1 \circ \rho_3 = \rho_2 \circ \rho_4 = \begin{cases} -2 & T^6/\mathbb{Z}_4 \\ -4 & T^6/\mathbb{Z}_2 \times \mathbb{Z}_4 \end{cases}. \tag{116}$$

To shorten the notation for the untilted or tilted shape of the first two-torus, it is useful to introduce

$$\begin{aligned}\tilde{Q} &\equiv Q + bV, & \tilde{U} &\equiv U - bP \\ \tilde{\rho}_1 &\equiv \rho_1 + b\rho_3, & \tilde{\rho}_4 &\equiv \rho_4 - b\rho_2.\end{aligned}\tag{117}$$

Using the identity $P\tilde{Q} = -V\tilde{U}$, the $(\text{length})^2$ of a three-cycle can then be rewritten as

$$\begin{aligned}\prod_{i=1}^3 V_{aa}^{(i)} &= \frac{1}{r} (P^2 + V^2) + r (\tilde{U}^2 + \tilde{Q}^2) \\ &= c_{\text{lattice}} \times \left[\frac{1}{r} (\tilde{X}^0 - r\tilde{X}^1)^2 + r \left(\tilde{Y}^0 - \frac{1}{r}\tilde{Y}^1 \right)^2 \right] \\ &\stackrel{\text{SUSY}}{=} \left(\frac{\sqrt{c_{\text{lattice}}}}{\sqrt{r}} \tilde{X}^0 - \sqrt{c_{\text{lattice}}} \sqrt{r} \tilde{X}^1 \right)^2,\end{aligned}$$

where we introduced the lattice dependent constant factor

$$c_{\text{lattice}} = \begin{cases} 1 & \mathbf{a/bAA}, \mathbf{a/bBB} \\ 2 & \mathbf{a/bAB} \end{cases},$$

and r is the ratio of radii on the first two-torus. The decomposition of a bulk three-cycle in terms of orientifold even and odd components,

$$\Pi_a^{\text{bulk}} = \sum_{i=0}^1 \left(\tilde{X}_a^i \Pi_i^{\text{even}} + \tilde{Y}_a^i \Pi_i^{\text{odd}} \right),$$

depends on the choice of the compactification background as detailed in table 33. The on-trivial intersection numbers of the $\Omega\mathcal{R}$ even and odd cycles in table 33 are

$$\Pi_i^{\text{even}} \circ \Pi_j^{\text{odd}} = -\delta_{ij} c_{\text{lattice}} \times \begin{cases} 2 & T^6/\mathbb{Z}_4 \\ 4 & T^6/\mathbb{Z}_2 \times \mathbb{Z}_4 \end{cases},$$

and the supersymmetry constraints read

$$\tilde{X}_a^0 - r\tilde{X}_a^1 > 0, \quad \tilde{Y}_a^0 - \frac{1}{r}\tilde{Y}_a^1 = 0.$$

The exceptional three-cycles do not contribute to the tree level value of the gauge coupling. Details on their orientifold projections can be found in [80, 46].

$\Omega\mathcal{R}$ even & odd 3-cycles on T^6/\mathbb{Z}_4 & $T^6/\mathbb{Z}_2 \times \mathbb{Z}_4$			
lattice	a/bAA	a/bAB	a/bBB
Π_0^{even}	$\tilde{\rho}_1$	$\tilde{\rho}_1 + \tilde{\rho}_4$	$\tilde{\rho}_4$
Π_1^{even}	ρ_2	$\rho_2 + \rho_3$	ρ_3
Π_0^{odd}	ρ_3	$\rho_3 - \rho_2$	$-\rho_2$
Π_1^{odd}	$\tilde{\rho}_4$	$\tilde{\rho}_4 - \tilde{\rho}_1$	$-\tilde{\rho}_1$
\tilde{X}_a^0	P_a	$\frac{P_a + V_a}{2}$	V_a
\tilde{X}_a^1	\tilde{Q}_a	$\frac{\tilde{Q}_a + \tilde{U}_a}{2}$	\tilde{U}_a
\tilde{Y}_a^0	\tilde{U}_a	$\frac{\tilde{U}_a - \tilde{Q}_a}{2}$	$-\tilde{Q}_a$
\tilde{Y}_a^1	V_a	$\frac{V_a - P_a}{2}$	$-P_a$

Table 33: Orientifold even and odd bulk three-cycles and bulk wrapping numbers for the six inequivalent lattices of the $T^6/(\mathbb{Z}_4 \times \Omega\mathcal{R})$ and $T^6/(\mathbb{Z}_2 \times \mathbb{Z}_4 \times \Omega\mathcal{R})$ orientifolds.

B.2 The T^6/\mathbb{Z}'_6 and $T^6/\mathbb{Z}_2 \times \mathbb{Z}_6$ orientifolds

The geometry of the T^6/\mathbb{Z}'_6 and $T^6/\mathbb{Z}_2 \times \mathbb{Z}_6$ orientifolds is explained in detail in [41] and [46], respectively. We review here the basic steps for rewriting the tree level gauge coupling as linear function of the dilaton and complex structure modulus.

A bulk three-cycle can be written as

$$\Pi^{\text{bulk}} = P \rho_1 + Q \rho_2 + U \rho_3 + V \rho_4$$

with the bulk wrapping numbers in the notation of $T^6/\mathbb{Z}_2 \times \mathbb{Z}_6$ (the abbreviations X, Y in this equation should not be mixed with the $\Omega\mathcal{R}$ even and odd bulk cycle wrapping numbers \tilde{X}_a^i and \tilde{Y}_a^i)

$$P \equiv n^1 X, \quad Q \equiv n^1 Y, \quad U \equiv m^1 X, \quad V \equiv m^1 Y,$$

$$\text{with } X \equiv n^2 n^3 - m^2 m^3, \quad Y \equiv n^2 m^3 + m^2 n^3 + m^2 m^3.$$

In order to shorten the notation, we define

$$\tilde{U} \equiv U + b P, \quad \tilde{V} \equiv V + b Q,$$

$$\tilde{\rho}_1 \equiv \rho_1 - b \rho_3, \quad \tilde{\rho}_2 \equiv \rho_2 - b \rho_4,$$

and decompose a bulk three-cycle into its $\Omega\mathcal{R}$ even and odd parts,

$$\Pi_a^{\text{bulk}} = \sum_{i=0}^1 \left(\tilde{X}_a^i \Pi_i^{\text{even}} + \tilde{Y}_a^i \Pi_i^{\text{odd}} \right),$$

with the explicit form of the three-cycles and bulk wrapping numbers given in table 34. The non-trivial intersection numbers read

$$\Pi_0^{\text{even}} \circ \Pi_0^{\text{odd}} = -c_{\text{lattice}} \times \begin{cases} 4 \\ 8 \end{cases} \quad \Pi_1^{\text{even}} \circ \Pi_1^{\text{odd}} = -\frac{3}{c_{\text{lattice}}} \times \begin{cases} 4 & T^6/\mathbb{Z}'_6 \\ 8 & T^6/\mathbb{Z}_2 \times \mathbb{Z}_6 \end{cases},$$

and supersymmetry conditions on the bulk cycles take the form

$\Omega\mathcal{R}$ even & odd 3-cycles on T^6/\mathbb{Z}'_6 & $T^6/\mathbb{Z}_2 \times \mathbb{Z}_6$			
lattice	a/bAA	a/bAB	a/bBB
Π_0^{even}	$\tilde{\rho}_1$	$\tilde{\rho}_1 + \tilde{\rho}_2$	$\tilde{\rho}_2$
Π_1^{even}	$-\rho_3 + 2\rho_4$	$-\rho_3 + \rho_4$	$-2\rho_3 + \rho_4$
Π_0^{odd}	$-\rho_3$	$-\rho_3 - \rho_4$	$-\rho_4$
Π_1^{odd}	$-\tilde{\rho}_1 + 2\tilde{\rho}_2$	$-\tilde{\rho}_1 + \tilde{\rho}_2$	$-2\tilde{\rho}_1 + \tilde{\rho}_2$
\tilde{X}_a^0	$\frac{2P_a+Q_a}{2}$	$\frac{P_a+Q_a}{2}$	$\frac{P_a+2Q_a}{2}$
\tilde{X}_a^1	$\frac{\tilde{V}_a}{2}$	$\frac{\tilde{V}_a-\tilde{U}_a}{2}$	$-\frac{\tilde{U}_a}{2}$
\tilde{Y}_a^0	$-\frac{2\tilde{U}_a+\tilde{V}_a}{2}$	$-\frac{\tilde{U}_a+\tilde{V}_a}{2}$	$-\frac{\tilde{U}_a+2\tilde{V}_a}{2}$
\tilde{Y}_a^1	$\frac{Q_a}{2}$	$\frac{Q_a-P_a}{2}$	$-\frac{P_a}{2}$

Table 34: $\Omega\mathcal{R}$ even and odd bulk three-cycles and bulk wrapping numbers for the six inequivalent lattices of the $T^6/(\mathbb{Z}'_6 \times \Omega\mathcal{R})$ and $T^6/(\mathbb{Z}_2 \times \mathbb{Z}_6 \times \Omega\mathcal{R})$ orientifolds.

$$\tilde{Y}_a^0 - \frac{\sqrt{3}}{c_{\text{lattice}}} \frac{1}{r} \tilde{Y}_a^1 = 0, \quad \tilde{X}_a^0 - \frac{\sqrt{3}}{c_{\text{lattice}}} r \tilde{X}_a^1 > 0 \quad \text{with} \quad c_{\text{lattice}} = \begin{cases} 1 & \text{a/bAA, a/bBB} \\ 3 & \text{a/bAB} \end{cases},$$

with the complex structure $r \equiv \frac{R_2}{R_1}$ on the first two-torus.

Using the relation $\tilde{Y}_a^0 \tilde{Y}_a^1 = -\tilde{X}_a^0 \tilde{X}_a^1$, the (length)² of a supersymmetric cycle can be brought to the form

$$\begin{aligned} \prod_{i=1}^3 V_{aa}^{(i)} &= \frac{4}{3r} \left([P^2 + PQ + Q^2] + r^2 [\tilde{U}^2 + \tilde{U}\tilde{V} + \tilde{V}^2] \right) \\ &= \frac{4}{3r} c_{\text{lattice}} \times \left[\left(\tilde{X}_a^0 - \frac{\sqrt{3}}{c_{\text{lattice}}} r \tilde{X}_a^1 \right)^2 + r^2 \left(\tilde{Y}_a^0 - \frac{\sqrt{3}}{c_{\text{lattice}}} \frac{1}{r} \tilde{Y}_a^1 \right)^2 \right] \\ &\stackrel{\text{SUSY}}{=} \left(\frac{2\sqrt{c_{\text{lattice}}}}{\sqrt{3}\sqrt{r}} \tilde{X}_a^0 - \frac{2}{\sqrt{c_{\text{lattice}}}} \sqrt{r} \tilde{X}_a^1 \right)^2. \end{aligned}$$

Details on the orientifold even and odd exceptional three-cycles can be found in [41, 46].

B.3 The T^6/\mathbb{Z}_6 and $T^6/\mathbb{Z}_2 \times \mathbb{Z}'_6$ orientifolds

While the other types of orbifolds have one or three complex structure moduli inherited from the torus, the tree level gauge coupling on the T^6/\mathbb{Z}_6 and $T^6/\mathbb{Z}_2 \times \mathbb{Z}'_6$ orientifolds depends only on the dilaton since all complex structures are frozen by the underlying \mathbb{Z}_3 symmetry.

A generic bulk cycle can be written as [6, 46]

$$\Pi^{\text{bulk}} = X \rho_1 + Y \rho_2.$$

with the bulk three-cycles

$$X \equiv n^1 n^2 n^3 - m^1 m^2 m^3 - \sum_{i \neq j \neq k \neq i} n^i m^j m^k, \quad Y \equiv \sum_{i \neq j \neq k \neq i} (n^i n^j m^k + n^i m^j m^k).$$

The decomposition into $\Omega\mathcal{R}$ even and odd components,

$$\Pi^{\text{bulk}} = \tilde{X}_a^0 \Pi_0^{\text{even}} + \tilde{Y}_a^0 \Pi_0^{\text{odd}},$$

is detailed in table 35 with intersection number

$\Omega\mathcal{R}$ even & odd 3-cycles on T^6/\mathbb{Z}_6 & $T^6/\mathbb{Z}_2 \times \mathbb{Z}'_6$				
lattice	AAA	AAB	ABB	BBB
Π_0^{even}	ρ_1	$\rho_1 + \rho_2$	ρ_2	$-\rho_1 + 2\rho_2$
Π_0^{odd}	$\rho_1 - 2\rho_2$	$\rho_1 - \rho_2$	$2\rho_1 - \rho_2$	ρ_1
\tilde{X}_a^0	$X_a + \frac{Y_a}{2}$	$\frac{X_a + Y_a}{2}$	$\frac{X_a}{2} + Y_a$	$\frac{Y_a}{2}$
\tilde{Y}_a^0	$-\frac{Y_a}{2}$	$\frac{X_a - Y_a}{2}$	$\frac{X_a}{2}$	$X_a + \frac{Y_a}{2}$

Table 35: $\Omega\mathcal{R}$ even and odd bulk three-cycles and bulk wrapping numbers for the four inequivalent lattices of the $T^6/(\mathbb{Z}_6 \times \Omega\mathcal{R})$ and $T^6/(\mathbb{Z}_2 \times \mathbb{Z}'_6 \times \Omega\mathcal{R})$ orientifolds.

$$\Pi_0^{\text{even}} \circ \Pi_0^{\text{odd}} = \begin{cases} -4 & T^6/\mathbb{Z}_6 \\ -8 & T^6/\mathbb{Z}_2 \times \mathbb{Z}'_6 \end{cases}$$

for all four lattice orientations. The bulk supersymmetry conditions are simply given by

$$\tilde{X}_a^0 > 0, \quad \tilde{Y}_a^0 = 0,$$

and the $(\text{length})^2$ of a supersymmetric bulk cycle can be rewritten as follows

$$\begin{aligned}
\prod_{i=1}^3 V_{aa}^{(i)} &= \left(\frac{2}{\sqrt{3}} \right)^3 (X^2 + XY + Y^2) \\
&= \frac{8 c_{\text{lattice}}}{3^{3/2}} \left[(\tilde{X}_a^0)^2 + \frac{3}{c_{\text{lattice}}} (\tilde{Y}_a^0)^2 \right] \\
&\stackrel{\text{SUSY}}{=} \left(\frac{2^{3/2} \sqrt{c_{\text{lattice}}}}{3^{3/4}} \tilde{X}_a^0 \right)^2,
\end{aligned} \tag{118}$$

where we introduced the factor

$$c_{\text{lattice}} = \begin{cases} 1 & \mathbf{AAA}, \mathbf{ABB} \\ 3 & \mathbf{AAB}, \mathbf{BBB} \end{cases} \tag{119}$$

for the different lattice orientations. Details on the orientifold projection on exceptional three-cycles can be found in [6, 46].

C Details of the $T^6/\mathbb{Z}_2 \times \mathbb{Z}_2$ models with magnetised T-duals

In this appendix, we collect some technical facts, which are required for matching the magnetised D9- and D5-brane models on $T^6/(\mathbb{Z}_2 \times \mathbb{Z}_2 \times \Omega)$ without torsion in [1] with the intersecting D6-brane models on $T^6/(\mathbb{Z}_2 \times \mathbb{Z}_2 \times \Omega\mathcal{R})$ with discrete torsion in section 4. For all these examples, the background lattice is **aaa**, and discrete Wilson lines are not taken into account, i.e. $\tau_x^i = 0$ for all D6_x-branes.

The $\mathbb{Z}_2^{(k)}$ fixed point sets F_k^x along the four-torus $T_i^2 \times T_j^2$ depend only on the wrapping numbers $(n_x^i, m_x^i; n_x^j, m_x^j)$ being odd or even combined with the discrete displacements (σ_x^i, σ_x^j) as displayed in table 36, for more details see appendix A.1 of [40].

\mathbb{Z}_2 fixed points and wrapping numbers				
(n_x^i, m_x^i)	σ_x^i	(odd,odd)	(odd,even)	(even,odd)
$\alpha_i \in T_i^2$	0	$\begin{pmatrix} 1 \\ 3 \end{pmatrix}$	$\begin{pmatrix} 1 \\ 2 \end{pmatrix}$	$\begin{pmatrix} 1 \\ 4 \end{pmatrix}$
	1	$\begin{pmatrix} 2 \\ 4 \end{pmatrix}$	$\begin{pmatrix} 3 \\ 4 \end{pmatrix}$	$\begin{pmatrix} 2 \\ 3 \end{pmatrix}$

Table 36: The fixed point sets F_k^x depend on the properties of the torus wrapping numbers and discrete displacements. The fixed point sets $F_k^x \in T_i^2 \times T_j^2$ are obtained by tensoring $\alpha_i \beta_j$.

C.1 Example 1

The rigid three-cycles of the first example in section 4.1 with wrapping numbers listed in table 21 have the form

$$\begin{aligned}
\Pi_{a_i} &= \frac{1}{4} (\Pi_{135}^{\text{bulk}} - \Pi_{146}^{\text{bulk}} - \Pi_{236}^{\text{bulk}} - \Pi_{245}^{\text{bulk}}) + \frac{1}{4} (-\Pi_{246}^{\text{bulk}} + \Pi_{235}^{\text{bulk}} + \Pi_{145}^{\text{bulk}} - \Pi_{136}^{\text{bulk}}) \\
&\quad + \frac{(-1)^{\tau_{a_i}^{Z_2^{(1)}}}}{4} \sum_{\beta\gamma \in F_1^i} (\varepsilon_{\beta\gamma}^{(1)} + \tilde{\varepsilon}_{\beta\gamma}^{(1)}) + \frac{(-1)^{\tau_{a_i}^{Z_2^{(2)}}}}{4} \sum_{\alpha\gamma \in F_2^i} (\varepsilon_{\alpha\gamma}^{(2)} + \tilde{\varepsilon}_{\alpha\gamma}^{(2)}) + \frac{(-1)^{\tau_{a_i}^{Z_2^{(3)}}}}{4} \sum_{\alpha\beta \in F_3^i} (\varepsilon_{\alpha\beta}^{(3)} - \tilde{\varepsilon}_{\alpha\beta}^{(2)}), \\
\Pi'_{a_i} &= \frac{1}{4} (\Pi_{135}^{\text{bulk}} - \Pi_{146}^{\text{bulk}} - \Pi_{236}^{\text{bulk}} - \Pi_{245}^{\text{bulk}}) - \frac{1}{4} (-\Pi_{246}^{\text{bulk}} + \Pi_{235}^{\text{bulk}} + \Pi_{145}^{\text{bulk}} - \Pi_{136}^{\text{bulk}}) \\
&\quad + \frac{(-1)^{\tau_{a_i}^{Z_2^{(1)}}}}{4} \sum_{\beta\gamma \in F_1^i} (-\varepsilon_{\beta\gamma}^{(1)} + \tilde{\varepsilon}_{\beta\gamma}^{(1)}) + \frac{(-1)^{\tau_{a_i}^{Z_2^{(2)}}}}{4} \sum_{\alpha\gamma \in F_2^i} (-\varepsilon_{\alpha\gamma}^{(2)} + \tilde{\varepsilon}_{\alpha\gamma}^{(2)}) + \frac{(-1)^{\tau_{a_i}^{Z_2^{(3)}}}}{4} \sum_{\alpha\beta \in F_3^i} (\varepsilon_{\alpha\beta}^{(3)} + \tilde{\varepsilon}_{\alpha\beta}^{(2)}), \\
\Pi_{a_i} + \Pi'_{a_i} &= \frac{1}{2} (\Pi_{135}^{\text{bulk}} - \Pi_{146}^{\text{bulk}} - \Pi_{236}^{\text{bulk}} - \Pi_{245}^{\text{bulk}}) \\
&\quad + \frac{(-1)^{\tau_{a_i}^{Z_2^{(1)}}}}{2} \sum_{\beta\gamma \in F_1^i} \tilde{\varepsilon}_{\beta\gamma}^{(1)} + \frac{(-1)^{\tau_{a_i}^{Z_2^{(2)}}}}{2} \sum_{\alpha\gamma \in F_2^i} \tilde{\varepsilon}_{\alpha\gamma}^{(2)} + \frac{(-1)^{\tau_{a_i}^{Z_2^{(3)}}}}{2} \sum_{\alpha\beta \in F_3^i} \varepsilon_{\alpha\beta}^{(3)}.
\end{aligned} \tag{120}$$

The bulk RR tadpoles cancel for $N_{a_1} = \dots = N_{a_4} = 4$, and the exceptional RR tadpoles cancel among the four different kinds of D6 $_{a_i}$ -branes if they have identical displacements and Wilson lines $(\vec{\sigma}_{a_i a_j}) = (\vec{0}) = (\vec{\tau}_{a_i a_j})$. For $(\vec{\sigma})_{a_i} = 0$, each fixed point set is of the form $F_k^{a_i} = \{(11), (31), (13), (33)\}$.

Relative $\mathbb{Z}_2^{(i)}$ eigenvalues in examples 1 & 3							
$(-1)^{\tau_{xy}^{(k)}}$	$a_i a_j$	$a_i a'_j$	$a_i b_j$	$a_i c_j$	$b_i b_j$	$c_i c_j$	$b_i c_j$
$(+++)$	$a_i a_i$ $i = 1 \dots 4$	$a_1 a'_4,$ $a_2 a'_3$	$a_1 b_1, a_2 b_2,$ $a_3 b_3 \equiv a_3 b'_2, a_4 b_4 \equiv a_4 b'_1$	$a_1 c_1, a_2 c_2$ $a_3 c_3 \equiv a_3 c'_1, a_4 c_4 \equiv a_4 c'_2$	$b_i b_i$ $i = 1, 2$	$c_i c_i$ $i = 1, 2$	$b_i c_i$ $i = 1, 2$
$(+--)$	$a_1 a_2,$ $a_3 a_4$	$a_1 a'_3,$ $a_2 a'_4$	$a_1 b_2, a_2 b_1$ $a_3 b_4 \equiv a_3 b'_1, a_4 b_3 \equiv a_4 b'_2$	$a_1 c_2, a_2 c_1$ $a_3 c_4 \equiv a_3 c'_2, a_4 c_3 \equiv a_4 c'_1$	$b_1 b_2$	$c_1 c_2$	$b_1 c_2, b_2 c_1$
$(-+-)$	$a_1 a_3,$ $a_2 a_4$	$a_1 a'_2,$ $a_3 a'_4$	$a_1 b_3 \equiv a_1 b'_2, a_2 b_4 \equiv a_2 b'_1$ $a_3 b_1, a_4 b_2$	$a_1 c_3 \equiv a_1 c'_1, a_2 c_4 \equiv a_2 c'_2$ $a_3 c_1, a_4 c_2$	$b_1 b'_2$	$c_i c'_i$	$b_1 c'_1, b_2 c'_2$
$(--+)$	$a_1 a_4,$ $a_2 a_3$	$a_i a'_i$	$a_1 b_4 \equiv a_1 b'_1, a_2 b_3 \equiv a_2 b'_2$ $a_3 b_2, a_4 b_1$	$a_1 c_4 \equiv a_1 c'_2, a_2 c_3 \equiv a_2 c'_1$ $a_3 c_2, a_4 c_1$	$b_i b'_i$	$c_1 c'_2$	$b_1 c'_2, b_2 c'_1$

Table 37: The first three columns contain the relative $\mathbb{Z}_2^{(i)}$ eigenvalues of the first example in [1]. These are the same signs as for the $D6_{a_i}$ -branes in the third example, for which also the $D6_{b_i}$ - and $D6_{c_i}$ -branes are listed in the remaining columns.

Intersection numbers for example 1				
xy	I_{xy}	$I_{xy}^{\mathbb{Z}_2^{(1)}}$	$I_{xy}^{\mathbb{Z}_2^{(2)}}$	$I_{xy}^{\mathbb{Z}_2^{(3)}}$
$a_i a'_j$	$(-2) \cdot (-2) \cdot 2$	$(-1)^{\tau_{a_i a'_j}^{\mathbb{Z}_2^{(1)}}} \cdot (-2) \cdot 4$	$(-1)^{\tau_{a_i a'_j}^{\mathbb{Z}_2^{(2)}}} \cdot (-2) \cdot 4$	$(-1)^{\tau_{a_i a'_j}^{\mathbb{Z}_2^{(3)}}} \cdot 2 \cdot 4$
x	$\eta_{\Omega \mathcal{R}} \tilde{I}_x^{\Omega \mathcal{R}}$	$\eta_{\Omega \mathcal{R} \mathbb{Z}_2^{(1)}} \tilde{I}_x^{\Omega \mathcal{R} \mathbb{Z}_2^{(1)}}$	$\eta_{\Omega \mathcal{R} \mathbb{Z}_2^{(2)}} \tilde{I}_x^{\Omega \mathcal{R} \mathbb{Z}_2^{(2)}}$	$\eta_{\Omega \mathcal{R} \mathbb{Z}_2^{(3)}} \tilde{I}_x^{\Omega \mathcal{R} \mathbb{Z}_2^{(3)}}$
a_i	$8 \times (-1) \cdot (-1) \cdot 1$	$8 \times (-1) \cdot 1 \cdot (-1)$	$8 \times 1 \cdot (-1) \cdot (-1)$	$-8 \times 1 \cdot (-1) \cdot 1$

Table 38: The torus and $\mathbb{Z}_2^{(i)}$ invariant intersection numbers of example 1 in section 4.1. The net-chiralities can be seen to match with those given in the main text by remembering that the orientifold projection changes the $\mathbb{Z}_2^{(1)}$ and $\mathbb{Z}_2^{(2)}$ eigenvalues while leaving $\mathbb{Z}_2^{(3)}$ invariant, $(\tau_{a'_j}^{\mathbb{Z}_2^{(1)}}, \tau_{a'_j}^{\mathbb{Z}_2^{(2)}}, \tau_{a'_j}^{\mathbb{Z}_2^{(3)}}) = (\tau_{a_j}^{\mathbb{Z}_2^{(1)}} + 1, \tau_{a_j}^{\mathbb{Z}_2^{(2)}} + 1, \tau_{a_j}^{\mathbb{Z}_2^{(3)}})$.

C.2 Example 3

The rigid D6-branes in section 4.2 with wrapping numbers listed in table 25 wrap the following three-cycles,

$$\begin{aligned}
\Pi_{a_i} &= \frac{1}{4} (\Pi_{135}^{\text{bulk}} - \Pi_{146}^{\text{bulk}} - 2 \Pi_{236}^{\text{bulk}} + 2 \Pi_{245}^{\text{bulk}}) + \frac{1}{4} (-2 \Pi_{246}^{\text{bulk}} + 2 \Pi_{235}^{\text{bulk}} + \Pi_{145}^{\text{bulk}} - \Pi_{136}^{\text{bulk}}) \\
&\quad + \frac{(-1)^{\tau_{a_i}^{z_2^{(1)}}}}{4} \sum_{\beta\gamma \in F_1^{a_i}} \left(\varepsilon_{\beta\gamma}^{(1)} + 2 \tilde{\varepsilon}_{\beta\gamma}^{(1)} \right) + \frac{(-1)^{\tau_{a_i}^{z_2^{(2)}}}}{4} \sum_{\alpha\gamma \in F_2^{a_i}} \left(\varepsilon_{\alpha\gamma}^{(2)} + \tilde{\varepsilon}_{\alpha\gamma}^{(2)} \right) + \frac{(-1)^{\tau_{a_i}^{z_2^{(3)}}}}{4} \sum_{\alpha\beta \in F_3^{a_i}} \left(\varepsilon_{\alpha\beta}^{(3)} - \tilde{\varepsilon}_{\alpha\beta}^{(3)} \right), \\
\Pi_{b_i} &= \frac{1}{4} \Pi_{135}^{\text{bulk}} + \frac{(-1)^{\tau_{b_i}^{z_2^{(1)}}}}{4} \sum_{\beta\gamma \in F_1^{b_i}} \varepsilon_{\beta\gamma}^{(1)} + \frac{(-1)^{\tau_{b_i}^{z_2^{(2)}}}}{4} \sum_{\alpha\gamma \in F_2^{b_i}} \varepsilon_{\alpha\gamma}^{(2)} + \frac{(-1)^{\tau_{b_i}^{z_2^{(3)}}}}{4} \sum_{\alpha\beta \in F_3^{b_i}} \varepsilon_{\alpha\beta}^{(3)}, \\
\Pi_{c_i} &= -\frac{1}{4} \Pi_{146}^{\text{bulk}} + \frac{(-1)^{\tau_{c_i}^{z_2^{(1)}}}}{4} \sum_{\beta\gamma \in F_1^{c_i}} \varepsilon_{\beta\gamma}^{(1)} + \frac{(-1)^{\tau_{c_i}^{z_2^{(2)}}}}{4} \sum_{\alpha\gamma \in F_2^{c_i}} \tilde{\varepsilon}_{\alpha\gamma}^{(2)} - \frac{(-1)^{\tau_{c_i}^{z_2^{(3)}}}}{4} \sum_{\alpha\beta \in F_3^{c_i}} \tilde{\varepsilon}_{\alpha\beta}^{(3)},
\end{aligned} \tag{121}$$

and their orientifold image three-cycles are given by

$$\begin{aligned}
\Pi_{a'_i} &= \frac{1}{4} (\Pi_{135}^{\text{bulk}} - \Pi_{146}^{\text{bulk}} - 2 \Pi_{236}^{\text{bulk}} + 2 \Pi_{245}^{\text{bulk}}) - \frac{1}{4} (-2 \Pi_{246}^{\text{bulk}} + 2 \Pi_{235}^{\text{bulk}} + \Pi_{145}^{\text{bulk}} - \Pi_{136}^{\text{bulk}}) \\
&\quad + \frac{(-1)^{\tau_{a'_i}^{z_2^{(1)}}}}{4} \sum_{\beta\gamma \in F_1^{a'_i}} \left(-\varepsilon_{\beta\gamma}^{(1)} + 2 \tilde{\varepsilon}_{\beta\gamma}^{(1)} \right) + \frac{(-1)^{\tau_{a'_i}^{z_2^{(2)}}}}{4} \sum_{\alpha\gamma \in F_2^{a'_i}} \left(-\varepsilon_{\alpha\gamma}^{(2)} + \tilde{\varepsilon}_{\alpha\gamma}^{(2)} \right) + \frac{(-1)^{\tau_{a'_i}^{z_2^{(3)}}}}{4} \sum_{\alpha\beta \in F_3^{a'_i}} \left(\varepsilon_{\alpha\beta}^{(3)} + \tilde{\varepsilon}_{\alpha\beta}^{(3)} \right), \\
\Pi_{b'_i} &= \frac{1}{4} \Pi_{135}^{\text{bulk}} - \frac{(-1)^{\tau_{b'_i}^{z_2^{(1)}}}}{4} \sum_{\beta\gamma \in F_1^{b'_i}} \varepsilon_{\beta\gamma}^{(1)} - \frac{(-1)^{\tau_{b'_i}^{z_2^{(2)}}}}{4} \sum_{\alpha\gamma \in F_2^{b'_i}} \varepsilon_{\alpha\gamma}^{(2)} + \frac{(-1)^{\tau_{b'_i}^{z_2^{(3)}}}}{4} \sum_{\alpha\beta \in F_3^{b'_i}} \varepsilon_{\alpha\beta}^{(3)}, \\
\Pi_{c'_i} &= -\frac{1}{4} \Pi_{146}^{\text{bulk}} - \frac{(-1)^{\tau_{c'_i}^{z_2^{(1)}}}}{4} \sum_{\beta\gamma \in F_1^{c'_i}} \varepsilon_{\beta\gamma}^{(1)} + \frac{(-1)^{\tau_{c'_i}^{z_2^{(2)}}}}{4} \sum_{\alpha\gamma \in F_2^{c'_i}} \tilde{\varepsilon}_{\alpha\gamma}^{(2)} + \frac{(-1)^{\tau_{c'_i}^{z_2^{(3)}}}}{4} \sum_{\alpha\beta \in F_3^{c'_i}} \tilde{\varepsilon}_{\alpha\beta}^{(3)},
\end{aligned} \tag{122}$$

where the orientifold transformation of exceptional cycles (98) was used.

Constraints on the consistent sets of discrete choices of displacements ($\vec{\sigma}$) can be derived

from the RR tadpole contributions of the individual three-cycles,

$$\begin{aligned}
\Pi_{a_i} + \Pi'_{a_i} &= \frac{1}{2} (\Pi_{135}^{\text{bulk}} - \Pi_{146}^{\text{bulk}} - 2\Pi_{236}^{\text{bulk}} + 2\Pi_{245}^{\text{bulk}}) \\
&\quad + (-1)^{\tau_{a_i}^{(1)}} \sum_{\beta\gamma \in F_1^{a_i}} \tilde{\varepsilon}_{\beta\gamma}^{(1)} + \frac{(-1)^{\tau_{a_i}^{(2)}}}{2} \sum_{\beta\gamma \in F_2^{a_i}} \tilde{\varepsilon}_{\beta\gamma}^{(2)} + \frac{(-1)^{\tau_{a_i}^{(3)}}}{2} \sum_{\alpha\beta \in F_3^{a_i}} \varepsilon_{\alpha\beta}^{(3)}, \\
\Pi_{b_i} + \Pi'_{b_i} &= \frac{1}{2} \Pi_{135}^{\text{bulk}} + \frac{(-1)^{\tau_{b_i}^{(3)}}}{2} \sum_{\alpha\beta \in F_3^{b_i}} \varepsilon_{\alpha\beta}^{(3)}, \\
\Pi_{c_i} + \Pi'_{c_i} &= -\frac{1}{4} \Pi_{146}^{\text{bulk}} + \frac{(-1)^{\tau_{c_i}^{(2)}}}{2} \sum_{\alpha\gamma \in F_2^{c_i}} \tilde{\varepsilon}_{\alpha\gamma}^{(2)}.
\end{aligned} \tag{123}$$

The consistent match to the third example in [1] is obtained by combining considerations on the cancellation of exceptional RR tadpoles and matching of the $a_i a_j$ and $a_i a'_j$ sectors of the matter spectrum as follows:

- Only the a_i branes contribute to the $\mathbb{Z}_2^{(1)}$ twisted RR tadpoles. This does not constrain the displacements $\sigma_{a_i}^1$ along the first two-torus $T_{(1)}^2$, but the fixed point sets $F_1^{a_i}$ and thus the displacements $(\sigma_{a_i}^2, \sigma_{a_i}^3)$ have to be pairwise identical among two different a_i -branes with opposite $\mathbb{Z}_2^{(1)}$ eigenvalue in order to achieve cancellation of the exceptional RR tadpole at each $\mathbb{Z}_2^{(1)}$ fixed point. Setting $(\vec{\sigma}_{a_i}) = (\vec{0})$ for all a_i branes leads to a matching of all $a_i a_j$ and $a_i a'_j$ sectors with [1] when including the corrections to the latter in table 2 of [67].
- The a_i branes have now been arranged in such a way that their exceptional $\mathbb{Z}_2^{(2)}$ and $\mathbb{Z}_2^{(3)}$ twisted RR tadpole contributions cancel. Therefore, also the $\mathbb{Z}_2^{(2)}$ twisted RR tadpole has to cancel among the c_i -branes and the $\mathbb{Z}_2^{(3)}$ twisted RR tadpole among the b_i -branes. This can only be achieved if the corresponding relative $\mathbb{Z}_2^{(k)}$ eigenvalue among each pair of branes is $(-)$ and the relative displacements are constrained to $(0, \sigma_{c_1 c_2}^2, 0)$ and $(0, 0, \sigma_{b_1 b_2}^3)$.
- The multiplicities in the $a_i b_j, a_i b'_j, a_i c_j$ and $a_i c'_j$ sectors are matched with [1] (up to the fact that the $\mathbf{4}$ and $\overline{\mathbf{4}}$ representations of $U(4)_{b_j}$ and $U(4)_{c_j}$ have to be distinguished) by setting $\sigma_{b_j}^1 = 0 = \sigma_{c_j}^1$. The above choice of all σ_x^i values implies that the overall amount of states with some a_i charge fits, and all $U(2)_{a_i}^3$ anomalies cancel.

- The multiplicities in the $b_i c_j$ and $b_i c'_j$ sectors match with [1] for $\sigma_{b_i}^1 = \sigma_{c_j}^1$ up to the issue of complex notations $\mathbf{4}$ and $\overline{\mathbf{4}}$ such that all $U(4)_{b_i}^3$ and $U(4)_{c_j}^3$ anomalies cancel.
- The $b_i b'_i$ and $c_i c'_i$ sectors provide each a non-chiral pair of antisymmetric representations of $U(4)_{x_i}$ which reduces to the one antisymmetric of $Sp(4)_{x_i}$ listed in [1]. Finally, for vanishing relative displacements $\sigma_{b_1}^3 = \sigma_{b_2}^3 = 0$ and $\sigma_{c_1}^2 = \sigma_{c_2}^2 = 0$ the $b_1 b_2$, $b_1 b'_2$, $c_1 c_2$ and $c_1 c'_2$ sectors provide also twice the amount of non-chiral bifundamental matter transforming under the unitary gauge factors compared to the matter in [1] transforming under the symplectic subgroups. This confirms the breaking pattern of the gauge symmetry discussed in section 4.2.

In summary, the assignments in table 25 provide the best match with [1], which gives full agreement in the $a_i a_j$ and $a_i a'_j$ sectors, and the differences involving branes b_i and c_i arise from the partial brane recombination discussed in section 4.2 and the associated breaking of unitary to symplectic subgroups.

The fixed point sets for the displacements ($\vec{\sigma}$) given in table 25 can be read off from the assignment per two-torus in table 36 to be $F_1^{a_i} = \{(11), (31), (13), (33)\}$ for all $D6_{a_i}$ -branes with $i = 1 \dots 4$ and $F_2^{a_i} = \{(11), (21), (13), (23)\} = F_3^{a_i}$. For the $D6_{b_i}$ -branes, all three fixed point sets are of the form $F_k^{b_i} = \{(11), (21), (12), (22)\}$ with $k = 1, 2, 3$. Finally, for the $D6_{c_i}$ -branes, the fixed point sets are given by $F_1^{c_i} = \{(11), (41), (14), (44)\}$ and $F_2^{c_i} = \{(11), (21), (14), (24)\} = F_3^{c_i}$.

The torus and $\mathbb{Z}_2^{(k)}$ invariant intersection numbers for all D6-branes in example 3 are listed in table 39.

Intersection numbers for example 3				
xy	I_{xy}	$I_{xy}^{\mathbb{Z}_2^{(1)}}$	$I_{xy}^{\mathbb{Z}_2^{(2)}}$	$I_{xy}^{\mathbb{Z}_2^{(3)}}$
$a_i a'_j$	$(-4) \cdot (-2) \cdot 2$	$(-1)^{\tau_{a_i a'_j}^{\mathbb{Z}_2^{(1)}}} \cdot (-4) \cdot (4 \delta_{(\sigma^2 + \sigma^3)_{a_i a_j}, 0})$	$(-1)^{\tau_{a_i a'_j}^{\mathbb{Z}_2^{(2)}}} \cdot (-2) \cdot (4 \delta_{(\sigma^1 + \sigma^3)_{a_i a_j}, 0})$	$(-1)^{\tau_{a_i a'_j}^{\mathbb{Z}_2^{(3)}}} \cdot 2 \cdot (4 \delta_{(\sigma^1 + \sigma^2)_{a_i a_j}, 0})$
$a_i b_j$	$(-2) \cdot (-1) \cdot 1$	$(-1)^{\tau_{a_i b_j}^{\mathbb{Z}_2^{(1)}}} \cdot (-2) \cdot 1$	$(-1)^{\tau_{a_i b_j}^{\mathbb{Z}_2^{(2)}}} \cdot (-1) \cdot (2 \delta_{\sigma^1_{a_i b_j}, 0})$	$(-1)^{\tau_{a_i b_j}^{\mathbb{Z}_2^{(3)}}} \cdot 1 \cdot (2 \delta_{\sigma^1_{a_i b_j}, 0})$
$a_i c_j$	$(-2) \cdot 1 \cdot (-1)$	$(-1)^{\tau_{a_i c_j}^{\mathbb{Z}_2^{(1)}}} \cdot (-2) \cdot 1$	$(-1)^{\tau_{a_i c_j}^{\mathbb{Z}_2^{(2)}}} \cdot 1 \cdot (2 \delta_{\sigma^1_{a_i c_j}, 0})$	$(-1)^{\tau_{a_i c_j}^{\mathbb{Z}_2^{(3)}}} \cdot (-1) \cdot (2 \delta_{\sigma^1_{a_i c_j}, 0})$
$b_i c_j$	$0_{\uparrow\uparrow} \cdot 1 \cdot (-1)$	$(-1)^{\tau_{b_i c_j}^{\mathbb{Z}_2^{(1)}}} \cdot 0_{\uparrow\uparrow} \cdot \delta_{(\sigma^2 + \sigma^3)_{b_i c_j}, 0}$	$(-1)^{\tau_{b_i c_j}^{\mathbb{Z}_2^{(2)}}} \cdot 1 \cdot (2 \delta_{(\sigma^1 + \sigma^3)_{b_i c_j}, 0})$	$(-1)^{\tau_{b_i c_j}^{\mathbb{Z}_2^{(3)}}} \cdot (-1) \cdot (2 \delta_{(\sigma^1 + \sigma^2)_{b_i c_j}, 0})$
x	$\eta_{\Omega\mathcal{R}} \tilde{I}_x^{\Omega\mathcal{R}}$	$\eta_{\Omega\mathcal{R}\mathbb{Z}_2^{(1)}} \tilde{I}_x^{\Omega\mathcal{R}\mathbb{Z}_2^{(1)}}$	$\eta_{\Omega\mathcal{R}\mathbb{Z}_2^{(2)}} \tilde{I}_x^{\Omega\mathcal{R}\mathbb{Z}_2^{(2)}}$	$\eta_{\Omega\mathcal{R}\mathbb{Z}_2^{(3)}} \tilde{I}_x^{\Omega\mathcal{R}\mathbb{Z}_2^{(3)}}$
a_i	$8 \times (-2) \cdot (-1) \cdot 1$	$8 \times (-2) \cdot 1 \cdot (-1)$	$8 \times 1 \cdot (-1) \cdot (-1)$	$-8 \times 1 \cdot (-1) \cdot 1$
b_i	$8 \times 0_{\uparrow\uparrow}^{123}$	$8 \times 0_{\uparrow\uparrow} \cdot 1 \cdot (-1)$	$8 \times 1 \cdot 0_{\uparrow\uparrow} \cdot (-1)$	$-8 \times 1 \cdot (-1) \cdot 0_{\uparrow\uparrow}$
c_i	$8 \times 0_{\uparrow\uparrow} \cdot (-1) \cdot 1$	8×0^{123}	$8 \times 1 \cdot (-1) \cdot 0_{\uparrow\uparrow}$	$-8 \times 1 \cdot 0_{\uparrow\downarrow} \cdot 1$

Table 39: The torus and $\mathbb{Z}_2^{(i)}$ invariant intersection numbers for example 3 in section 4.2 match with the net-chiralities given in the main text when taking into account that $(\tau_{a'_j}^{\mathbb{Z}_2^{(1)}}, \tau_{a'_j}^{\mathbb{Z}_2^{(2)}}, \tau_{a'_j}^{\mathbb{Z}_2^{(3)}}) = (\tau_{a_j}^{\mathbb{Z}_2^{(1)}} + 1, \tau_{a_j}^{\mathbb{Z}_2^{(2)}} + 1, \tau_{a_j}^{\mathbb{Z}_2^{(3)}})$ for the orientifold image D6-branes a_j and a'_j .

References

- [1] C. Angelantonj, C. Condeescu, E. Dudas, and M. Lennek, “Stringy Instanton Effects in Models with Rigid Magnetised D-branes,” *Nucl. Phys.*, vol. B818, pp. 52–94, 2009.
- [2] F. Gmeiner and G. Honecker, “Millions of Standard Models on \mathbb{Z}'_6 ,” *JHEP*, vol. 07, p. 052, 2008.
- [3] M. Cvetič, G. Shiu, and A. M. Uranga, “Three-family supersymmetric standard like models from intersecting brane worlds,” *Phys. Rev. Lett.*, vol. 87, p. 201801, 2001.
- [4] M. Cvetič, G. Shiu, and A. M. Uranga, “Chiral four-dimensional $N = 1$ supersymmetric type IIA orientifolds from intersecting D6-branes,” *Nucl. Phys.*, vol. B615, pp. 3–32, 2001.
- [5] G. Honecker, “Chiral supersymmetric models on an orientifold of $\mathbb{Z}_4 \times \mathbb{Z}_2$ with intersecting D6-branes,” *Nucl. Phys.*, vol. B666, pp. 175–196, 2003.
- [6] G. Honecker and T. Ott, “Getting just the supersymmetric standard model at intersecting branes on the \mathbb{Z}_6 -orientifold,” *Phys. Rev.*, vol. D70, p. 126010, 2004.
- [7] G. Honecker, “Chiral $N = 1$ 4D orientifolds with D-branes at angles,” *Mod. Phys. Lett.*, vol. A19, pp. 1863–1879, 2004.
- [8] F. Gmeiner, R. Blumenhagen, G. Honecker, D. Lüst, and T. Weigand, “One in a billion: MSSM-like D-brane statistics,” *JHEP*, vol. 01, p. 004, 2006.
- [9] A. M. Uranga, “Chiral four-dimensional string compactifications with intersecting D-branes,” *Class. Quant. Grav.*, vol. 20, pp. S373–S394, 2003.
- [10] R. Blumenhagen, M. Cvetič, P. Langacker, and G. Shiu, “Toward realistic intersecting D-brane models,” *Ann. Rev. Nucl. Part. Sci.*, vol. 55, pp. 71–139, 2005.
- [11] R. Blumenhagen, B. Körs, D. Lüst, and S. Stieberger, “Four-dimensional String Compactifications with D-Branes, Orientifolds and Fluxes,” *Phys. Rept.*, vol. 445, pp. 1–193, 2007.
- [12] E. Dudas, “*Orientifolds and model building*,” *J. Phys. Conf. Ser.*, vol. 53, pp. 567–600, 2006.
- [13] F. Marchesano, “*Progress in D-brane model building*,” *Fortsch. Phys.*, vol. 55, pp. 491–518, 2007.
- [14] D. Lüst, “*String Landscape and the Standard Model of Particle Physics*,” 2007.

- [15] W. Buchmüller, K. Hamaguchi, O. Lebedev, and M. Ratz, “Supersymmetric standard model from the heterotic string,” *Phys. Rev. Lett.*, vol. 96, p. 121602, 2006.
- [16] O. Lebedev *et al.*, “A mini-landscape of exact MSSM spectra in heterotic orbifolds,” *Phys. Lett.*, vol. B645, pp. 88–94, 2007.
- [17] W. Buchmüller, K. Hamaguchi, O. Lebedev, and M. Ratz, “Supersymmetric standard model from the heterotic string. II,” *Nucl. Phys.*, vol. B785, pp. 149–209, 2007.
- [18] O. Lebedev, H. P. Nilles, S. Ramos-Sanchez, M. Ratz, and P. K. S. Vaudrevange, “Heterotic mini-landscape (II): completing the search for MSSM vacua in a \mathbb{Z}_6 orbifold,” *Phys. Lett.*, vol. B668, pp. 331–335, 2008.
- [19] V. Braun, Y.-H. He, B. A. Ovrut, and T. Pantev, “The exact MSSM spectrum from string theory,” *JHEP*, vol. 05, p. 043, 2006.
- [20] V. Bouchard and R. Donagi, “An $SU(5)$ heterotic standard model,” *Phys. Lett.*, vol. B633, pp. 783–791, 2006.
- [21] R. Blumenhagen, G. Honecker, and T. Weigand, “Loop-corrected compactifications of the heterotic string with line bundles,” *JHEP*, vol. 06, p. 020, 2005.
- [22] R. Blumenhagen, G. Honecker, and T. Weigand, “Supersymmetric (non-)Abelian bundles in the Type I and $SO(32)$ heterotic string,” *JHEP*, vol. 0508, p. 009, 2005.
- [23] R. Blumenhagen, G. Honecker, and T. Weigand, “Non-Abelian brane worlds: The Heterotic string story,” *JHEP*, vol. 0510, p. 086, 2005.
- [24] R. Blumenhagen, S. Moster, and T. Weigand, “Heterotic GUT and standard model vacua from simply connected Calabi-Yau manifolds,” *Nucl. Phys.*, vol. B751, pp. 186–221, 2006.
- [25] T. Weigand, “Lectures on F-theory compactifications and model building,” *Class. Quant. Grav.*, vol. 27, p. 214004, 2010.
- [26] T. P. T. Dijkstra, L. R. Huiszoon, and A. N. Schellekens, “Chiral supersymmetric standard model spectra from orientifolds of Gepner models,” *Phys. Lett.*, vol. B609, pp. 408–417, 2005.
- [27] T. P. T. Dijkstra, L. R. Huiszoon, and A. N. Schellekens, “Supersymmetric Standard Model Spectra from RCFT orientifolds,” *Nucl. Phys.*, vol. B710, pp. 3–57, 2005.
- [28] G. Aldazabal, S. Franco, L. E. Ibanez, R. Rabadan, and A. Uranga, “Intersecting brane worlds,” *JHEP*, vol. 0102, p. 047, 2001.

- [29] P. G. Camara, L. E. Ibanez, and F. Marchesano, “RR photons,” 2011.
- [30] T. W. Grimm and D. V. Lopes, “The N=1 effective actions of D-branes in Type IIA and IIB orientifolds,” 2011.
- [31] M. Kerstan and T. Weigand, “The Effective action of D6-branes in N=1 type IIA orientifolds,” *JHEP*, vol. 1106, p. 105, 2011.
- [32] J. Derendinger, S. Ferrara, C. Kounnas, and F. Zwirner, “On loop corrections to string effective field theories: Field dependent gauge couplings and sigma model anomalies,” *Nucl.Phys.*, vol. B372, pp. 145–188, 1992. Revised version.
- [33] V. Kaplunovsky and J. Louis, “On Gauge couplings in string theory,” *Nucl.Phys.*, vol. B444, pp. 191–244, 1995.
- [34] C. Angelantonj and A. Sagnotti, “Open strings,” *Phys. Rept.*, vol. 371, pp. 1–150, 2002.
- [35] I. Antoniadis, C. Bachas, and E. Dudas, “Gauge couplings in four-dimensional type I string orbifolds,” *Nucl.Phys.*, vol. B560, pp. 93–134, 1999.
- [36] M. Billo *et al.*, “Instantons in N=2 magnetized D-brane worlds,” *JHEP*, vol. 10, p. 091, 2007.
- [37] M. Billo *et al.*, “Instanton effects in N=1 brane models and the Kahler metric of twisted matter,” *JHEP*, vol. 12, p. 051, 2007.
- [38] J. P. Conlon, “Gauge Threshold Corrections for Local String Models,” *JHEP*, vol. 04, p. 059, 2009.
- [39] J. P. Conlon and E. Palti, “Gauge Threshold Corrections for Local Orientifolds,” *JHEP*, vol. 09, p. 019, 2009.
- [40] F. Gmeiner and G. Honecker, “Complete Gauge Threshold Corrections for Intersecting Fractional D6-Branes: The \mathbb{Z}_6 and \mathbb{Z}'_6 Standard Models,” *Nucl. Phys.*, vol. B829, pp. 225–297, 2010.
- [41] F. Gmeiner and G. Honecker, “Mapping an Island in the Landscape,” *JHEP*, vol. 09, p. 128, 2007.
- [42] F. Gmeiner, D. Lüst, and M. Stein, “Statistics of intersecting D-brane models on T^6/\mathbb{Z}_6 ,” *JHEP*, vol. 05, p. 018, 2007.
- [43] D. Lüst and S. Stieberger, “Gauge threshold corrections in intersecting brane world models,” *Fortsch. Phys.*, vol. 55, pp. 427–465, 2007.

- [44] N. Akerblom, R. Blumenhagen, D. Lüst, and M. Schmidt-Sommerfeld, “Thresholds for intersecting D-branes revisited,” *Phys. Lett.*, vol. B652, pp. 53–59, 2007.
- [45] R. Blumenhagen and M. Schmidt-Sommerfeld, “Gauge Thresholds and Kähler Metrics for Rigid Intersecting D-brane Models,” *JHEP*, vol. 12, p. 072, 2007.
- [46] S. Förste and G. Honecker, “Rigid D6-branes on $T^6/[\mathbb{Z}_2 \times \mathbb{Z}_{2M} \times \Omega\mathcal{R}]$ with discrete torsion,” *JHEP*, vol. 01, p. 091, 2011.
- [47] S. Förste, G. Honecker, and R. Schreyer, “Supersymmetric $\mathbb{Z}_N \times \mathbb{Z}_M$ orientifolds in 4D with D-branes at angles,” *Nucl. Phys.*, vol. B593, pp. 127–154, 2001.
- [48] G. Honecker, “Supersymmetric intersecting D6-branes and chiral models on the $T^6/(\mathbb{Z}_4 \times \mathbb{Z}_2)$ orbifold,” 2003.
- [49] R. Blumenhagen, M. Cvetič, F. Marchesano, and G. Shiu, “Chiral D-brane models with frozen open string moduli,” *JHEP*, vol. 03, p. 050, 2005.
- [50] S. Förste, C. Timirgaziu, and I. Zavala, “Orientifold’s Landscape: Non-Factorisable Six-Tori,” *JHEP*, vol. 10, p. 025, 2007.
- [51] S. Förste and I. Zavala, “Oddness from Rigidness,” *JHEP*, vol. 07, p. 086, 2008.
- [52] R. Blumenhagen, L. Görlich, and B. Körs, “Supersymmetric 4D orientifolds of type IIA with D6-branes at angles,” *JHEP*, vol. 01, p. 040, 2000.
- [53] G. Honecker and J. Vanhoof, “to appear,”
- [54] D. Cremades, L. E. Ibáñez, and F. Marchesano, “Yukawa couplings in intersecting D-brane models,” *JHEP*, vol. 07, p. 038, 2003.
- [55] D. Cremades, L. E. Ibáñez, and F. Marchesano, “Computing Yukawa couplings from magnetized extra dimensions,” *JHEP*, vol. 05, p. 079, 2004.
- [56] D. M. Ghilencea, L. E. Ibáñez, N. Irges, and F. Quevedo, “TeV-Scale Z’ Bosons from D-branes,” *JHEP*, vol. 08, p. 016, 2002.
- [57] M. A. Shifman and A. Vainshtein, “Solution of the Anomaly Puzzle in SUSY Gauge Theories and the Wilson Operator Expansion,” *Nucl. Phys.*, vol. B277, p. 456, 1986.
- [58] M. A. Shifman and A. Vainshtein, “On holomorphic dependence and infrared effects in supersymmetric gauge theories,” *Nucl. Phys.*, vol. B359, pp. 571–580, 1991.
- [59] R. Blumenhagen, F. Gmeiner, G. Honecker, D. Lüst, and T. Weigand, “The statistics of supersymmetric D-brane models,” *Nucl. Phys.*, vol. B713, pp. 83–135, 2005.

- [60] T. W. Grimm and J. Louis, “The effective action of type IIA Calabi-Yau orientifolds,” *Nucl. Phys.*, vol. B718, pp. 153–202, 2005.
- [61] N. Akerblom, R. Blumenhagen, D. Lüst, and M. Schmidt-Sommerfeld, “Instantons and Holomorphic Couplings in Intersecting D-brane Models,” *JHEP*, vol. 08, p. 044, 2007.
- [62] S. Abel and B. Schofield, “Brane anti-brane kinetic mixing, millicharged particles and SUSY breaking,” *Nucl.Phys.*, vol. B685, pp. 150–170, 2004.
- [63] S. Abel, M. Goodsell, J. Jaeckel, V. Khoze, and A. Ringwald, “Kinetic Mixing of the Photon with Hidden U(1)s in String Phenomenology,” *JHEP*, vol. 0807, p. 124, 2008.
- [64] L. E. Ibáñez and A. M. Uranga, “Neutrino Majorana masses from string theory instanton effects,” *JHEP*, vol. 03, p. 052, 2007.
- [65] R. Blumenhagen, M. Cvetič, and T. Weigand, “Spacetime instanton corrections in 4D string vacua - the seesaw mechanism for D-brane models,” *Nucl. Phys.*, vol. B771, pp. 113–142, 2007.
- [66] R. Blumenhagen, M. Cvetič, S. Kachru, and T. Weigand, “D-Brane Instantons in Type II Orientifolds,” *Ann. Rev. Nucl. Part. Sci.*, vol. 59, pp. 269–296, 2009.
- [67] P. G. Camara, C. Condeescu, E. Dudas, and M. Lennek, “Non-perturbative Vacuum Destabilization and D-brane Dynamics,” *JHEP*, vol. 1006, p. 062, 2010.
- [68] M. Bianchi and A. Sagnotti, “On the systematics of open string theories,” *Phys.Lett.*, vol. B247, pp. 517–524, 1990.
- [69] E. G. Gimon and J. Polchinski, “Consistency Conditions for Orientifolds and D-Manifolds,” *Phys. Rev.*, vol. D54, pp. 1667–1676, 1996.
- [70] D. Bailin and A. Love, “Towards the supersymmetric standard model from intersecting D6-branes on the Z-prime(6) orientifold,” *Nucl.Phys.*, vol. B755, pp. 79–111, 2006.
- [71] D. Bailin and A. Love, “Almost the supersymmetric standard model from intersecting D6-branes on the Z(6)-prime orientifold,” *Phys.Lett.*, vol. B651, pp. 324–328, 2007.
- [72] D. Bailin and A. Love, “Constructing the supersymmetric Standard Model from intersecting D6-branes on the Z(6)-prime orientifold,” *Nucl.Phys.*, vol. B809, pp. 64–109, 2009.
- [73] L. E. Ibáñez, F. Marchesano, and R. Rabadan, “Getting just the standard model at intersecting branes,” *JHEP*, vol. 0111, p. 002, 2001.

- [74] D. Lüüst, P. Mayr, R. Richter, and S. Stieberger, “Scattering of gauge, matter, and moduli fields from intersecting branes,” *Nucl.Phys.*, vol. B696, pp. 205–250, 2004.
- [75] D. Lüüst, S. Stieberger, and T. R. Taylor, “The LHC String Hunter’s Companion,” *Nucl. Phys.*, vol. B808, pp. 1–52, 2009.
- [76] D. Lüüst, O. Schlotterer, S. Stieberger, and T. R. Taylor, “The LHC String Hunter’s Companion (II): Five-Particle Amplitudes and Universal Properties,” *Nucl. Phys.*, vol. B828, pp. 139–200, 2010.
- [77] W.-Z. Feng, D. Lüüst, O. Schlotterer, S. Stieberger, and T. R. Taylor, “Direct Production of Lightest Regge Resonances,” 2010.
- [78] L. A. Anchordoqui, I. Antoniadis, H. Goldberg, X. Huang, D. Lüüst, *et al.*, “Z’-gauge Bosons as Harbingers of Low Mass Strings,” 2011.
- [79] C. Angelantonj, C. Condeescu, E. Dudas, and G. Pradisi, “Non-perturbative transitions among intersecting-brane vacua,” 2011.
- [80] R. Blumenhagen, L. Görlich, and T. Ott, “Supersymmetric intersecting branes on the type IIA $T^6/Z(4)$ orientifold,” *JHEP*, vol. 01, p. 021, 2003.
- [81] M. Cvetič and P. Langacker, “New grand unified models with intersecting D6-branes, neutrino masses, and flipped $SU(5)$,” *Nucl. Phys.*, vol. B776, pp. 118–137, 2007.